2021

Identification and Characterization of Calcium as a Biofilm Promoting Signal by Vibrio Fischeri

Alice Hannah Tischler

LOYOLA UNIVERSITY CHICAGO

IDENTIFICATION AND CHARACTERIZATION OF CALCIUM AS A BIOFILM PROMOTING SIGNAL BY *VIBRIO FISCHERI*

A DISSERTATION SUBMITTED TO

THE FACULTY OF THE GRADUATE SCHOOL

IN CANDIDACY FOR THE DEGREE OF

DOCTOR OF PHILOSOPHY

PROGRAM IN MICROBIOLOGY AND IMMUNOLOGY

BY

ALICE HANNAH TISCHLER

CHICAGO, ILLINOIS

DECEMBER 2021

ACKNOWLEDGEMENTS

First and foremost, I have to thank my family for their unending love and support. My parents especially who when I was young, always cultivated, but never pushed my love of science. It has been such a privilege to be able to have shared this intellectual journey with you. To my sister Dory for being an oasis outside of science, and supporting me through the most trying times.

I am particularly grateful to my mentor, Dr. Karen L. Visick who has given me guidance and has fostered my growth as a scientist. Her enthusiasm for research inspires me to see the joy in science every day. I would like to thank the past and present members of the Visick lab for all of their support, humor, advice, and most importantly, teamwork. Thank you to my committee for your excellent advice and encouragement along the way, I appreciate all of your insight. I would also like to give a very special thanks to the Microbiology and Immunology department. It has been a wonderful experience to have gone on this journey with such a supportive and bright community, especially with my fellow graduate students who have become true friends.

TABLE OF CONTENTS

LIST OF TABLES

LIST OF FIGURES

ABSTRACT

The marine bacterium, *V. fischeri* actively engages in an exclusive partnership in the light organ of its squid host, *Euprymna scolopes*. A critical step in this colonization process is the formation of a bacterial aggregate, or biofilm, which is a community of bacteria embedded within a protective extracellular matrix. While *V. fischeri* readily forms biofilms in nature, genetic overexpression must be utilized to achieve biofilm formation in the laboratory. Recent work investigating media composition led myself and others to evaluate how seawater salts impacted growth and biofilm formation in a number of mutant backgrounds, leading to the identification of calcium as a strong biofilm promoting signal. We identified that in our WT strain, ES114, calcium could induce formation of a cellulose dependent ring adherent to the sides of the test tube. Surprisingly, calcium was also permissive to allow formation of adherent rings and cohesive cellular clumps, in a biofilm competent *rscS*$^{++}$ strain, and in strains lacking the novel regulator BinK. These rings and clumps were dependent on cellulose and SYP, respectively. A *binK* mutant was only biofilm competent in the presence of calcium.

The ability to induce biofilm formation in the absence of genetic overexpression allowed us to probe the roles of known SYP regulators, SypF, SypG, and RscS. This led to the identification of HahK, and subsequent identification of HnoX, two biofilm regulators whose input had previously been masked due to overexpression conditions. These conditions also allowed us for the first time to identify a phenotype when the positive regulator RscS was deleted.

To further examine how calcium is able to promote biofilm phenotypes, I assessed the contribution of the signaling molecule, c-di-GMP, determining that calcium induces c-di-GMP dependent on a specific diguanylate cyclase, CasA. CasA is directly activated by calcium, dependent on residues in an N-terminal sensory domain, and synthesizes c-di-GMP through an enzymatic C-terminal domain. CasA regulates cellulose polysaccharide at the level of transcription, dependent on the transcription factor VpsR, and provides insight into potential function of the *V. cholerae* homolog, CdgK. Together, these results firmly establish calcium as a key signal for biofilm formation by *V. fischeri* and provide one mechanism for how calcium works to impact these phenotypes.

CHAPTER ONE

LITERATURE REVIEW

Introduction

Bacteria adapt to their surroundings by recognizing environmental signals, resulting in changes in gene expression, protein production and/or activity, and other processes that permit them to survive and/or thrive accordingly. In many cases, this adaptation process results in development of biofilms, sessile communities encased within a protective extracellular matrix. Biofilms can be incredibly advantageous, and a staggering $3.5x10^{29}$ bacterial and archaeal cells are estimated to live in biofilms (Flemming & Wuertz, 2019). While the vast majority of bacterial biofilms are environmental, a prodigious number (~$4x10^{23}$) reside in and/or on humans at an approximate 1:1 ratio of bacterial to human cells (Flemming & Wuertz, 2019, Whitman *et al.*, 1998, Sender *et al.*, 2016). Both scientists and the general public have been increasingly appreciating the ways that bacteria interact with humans and other host organisms through mechanisms other than disease. These interactions highlight the need to study how bacteria regulate and form biofilms in the context of a host.

The symbiosis between the marine bacterium *Vibrio fischeri,* and its eukaryotic host the Hawaiian bobtail squid, *Euprymna scolopes*, is an excellent model to study bacterial-host interactions in the context of biofilm formation. This symbiosis is well characterized and will be explored in great detail later in this chapter. Colonization is driven coordinately by both symbiont and host, and biofilm formation is a key step in colonization initiation. Several signals

have been identified thus far that can alter *V. fischeri* biofilm formation: arabinose, calcium, and nitric oxide (NO) (Thompson *et al.*, 2019, Visick *et al.*, 2013). My dissertation work has focused on the identification and characterization of calcium as a major signal promoting biofilm formation. In this first section I will provide a review of the literature necessary to understand and give context to the data I present here.

I will first describe the properties and characteristics of calcium, the proteins that bind calcium, and its emerging role as a signal in bacteria. I will then introduce and discuss generalized biofilm formation before transitioning into the role of the small signaling molecule c-di-GMP, as biofilms and c-di-GMP go hand-in-hand. Next, I will detail the stages of colonization and symbiosis between *V. fischeri* and *E. scolopes*, and finally conclude with a review of what we know about biofilm formation and regulation by *V. fischeri*.

Calcium

Introduction

At its most basic level, calcium is an element. It is classified as a group 2 alkali earth metal with a +2 oxidation state, allowing it to be highly reactive and is therefore always found as part of a compound in nature, often with carbonate or chloride. Calcium is both the 5th most abundant element in the earth's crust and the 5th most abundant ion in seawater, at an average concentration of 10.28 mM (PubChem, 2021). In a biological sense, calcium is both problematic and advantageous to cells, as it can be cytotoxic at high levels but has also evolved to be a ubiquitous tool for signal transduction across all forms of life (Clapham, 2007).

Calcium as a signal has historically been investigated in eukaryotic cells, and has long been lauded as a key signal, resulting in detailed knowledge of regulatory networks controlling a variety of cellular processes, including cell division, motility, and apoptosis (Clapham, 2007,

King *et al.*, 2020). Comparatively, the study and understanding of calcium as a signal and regulatory factor in bacteria has been relatively underappreciated, and remains fragmented at best (Domínguez *et al.*, 2015, Dominguez, 2004, Dominguez, 2018, King *et al.*, 2020). However, this is a growing field of research, and calcium has been identified as a signal for diverse bacterial processes including, but not limited to, chemotaxis, sporulation, biofilm formation, and pathogenesis (Domínguez *et al.*, 2015, Dominguez, 2004, Dominguez, 2018, King *et al.*, 2020). Bacterial responses to calcium in the context of a host is a particular area of interest, as calcium can be a major determinant of host colonization and pathogenesis. New insights into how bacteria use and respond to calcium are often framed as similar or different to eukaryotes, revealing quite a lot of evolutionary conservation across domains of life, from the ways that cells utilize and control calcium levels, to proteins that bind calcium. This section serves as an overview of calcium signaling in bacteria, taking into account mechanisms conserved across domains.

Calcium Binding Proteins

Unchecked, calcium can be quite toxic to cells, but when properly utilized it can be a powerful tool. Mechanisms to mediate calcium concentrations and localization often involve calcium binding proteins (CBP), which are able to bind to calcium for sequestration and/or signaling. Several CBPs binding domains are universal across taxonomic domains, including the well-studied EF-hand domain superfamily. This domain is characterized by two perpendicular alpha helices connected by a negatively charged loop, which can bind to either calcium or magnesium (Figure 1A). This loop consists of ~12 amino acids, and the binding affinities have a wide range, and can vary up to ~100,000 fold, dependent on several protein properties including the amino acids inside the loop and protein geometry (Clapham, 2007, Elíes *et al.*, 2020, Lewit-

Bentley & Réty, 2000). Calmodulin (CaM), which is perhaps the most extensively studied, is a classic example of this superfamily, as it contains two pairs of two EF-hand motifs that coordinate calcium binding (Zhang *et al.*, 1995, Elíes *et al.*, 2020, Kretsinger *et al.*, 2004). In bacteria, 5 different classes of EF-hand domains have been reported, binned by loop size and helix structures. Classes I-III retain the typical eukaryotic helix-loop-helix structure, varying in the length of their loop, containing 12, 10, or 15 residues, respectively. Classes IV and V lack either the first or second helix, respectively, resulting in variations that include strand-loop-helix, strand-loop-strand, helix-loop-strand, and helix-loop-loop (Domínguez *et al.*, 2015, Dominguez, 2018). Overall, these EF-hand motifs demonstrate both impressive conservation and variety across species and domains.

On the opposite side of the spectrum, the much less well studied βγ-crystallin superfamily is also conserved across domains and contains a calcium binding motif (Aravind *et al.*, 2009). This superfamily contains a Greek key motif that is specifically characterized by highly ordered β-hairpin loops between the first and second strands of each motif (Figure 1B) (Aravind *et al.*, 2009). Calcium binding is mediated by a specific conserved motif, N/D-N/D-#-I-S/T-S, and both structure and binding motif are conserved across all domains of life. While biologically relevant in bacteria, archaea, and eukaryotes, many vertebrates with these domains have lost the ability to bind calcium due to poorly positioned large residues that interfere with binding. However, in addition to and/or in place of binding, many proteins in this superfamily retain the ability to sense and/or sequester calcium, all together representing a versatile superfamily (Aravind *et al.*, 2009, Dominguez, 2018).

Several other bacteria specific conserved domains have been identified in CBPs, including repeats-in-toxin (RTX), proline glutamate polymorphic GC-rich repetitive sequence

(PE_PGRS), and the bacterial immunoglobulin like (Big) domains (Domínguez *et al.*, 2015, Dominguez, 2018). As of yet, most proteins containing these domains have been identified bioinformatically and have not been biologically assessed but are predicted to be involved in a variety of roles including structural, buffering, sensors and signal transducers (Dominguez, 2018). Many proteins that biologically have been shown to bind and/or sense/respond to calcium do not contain any of these known calcium binding structures, suggesting that multiple classes of bacterial CBPs and the domains and motifs responsible for binding calcium have yet to be identified.

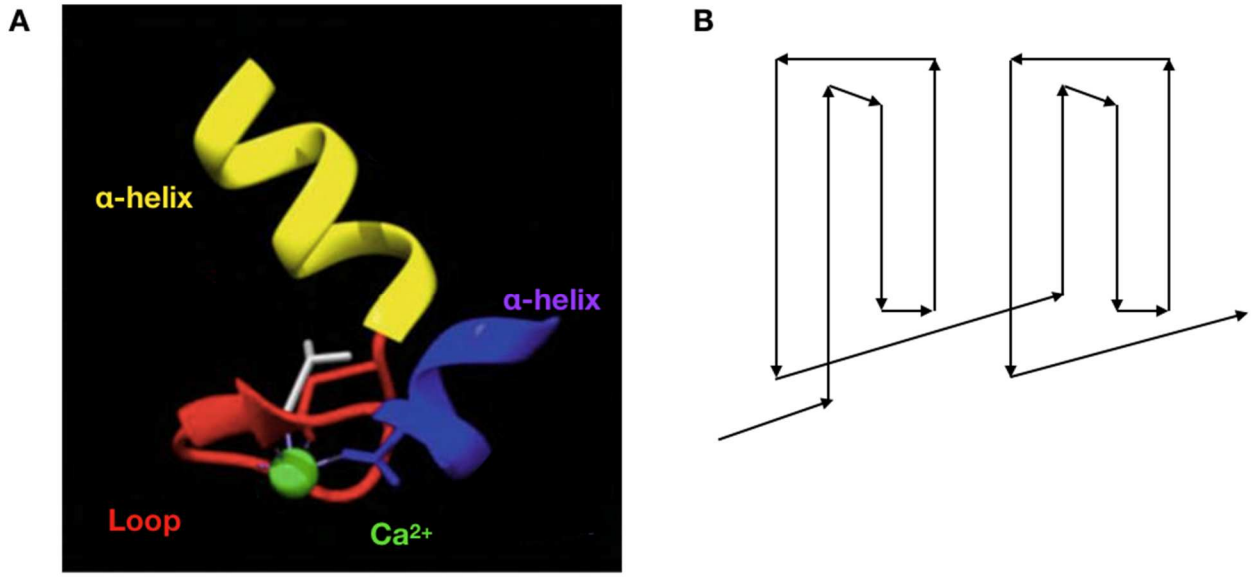

Figure 1. Structure of Calcium-Binding Motifs. (A) Modified from (Elíes *et al.*, 2020), general structure of a canonical EF-hand domain bound to calcium. (B) Adapted based on (Graw, 1997), pattern forming a βγ-crystalline Greek key motif.

Calcium Signaling in Bacteria- Two Component Regulatory Systems

Two component regulatory systems (TCS) are a common mechanism bacteria use to sense their environment. In the simplest version of this system, a sensor kinase (SK) detects a signal, triggering autophosphorylation of a conserved histidine. This phosphoryl group is then

donated to a response regulator (RR) on a conserved aspartate residue, and the activated RR can carry out a response such as activating transcription (Stock *et al.*, 2000, West & Stock, 2001). Several TCSs have been identified that sense calcium, both negatively and positively. Of these, the most well-known is PhoPQ, which can be regulated by many signals, including negative regulation by calcium in numerous Gram-negative bacteria including: *E. coli, Pseudomonas aeruginosa, Yersinia pestis, Shigella flexneri, Salmonella enterica* (García Véscovi *et al.*, 1996, Véscovi *et al.*, 1997, Lesley & Waldburger, 2001, Chamnongpol *et al.*, 2003, King *et al.*, 2020). Of note, *V. fischeri* contains PhoPQ, but it does not sense/respond to calcium (Lyell *et al.*, 2010). The variety in signals sensed by PhoPQ systems is reflected in the responses elicited, which include regulation of virulence factors, motility, and lipid A modification (King *et al.*, 2020) However, magnesium and calcium binding regions in PhoQ have been identified, and remain fairly well conserved across species, despite the range of downstream responses (Véscovi *et al.*, 1997, Chamnongpol *et al.*, 2003, Regelmann *et al.*, 2002).

Another TCS negatively regulated by calcium is CarRS in *V. cholerae* (Bilecen & Yildiz, 2009). CarRS responds to calcium by downregulating transcription of VpsR. VpsR is the main transcriptional regulator of the *Vibrio p*oly*s*accharide (*vps*) locus, which is responsible for synthesis of VPS, the biofilm polysaccharide in *V. cholerae* (Bilecen & Yildiz, 2009, Casper-Lindley & Yildiz, 2004, Conner *et al.*, 2017). Ultimately this downregulation results in a decrease in *V. cholerae* biofilm formation in the presence of calcium.

Several TCSs have been identified as positively responding to calcium, including two in *Pseudomonas* spp., CarSR, and CvsSR. CarSR is found in *P. aeruginosa*, and positively regulates at least two identified targets, CarO and CarP. These two regulators are involved in calcium-mediated induction of the virulence factors pyocyanin and pyoverdine, and additionally

contribute to calcium homeostasis and tolerance to elevated calcium levels (Guragain *et al.*, 2016, King *et al.*, 2020). CvsSR is found in *P. syringae*, and is required for pathogenicity, enhancing transcription of genes for the type 3 secretion system and sRNAs, while also repressing alginate and flagella biosynthesis (Fishman *et al.*, 2018).

While TCSs can be a wonderful tool to sense and respond to environmental stimuli, including calcium, the diversity of sensors and specificity to a particular species described here highlights one of the biggest challenges surrounding investigation of gene regulation on a broad scale. Even among a conserved TCS like PhoPQ, the signals and downstream responses can be wildly diverse. This makes TCSs an excellent tool for bacterial adaptation to adjust to specific environments but can present difficulties for broad scale analysis and inferences by researchers.

Host-Associated Calcium

Calcium is extremely tightly regulated in eukaryotes, and colonization by bacteria can trigger changes in calcium that affect both bacteria and host. This is an emerging area of study, so while many gaps remain, common trends include pathogen manipulation of calcium signaling networks and their outcomes to benefit bacterial survival and persistence in the host. Below are brief overviews of known ways that several bacteria are able to utilize calcium to their advantage in the context of a host.

Pili are one of the major virulent factors for *Neisseria meningitidis*, the etiological agent of bacterial meningitis. The pilus protein, PilC1, is vital for adherence to and internalization of host endothelial cells. PilC1 works by activating host phospholipase C, resulting in a significant increase in cytosolic calcium levels, and without this calcium increase, PilC1-mediated adherence is significantly reduced (Asmat *et al.*, 2014, Dominguez, 2018). Several other bacterial species also use similar mechanisms calcium-mediated adherence/internalization of

host cells, including *P. aeruginosa, Campylobacter jejuni*, and *Borrelia burgdorferi* (Johnson *et al.*, 2011, Hu *et al.*, 2005, Grab *et al.*, 2009, Dominguez, 2018).

Mycobacterium tuberculosis (Mtb), the causative agent of tuberculosis, is well-adapted to human hosts and utilizes many mechanisms to resist the host immune system and persist with the host. Within macrophages, Mtb induces interferon signals that result in increased endoplasmic reticulum (ER) production (Watson *et al.*, 2015, Saquib *et al.*, 2015, Cui *et al.*, 2016). The ER is a major site for calcium storage in eukaryotic cells, and Mtb can decrease calcium levels, triggering ER stress (Sano & Reed, 2013, Cui *et al.*, 2016). Ultimately, this leads to cell apoptosis through multiple pathways, including the unfolded protein response, oxidative stress in mitochondria, and reduction of membrane integrity leading to a release of cytochrome C (Sano & Reed, 2013, Cui *et al.*, 2016). While apoptosis is typically considered a good mechanism to control bacterial spread, Mtb is often able to survive (Cui *et al.*, 2016), suggesting that Mtb is benefitting through induction of these pathways via manipulation of host calcium levels.

Shigella, the causative agent of bacillary dysentery, uses host calcium in a variety of ways to promote invasion, slow host cell death, and modulate the immune response (Bonnet & Tran Van Nhieu, 2016, Tran Van Nhieu *et al.*, 2018, Dominguez, 2018). As soon as five minutes after the bacteria encounter host cells, *Shigella* alters host calcium levels, leading to cytoskeletal remodeling and bacterial entry. *Shigella* invasion triggers the p53-mediated apoptotic-signaling pathway, but uses a calcium-regulated bacterial effector to degrade p53 (Bergounioux *et al.*, 2012). Therefore, instead of dying by apoptosis, host cells instead undergo a slow, necrotic death associated with high intracellular calcium and plasma membrane permeabilization through a yet unknown mechanism (Carneiro *et al.*, 2009, Dupont *et al.*, 2009, Bonnet & Tran Van Nhieu, 2016). Lastly, *Shigella* uses calcium-mediated mechanisms to dampen the immune response

through calcium activation of a signaling cascade that antagonizes inflammatory factors (Andree *et al.*, 2014, Bonnet & Tran Van Nhieu, 2016).

As seen here, the ways that bacteria interact with host cells via calcium is quite diverse, and many questions remain on exactly how these pathogens interact with host cells and vice versa. Pathogenic interactions between bacteria and host have typically been studied in the context of virulence factors, examining the specific cellular targets and catalytic activity of each factor. While these interactions are clearly critical for pathogenesis, work delving into the murkier waters of how second messengers like calcium are modulated during infection will shed light on what are likely to be crucial contributions to infection dynamics.

Summary

Right now is a very exciting time to be studying calcium in the context of both bacteria and bacterial-host interactions. Calcium has been appreciated and investigated as a critical global signal in eukaryotic cells for years, which has led to an incredibly detailed understanding of how calcium functions in various cell types and conditions. In contrast, the ways that calcium is utilized in bacteria, or even in the context of bacterial-host interactions has only just begun to be acknowledged. The extent of calcium as a bacterial signal is still unclear, and future research will determine if calcium is an essential universal bacterial regulator like in eukaryotes, or if it is a more specific, niche environmental cue.

Biofilm Formation and Cyclic-di-GMP

Introduction- Biofilm Formation

The most common bacterial lifestyle in the environment are protected communities called biofilms (Flemming & Wuertz, 2019, O'Toole *et al.*, 2000). Bacteria within biofilms are embedded within a secreted and protective extracellular matrix comprised of a mix of proteins,

polysaccharides, extracellular DNA and lipids (Flemming & Wingender, 2010, Flemming *et al.*, 2016). The matrix is not necessarily just a static amorphous secretion, but is both viscous and elastic, filling in space between and around cells, providing spatial arrangement of cells and mechanical stability to the whole structure (Flemming *et al.*, 2016, Persat *et al.*, 2015). Biofilms can be incredibly advantageous, providing benefits including, but not limited to, protection from desiccation, environmental stressors, antibiotics, and predation (Chang *et al.*, 2007, Matz *et al.*, 2005, Flemming *et al.*, 2016). These strong advantages present significant challenges to the medical field and environmental industries where biofilms lead to recurrent infection, biofouling, and corrosion (Costerton *et al.*, 1987, Wingender & Flemming, 2011, Flemming *et al.*, 2016). Therefore, understanding how and why biofilms form is of particular scientific importance. In the beginning of this section, I first introduce the stages of biofilm development to give context to how biofilms form. Next, I introduce the small molecule c-di-GMP before exploring the connection between c-di-GMP and biofilm formation that is a major factor in my dissertation work.

Stages of Biofilm Development

Attachment. The stages of biofilm formation are typically considered in relation to a foreign surface, beginning with the initial sensing of and interacting with the surface (Kostakioti *et al.*, 2013, Rumbaugh & Sauer, 2020). Surface properties can either be attractive or repulsive, and a bacterium's ability to overcome these properties can depend on behaviors like motility or chemotaxis to reach the surface. This initial attachment can be reversed if bacteria are perturbed by outside forces, or if the conditions are sensed to be unfavorable (Figure 2) (Donlan, 2002, Kostakioti *et al.*, 2013). Irreversible attachment happens when the bacteria are able to maintain their grip on the surface, even in the presence of outside forces, and is often mediated by

attachment organelles and proteins including pili, curli, and adhesins (Donlan, 2002, Kostakioti *et al.*, 2013).

Maturation. Attachment triggers changes in gene expression to mediate the shift to a sessile lifestyle (Figure 2). Bacteria must produce and secrete substantial amounts of different matrix components in order to fully form a biofilm, as the matrix contains nearly 90% of the biofilm's dry weight mass (Flemming & Wingender, 2010). The matrix not only is protective, but it also gives the biofilm shape, which can vary greatly from microclusters and monolayers, to bulbous mushroom shaped forms, and dense, diverse microbial mats (Flemming *et al.*, 2016, Persat *et al.*, 2015, Kostakioti *et al.*, 2013). These shapes and stabilization are often dependent on components, including extracellular DNA, proteins, and ions, that are able to physically interact with the cells, matrix, and/or surfaces to provide stability to the structure (Flemming *et al.*, 2016, Persat *et al.*, 2015). The same matrix properties that are protective also limit diffusion of resources to reach the lower layers of cells. Pores and channels can form within the matrix to aid in communication and resource sharing, but gradients of oxygen, pH, nutrients, and quorum sensing molecules arise, leading to a heterogenous bacterial population with differences in gene expression, gene mutations, and genetic transfer dependent on the niche within the matrix (O'Toole *et al.*, 2000, López *et al.*, 2010, Kostakioti *et al.*, 2013, Flemming *et al.*, 2016, Spormann, 2008, Donlan, 2002).

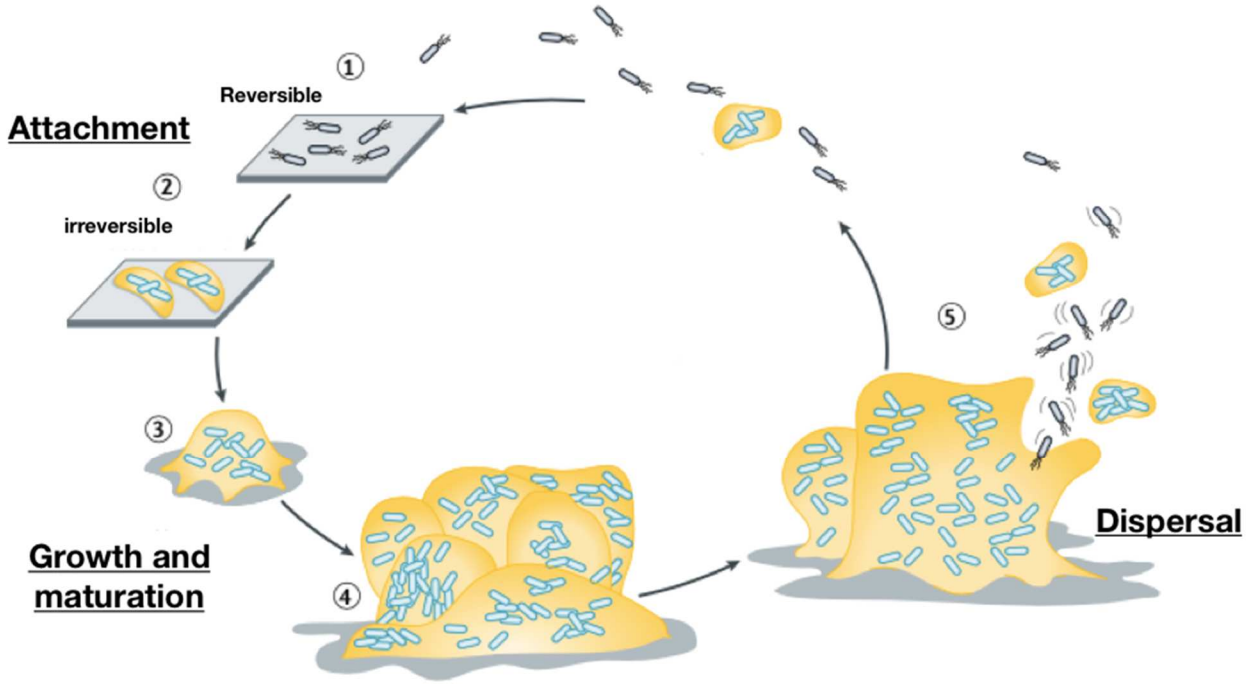

Figure 2. Stages of Biofilm Lifecycle Modified from Rumbaugh and Sauer 2020. Planktonic cell undergo an initial attachment (1) to a surface via electrostatic and hydrophobic interactions, which are unstable before forming a stronger irreversible attachment (2) where flagella are lost and cells begin secreting matrix. This leads to the beginning of biofilm maturation (3) when communities are several cells thick and embedded within the matrix, and continues until a maximum number of cells and thickness of community is reached (4). Dispersal (5) occurs when sessile cells transition to planktonic and leave the biofilm community.

Dispersal. The final stage in biofilm development is dispersal (Figure 2). Dispersal is defined as an active event, where sessile, matrix-enclosed cells convert to a planktonic mode, and is caused by a variety of factors including fatty acid signaling, nitric oxide (NO), oxygen, nutrient availability, and iron (Rumbaugh & Sauer, 2020, Kostakioti *et al.*, 2013). After receiving the signal to leave, a key step is breakdown of the matrix by endonucleases and glycoside hydrolases, allowing cells to physically able to escape the confines of the matrix (Rumbaugh & Sauer, 2020). Interestingly, the cells that leave are not quite the same as either biofilm or planktonic cells, but somewhere in between. Dispersed cells are more motile and more

virulent and retain enhanced adhesion abilities than either biofilm or planktonic cells. These phenotypes are often short-lived, and bacteria that remain planktonic quickly readjust to the norms associated with planktonic cells (Rumbaugh & Sauer, 2020).

Overall, biofilm formation is a dynamic process that allows individual bacteria to function as part of a protective, advantageous community. It should be noted that biofilm in the context of surface attachment was described here; however, surface attachment is not required for bacterial aggregation (Costerton *et al.*, 1987, Flemming *et al.*, 2016, Flemming & Wuertz, 2019, Bossier & Verstraete). This highlights how diverse biofilms can be, which allows them to be tailored to fit the specific needs of bacteria within a niche.

Introduction– C-di-GMP

In many bacteria, internal signaling relies on cyclic dinucleotides, such as bis(3'-5')-cyclic dimeric guanosine monophosphate (c-di-GMP), a small ubiquitous second messenger that regulates numerous bacterial behaviors, including biofilm formation, motility, and virulence (Römling *et al.*, 2013, Valentini & Filloux, 2016). C-di-GMP is synthesized by diguanylate cyclases (DGC) from 2 GTP molecules in a two-step reaction, via a 5'-pppGpG intermediate and two pyrophosphate byproducts (Figure 3) (Ross *et al.*, 1987). DGCs contain a conserved GGDEF domain, which when activated, form catalytically competent homodimers with an active site at the dimer interface (Tal *et al.*, 1998, Paul *et al.*, 2007, Römling *et al.*, 2013). Degradation of c-di-GMP into 5' -pGpG is mediated by phosphodiesterases (PDE), containing either EAL or HD-GYP domains, and then further degraded into GMP (Figure 3) (Ross *et al.*, 1987, Tal *et al.*, 1998, Galperin *et al.*, 1999). While DGCs and PDEs have opposite functions, GGDEF domains are frequently found with EAL domains within the same proteins, and to a lesser extent with HY-GYP domains (Römling *et al.*, 2013, Tal *et al.*, 1998). Out of all the GGDEF and EAL

domain containing proteins, approximately 1/3 of GGDEF and 2/3 of EAL domains are found within the same protein. The *V. fischeri* genome alone contains 8 predicted GGDEF/EAL genes (out of 50); however, 3 of these contain degenerate GGDEF domains, and one, BinA, has been reported to lack GGDEF activity (Figure 4) (Mandel *et al.*, 2008, Ruby *et al.*, 2005, Wolfe & Visick, 2010, Bassis & Visick, 2010). Although the number of DGCs and PDEs encoded within bacterial genomes can differ greatly, many organisms contain dozens of such genes, highlighting the importance of c-di-GMP as an intracellular signal (Römling *et al.*, 2013). Activation of DGCs and PDEs is similarly diverse and is often linked to environmental signals and signal transduction pathways, and sensory domains are common domain types associated with DGCs and PDEs (Römling *et al.*, 2013). This variety of sensory domains is matched by the diversity of known signals that impact c-di-GMP. For example, in *V. cholerae* polysaccharide production alone, known signals include temperature, bile acids, polyamines, and ferrous iron (Conner *et al.*, 2017, Townsley & Yildiz, 2015, Koestler & Waters, 2014, Karatan *et al.*, 2005, Schaller *et al.*, 2012). For the remainder of this section, I will explore the connection between c-di-GMP and biofilm formation.

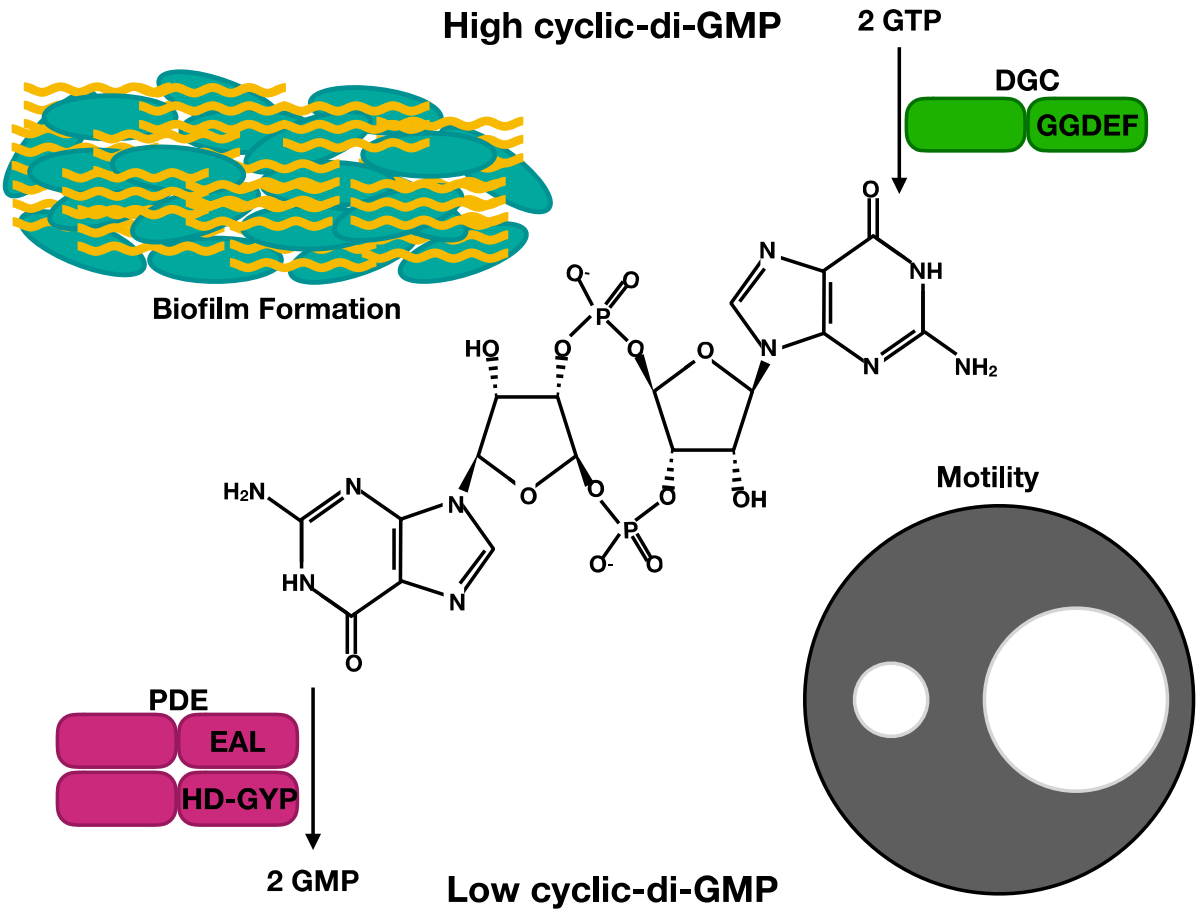

Figure 3. C-di-GMP Schematic. C-di-GMP is synthesized from 2 GTP by DGC proteins containing GGDEF domains with a 5'- pppGpG intermediary. C-di-GMP (pictured in the middle) can be hydrolyzed into 5'- pGpG by PDE proteins that contain either EAL or HD-GYP domains, and then gets further degraded into GMP. High levels of c-di-GMP are associated with biofilm formation (top left-cartoon biofilm, bacteria are teal, matrix is yellow), and low levels are associated with motility (bottom right- cartoon motility plate, migrating bacteria are white).

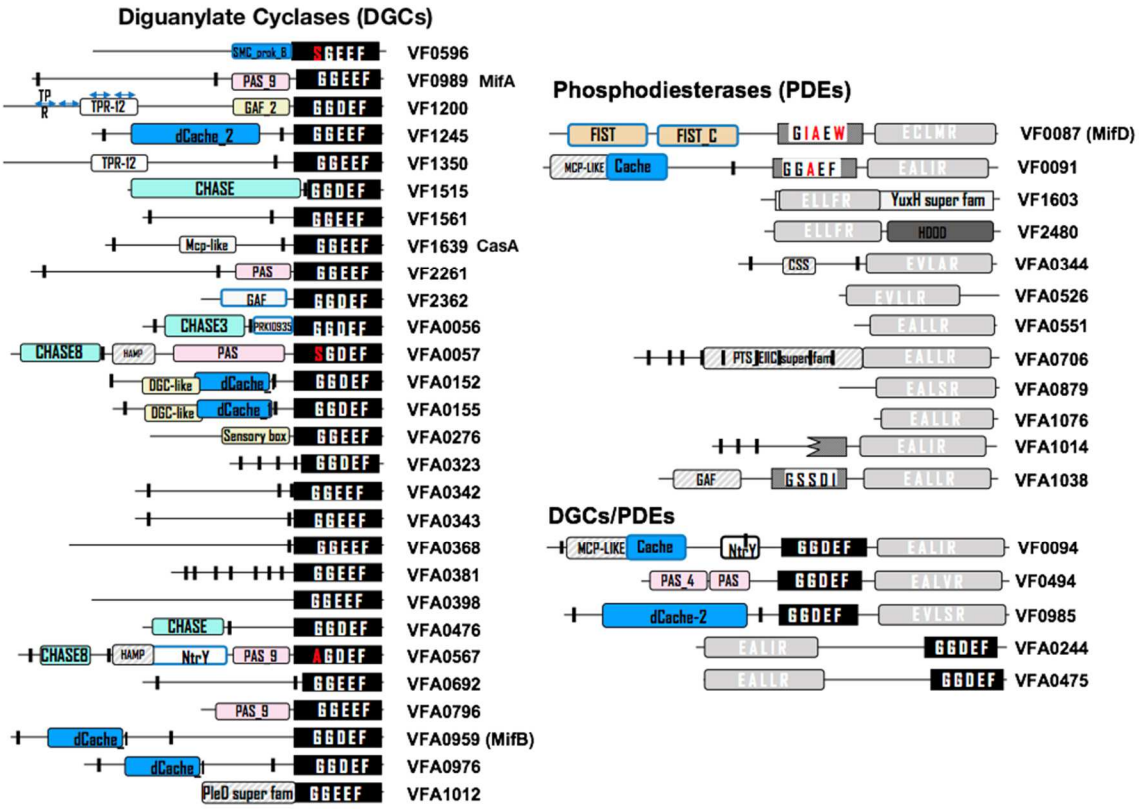

Figure 4. Cartoon of Putative DGCs and PDEs in *V. fischeri*. Adapted from Wolfe and Visick, 2010. Cartoon of predicted DGCs and PDEs in *V. fischeri*. Note, several genes with degenerative domains are not included on this list, or have been moved from the DGC/PDE section to just the PDE section (MifD, VF_0091, BinA).

C-di-GMP and Biofilm Formation

The bottom line for studies investigating bacterial phenotypes in relation to c-di-GMP is that high and low levels of c-di-GMP lead to sessile and planktonic phenotypes, respectively (Figure 3) (Römling *et al.*, 2013). Impressively, this theory has held true across all types of biofilms and species investigated, although the mechanism of how c-di-GMP induces a sessile lifestyle can vary wildly and can be species specific (Römling *et al.*, 2013, Römling & Galperin, 2015). C-di-GMP was first discovered as an activator of bacterial cellulose synthase, and ever since, c-di-GMP and cellulose have been inextricably linked (Ross *et al.*, 1987). In fact, a role for c-di-GMP outside of cellulose synthesis was not hypothesized until 1998, and was confirmed

in 2004 (Tal *et al.*, 1998, Paul *et al.*, 2004, Tischler & Camilli, 2004). Since then, c-di-GMP has been implicated in activation of numerous polysaccharides in a variety of species at multiple levels of control. For example, in *V. cholerae*, c-di-GMP activates the *V*ibrio *p*oly*s*accharide (*vps*) locus through binding and increasing activity of transcriptional regulators VpsR and VpsT (Conner *et al.*, 2017, Srivastava *et al.*, 2011, Krasteva *et al.*, 2010, Hsieh *et al.*, 2018). In *V. vulnificus,* c-di-GMP increases transcription of the *b*iofilm *r*ugose *p*olysaccharide (*brp*) locus, although the mechanism of how this occurs is unknown (Chodur *et al.*, 2018). Beyond *Vibrio* spp., c-di-GMP-mediated biofilm initiation and formation has been well described in *Pseudomonas* spp.. The DGC SadC and PDE BifA both impact swarming motility and alter biofilm formation at step 2, irreversible attachment (Figure 2) (Kuchma *et al.*, 2007, Merritt *et al.*, 2007). BifA, and another DGC, RoeA, but not SadC, are able to modulate production of the Pel polysaccharide, further impacting attachment (Merritt *et al.*, 2010, Ha & O'Toole, 2015). Additionally, the DGC WspR is thought to be phosphorylated in response to surface sensing, and activated WspR leads to an increase in biofilm matrix production through an unknown mechanism that requires both Pel and Psl polysaccharides (Ha & O'Toole, 2015, Hickman *et al.*, 2005, Valentini & Filloux, 2016). Once *Pseudomonas* biofilms are attached and begin to mature, the DGC MucR is activated to increase alginate, another polysaccharide in the biofilm matrix (Ha & O'Toole, 2015, Hay *et al.*, 2009). Beyond biofilm formation, *Pseudomonas* spp. have a whole host of DGCs and PDEs that mediate biofilm dispersal through a variety of mechanisms including adhesin cleavage and NO-sensing (Barraud *et al.*, 2009, Ha & O'Toole, 2015, Rumbaugh & Sauer, 2020). Overall, the mechanisms of biofilm formation mediated by c-di-GMP are incredibly diverse within organisms, with the common thread being that high levels of c-di-GMP skew the cell towards biofilm phenotypes.

Cellulose-Dependent Biofilm and C-di-GMP

Cellulose is the most abundant polysaccharide in the world and hypothesized to be the most common exopolysaccharide found in the biofilm matrix (Serra & Hengge, 2019, Römling & Galperin, 2015). Cellulose biofilms are efficient for establishing physical contact with a host, and several host-associated bacteria, both symbiotic and pathogenic, use cellulose as a colonization factor (Augimeri *et al.*, 2015). Despite this widespread occurrence, regulation of cellulose biofilms remains fairly consistent across species as all known *b*acterial *c*ellulose *s*ynthase (*bcs*) loci contain the main synthase subunits, *bcsA* and *bcsB*. Variety in the remaining *bcs* genes has led to the classification of 3 distinct operon types defined by gene content (Römling & Galperin, 2015). Type one is distinguished by the presence of *bcsD*, which is responsible for forming a huge pore located in the periplasm that directs glucan chains to the outer membrane (Römling & Galperin, 2015). Type two has no *bcsD*, but has both *bcsE* and *bcsG*, which are thought to modify cellulose with phosphoethanolamine (pEtN) in the periplasm (Figure 5) (Thongsomboon *et al.*, 2018, Serra & Hengge, 2019, Römling & Galperin, 2015). Type three lacks *bcsD, bcsE,* and *bcsG*, but typically encode a cellulase, *bcsZ*, and *bscK*, which is thought to interact with the peptidoglycan to organize polysaccharide (Römling & Galperin, 2015). *V. fischeri* contains a type two *bcs* operon (Figure 5)- and is most similar to the operons in *E. coli* and *Salmonella* spp. (Römling & Galperin, 2015).

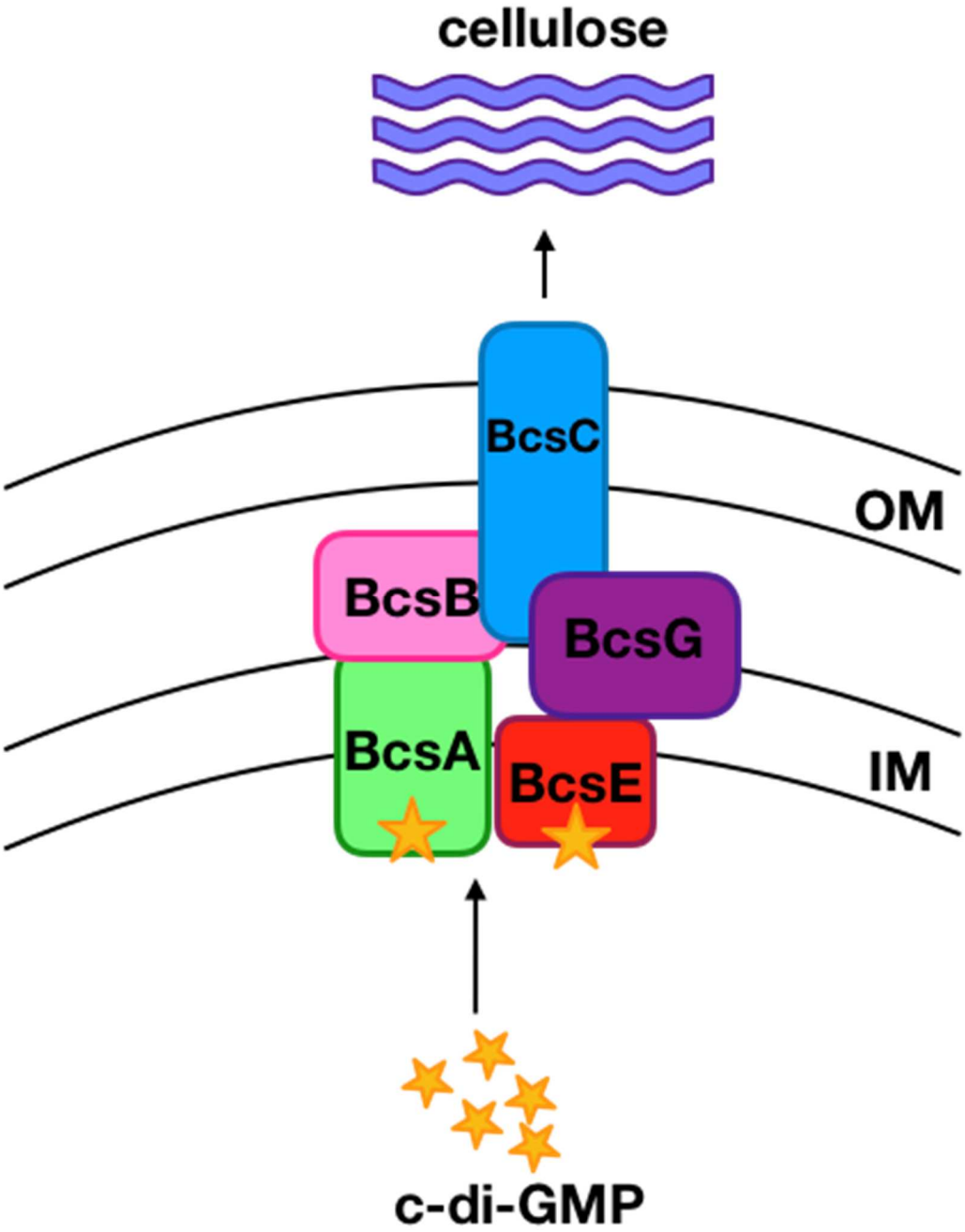

Figure 5. Generalized Cellulose Synthesis Complex. Adapted from Romling and Galperin 2015. BcsA and BcsB are the main cellulose synthase subunits, synthesizing and exporting cellulose polysaccharide via BcsC. BcsA is allosterically activated by c-di-GMP. BcsE also binds c-di-GMP, and is thought to activate BcsG for post-synthesis modification of cellulose in the periplasm.

Cellulose has been studied quite extensively in both of these genera because cellulose and curli are the main components of *Salmonella* and *E. coli* biofilms (Zogaj *et al.*, 2001, Römling *et al.*, 2000, Serra *et al.*, 2013). These biofilms are characterized by their colors on Congo red agar and 3D structures that are characterized as "rdar" or *r*ed *d*ry *a*nd *r*ough (Römling, 2005, Serra *et al.*, 2013). Regulation of these biofilms begins in early stationary phase, via RpoS (σ^s)-dependent transcription factor CsgD (Römling *et al.*, 2000). CsgD controls regulation of both curli and cellulose, driving transcription of the curlin subunits *csgAB*, and *dgcC* (Römling *et al.*, 2000, Zogaj *et al.*, 2001, Simm *et al.*, 2004, Serra & Hengge, 2019). DgcC is the main DGC that provides the c-di-GMP that allows for allosteric activation of BcsA (Zogaj *et al.*, 2001, Brombacher *et al.*, 2006, Chan *et al.*, 2004). Until recently, the reason for the specificity of DgcC was unknown; however, it was recently determined that DgcC, and its partner PDE, PdeK, are able to directly interact with both each other and BcsB, providing a localized c-di-GMP source and sink for activation of BcsA (Richter *et al.*, 2020). This localization mechanism is likely to be widespread as a mechanism for DGC/PDE specificity. After activation of BcsA, and cellulose synthesis, BcsE binds c-di-GMP, likely activating BcsG to modify the nascent cellulose with pEtN (Serra & Hengge, 2019, Thongsomboon *et al.*, 2018, Fang *et al.*, 2014). This newly described modification seems to be required for proper functioning polysaccharide, as unmodified fibers are short, thin, and curled, compared to long, thick, pEtN-cellulose filaments (Thongsomboon *et al.*, 2018). pEtN-cellulose has been likened to "steel" as a building material, allowing for strong cohesion paired with remarkable elasticity to produce complex 3-D architecture in microcolonies (Serra *et al.*, 2013, Serra & Hengge, 2019). Overall, cellulose is a diverse polysaccharide produced by many bacteria, and a hallmark of cellulose production is activation by c-di-GMP, minimally through allosteric activation of BcsA.

Summary

Any discussion of either biofilm formation or c-di-GMP has to include the other, as these concepts go hand-in-hand. The general mechanics of biofilm formation are well understood compared to current knowledge about c-di-GMP, and future research will likely strengthen these connections. At the most basic level, high c-di-GMP is able to induce biofilm formation through any number of mechanisms including attachment, gene expression, and polysaccharide synthesis. Environmental cues and signals can induce c-di-GMP production by DGCs or stop degradation by PDEs, and is one way that bacteria can respond to environmental signals to promote biofilms.

***Vibrio fischeri-Euprymna scolopes* Symbiosis**

Introduction

In nature, some organisms form mutually beneficial symbioses, with each organism providing a net positive benefit for the other. The mutualistic symbiotic relationship between *V. fischeri* and the invertebrate squid host *Euprymna scolopes* is a well-established model for microbe-host interactions. The *Vibrio*-squid colonization model provides tremendous scientific insight due, in part, to the ability of researchers to easily assess both partners, both separately and together. *V. fischeri* is a highly genetically tractable organism that is readily grown, maintained, and manipulated in the laboratory environment (Visick *et al.*, 2018, McFall-Ngai, 2014, Visick *et al.*, 2021, McFall-Ngai & Bosch, 2021). Many host-relevant phenotypes have been well defined for *V. fischeri*, including motility, chemotaxis, biofilm formation, and luminescence. Adult *E. scolopes* can be maintained and bred over a period of months in seawater (real or artificial) in tanks in a laboratory environment. Juvenile squid hatch free of *V. fischeri* symbionts, and colonization can occur quickly, in as little as 15 minutes under laboratory conditions (Bongrand *et al.*, 2016). Colonization dynamics can be monitored through techniques such as bacterial

enumeration, luminescence, RNAseq, and microscopy. These techniques illuminate the squid's response to bacterial colonizers, from alterations in gene transcription, to physical remodeling of the symbiotic organ. As *V. fischeri* is the exclusive colonizer of *E. scolopes's* symbiotic (light) organ, this model is primed to assess specific colonization requirements and factors for both partners. In this section, I will detail the dynamics of both the symbiont and host during symbiosis to demonstrate the interdependency of these organisms and the variety of behaviors required by *V. fischeri* for successful symbiosis.

Initiation

The initiation of a mutualistic symbiosis is the start of a life-long partnership that begins with both bacterial recruitment and restriction by the host, active bacterial engagement via aggregation (biofilm formation), and subsequent movement into the host's symbiotic light organ.

Recruitment and Restriction of Bacteria by the Host. Juvenile squid hatch free of *V. fischeri* and must acquire this symbiont from the seawater environment (Wei & Young, 1998). The squid pulls bacteria-containing seawater into its mantle cavity, across the symbiotic light organ, and then out through a funnel during ventilation (Figure 6) (Nyholm & McFall-Ngai, 2004). *V. fischeri* may represent as little as 0.01% of the local bacterial population, yet it is able to successfully and exclusively colonize the host (Nyholm & McFall-Ngai, 2004). Although the factors that control this specificity have yet to be fully elucidated, current evidence indicates that both squid and bacteria actively employ strategies to ensure *V. fischeri* is the exclusive symbiont.

The surface of the bilobed uncolonized light organ includes two sets of ciliated appendages that serve important functions in actively recruiting bacteria (Figure 6) (Nyholm & McFall-Ngai, 2004). Two types of cilia, long (~25 μm) and short (~10 μm), adorn the appendages, ultimately working together to create a flow that draws in smaller particles or

organisms (<4 μm) to a sheltered zone near the entry pores and moves larger particles (>4 μm) away from the light organ entrance (Nawroth *et al.*, 2017). This generalized size sorting mechanism allows the squid to actively recruit small bacterial species like *V. fischeri* (1 μm) to the sheltered zone. In the sheltered zone, the bacteria encounter an environment full of signaling, specificity, and effector molecules provided and sensed both by the host and symbiont (Nawroth *et al.*, 2017). Furthermore, the ciliated epithelial tissue on the light organ surface actively secretes mucus, starting within 1-2 hours after hatching (Nyholm & McFall-Ngai, 2004). Mucus secretion can be triggered by bacteria or by the bacterial product peptidoglycan (PG) alone, suggesting this response is a general bacteria-sensing mechanism, rather than a specific strategy to identify *V. fischeri* (Nyholm & McFall-Ngai, 2004).

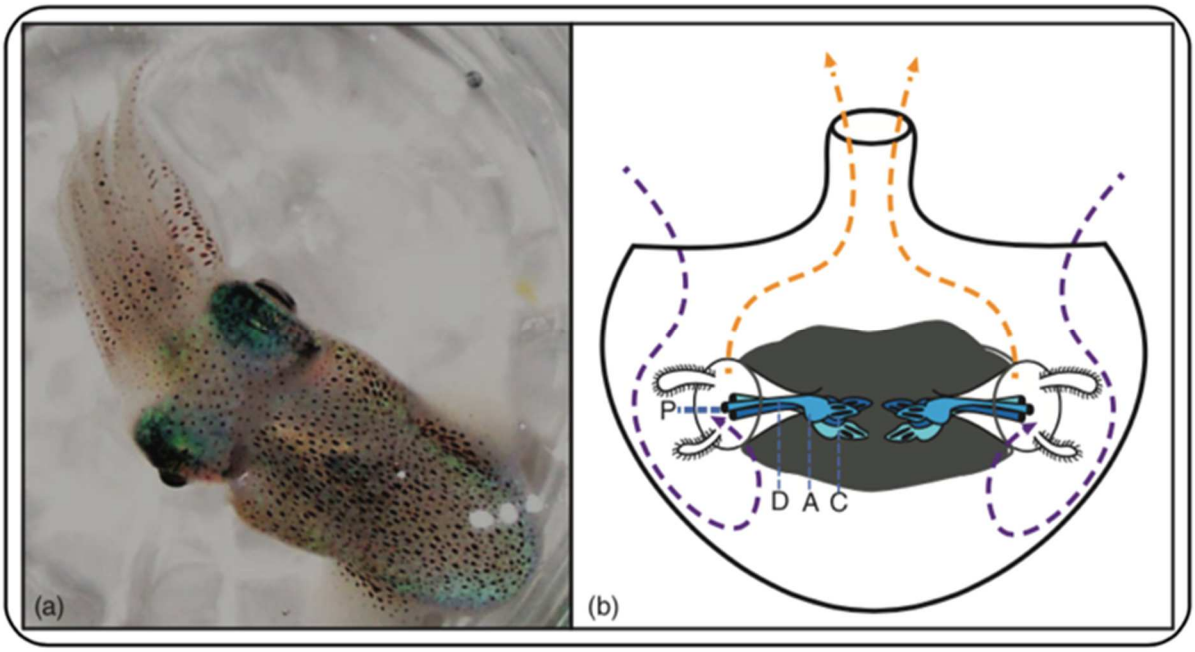

Figure 6. Anatomy of *Euprymna scolopes*. From Tischler *et al*. 2019, created by Dr. Kelsey Hodge-Hanson. (a) Photograph of an adult *E. scolopes*. (b) Cartoon of the central body (mantle) cavity of an immature juvenile *E. scolopes* depicting the symbiotic light organ and the water flow that is important for *V. fischeri* to colonize the squid (inspired by Nyholm *et al*., 2002). Ciliated epithelial appendages present on both halves of the organ help direct bacteria in the seawater towards sheltered zones located near the pores. Each of the six pores (P) leads to a separate duct (D), antechamber (A) and deep crypt region (C).

One well-studied factor in the mucus is nitric oxide (NO), a small, diffusible molecule involved in eukaryotic cell signaling and innate immunity (Wang & Ruby, 2011). During colonization, NO acts as an antimicrobial molecule, restricting aggregation of both symbiotic and non-symbiotic *Vibrio* spp. within the host mucus (Davidson *et al.*, 2004). *V. fischeri* responds to NO signals through the NO-responsive proteins HnoX and NsrR, altering iron metabolism and inducing detoxification pathways, respectively, presumably to prepare the bacteria for later stages of colonization (Davidson *et al.*, 2004, Wang & Ruby, 2011). Counterintuitively, NO can also have a negative effect on symbiosis. Strains lacking *hnoX*, and therefore the ability to sense

NO, form larger symbiotic aggregates and outcompete wild-type (WT) bacteria for colonization (Thompson *et al.*, 2019, Wang & Ruby, 2011). Once colonized, *V. fischeri* releases two molecules, a derivative of PG called tracheal cytotoxin (TCT), and lipopolysaccharide (LPS), which signal *E. scolopes* to reduce NO production (Altura *et al.*, 2011). This interplay between host and symbiont sensing and signaling highlights the importance of NO as a specificity factor for successful colonization.

Biofilm Formation Promotes Colonization. Despite the inhospitable composition of the squid's mucus, *V. fischeri* successfully initiates symbiotic colonization by first binding to the cilia, then forming an aggregate in the mucus on the surface of the light organ (Figure 7) (Altura *et al.*, 2013, Nyholm *et al.*, 2000). Evidence indicates that this aggregate represents a form of biofilm, a protected microbial community embedded in excreted matrix components such as polysaccharides, nucleic acids, and proteins (Nyholm *et al.*, 2000, Yip *et al.*, 2006, Flemming & Wingender, 2010). Biofilm-defective *V. fischeri* strains unable to make the symbiosis polysaccharide (SYP) cannot form symbiotic aggregates or proficiently colonize *E. scolopes* (Yip *et al.*, 2006). Additionally, hyper-biofilm forming strains demonstrate a colonization advantage (Bongrand & Ruby, 2018, Yip *et al.*, 2005, Yip *et al.*, 2006). Thus, biofilm formation is a key mechanism *V. fischeri* employs to initiate symbiosis.

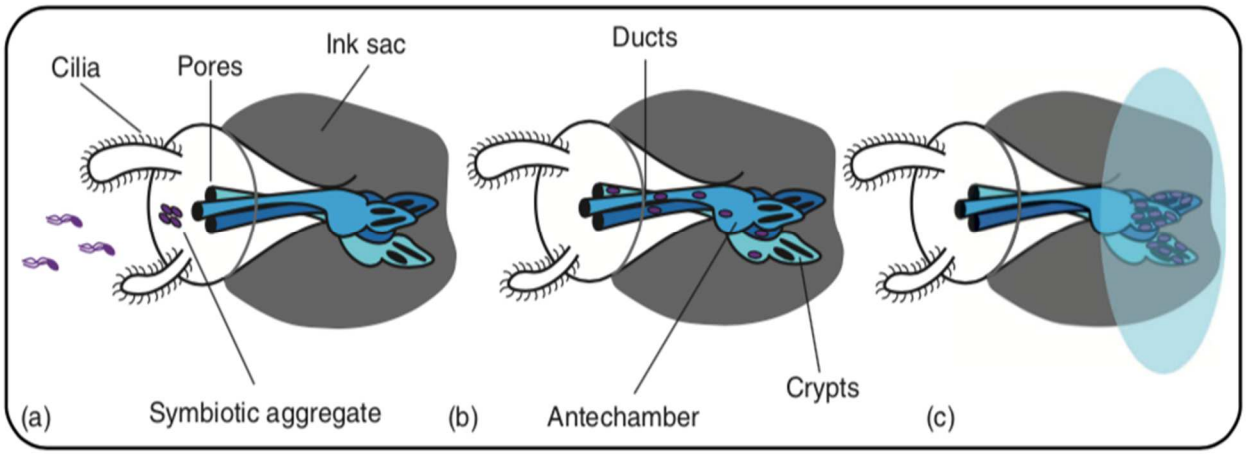

Figure 7. Initiation of the *Vibrio*-Squid Symbiosis. From Tischler *et al*. 2019, created by Dr. Kelsey Hodge-Hanson. Cartoon of the earliest stages of symbiotic colonization of one lobe of the light organ. (a) Planktonic *V. fischeri* (purple ovals) are swept toward the light organ by the ciliary action of the appendage surface. The bacteria form a symbiotic aggregate, or a biofilm, at the entry pores leading into the light organ. Although bacterial flagella (represented by wavy purple lines) are not required for aggregate formation, motility is required for colonization. (b) The cells disperse from the aggregate to enter a pore, traverse through the corresponding duct and antechamber, and ultimately reach the deep crypt region. The six crypts may be colonized by distinct strains of *V. fischeri*. (c) In the crypts, the *V. fischeri* population grows until a quorum is reached that induces bioluminescence (translucent blue oval).

V. fischeri exerts extensive control over biofilm formation through a complex network of regulators that ultimately control production of SYP, presumably to ensure that it occurs at the proper time and place (Stabb & Visick, 2013, Visick *et al.*, 2021). Much of the control occurs at the level of transcription of the *syp* locus, which directs SYP production, although at least one regulator post-transcriptionally controls SYP (Stabb & Visick, 2013). Most of these regulators are classified as two-component systems, comprised of sensor kinases (SK) and response regulators (RR) that allow bacteria to sense and respond to the environment. For example, the SK RscS promotes robust biofilm formation in laboratory culture, and is necessary for both symbiotic aggregation and colonization (Visick & Skoufos, 2001, Yip *et al.*, 2006). Another SK, BinK, appears to negatively regulate the same processes (Pankey *et al.*, 2017, Brooks & Mandel,

2016). Bacterial aggregation, and biofilm formation will be explored in more depth in subsequent sections.

Dispersal and Movement into the Light Organ. The aggregated bacteria must transition to a planktonic lifestyle to enter the light organ through one of six pores as individual cells (Figure 7). While the mechanism of bacterial dispersal from the aggregate is yet unknown, flagella-based motility and chemotaxis direct movement towards the pores (Nyholm *et al.*, 2000, Mandel *et al.*, 2012). Motility in *V. fischeri* is mediated by a polar tuft of 1-7 flagella (Ruby & Asato, 1993, Millikan & Ruby, 2002). Non-flagellated and hyper-flagellated mutants both fail to colonize the squid, indicating proper flagellation and/or propulsion is crucial for colonization (Millikan & Ruby, 2002).

A chemotaxis gradient guides *V. fischeri* through the entry pores leading into the light organ. *In vitro, V. fischeri* chemotaxes to a variety of substrates, including *N*-acetylglucosamine (GlcNAc), a monosaccharide derivative of chitin (Wier *et al.*, 2010, Mandel *et al.*, 2012). In the squid, the apical surfaces of the ciliated epithelium contain chitin synthases that are concentrated around the pores (Kremer *et al.*, 2013). Farther inside (approximately 10-20 μm), the epithelial surface contains chitin derivatives like GlcNAc, likely generated by host chitotriosidase degradation of chitin (Kremer *et al.*, 2013). During colonization, the most probable chemoattractant is a disaccharide of two GlcNAc monomers (chitobiose); experimental addition of chitobiose to seawater disrupts the sugar gradient and *V. fischeri* entry into pores (Mandel *et al.*, 2012). The exchange of beneficial factors is a hallmark of mutualistic symbioses, and it is likely that additional molecules play a role in establishing this symbiosis.

Colonization

Once a *V. fischeri* cell reaches a pore, it travels through a narrow duct to reach the antechamber (Nyholm 2002). To colonize, the cell must survive the antechamber and passage through a bottleneck to reach deep crypt spaces. There, the environment facilitates metabolite exchange, sustains cellular growth, and signals for induction of luminescence. In part because the six pores each ultimately lead to a distinct crypt, multiple strains of *V. fischeri* can colonize a single light organ (Bongrand & Ruby, 2018, Visick *et al.*, 2021). Thus, both bacteria-bacteria and bacteria-host interactions contribute to a dynamic partnership.

Bioluminescence. *E. scolopes* does not require *V. fischeri* for viability (Claes & Dunlap, 2000), suggesting that the major contribution *V. fischeri* brings to the *Vibrio*-squid symbiosis is the bacteria's ability to bioluminesce. Beginning 12 hours after initial colonization, bioluminescence is thought to benefit the host via a method of camouflage called counterillumination, in which bacterial light matches the downwelling moonlight to obscure the nocturnal squid's silhouette in shallow waters (Stabb & Millikan, 2009, Jones & Nishiguchi, 2004). *E. scolopes* modulates the direction and intensity of bacterial light (Jones & Nishiguchi, 2004, McFall-Ngai & Montgomery, 1990) through a muscle-controlled ink sac, a lens, and reflective proteins called reflectins in the tissues surrounding the light organ (Mandel & Dunn, 2016, Montgomery & McFall-Ngai, 1992). The squid's ability to regulate light is essential to adapt to changing environmental conditions such as lunar status or cloud cover.

Light production is directed by the *lux* operon, which encodes the light-producing enzyme luciferase as well as enzymes that make substrates, recycle byproducts, and siphon metabolites from cellular processes for the light reaction (Reviewed in (Stabb *et al.*, 2008) and (Visick *et al.*, 2021). Activation of the *lux* operon is controlled by quorum sensing. Quorum

sensing enables bacterial populations to coordinate behavior using signaling molecules, or autoinducers (also termed pheromones), to induce gene expression dependent on the population density (Stabb *et al.*, 2008). This is crucial for group behaviors such as bioluminescence, for which light production by a single cell would be energetically wasteful. To control the *lux* pathway, LuxI produces the autoinducer *N*-3-oxohexanoyl-homoserine lactone (3-oxo-C6), which rapidly diffuses across the bacterial membrane to equilibrate autoinducer levels inside and outside the cells. With increasing density of the *V. fischeri* population, 3-oxo-C6 levels rise, permitting this molecule to bind to the *lux* activator LuxR. In turn, LuxR activates transcription of the *lux* genes, inducing bioluminescence. While the LuxI/LuxR interaction is considered to be the main bioluminescence inducer, two other quorum sensing systems (AinS/AinR and LuxS/LuxP/LuxQ) also regulate this pathway and provide a link to other environmental conditions (Miyashiro & Ruby, 2012, Stabb *et al.*, 2008).

V. fischeri must bioluminesce to support a successful, long-term colonization with *E. scolopes*. Mutants defective for luminescence initially colonize the host, but neither persist nor induce normal development of a mature host light organ (Visick *et al.*, 2000). Additionally, squid that are initially colonized with *lux* mutants can be recolonized with luminescent bacteria, indicating that the mutants may be unable to properly signal to the host that colonization has occurred (Koch *et al.*, 2014). Thus, light itself may signal to the squid that colonization has been achieved, perhaps through light-responsive phototransduction proteins (Chun *et al.*, 2008, Stabb & Visick, 2013, Mandel & Dunn, 2016). These data highlight the importance of light as a symbiotic commodity.

Bacterial Interactions in the Light Organ. Historically, colonization and symbiosis were studied almost exclusively with a single bacterial strain isolated from the *E. scolopes* light

organ: *V. fischeri* ES114. Interest in strain-level differences of *V. fischeri* prompted exploration of additional isolates, including those from symbiotic association with the pinecone fish, *Monocentris japonica*, as well as those collected from *E. scolopes* located in two distinct Hawaiian bays (Bongrand *et al.*, 2016). The best-studied pinecone fish isolate, MJ11, colonizes squid very poorly. Experiments to evolve MJ11 to colonize *E. scolopes* yielded strains with adapted colonization factors, including altered bioluminescence (Pankey *et al.*, 2017). Understanding the changes that permit an isolate to become a better symbiont will provide needed insight into the most important symbiotic processes.

The study of diverse isolates from squid has shown that strains of *V. fischeri* can compete with each other for space within the light organ. Comparative studies grouped these strains into two broad categories, dependent on their ability to share (S) or dominate (D) a single light organ crypt (Bongrand *et al.*, 2016). The presence of six separate crypts means that a single squid may be colonized with multiple S and/or D strains. The ability of both S and D strains to successfully colonize *E. scolopes* begs the questions: what differentiates S and D strains, and is there an evolutionary advantage for the persistence of both strain types in the environment? Sequence comparisons showed a highly conserved core genome, and ~200 open reading frames exclusive to D strain genomes that are likely responsible for the dominance phenotypes (Bongrand *et al.*, 2016). Phenotypic characterization of D strains revealed an increased aggregate size, accelerated time to aggregate formation, and speedier entrance into the light organ (Koehler *et al.*, 2018, Bongrand & Ruby, 2018). However, aggregate size did not fully correlate with relative success, so it is unlikely that hyper-aggregation is exclusively responsible for dominance (Bongrand & Ruby, 2018). Instead, dominance is likely multi-factorial, mediated by mechanisms that represent ecologically exploitative tactics in colonization.

Indeed, some *V. fischeri* strains gain a colonization advantage mediated by an interference mechanism using a Type VI Secretion System (T6SS) (Speare *et al.*, 2018). T6SSs promote contact-dependent killing using molecular syringes that translocate toxins directly into target bacteria, while sister bacteria are protected by the cognate anti-toxin gene (Speare *et al.*, 2018). Whereas all known *V. fischeri* strains contain a T6SS (T6SS1), lethal strains of *V. fischeri* encode a second T6SS (T6SS2) that permits killing of non-lethal strains. Furthermore, not all lethal strains contain the same toxin/anti-toxin pairs, meaning that lethal strains can kill each other (Speare *et al.*, 2018). As of yet, the utility of T6SS1 is unknown, but it may be used to interact with eukaryotic cells or ensure mono-colonization by *V. fischeri*. The classification of lethal strain-types does not fully correlate with the D group classification (Bongrand & Ruby, 2018), supporting the idea that *V. fischeri* strains employ diverse strategies to become successful colonists.

Persistence

The intimate association between microbe and host is sustained over the lifetime of the host. However, rather than the static association found in some symbioses, the *V. fischeri*-squid symbiosis is dynamic, impacted both by developmental events early in the symbiosis and by daily fluctuations that occur throughout the course of the symbiosis.

Bacterial Changes During Colonization. Once inside the light organ, *V. fischeri* cells undergo two distinct morphological changes within 24 hours. First, there is a reduction in cell size that may reflect a cellular response to the specific environmental growth conditions (Ruby & Asato, 1993). In support of this possibility, *V. fischeri* released from the light organ after 24 hours exhibit a lag in growth in laboratory medium not seen when they are released at an earlier time (Ruby & Asato, 1993). Second, the tuft of polar flagella is lost (Ruby & Asato, 1993).

Presumably, the flagella are unnecessary and perhaps even detrimental once the bacteria have reached the crypts and achieved a high cell density. Once released from the squid, non-motile *V. fischeri* can rapidly regrow their flagella (~45-60 minutes) (Ruby & Asato, 1993). The signal(s) and mechanism(s) that control these events are unknown, although magnesium is required for flagellation of *V. fischeri* (Stabb & Visick, 2013). Because magnesium is plentiful in seawater, the squid may restrict magnesium as a way to control symbiont flagellation.

Host Responses- Immunity and Maturation. Like other invertebrates, *E. scolopes* has an innate immune system, with hemocytes serving as the primary component (Castillo *et al.*, 2009). Hemocytes are phagocytic cells, generally associated with pathogen control, but also play key roles during interactions with beneficial microbes. *E. scolopes* contains a single morphological type of circulating hemocyte found throughout the squid, including the blood, light organ crypts, and sinuses of the ciliated epithelium (Nyholm & McFall-Ngai, 1998, Koropatnick *et al.*, 2004). Bacterial colonization induces changes in hemocyte transcript and protein expression, indicating a specific host response to symbiont activity and bacteria-host communication (Collins *et al.*, 2012, Schleicher *et al.*, 2014). These hemocytes play at least three critical roles in sustaining the symbiosis. First, bacterial growth is supported by hemocyte-supplied chitin (Schwartzman *et al.*, 2015). Second, bacteria-derived molecules provide signals for hemocyte recruitment and trafficking to deliver information for light organ maturation (Koropatnick *et al.*, 2007, Altura *et al.*, 2013). Third, phagocytic activity associated with hemocytes likely contributes to the exclusivity of the symbiosis; in contrast to other species, which are readily engulfed, *V. fischeri* cells bind poorly to hemocytes and are thus protected from phagocytosis (Nyholm *et al.*, 2009). This phenomenon depends on exposure to *V. fischeri*, as hemocytes from hosts lacking symbionts effectively engulf *V. fischeri* (Nyholm *et al.*, 2009).

One bacterial factor responsible for inhibiting phagocytosis is the outer membrane porin OmpU, as loss of this protein results in increased bacteria-hemocyte binding (Nyholm *et al.*, 2009).

In addition to an immune response, *V. fischeri* colonization provides signals that induce substantial structural remodeling of the juvenile light organ. Specifically, *V. fischeri* cells release microbe-associated molecular patterns (MAMPs), TCT and LPS, that synergistically trigger organ morphogenesis (Koropatnick *et al.*, 2004). TCT is thought to be released as a soluble molecule, whereas LPS is contained within outer membrane vesicles (OMVs) (Aschtgen *et al.*, 2016). The OMVs alone are sufficient to induce organ morphogenesis, and are generated by blebbing from rotating flagella before delivery to the host via hemocyte phagocytosis (Aschtgen *et al.*, 2016). Within hours of colonization, cells in the ciliated appendages detach and undergo apoptosis, or programmed cell death, ultimately resulting in regression of the appendages. Additional changes occur, including: attenuation of NO signaling, constriction of the ducts, cell swelling in the crypts, and cessation of mucus secretion (Nyholm & McFall-Ngai, 2004). Symbiont-induced maturation occurs rapidly in the first few days and is complete around four weeks post colonization, resulting in substantial and irreversible morphological changes (Montgomery & McFall-Ngai, 1998, Koch *et al.*, 2014). Symbiont-induced hemocyte trafficking to the ciliated epithelium marks the first step in morphogenesis, beginning as quickly as 2 hours after inoculation and peaking at 18 hours (Koropatnick *et al.*, 2007). Another factor that may contribute to development is cathepsin L, a cysteine protease that is associated with apoptosis in animals (Peyer *et al.*, 2018). During colonization, cathepsin L is present and active in cells, including symbiotic hemocytes, interacting with *V. fischeri* in the appendages and crypt spaces and is capable of inducing host-cell death (Peyer *et al.*, 2018, Schleicher *et al.*, 2014). These

critical developmental changes are precipitated by the presence of bacterial symbionts, demonstrating the importance of host-microbe interactions in many facets of animal biology.

Daily Rhythm. The stable, long-term symbiotic relationship between *V. fischeri* and *E. scolopes* is dynamic in nature, with daily changes occurring on a diel rhythm, based on a light/dark cycle (Nyholm & McFall-Ngai, 1998, Boettcher *et al.*, 1996). Every day at dawn, ~90% of the symbionts are expelled from the light organ by a muscle-induced contraction, and the remaining 5-10% of bacterial cells rapidly grow to repopulate the crypts (Nyholm & McFall-Ngai, 1998). The interiors of the host crypts are effaced during this process, and the expulsion products consist of a toothpaste-like gel containing bacteria and host cells along with acellular matrix material (Nyholm & McFall-Ngai, 1998, Wier *et al.*, 2010, Graf & Ruby, 1998). This process of growth and expulsion repeats daily in response to light throughout the lifetime of a colonized squid.

The long-term dynamic equilibrium between both symbiotic partners is anchored in metabolism. Just after dawn in the early hours after expulsion, the bacteria use the available resources—primarily amino acids and glycerophospholipids—to quickly repopulate the light organ with a generation time of approximately 30 min (Ruby & Asato, 1993, Graf & Ruby, 1998). Expression of genes utilized in glycerol metabolism is increased just after dawn, and symbiotic bacteria have altered lipid profiles compared to lab-grown bacterial cells, suggesting incorporation of glycerophospholipids (Wier *et al.*, 2010). At night, the bacterial population reaches a quorum, and chitin utilization becomes critical, with chitin catabolism genes highly expressed before dawn (Schwartzman *et al.*, 2015, Wier *et al.*, 2010). In parallel, lysed hemocytes, a key source of chitin, are present in the light organ at night, and transcripts of the chitin-synthesizing enzyme chitotriosidase are elevated (Schwartzman *et al.*, 2015). Utilization

of chitin at night acidifies the surrounding tissues, which subsequently release oxygen molecules from hemocyanin carriers (Schwartzman *et al.*, 2015). Oxygen is the limiting reagent for luciferase activity in the light organ, and it is likely that luminescence is controlled via oxygen availability; bioluminescence peaks immediately after expulsion into oxygen-replete seawater (Stabb & Visick, 2013, Boettcher *et al.*, 1996, Miyashiro & Ruby, 2012). Levels of luminescence continue to fluctuate based on the daily diel rhythm (Boettcher *et al.*, 1996), mirroring variations in host-provided nutrients and bacterial metabolism to create a dynamic, yet stable, symbiosis.

Conclusions

The *Vibrio*-squid symbiosis provides an excellent model for studying microbial interactions with animal tissues. The specificity of the association, genetic tractability of the bacteria, and dynamic nature of the symbiosis has led to a model in which bacterial behaviors may be easily investigated in the laboratory and efficiently evaluated during colonization. This experimental pipeline lays a solid foundation to deeply explore communication and complex factors within the bacteria-squid partnership. As with numerous organisms, including humans, the squid's association with bacteria is integral to animal biology. Each aspect of the colonization process builds toward an exquisite match between a squid and a bioluminescent bacterium.

Biofilm Formation by *V. fischeri*

Introduction

Biofilms are the natural state of living for the majority of bacteria, both in the environment, and in the context of a host (Flemming & Wuertz, 2019). The *V. fischeri*-*E. scolopes* model is a natural model to study host-associated biofilms (Nyholm & McFall-Ngai, 2021, McFall-Ngai & Bosch, 2021), as bacteria aggregate on the surface of the light organ during the colonization process (Nyholm *et al.*, 2000). Bacterial aggregation is directly related to

colonization, as bacterial strains defective for biofilm formation are unable to colonize, while hyper-aggregating strains have a colonization advantage (Yip *et al.*, 2005, Yip *et al.*, 2006, Bongrand *et al.*, 2016, Bongrand & Ruby, 2018, Koehler *et al.*, 2018, Morris & Visick, 2013, Thompson *et al.*, 2019). While squid-isolated strains, including our WT strain, ES114, readily form biofilms in the context of a host, biofilm formation in the laboratory requires overexpression to induce biofilm formation. *V. fischeri* is known to induce two separate types of biofilms, one dependent on the symbiosis polysaccharide, SYP, and the other dependent on cellulose polysaccharide (Yip *et al.*, 2006, Bassis & Visick, 2010). SYP is well characterized compared to cellulose as a biofilm component. In this section, I will describe the different types of biofilms induced by *V. fischeri,* and what is known about how these biofilms are formed and regulated.

SYP-Dependent Biofilm Formation

The main polysaccharide that contributes to biofilm formation by *V. fischeri* is the symbiosis polysaccharide (SYP). Control of SYP occurs at multiple levels, including transcription of the 18 gene *syp* locus, which encodes proteins predicted to produce and export SYP, and at a yet unknown post-transcriptional level (Shibata *et al.*, 2012, Yip *et al.*, 2006, Visick & Ruby, 2006, Morris *et al.*, 2011). Perhaps because if its importance, *syp* has a high level of regulation, including at multiple levels with numerous regulators (Figure 8) (Visick *et al.*, 2021). The first identified regulator was RscS, an orphan SK, which was hypothesized to be acquired through horizontal gene transfer, and is required for symbiotic aggregation (Visick & Skoufos, 2001, Yip *et al.*, 2006, Mandel *et al.*, 2009, Ludvik *et al.*, 2021). Overproduction of RscS has historically been an excellent tool to induce biofilm formation at the bench. Similar in structure to RscS is the SK SypF, which contains HisKA, REC, and Hpt domains (Norsworthy &

Visick, 2015). While both RscS and SypF contain Hpt domains, the Hpt domain of RscS is dispensable for biofilm formation and a phenotype has yet to be found which requires this domain (Geszvain & Visick, 2008); however, SypF-Hpt is required, and sufficient, for RscS induced *syp* transcription, and subsequent biofilm formation (Norsworthy & Visick, 2015). RscS and SypF induce *syp* transcription dependent on the direct transcriptional activator, SypG (Yip *et al.*, 2005, Hussa *et al.*, 2007, Ray *et al.*, 2013). Despite being the direct activator, overproduction of SypG alone is insufficient to produce biofilm phenotypes, and requires simultaneous deletion of the gene for RR SypE (Hussa *et al.*, 2008, Morris & Visick, 2013). SypE is both a strong negative and positive regulator, with a N-terminal serine kinase domain that inhibits biofilm formation, and C-terminal serine phosphatase domain that promotes biofilm formation, and a central REC domain (Morris *et al.*, 2011, Morris & Visick, 2013). SypE is also able control activation of SypA through phosphorylation, and although SypA is required post-transcriptionally for biofilm formation, its exact role is not yet clear (Morris & Visick, 2013, Thompson & Visick, 2015).

Within the last few years, the novel *syp* regulator BinK has been identified as a strong negative regulator of *syp* transcription and subsequent biofilm formation (Brooks & Mandel, 2016, Pankey *et al.*, 2017). Strains lacking BinK form larger aggregates *in vivo*, but the *in vitro* effects of a *binK* mutation required RscS overproduction (Brooks & Mandel, 2016). While a *binK* mutant strain has a colonization advantage, a *rscS* mutant strain is deficient for colonization; however, recent work has identified that a *binK rscS* double mutant strain is competent to initiate squid colonization, which marks the first time a strain lacking RscS has been seen to colonize squid (Ludvik *et al.*, 2021). While both *binK* single and *binK rscS* double mutant strains could colonize, a competition experiment revealed the strain lacking RscS was

significantly outcompeted, suggesting a phenotype for RscS, and possibly SYP, after initial aggregation, during later stages of symbiosis (Ludvik *et al.*, 2021).

Another component of SYP-dependent biofilms are the Bmp proteins (Ray *et al.*, 2015). A combination of SYP and Bmp is responsible for creating the wrinkles indicative of wrinkled colony formation (Ray *et al.*, 2015). Wrinkled colonies lacking Bmp are smooth looking, but when disrupted with a toothpick are cohesive, indicative of SYP (Ray *et al.*, 2015).

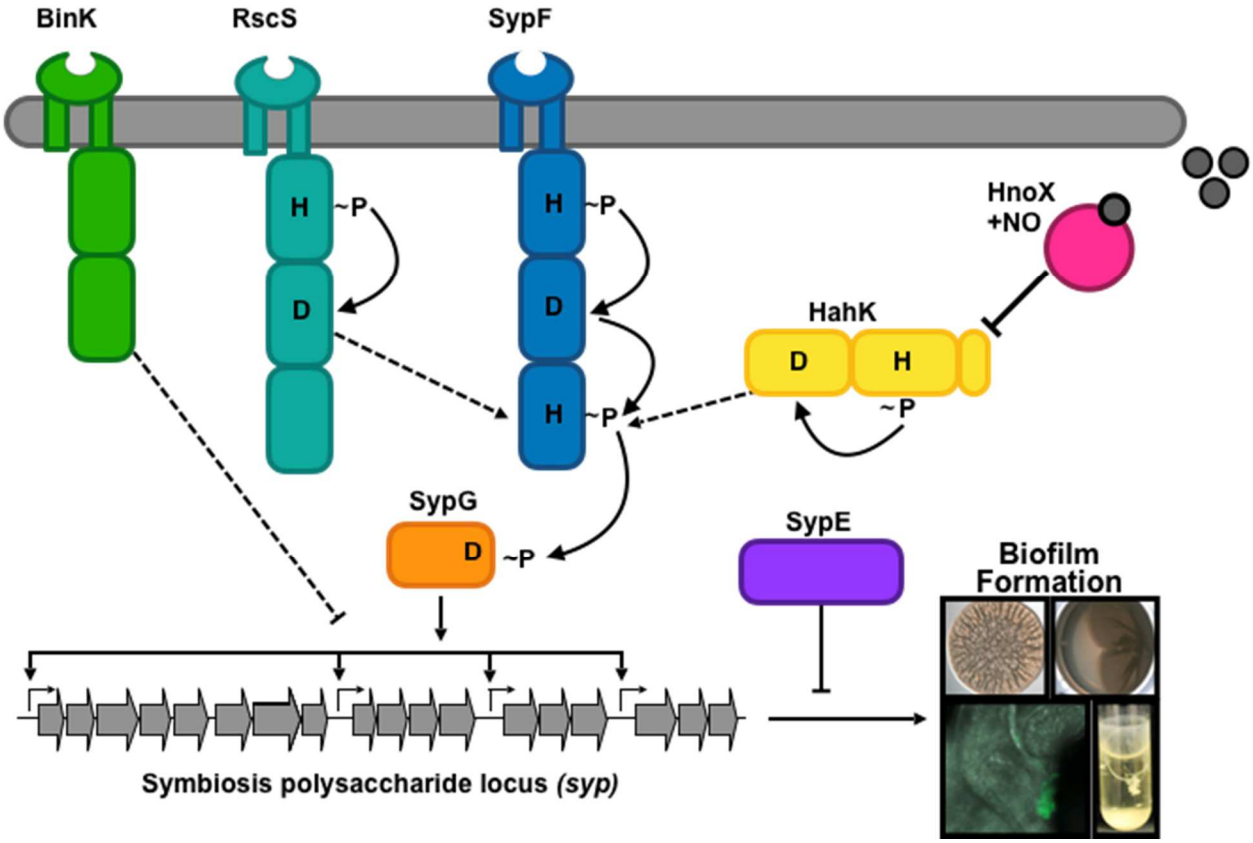

Figure 8. Model of Regulatory Control Over s*yp*-Dependent Biofilm Formation by *V. fischeri*. The hybrid sensor kinase RscS induces biofilm formation in a manner that depends on the *syp* locus and the *syp* regulators SypF and SypG. The activity of RscS requires the indicated conserved residues (H412 and D709) in RscS as well as the conserved histidine (H705) within the last (Hpt) domain of SypF but not the conserved histidine (H250) or aspartate (D549) in the HisKA and REC domains of SypF. SypF donates phosphoryl groups to both the response regulator SypG, the direct activator of the *syp* locus, and to the response regulator SypE, which controls *syp*-dependent biofilm formation at a level below *syp* transcription. BinK functions as a negative regulator of *syp*-dependent biofilm formation, at least in part due to the inhibition of *syp* transcription. HnoX is activated by NO and inhibits HahK, which activates *syp* transcription through the Hpt domain of SypF.

Cellulose-Dependent Biofilm Formation

The first connection between *V. fischeri* and cellulose polysaccharide was discovered in relation to VpsR, where a SypF variant, SypF1, was able to induce both SYP and cellulose-dependent phenotypes, dependent on SypG and VpsR, respectively (Darnell *et al.*, 2008). This

put into new perspective earlier data showing that a *vpsR* mutant strain was outcompeted by WT for colonization (Hussa *et al.*, 2007). Shortly after, investigation of c-di-GMP via the PDE BinA revealed that a *binA* mutant exhibited a very strong cellulose-dependent phenotype (Bassis & Visick, 2010). Interestingly, *binA* is located just downstream of the *syp* locus, which is not located near the *bcs* locus, and BinA seemed to have no impact on SYP. It was revealed that BinA functioned to change the c-di-GMP levels within the cell, and while it contains both an EAL and GGDEF domain, the GGDEF domain is degenerate (Figure 4), and does not seem to be catalytically active (Bassis & Visick, 2010). Overall, these data identify cellulose as a polysaccharide that contributes to biofilm formation by *V. fischeri*, and identifies both a positive (VpsR) and negative (BinA) regulator (Figure 9).

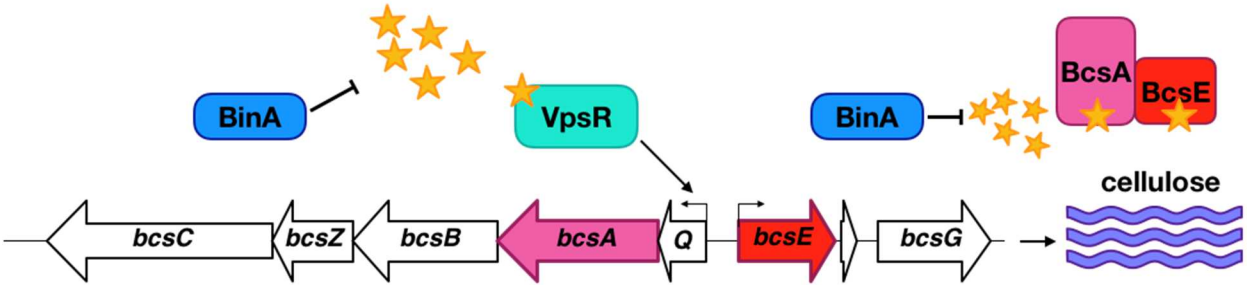

Figure 9. Model for Regulation of Cellulose-Dependent Biofilm Formation. VpsR and BinA are positive and negative regulators of cellulose, respectively. This is one model of how these regulators could be impacting cellulose. BinA is a PDE which negatively regulates cellulose, and this could occur transcriptionally or post-transcriptionally.

Summary

Biofilm formation by *V. fischeri* is a complicated process that involves numerous polysaccharides, proteins, and is controlled by a network of regulators. As a highly tractable genetic organism, and a model for symbiont-host biofilm formation, *V. fischeri* is an ideal organism with which to explore biofilm formation. Many regulators have been identified, but

many more questions remain, including the ability to produce biofilms *in vitro* in our WT strain, ES114. Future studies will be sure to shed more light on the dynamic process of biofilm formation by *V. fischeri*

CHAPTER TWO

MATERIALS AND METHODS

Bacterial Strains and Media.

V. fischeri strains used in this study are listed in Table 1, plasmids in Table 2, and primers in Table 3. All strains used in this study were derived from strain ES114, a bacterial isolate from *Euprymna scolopes* (Boettcher & Ruby, 1990). *Escherichia coli* strains TAM1 (Active Motif), TAM1 λ *pir* (Active Motif), DH5∝, π3813 and GT115 were used for cloning and plasmid maintenance (Le Roux *et al.*, 2007). For routine culturing, *V. fischeri* strains were grown in LBS (Graf *et al.*, 1994, Stabb *et al.*, 2001) and *E. coli* strains were grown in LB (Davis *et al.*, 1980), in some cases supplemented with thymidine. For TfoX-mediated transformation (TT) of *V. fischeri*, Tris minimal medium (TMM) (100 mM Tris, pH 7.5, 300 mM NaCl, 0.1% ammonium chloride, 10 mM *N*-acetylglucosamine, 50 mM $MgSO_4$, 10 mM KCl, 10 mM $CaCl_2$, 0.0058% K_2HPO_4, 10 μM ferrous ammonium sulfate) was used. Soft-agar motility medium contained tryptone (1%), NaCl (2%), agar (0.25%), and $MgSO_4$ (35 mM), and $CaCl_2$ was added to indicated concentration. Antibiotics were added as appropriate at the following final concentrations: ampicillin (Amp), 100 μg ml^{-1}; chloramphenicol (Cm), 1 μg ml^{-1}; erythromycin (Em), 2.5 μg ml^{-1} (*V. fischeri*) or 150 μg ml^{-1} (*E. coli*); kanamycin (Kn), 100 μg ml^{-1} (*V. fischeri*) or 50 μg ml^{-1} (*E. coli*); tetracycline (Tet), 2.5 μg ml^{-1}; trimethoprim (Trim), 10 μg ml^{-1}; spectinomycin (Sp), 200 μg ml^{-1}; and gentamicin (Gen), 5 μg ml^{-1}. For Sp and Gen, LB was used as the medium instead of LBS for outgrowth and plating.

Molecular Techniques and Strain Construction

Mutations in ES114 were generated through TfoX-mediated transformation (TT) (Pollack-Berti *et al.*, 2010, Brooks *et al.*, 2014, Christensen *et al.*, 2020b, Cohen *et al.*, 2021). Briefly, ~500 bp segments upstream and downstream of genes of interest were PCR amplified using high fidelity KOD polymerase (Novagen, EMD Millipore), and PCR SOE (Splicing by Overlap Extension (Horton *et al.*, 1989) was used to fuse segments to an antibiotic cassette as described previously (Visick *et al.*, 2018). The fused product was amplified and transformed into the recipient *V. fischeri* strain (typically ES114) carrying a TfoX-overproducing plasmid (plostfoX (Brooks *et al.*, 2014), plostfoX-Kan (Brooks *et al.*, 2014), or pJJC4 (Cohen *et al.*, 2021)), and recombinant cells were selected on media containing the appropriate antibiotic. The allelic replacement was confirmed by PCR with outside primers using Promega *Taq* polymerase (Table 3). After the initial deletion was made, genomic DNA (gDNA) was isolated from the recombinant strains using the Quick-DNA Miniprep plus kit (Zymo Research) and used to introduce the mutation into other desired strain backgrounds. Insertion at the Tn*7* site was performed via tetraparental mating (McCann *et al.*, 2003) between the *V. fischeri* recipient and three *E. coli* strains, carrying the conjugal plasmid pEVS104 (Stabb & Ruby, 2002), the Tn*7* transposase plasmid pUX-BF13 (Bao *et al.*, 1991), and relevant donor plasmid. Insertions were also introduced adjacent to the Tn*7* site at the intergenic (IG) region between *yeiR-glmS* as previously described (Visick *et al.*, 2018). These insertions were made using the PCR amplification and SOE method described above, with genes of interest fused to an upstream Erm^r cassette for selection, driven by the constitutive P*ndrR* promoter, and containing an idealized ribosome binding site (RBS). In some cases, the antibiotic resistance cassette was removed from *V. fischeri* deletion mutants using Flp recombinase, which acts on FRT sequences to delete the

intervening sequences, as has previously been shown (Cherepanov & Wackernagel, 1995). Overexpression plasmids were constructed by amplifying genes of interest from the IG region of *V. fischeri* strains, and the resulting PCR product was ligated into the pJET1.2 blunt cloning vector (ThermoFisher), transformed into chemically competent *E. coli* DH5α, and selected using Amp. The resulting plasmids were purified using the Plasmid Miniprep kit (Zymo Research), sequenced (IDT), and transformed into chemically competent *E. coli* GT115 containing the pFY4535 biosensor where indicated.

Bioinformatics

Amino acid and DNA sequences were obtained from the National Center for Biotechnology Information (NCBI) database. Conserved protein domains and residues were identified using NCBI. Alignments were generated using BLAST and the Clustal Omega multiple-sequence alignment program from EMBL-EBI (https://www.ebi.ac.uk/Tools/msa/clustalo/) (Altschul *et al.*, 1990, Altschul *et al.*, 1997, Boratyn *et al.*, 2012, Madeira *et al.*, 2019).

Wrinkled Colony Formation Assay

To observe wrinkled colony formation, the indicated *V. fischeri* strains were streaked onto LBS agar plates. Single colonies were cultured with shaking in 5 ml LBS broth overnight at 28°C. The strains were then sub-cultured the following day in 5 ml of fresh medium. Following growth to early log phase, the cultures were standardized to an optical density at 600 nm (OD_{600}) of 0.2 using LBS. 10 µl of diluted cultures were spotted onto LBS agar plates and grown at 24°C. Images of the spotted cultures were acquired over the course of wrinkled colony formation at the indicated times using a Zeiss Stemi 2000-C dissecting microscope. At the end of the time course,

the colonies were disrupted with a toothpick to assess colony cohesiveness, which is an indicator of Syp-PS production (Ray *et al.*, 2015).

Pellicle Formation Assay

To assess pellicle formation, *V. fischeri* strains were grown overnight and sub-cultured with shaking as described above. Following growth to mid-log phase, the cultures were standardized to an optical density at 600 nm (OD_{600}) of 0.2 in 2 ml of LBS in a 24- well microtiter plate. Inoculated microtiter plates were sealed in a plastic bag and incubated statically at 24°C. Images of the microtiter wells were acquired over the course of pellicle formation at the indicated times using a Zeiss Stemi 2000-C dissecting microscope. At the end of the time course, the pellicles were disrupted with a toothpick to estimate pellicle strength.

C-di-GMP Biosensor Assay

Relative c-di-GMP levels were assessed in either LBS or LB broth at 24 or 28°C for *V. fischeri* and *E. coli*, respectively, and cultures inoculated from single colonies contained added calcium chloride as indicated. The biosensor was not selected using antibiotics as it contains a toxin/antitoxin system (Zamorano-Sánchez *et al.*, 2019), but Amp was used to select for overexpression plasmids in *E. coli* strains. Samples were diluted 1:1000 in phosphate-buffered saline (PBS) and assessed via flow cytometry on a LSRFortessa (BD Biosciences). Forward scatter (FSC) and side scatter (SSC) were collected in a log scale with a threshold of 200, and AmCyan and PE-TexasRed channels were used to measure AmCyan and RFP, respectively. Data were analyzed using FlowJo 10, gating first on live cells as determined by FSC and SSC, then AmCyan to confirm singlets, and finally RFP to assess relative c-di-GMP. This resulting population was used to create representative histograms, and the geometric mean fluorescence

intensity (MFI) of each curve was used to quantify and compare samples. Data were graphed using GraphPad Prism 6 and analyzed via linear regression or one-way ANOVA as indicated.

Motility Assay

Single colonies were inoculated in TBS. Cultures were grown overnight shaking at 28˚C, subcultured 1:100 in fresh broth, and incubated shaking until exponential growth phase. Cultures were normalized to a final OD_{600} of 0.2, and 10 µl aliquots were spotted on soft-agar motility plates supplemented with indicated concentrations of $CaCl_2$. Plates were incubated at 28˚C, and the diameter of each zone of migration was measured and imaged over time. Pictures were taken using an iPhone 7 camera.

Shaking Biofilm Assay

To assess calcium-induced biofilm formation under shaking liquid conditions, LBS broth containing between 10-100 mM calcium chloride (as indicated) was inoculated with single colonies of *V. fischeri* strains and grown with shaking overnight at 24°C. For these experiments only, test tubes (13 by 100 mm) were used with a culture volume of 2 ml LBS broth. For crystal violet staining, 200 µl of a 1% crystal violet solution was added to cultures for 30 min. Tubes were washed with deionized H_2O, and destained with ethanol. OD_{600} was measured suing a Synergy H1 microplate reader (BioTek). Pictures were captured via iPhone 7or 12 mini camera and data are representative of at least 3 independent experiments. Linear regression analysis was performed in GraphPad Prism 6.

Congo Red Assay

Bacteria were streaked onto LBS plates containing Congo red and Coomassie blue dyes (40 µg ml^{-1} and 15 µg ml^{-1}, respectively), and either 10 mM or 40 mM calcium as indicated, and grown overnight at 24°C. To better visualize color differences, cells were transferred onto

white paper in a replica plating-like approach by briefly smoothing the paper onto the agar plate and then lifting it off (Visick *et al.*, 2018). The result was photographed with an iPhone 7 or 12 mini camera.

β-galactosidase Assay

Strains carrying a *lacZ* reporter fusion to the *sypA, bcsQ* or *vpsR* promoter were grown in duplicate at 24°C in LBS containing calcium chloride as indicated. Strains were subcultured into 20 ml of fresh medium in 125-ml baffled flasks, and samples were collected after 22 h or 4 h of growth, or at time indicated. OD_{600} was measured and cells were resuspended in Z-buffer, and lysed with chloroform. The β-galactosidase activity of each sample was assayed as described previously (Miller, 1972) and measured using a Synergy H1 microplate reader (BioTek). Assays were performed at least 2 independent times and analyzed via a one-way ANOVA in GraphPad Prism 6.

GFP Reporter Assay

Strains of *V. fischeri* carrying a plasmid-based P*sypA- GFP* reporter were cultured overnight in duplicate in TMM. The next day, strains were subcultured; the strains were transferred into fresh media at an OD_{600} normalized to 0.05 and grown at 24°C for 3 h. The levels of *syp* transcription were measured over time using fluorescence (arbitrary units) per cell (per optical density (OD_{600})) as a read-out for transcription using a Synergy H1 microplate reader (BioTek). Fluorescence per cell was normalized to the background transcription induction of a biofilm-deficient strain, which is indicated by a dotted line. Graphed data are from at least three independent experiments. Error bars indicate standard deviation. The data were analyzed using a one-way ANOVA using Graphpad Prism 6.

Aggregation Experiments

Juvenile *E. scolopes* were collected within 12 h of hatching and incubated with approximately 3×10^6 bacteria containing GFP-encoding plasmid pVSV102 for three hours at room temperature in filter-sterilized instant ocean. Squid were anesthetized in 2% ethanol and dissected to expose the light organ using a Leica EZ4 stereomicroscope. Aggregates were visualized on a Zeiss AxioZoom V16 microscope and measured using Zeiss ZEN Blue software. Bacterial colonies from inoculum seawater samples were visualized to confirm the expression of GFP. The data were analyzed using a Mann-Whitney test on Graphpad Prism 6.

Western Immunoblotting

V. fischeri cells were grown overnight in LBS, and cultures were normalized to an OD_{600} of 1. One-ml aliquots were pelleted and lysed in 200 µl 2X sample buffer (4% SDS, 40 mM Tris, pH 6.3, 10% glycerol). Samples were loaded in two separate gels in tandem, and separated by SDS-PAGE (8% acrylamide). One gel was stained with Coomassie blue (40% MeOH, 10% acetic acid, 0.1% Coomassie Blue R250) as a loading control, destained (40% MeOH, 10% acetic acid) and imaged using FluorChem (ProteinSimple). The second gel was transferred to a polyvinylidene difluoride (PVDF) membrane. After blocking with dry milk in PBS-T (137 mM NaCl, 2.7 mM KCl, 4.3 mM Na_2HPO_4, 1.47 mM KH_2PO_4, and 0.05% Tween 20), the membrane was treated with rabbit anti-HA antibody (Sigma-Aldrich), followed by exposure to a secondary antibody, goat anti-rabbit IgG antibody (Fisher Scientific) conjugated to horseradish peroxidase. Finally, to visualize HA-tagged proteins, the membrane was incubated with Super-Signal West Pico plus chemiluminescent substrate (Thermo Fischer Scientific, Rockford, IL) visualized using a FluorChem E System (ProteinSimple, San Jose, California) or exposed to autoradiography film (Dot Scientific), which was developed in an autoprocessor.

Table 1. Strains Used in this Study

Strain	Genotype	Construction[1]	Source or Reference
ES114	WT	N/A	(Boettcher & Ruby, 1990)
KV1715	*vpsR*::pEAH11	N/A	(Hussa *et al.*, 2007)
KV3299	Δ*sypE sypF2*	N/A	(Hussa *et al.*, 2008)
KV4131	Δ*binA*	N/A	(Bassis & Visick, 2010)
KV4197	Δ*binA sypG*::pAIA4	N/A	(Bassis & Visick, 2010)
KV4203	Δ*binA sypC*::pBTG49	N/A	(Bassis & Visick, 2010)
KV4212	Δ*binA sypO*::pTMB55	N/A	(Bassis & Visick, 2010)
KV4567	attTn*7*::P*bcsQ-lacZ*	N/A	(Tischler *et al.*, 2018)
KV4607	Δ*binA bcsA*::Tn*5*	N/A	(Bassis & Visick, 2010)
KV4608	Δ*binA bcsC*::Tn*5*	N/A	(Bassis & Visick, 2010)
KV4611	Δ*binA bcsZ*::Tn*5*	N/A	(Bassis & Visick, 2010)
KV5367	Δ*sypF*	N/A	(Norsworthy & Visick, 2015)
KV6439	Δ*sypEF*	N/A	(Thompson *et al.*, 2018)
KV6567	Δ*sypE sypF2* Δ*sypG*	N/A	(Thompson *et al.*, 2019)
KV6576	IG (*yeiR-glmS*)::*lacI-Q*	N/A	(Ondrey & Visick, 2014)
KV7226	Δ*sypF* attTn*7*::*sypF*-HPT-FLAG	N/A	(Norsworthy & Visick, 2015)
KV7371	IG::P*sypA-lacZ*	N/A	(Norsworthy & Visick, 2015)
KV7410	IG (yeiR-glmS)::P*sypA-lacZ* attTn*7*::Em	N/A	(Norsworthy & Visick, 2015)

KV7485	Δ*sypF* attTn*7*::*sypF*-HPT-H705Q-FLAG	N/A	(Norsworthy & Visick, 2015)
KV7655	attTn*7*::*rscS*	N/A	(Tischler *et al.*, 2018)
KV7856	Δ*binK* Δ*sypE sypF2*	N/A	(Thompson *et al.*, 2018)
KV7860	Δ*binK*	N/A	(Tischler *et al.*, 2018)
KV7861	Δ*binK* Δ*rscS*	N/A	(Tischler *et al.*, 2018)
KV7862	Δ*binK* Δ*sypF*	N/A	(Tischler *et al.*, 2018)
KV7871	Δ*sypF* Δ*binK* attTn*7*::*sypF*-Hpt-H705Q-FLAG	N/A	(Tischler *et al.*, 2018)
KV7873	Δ*sypF* Δ*binK* attTn*7*::*sypF*-H705Q-FLAG	N/A	This study
KV7875	Δ*sypF* Δ*binK* attTn*7*::*sypF*-H250Q-FLAG	N/A	This study
KV7877	Δ*sypF* Δ*binK* attTn*7*::*sypF*-Hpt-FLAG	N/A	This study
KV7878	Δ*sypF* Δ*binK* attTn*7*::*sypF*-FLAG	N/A	This study
KV7879	Δ*sypF* Δ*binK* attTn*7*::*sypF*-D549A-FLAG	N/A	This study
KV7894	Δ*bcsA*	Derived from ES114 using pKPQ22 (Visick *et al.*, 2013)	This study
KV7906	Δ*binK* Δ*sypK*	N/A	This study
KV7908	Δ*binK* Δ*bcsA*	N/A	This study
KV7914	Δ*binK* Δ*sypK* Δ*bcsA*	N/A	This study
KV7933	Δ*binK* Δ*sypG*	N/A	This study
KV7949	Δ*sypF* Δ*binK rscs*::Tn*10* attTn*7*::*sypF*-HPT	N/A	This study
KV7996	Δ*binK* Δ*sypF* Δ*hahK*::FRT-Cm IG (*yeiR-glmS*)::P*sypA-lacZ* attTn*7*::*sypF*-HPT-FLAG	N/A	This study
KV7997	Δ*binK* Δ*sypF* Δ*hahK*::FRT-Cm IG (*yeiR-glmS*)::P*sypA-lacZ* attTn*7*::*sypF*-FLAG	N/A	This study

KV8005	Δ*binK* Δ*sypF* Δ*hahK*::FRT-Cm IG (*yeiR-glmS*)::P*sypA-lacZ* attTn*7*::Erm	N/A	Karen Visick
KV8014	Δ*binK* Δ*sypF* IG (*yeiR-glmS*)::P*sypA-lacZ* attTn*7*::*sypF*-HPT-FLAG	N/A	Karen Visick
KV8015	Δ*binK* Δ*sypF* IG (*yeiR-glmS*)::P*sypA-lacZ* attTn*7*::*sypF*-FLAG	N/A	Karen Visick
KV8016	Δ*binK* Δ*sypF* IG (*yeiR-glmS*)::P*sypA-lacZ* attTn*7*::Erm	N/A	Karen Visick
KV8025	Δ*hnoX*::FRT- Erm	N/A	(Thompson *et al.*, 2019)
KV8027	Δ*sypE sypF2* Δ*hnoX*::FRT-Erm	N/A	(Thompson *et al.*, 2019)
KV8037	Δ*binK* attTn*7*::P*bcsQ-lacZ*	TT of KV7860 with gDNA KV4567	This study
KV8038	Δ*binK* IG (*yeiR-glmS*)::P*sypA-lacZ* attTn*7*::Erm	TT of KV7860 with gDNA KV7410	This study
KV8069	Δ*sypQ*::Cm	TT of ES114 using PCR DNA generated with primers 443, 2174, 2089, 2090, 1188 and 2175	This study
KV8070	Δ*binK* Δ*sypF* Δ*sypQ*::FRT-Cm	TT KV7862 with gDNA KV8069	This study
KV8076	Δ*binK* Δ*sypQ*::Cm attTn*7*::P*bcsQ-lacZ*	TT of KV8037 with gDNA KV8069	This study
KV8077	Δ*binK* Δ*sypQ*::Cm IG (*yeiR-glmS*)::P*sypA-lacZ* attTn*7*::Erm	TT KV8038 with gDNA KV8069	This study
KV8078	Δ*sypQ*::FRT-Cm attTn*7*::P*bcsQ-lacZ*	TT of KV4567 with gDNA KV8069	This study
KV8079	Δ*sypQ*::Cm IG (*yeiR-glmS*)::P*sypA-lacZ* attTn*7*::Erm	TT of KV7410 with gDNA KV8069	This study
KV8086	Δ*binK* Δ*sypEF* attTn*7*::*sypF*-HPT-FLAG	N/A	(Thompson *et al.*, 2018)
KV8091	Δ*binK* Δ*sypF* Δ*hahK*::FRT Δ*sypQ*::Cm IG (*yeiR-glmS*)::P*sypA-lacZ* attTn*7*::*sypF*-HPT-FLAG	TT of KV7996 (flp with pKV496) gDNA KV8070	This study
KV8092	Δ*binK* Δ*sypF* Δ*hahK*::FRT Δ*sypQ*::Cm IG (*yeiR-glmS*)::P*sypA-lacZ* attTn*7*::*sypF*-FLAG	TT of KV7997 (flp with pKV496) gDNA KV8070	This study

KV8093	Δ*binK* Δ*sypF* Δ*sypQ*::FRT-Cm IG (*yeiR-glmS*)::P*sypA-lacZ* attTn*7*::*sypF*-HPT-FLAG	TT KV8014 with gDNA KV8070	This study
KV8094	Δb*inK* Δ*sypF* Δ*sypQ*::FRT-Cm IG (*yeiR-glmS*)::P*sypA-lacZ* attTn*7*::*sypF*-FLAG	TT KV8015 with gDNA KV8070	This study
KV8095	Δ*binK* Δ*sypF* Δ*sypQ*::FRT-Cm IG (*yeiR-glmS*)::P*sypA-lacZ* attTn*7*::Erm	TT KV8016 with gDNA KV8070	This study
KV8107	Δ*binK* Δ*sypEF* Δ*hahK*::FRT-Cm attTn*7*::*sypF*-HPT-FLAG	N/A	Cecilia Thompson
KV8112	Δ*binK* Δ*sypF* Δ*hahK*::FRT Δ*sypQ*::Cm IG (*yeiR-glmS*)::P*sypA-lacZ* attTn*7*::Erm	TT KV8005 with gDNA KV8070	This study
KV8150	Δ*binK* Δ*sypE sypF2* Δ*hnoX*::FRT	N/A	(Thompson *et al.*, 2019)
KV8232	IG (*yeiR-glmS*)::ErmR-trunc TrimR	N/A	(Visick *et al.*, 2018)
KV8297	Δ*hahK*::FRT-Trim IG (*yeiR-glmS)::lacI-Q*	N/A	(Tischler *et al.*, 2018)
KV8323	Δ*sypF* Δ*binK* Δ*hahK*::FRT-Trim attTn*7*::*sypF*-Hpt-FLAG	TT of KV7878 with gDNA KV8297	This study
KV8324	Δ*sypF* Δ*binK* Δ*hahK*::FRT-Trim attTn*7*::*sypF*-FLAG	TT of KV7949 with gDNA KV8297	This study
KV8325	Δ*sypF* Δ*binK* Δ*hahK*::FRT-Trim *rscS*::Tn*10* attTn*7*::*sypF*-HPT	TT of KV7949 with gDNA KV8297	This study
KV8458	Δ*binK*::FRT- Trim	N/A	(Thompson *et al.*, 2019)
KV8607	Δ*sypE sypF2* Δ*sypG* Δ*binK*::FRT- Trim	TT KV6567 with gDNA KV8458	This study
KV8611	Δ*sypE sypF2* Δ*sypG* Δ*binK*::FRT- Trim Δ*hnoX*::FRT-Erm	TT KV8607 with gDNA KV8025	This study
KV8897	Δ*qrr* Δ*casA*::FRT-Spec	N/A	Tischler *et al* 2021 submitted.
KV8920	Δ*casA*::FRT-Spec	N/A	This study
KV8938	Δ*binK* Δ*casA*::FRT-Spec	TT KV7860 with gDNA KV8897	This study
KV9179	Δ*casA*::FRT	N/A	Tischler *et al* 2021 submitted.

KV9341	Δ*vpsR*::FRT-Spec	N/A	Tischler *et al* 2021 submitted.
KV9573	IG::Erm-P*vpsR-lacZ*	TT KV7371 with SOE using primers 2185 & 2090 (pKV502), 2932 & 2933 (ES114), 2822 & 2876 (KV7371)	This study
KV9818	Δ*casA*::FRT-Spec IG (*yeiR-glmS*)::ErmR-trunc TrimR	TT KV8232 with gDNA KV8920	This study
KV9820	Δ*casA*::FRT-Spec IG::Erm-P*nrdR-casA*-HA	TT KV9818 with SOE using primers 2290 & 2090 (pKV506), 2905 & 3042(ES114), 2089 & 1487 (pKV505)	This study
KV9821	Δ*casA*::FRT-Spec IG::Erm-P*nrdR*-RBS-*casA*-HA	TT KV9818 with SOE using primers 2290 & 2090 (pKV506), 3057 & 1487 (KV9820)	This study
KV9822	Δ*casA*::FRT-Spec IG::Erm-P*nrdR*-RBS-*casA-G410A*-HA	TT KV9818 with SOE using primers 2290 & 2911 (KV9821) and 2910 & 1487 (KV9821)	This study
KV9823	Δ*casA*::FRT-Spec IG::Erm-P*nrdR*-RBS-*casA-R400A*-HA	TT KV9818 with SOE using primers 2290 & 3048 (KV9821) and 3047 & 1487 (KV9821)	This study
KV9824	Δ*casA*::FRT-Spec IG::Erm-P*nrdR*-RBS-*casA-G231A*-HA	TT KV9818 with SOE using primers 2290 & 3112 (KV9821) and 3111 & 1487 (KV9821)	This study
KV9825	Δ*casA*::FRT-Spec IG::Erm-P*nrdR*-RBS-*casA-D111A*-HA	TT KV9818 with SOE using primers 2290 & 3118 (KV9821) and 3117 & 1487 (KV9821)	This study
KV9826	Δ*casA*::FRT-Spec IG::Erm-P*nrdR*-RBS-*casA-D236A*-HA	TT KV9818 with SOE using primers 2290 & 3120 (KV9821) and 3119 & 1487 (KV9821)	This study
KV9827	Δ*casA*::FRT-Spec IG::Erm-P*nrdR*-RBS-*casA-E293A*-HA	TT KV9818 with SOE using primers 2290 & 3122 (KV9821) and 3121 & 1487 (KV9821)	This study
KV9828	Δ*casA*::FRT-Spec IG::Erm-P*nrdR*-RBS-*cdgK*-HA	TT KV9818 with SOE using primers 2290 & 2090 (pKV506), *cdgK* gblock (IDT), 2089 & 1487 (pKV505)	This study
KV9864	Δ*sypQ*::FRT-Cm Δ*casA*::FRT-Spec attTn*7*::P*bcsQ-lacZ*	TT KV8078 with gDNA KV8920	This study
KV9865	Δ*sypQ*::FRT-Cm Δ*vpsR*::FRT-Spec attTn*7*::P*bcsQ-lacZ*	TT KV8078 with gDNA KV9341	This study
KV9866	Δ*casA*::FRT Δ*vpsR*::FRT-Spec	TT KV9179 with gDNA KV9341	This study
KV9867	Δ*vpsR*::FRT-Spec IG::Erm-P*vpsR-lacZ*	TT KV9573 with gDNA KV9341	This study

KV9868	Δ*casA*::FRT Δ*vpsR*::FRT-Spec attTn*7*::P*bcsQ-lacZ*	Derived from KV9866 using pCMA26	This study

[1]Construction of unpublished strains

Table 2. Plasmids Used in this Study

Name	Description	Derivation	Source
pAT100	pJET + FRT-Erm *casA*-HA	pJET + PCR product with primers 975 & 1487 (KV9821)	This study
pAT101	pJET + FRT-Erm *casA+G410A*-HA	pJET + PCR product with primers 975 & 1487 (KV9822)	This study
pAT102	pJET + FRT-Erm *casA+D236A*-HA	pJET + PCR product with primers 975 & 1487 (KV9826)	This study
pCLD42	pKV69 + *vpsR*	N/A	(Darnell *et al.*, 2008)
pCMA9	pKV69 + *binA*	N/A	(Bassis & Visick, 2010)
pCMA26	P*bcsQ-lacZ* reporter	N/A	(Tischler *et al.*, 2018)
pFY4535	c-di-GMP biosensor, Gent^R, *hok/sok*	N/A	(Zamorano-Sánchez *et al.*, 2019)
pJJC4	*tfoX*$^+$ + Cm^R	N/A	(Cohen *et al.*, 2021)
pKPQ22	pKV363 + sequences flanking *bcsA* to generate *bcsA* deletion	N/A	(Visick *et al.*, 2013)
pKV496	Kan^R + *flp*$^+$	N/A	(Visick *et al.*, 2018)
pKV498	pKV69 + *hahK*	N/A	(Tischler *et al.*, 2018)
pKV502	pJET + *yeiR*-FRT-Erm^R	N/A	(Visick *et al.*, 2018)
pKV505	pJET + HA-*glmS*	N/A	(Visick *et al.*, 2018)
pKV506	pJET + yeiR-FRT-Erm^R-P*nrdR*	N/A	(Visick *et al.*, 2018)
pKV521	pJET + FRT-Spec^R	N/A	(Visick *et al.*, 2018)
pKV522	pJET + *hahK*-HA	N/A	(Thompson *et al.*, 2019)
pKV523	pJET + *hahK*-H222Q-HA	N/A	(Thompson *et al.*, 2019)
pKV524	pJET + *hahK*-D506A-HA	N/A	(Thompson *et al.*, 2019)
pKV69	Vector, Cm^R, Tet^R	N/A	(Visick & Skoufos, 2001)
pLL3	pVSV209 + P*sypA-GFP*	N/A	(Thompson *et al.*, 2019)
plostfoX-Kan	*tfoX*$^+$ + Kan^R	N/A	(Brooks *et al.*, 2014)

pVSV102	Constitutive GFP expression vector	N/A	(Dunn *et al.*, 2006)

Table 3. Primers Used in this Study

Primer	Sequence
443	CGGTAATACTCCATAAGTTCTTTCAC
975	CCTCACCCCAGATGGTTTGGCA
1188	GGTAATGCTGGGCGACTAG
1487	GGTCGTGGGGAGTTTTATCC
2089	CCATACTTAGTGCGGCCGCCTA
2090	CCATGGCCTTCTAGGCCTATCC
2116	agagctcTCTGGCGGTGATAATGGTTG
2117	aggtaccGGCATAGTGCGTGTTTATGC
2174	TAGGCGGCCGCACTAAGTATGGAGCATGATGGTATATTACGATACC
2175	GGATAGGCCTAGAAGGCCATGGTGGACTCGAGTTCAAAAATAACA
2185	CTTGATTTATACAGCGAAGGAG
2290	AAGAAACCGATACCGTTTACG
2822	AGGAAACAGCTatgACCATGATTACGGATTCAC
2876	GAAACGCCGAGTTAACGCC
2905	ggataggcctagaaggccatggCACTTCGTGTTAAAGAATTTATAC
2910	CGATTTGGCGCTGAAGAATTTGTTATCTGTATTAATG
2911	CAAATTCTTCAGCGCCAAATCGAGACACAATATC
2932	ggataggcctagaaggccatggCCATCAATGCGTCCACAAGC
2933	catggtcatagctgtttcctCATAACACTACCTCTAAATTCTTATATC
3042	ttatgcataatctggaacatcatatggataTGAAAAGTAAACTCGGTTTTTACC
3047	GAATAAGAGTGTGGCTGATAGTGATATTGTGTCTCG
3048	CAATATCACTATCAGCCACACTCTTATTCAGCATTCTC
3057	ggataggcctagaaggccatggAGGAGGATTTATACATGCCGAAATTTAATTTAAAAC
3111	GTATATTCAAAGCTGTATTGGTCATTGATCTTTC
3112	GACCAATACAGCTTTGAATATACCTTTATAG
3117	GGACGTCTTGCTTATAGTATCGCTGGTAAAAAAG
3118	GATACTATAAGCAAGACGTCCTTCTGCAAC

3119	GTATTGGTCATTGCTCTTTCAGTTGAAAAGC
3120	CTGAAAGAGCAATGACCAATACACCTTTG
3121	GATAAAAGAAGCGTTGAAAGGTTTTCTTGTG
3122	CTTTCAACGCTTCTTTTATCGATGTTTTG

Lowercase letters indicate nonnative or tail sequences

CHAPTER THREE

EXPERIMENTAL RESULTS

Identification and Characterization of Calcium as a Biofilm-Promoting Signal

Introduction

Biofilm formation is a key behavior by *V. fischeri* and required for colonization of the squid host. However, while our canonical WT strain, ES114, is a successful colonizer, it does not readily form biofilms under standard laboratory conditions. Therefore, genetically modified strains have been used to investigate biofilm formation *in vitro*. Biofilm-competent strains feature either (1) overexpression of the SK *rscS*, a positive regulator of *syp* transcription, or (2) overexpression of the σ^{54}-dependent transcription factor, *sypG*, and deletion of the post-transcriptional negative regulator*, sypE* (Yip *et al.*, 2006, Hussa *et al.*, 2008, Morris & Visick, 2013). Both of these genetic backgrounds allow for wrinkled colony formation, indicative of SYP-dependent biofilms, at the bench. However, the need to overexpress positive regulators (and delete negative regulator(s)) suggests that our laboratory conditions lack some factor(s) that signal bacterial behavior towards biofilm formation.

Recent work began exploring various media compositions, and how those conditions impacted wrinkled colony formation as a readout of SYP-dependent biofilms in a RscS-overproducing derivative of ES114 (Marsden *et al.*, 2017). This work identified substantial differences in the wrinkling patterns of bacteria grown on LBS (Luria-Bertani salt) versus SWT (seawater tryptone) media (Marsden *et al.*, 2017). LBS and SWT differ in two main ways-

nutrient composition and salt content. LBS is more nutrient-rich than SWT, containing greater amounts of both tryptone and yeast extract (Marsden *et al.*, 2017, Stabb *et al.*, 2001). SWT contains a greater diversity of salts than LBS (NaCl, $MgSO_4$, KCl, and $CaCl_2$ in SWT vs NaCl in LBS), mirroring the high salt composition of seawater. Isolating each individual component revealed impacts on wrinkled colony formation, but both NaCl and $CaCl_2$ were identified to promote biofilm formation. Calcium had the strongest overall impact on biofilm formation, specifically promoting both wrinkled colony biofilms, and pellicles- biofilms that form at the air-liquid interface of static cultures (Marsden *et al.*, 2017).

In addition to the work exploring media components, several reports noted bacterial adherence to the surface of test tubes and/or formation of stringy cell aggregates (Geszvain & Visick, 2008, O'Shea *et al.*, 2006, Bassis & Visick, 2010, Darnell *et al.*, 2008). These results coupled with an observation in former student Jakob Ondrey's lab notebook about liquid aggregation phenotypes in different media led me to initially explore phenotypic differences between the various metabolism mutants that Jakob investigated with different media. Ultimately, I confirmed that Jakob's observations with the metabolism mutants were media-dependent, and identified calcium as the major contributor. More importantly, I determined that calcium supplementation induced a biofilm phenotype by the wild-type strain ES114 harboring an empty vector control, notably a ring that formed in shaking liquid culture as described below. These rings seemed to require two signals, (1) calcium and (2) tetracycline to hold selection of the empty vector control plasmid. From these preliminary data, my goals were to understand the basis for this phenomenon- specifically how the rings were being induced and what bacterial process(es) was responsible.

BinA and VpsR Regulate Adherent Ring Formation

We know ES114 must be biofilm-competent in nature since it successfully colonizes the squid host, but we had previously never seen substantial ES114-dependent biofilm formation under these laboratory conditions. Therefore, I decided to first focus on investigating the calcium and tetracycline-dependent biofilms in ES114. Screening various mutants in the lab's strain collection to identify any changes in ring formation led me to two regulators of interest: BinA and VpsR. For BinA, I observed that deletion of *binA* allowed for increased calcium-dependent ring formation, while overexpression of *binA* decreased ring formation compared to a WT vector control (Figure 10). VpsR had an opposite phenotype to BinA, where a *vpsR* mutant strain lost the ability to form a ring, while overexpression of *vpsR* allowed for robust ring formation (Figure 11). Additionally, overexpression of *vpsR* in a *binA* mutant background was insufficient to overcome the need for calcium to induce ring formation (Figure 11). These data indicate that both BinA and VpsR regulate ring formation, dependent on calcium.

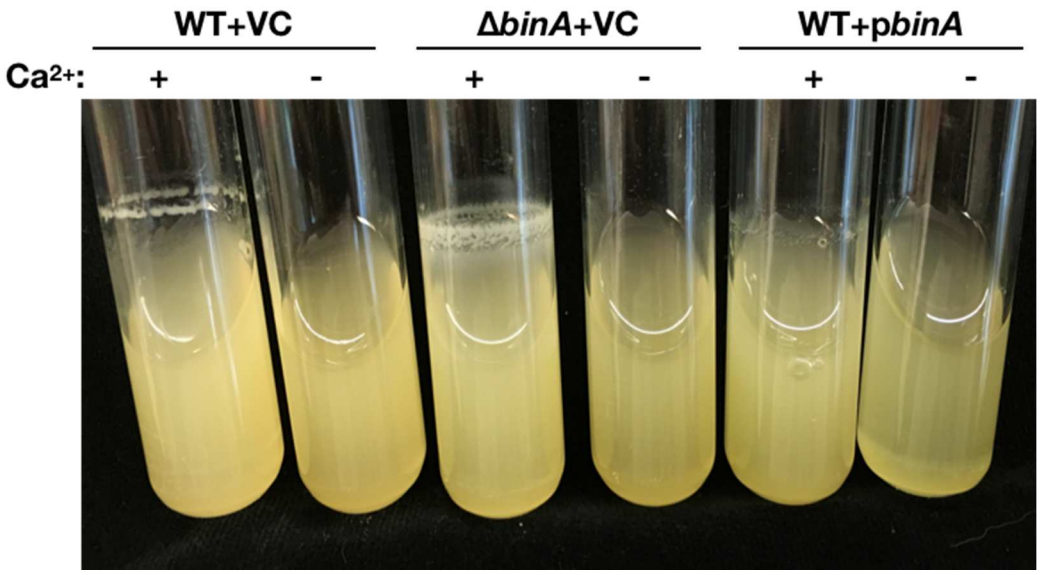

Figure 10 BinA Negatively Regulates Ring Formation. WT and Δ*binA* strains with a vector control, and WT overexpressing *binA* (p*binA*) were grown either in the presence or absence of 10 mM $CaCl_2$ as indicated.

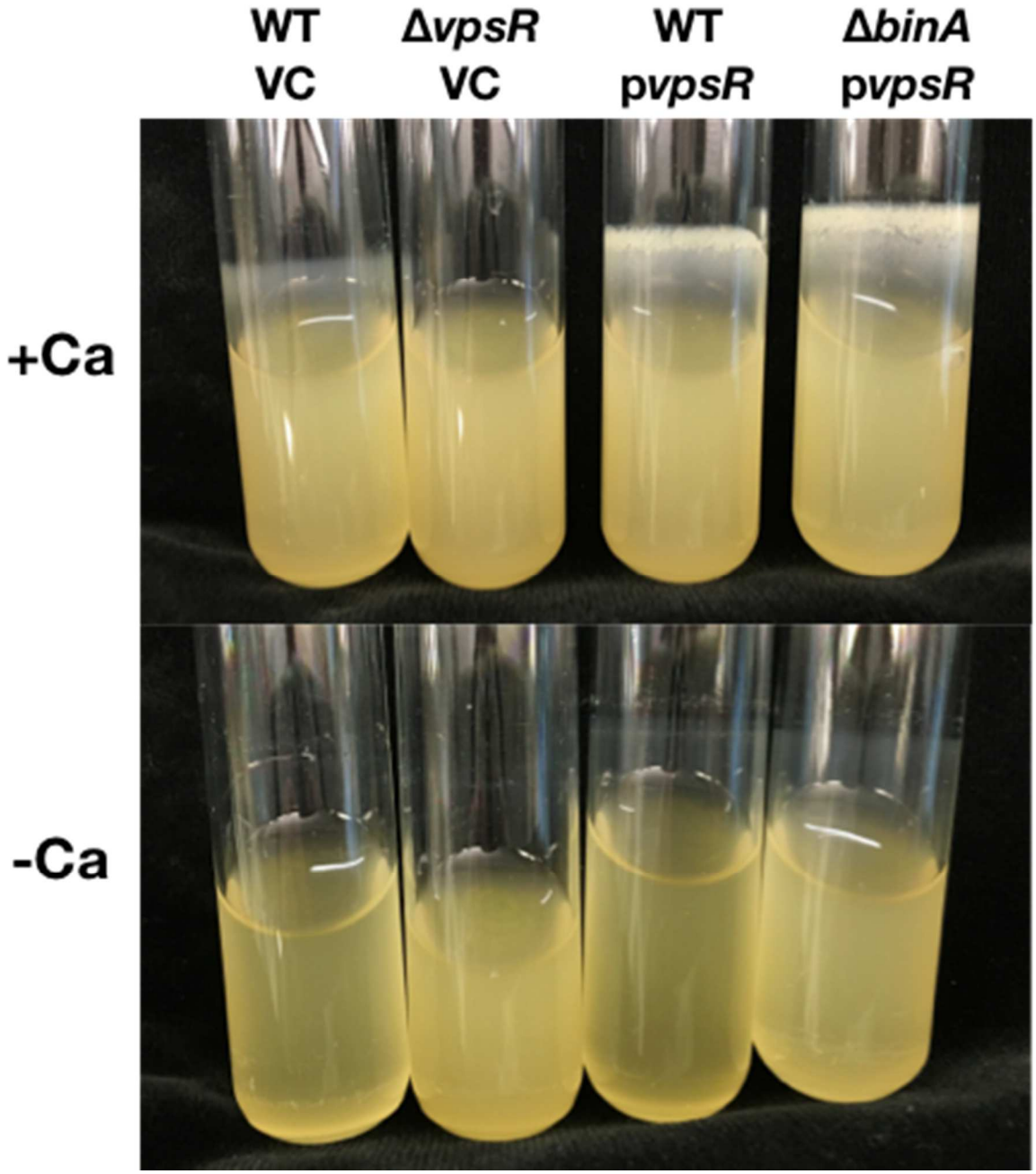

Figure 11 VpsR Positively Regulates Ring Formation. WT, Δ*vpsR* and Δ*binA* mutant strains containing either a vector control (VC) or *vpsR* overexpression (p*vpsR*) as indicated were grown either with (top) or without (bottom) 10 mM $CaCl_2$.

Antibiotics and Temperature Impact Ring Formation

My preliminary data had suggested that both calcium and an empty vector maintained via tetracycline were required to induce ring formation by ES114 in overnight cultures grown shaking at 28°C, and I found this to be consistent in a *binA* mutant strain and during *vpsR* overexpression. I hypothesized that this could be due to either the antibiotics or the plasmid backbone itself. Using a *binA* mutant, I grew a strain containing the vector control in the presence of calcium with either no selection or selection with tetracycline (tet), or chloramphenicol (cm), as the plasmid is resistant to both drugs. The tube grown without selection had noticeably reduced ring formation compared to ones grown with tet or cm (Figure 12A). I also grew a *binA* mutant with no vector control with and without calcium, and only a very faint ring formed in the presence of calcium (Figure 12A). These results suggested that the presence of the vector and/or antibiotic selection does indeed impact ring formation.

To specifically look at the contribution of antibiotics, I added a range of concentrations of tet to a *binA* mutant strain grown in the presence of calcium, either with or without the vector control. The lower concentrations were subinhibitory, allowing for survival and growth of the strain lacking the plasmid. Ring formation was induced in all concentrations of tet for the strain containing the vector control, as well as with no antibiotic addition (Figure 12B). In the strain lacking the vector control, ring formation was not seen at 0 or 0.25 μg/ml tet but was induced starting at 0.5 μg/ml, and very robust at 1 μg/ml tet addition (Figure 12B). Concentrations higher than 1 μg/ml could not support sufficient bacterial growth, although a light ring was visible at 2.5 μg/ml tet (Figure 12B). Together these results suggest that two signals, calcium and antibiotics can together induce ring formation under certain conditions.

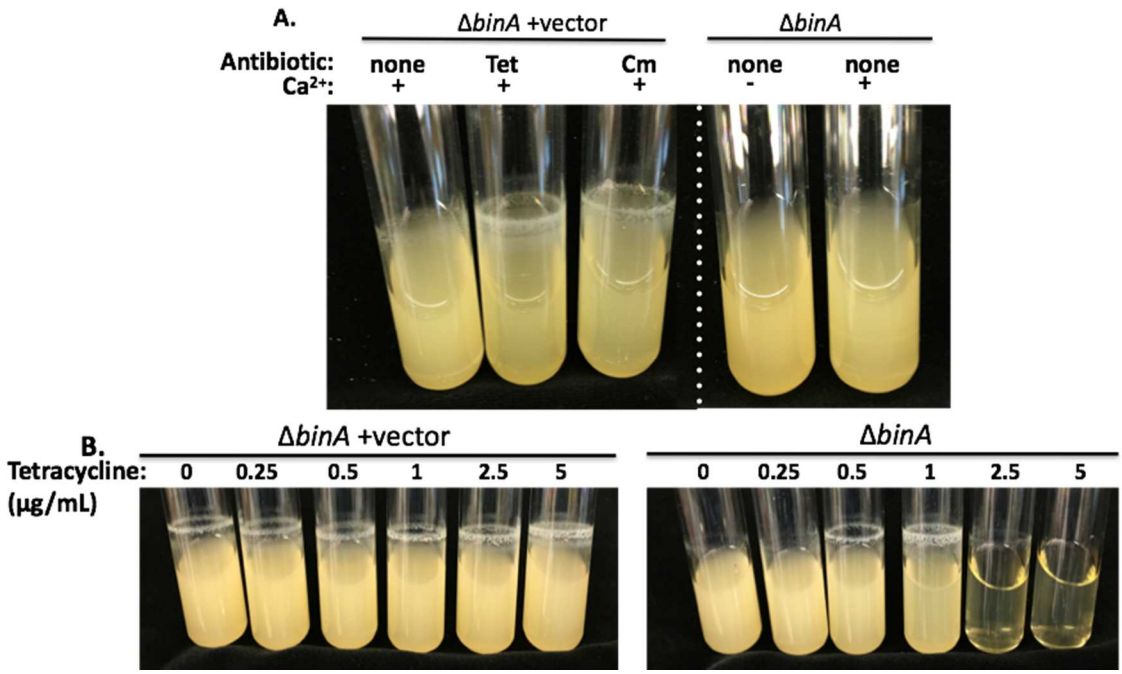

Figure 12. Tetracycline Induces Ring Phenotype in the Presence of Calcium. (A) The Δ*binA* strain with vector control was grown in the presence of $CaCl_2$ (10mM) with either no antibiotic, tetracycline (Tet), or chloramphenicol (Cm) (left). The Δ*binA* strain with no vector was grown overnight with no antibiotics in the absence or presence of 10 mM calcium (right). (B) The Δ*binA* strain with (left) and without (right) vector control was grown in the presence of calcium with increasing concentrations of tetracycline.

While the dual signals of calcium and tetracycline do not require genetic overexpression, we hypothesized that antibiotics may be inducing a general stress response, and therefore might be misleading as a signal promoting biofilm formation. We noted that all of these experiments were performed overnight at 28°C, which is the standard to grow overnight cultures, and the first condition where I saw this phenotype. However, wrinkled colony and pellicle biofilm assays are performed at room temperature (~25°C), which promotes better biofilm formation (Yip *et al.*, 2006, Mandel *et al.*, 2009). In addition to temperature, oxygenation can impact *V. fischeri* adherence to the surface of a test tube (Geszvain & Visick, 2008). Therefore, I investigated ring formation by ES114 with only calcium addition, no antibiotics/vector, at 28°C and 24°C and in smaller tubes (13 by 100 mm with 2 ml of media vs 18 by 150 mm with 5 ml of media). Without

antibiotics, calcium alone was able to promote ring formation at 24°C but not at 28°C (Figure 13). Additionally, ring formation was more consistent and robust in smaller tubes (data not shown). These data suggest that only calcium, not antibiotics, is required to induce ring formation when cells were grown at 24°C.

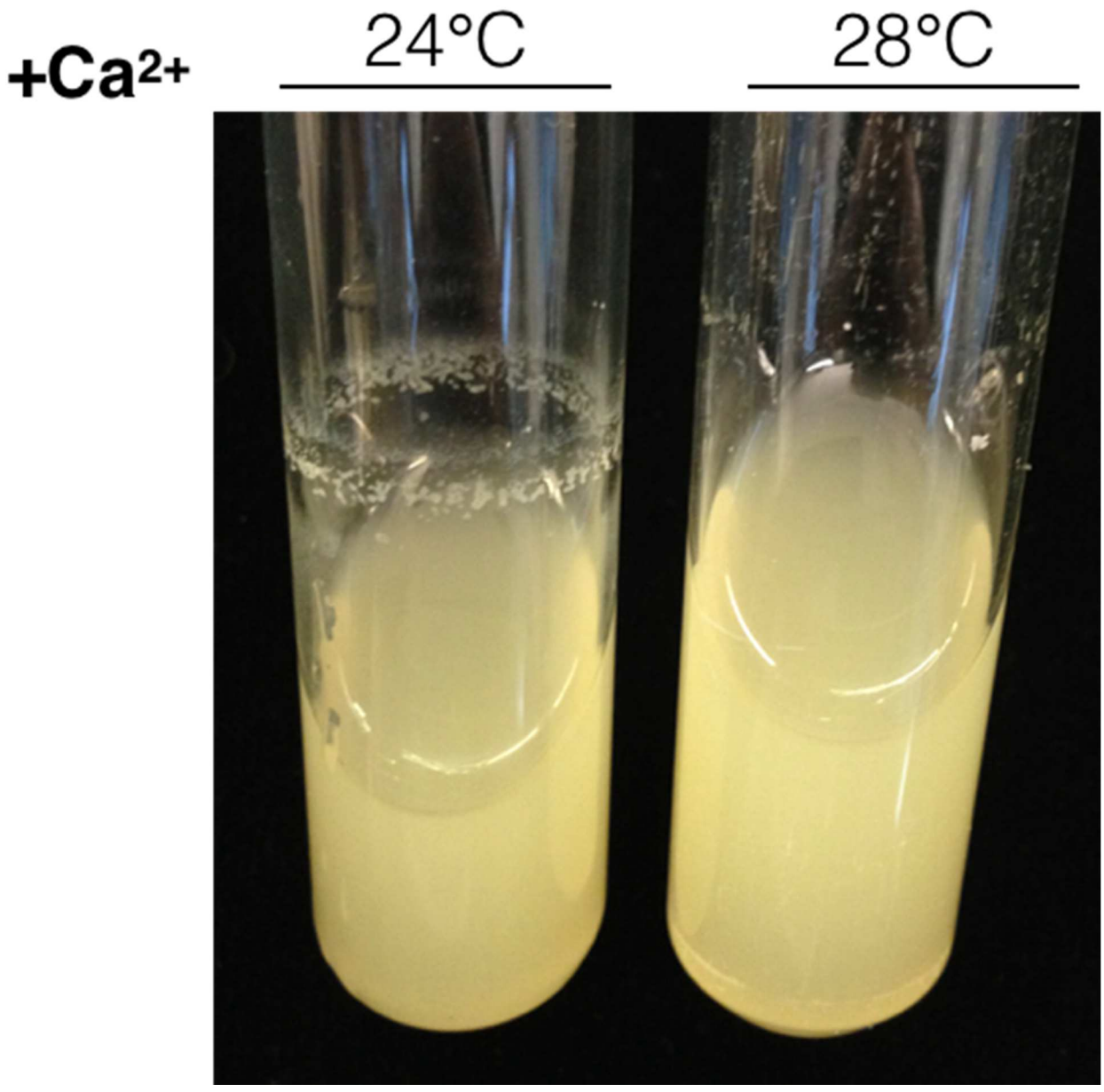

Figure 13. 24°C but not 28°C is Permissive for Ring Formation by ES114 Without Antibiotics. ES114 grown in LBS supplemented with 10 mM $CaCl_2$, grown overnight at either 24°C or 28°C, as indicated.

Adherent Rings Depend on Cellulose Polysaccharide

Both BinA and VpsR have previously been reported to impact cellulose polysaccharide in *V. fischeri*, negatively and positively, respectively (Bassis & Visick, 2010, Darnell *et al.*, 2008), which is the same direction that both proteins influence ring formation. I therefore hypothesized that ring formation would be dependent on cellulose polysaccharide. *V. fischeri* has been shown to form cellulose-dependent biofilms, but biofilm formation dependent on SYP is a much more well-studied phenotype. Therefore, I utilized the strong phenotype of a *binA* mutant background to assess ring formation in strains with mutations in several individual *syp* or *bcs* genes. A *binA* mutant strain with additional mutations in *sypG, sypC,* and *sypO* phenocopied a single *binA* mutant, displaying robust calcium-dependent ring formation (Figure 14). Conversely, mutations in *bcsC, bcsZ,* and *bcsA* all resulted in a complete loss of ring formation (Figure 14). These data suggest that calcium-induced ring formation is dependent on cellulose polysaccharide, but not on SYP.

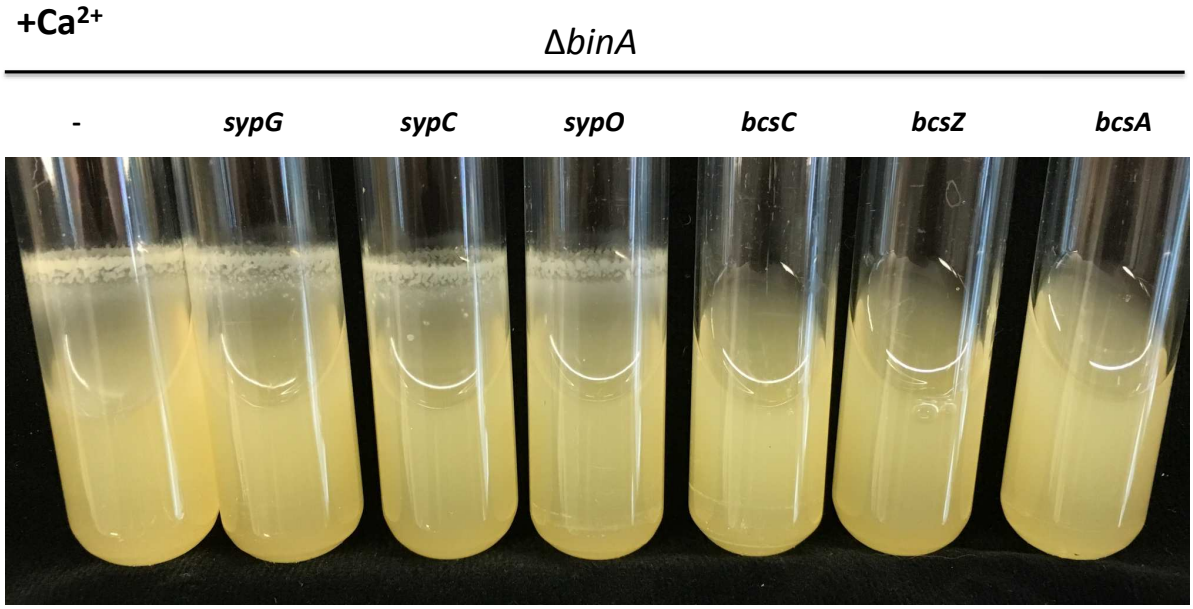

Figure 14. Adherent Rings Depend on Cellulose Polysaccharide. A *binA* single mutant strain and double mutants of the indicated *syp* or *bcs* genes were grown shaking in LBS supplemented with 10 mM $CaCl_2$.

VpsR and BinA Impact *bcs* Transcription

Cellulose-dependent rings are regulated by both VpsR and BinA, and I hypothesized that this regulation may occur at the level of transcription. I overexpressed *vpsR* and *binA* in a P*bcsQ-lacZ* reporter strain background to ask if either regulator impacted *bcs* transcription, and if calcium affected this regulation. Samples were taken over a 7h time course, and I noted a few observations. First, *bcs* transcription increased over time, regardless of calcium supplementation (Figure 15). Second, overexpression of *vpsR* and *binA* also revealed consistent trends independent of calcium; *vpsR* overexpression resulted in increased activity compared to the vector control, while *binA* overexpression resulted decreased activity (Figure 15). These effects on *bcs* transcription correlated to how each regulator impacted ring formation in liquid culture. Interestingly, both VpsR and BinA impacted *bcs* transcription even in the absence of calcium, but ring formation only occurred in the presence of calcium, suggesting that while VpsR and BinA regulate *bcs* transcription, this regulation alone is likely not sufficient to induce ring formation.

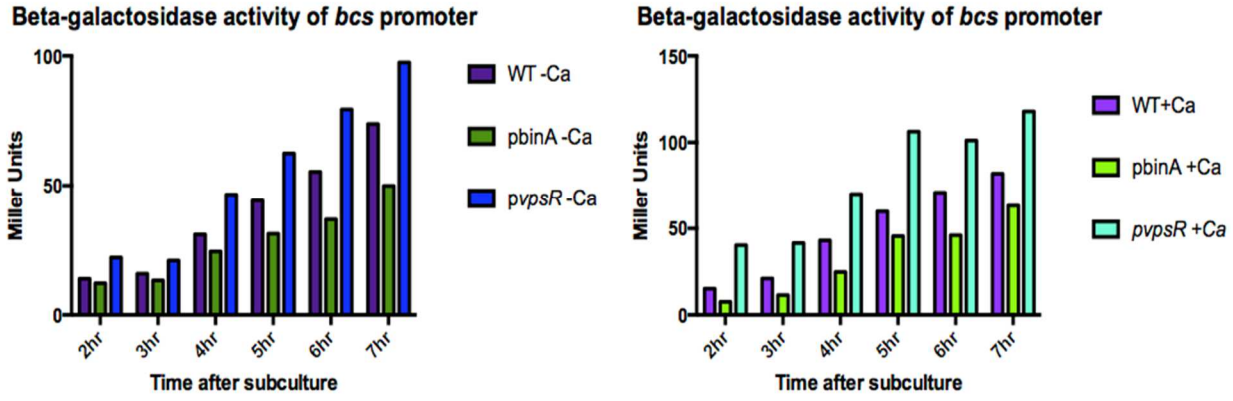

Figure 15. Impact of *vpsR* and *binA* Overexpression on *bcs* Transcription Over Time. WT containing a P*bcsQ-lacZ* reporter containing either a vector control, p*binA*, or p*vpsR* was grown without (left) or with (right) 10 mM calcium supplementation. Samples were taken between 2-7h after subculturing as indicated. Graphs are representative of at least three individual experiments.

To probe the impact of calcium, and confirm the contribution of VpsR to *bcs* transcription, I evaluated a WT and a Δ*vpsR* mutant containing a *bcs* transcriptional reporter grown in the absence and presence of calcium. The WT strain had a significant increase in *bcs* transcription in response to calcium. The Δ*vpsR* mutant strain resulted in overall minimal *bcs* transcription, and demonstrated no calcium-dependent increase in transcription (Figure 16A). Complementation of *vpsR* restored both *bcsQ* transcription and the significant calcium-mediated increase in *bcs* transcription (Figure 16B). These results suggest that VpsR is required for *bcs* transcription, under both calcium and no calcium conditions.

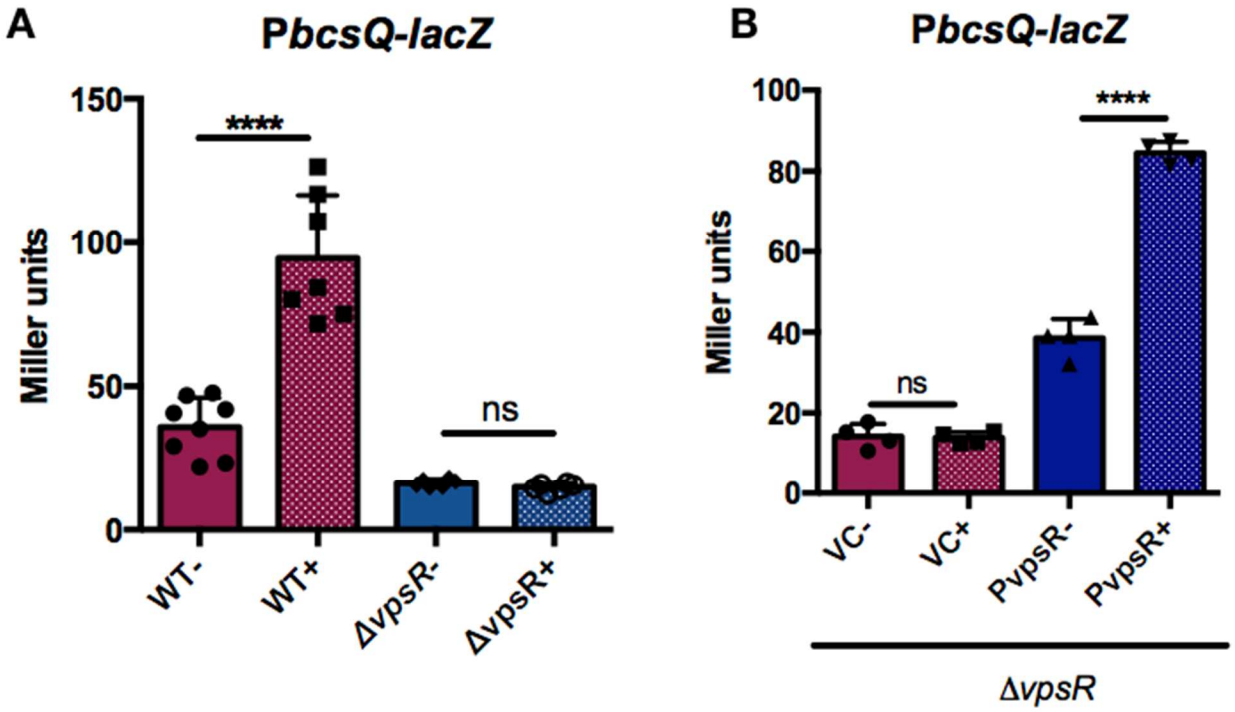

Figure 16. VpsR Regulates *bcs* Transcription. (A) WT or Δ*vpsR* strains with a P*bcsQ-lacZ* reporter were grown with and without calcium as indicated, and β-galactosidase activity was assessed at a 4 hour end point. Miller units increase significantly in WT in response to calcium (p=0.0001), the Δ*vpsR* mutant strain has no significant difference (ns). (B) Δ*vpsR* mutant strains containing either a vector control or *vpsR* overexpression grown with or without calcium as indicated. β-galactosidase activity was assessed at a 4 hour end point. Vector control shows no significance in response to calcium, while *vpsR* overexpression increases significantly in response to calcium (p=0.0001)

Calcium Specifically Induces Shaking-Liquid Biofilm Formation

LBS is normally non-permissive for biofilm formation in liquid culture, even by RscS-overproducing cells. Given the positive contribution of calcium to biofilm formation observed by Dr. Anne Marsden and my work described above, Dr. Karen Visick added calcium to LBS cultures of an RscS-overproducing strain, and found that these conditions induced robust biofilm formation, with cohesive clumps of cells following overnight growth at 28°C. I followed up on this important finding by assessing if this effect was specific to calcium. To examine the specific contribution of each major salt in seawater (and SWT), I grew WT (ES114) and a strain with a second copy of *rscS* (*rscS*$^{++}$) overnight in LBS supplemented individually with $CaCl_2$, KCl, NaCl, or $MgSO_4$. Only calcium supplementation permitted biofilm formation: ES114 maintained a turbid culture, but displayed a ring adherent to the side of the test tube precisely where the culture hit the sides of the tube while shaking (Figure 17). The *rscS*$^{++}$ strain displayed a clear, non-turbid culture, and two biofilm phenotypes, the ring seen in ES114, and a cohesive cellular clump free floating at the bottom of the test tube (Figure 17). The ring and clump were connected via stringy branches that came down from the ring, twisting to form a rope, before connecting to the clump in an overall "tree-like" structure (Figure 17). These phenotypes validate previous observations of bacterial adhesion, and suggest that calcium is a specific inducer of biofilm formation.

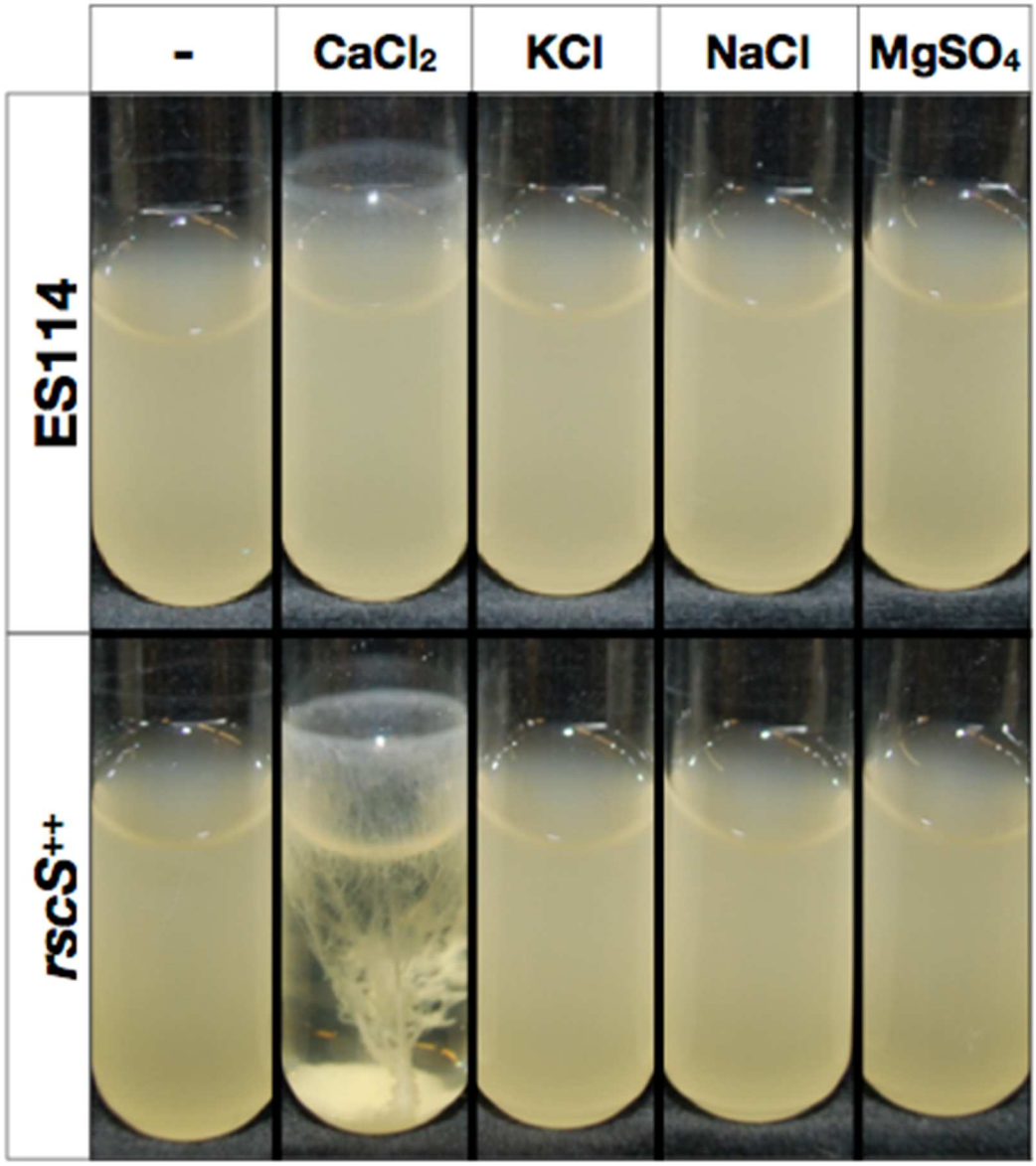

Figure 17. Calcium Induces Shaking-Liquid Biofilm Formation. ES114 and *rscS*$^{++}$ strains were grown overnight in LBS medium alone or medium supplemented with 10 mM $CaCl_2$, KCl, NaCl, or $MgSO_4$, as indicated.

I next asked if calcium also promoted the known biofilm phenotypes of wrinkled colony and pellicle formation by ES114 and *rscS*$^{++}$. Calcium addition to plates promoted subtle changes in wrinkled colony formation by *rscS*$^{++}$, but these colonies maintained the cohesiveness that is indicative of SYP (Figure 18A). As Dr. Marsden had seen, ES114 displayed changes in colony architecture in response to calcium, but this architecture was not wrinkled, nor were the colonies cohesive (Figure 18A). *rscS*$^{++}$ was only able to produce pellicles in the presence of calcium (Figure 18B, black arrow), and ES114 was unable to form pellicles either in the presence or absence of calcium, although cultures were noticeably darker when calcium was added (Figure 18B). These results suggested that calcium can influence/alter several types of biofilm phenotypes.

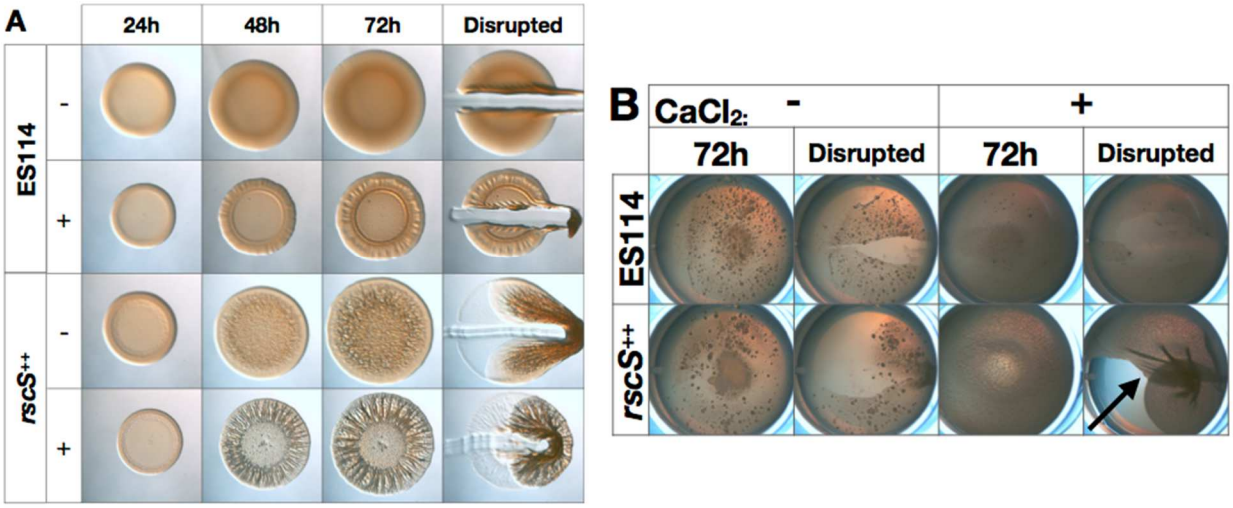

Figure 18. Calcium Induces Wrinkled Colony and Pellicle Formation. Biofilm formation was assessed for wild-type *V. fischeri* (ES114) and *rscS*$^{++}$ (KV7655) strains. (A) Wrinkled colony formation was assessed by a time course on LBS agar plates lacking or containing 10 mM $CaCl_2$ as indicated. Colonies were disrupted at the final time point to evaluate SYP production. (B) Pellicle formation was assessed at 72 h after static incubation in LBS either lacking or containing 10 mM $CaCl_2$, as indicated. Pellicles were disrupted to determine cohesiveness. The arrow indicates a cohesive pellicle.

A *binK* Mutant Phenocopies RscS Overproduction in the Presence of Calcium

Others in the field had recently identified the SK BinK as a negative regulator of biofilm formation, and they reported that BinK inhibited RscS-dependent biofilm formation at 28°C (Brooks & Mandel, 2016). As we saw RscS could induce shaking-liquid biofilms at 28°C when calcium was added, we hypothesized that a *binK* mutant may influence calcium-dependent biofilm phenotypes. Lab member Louise Lie, observed that a *binK* mutant alone –without overexpression of *rscS*- was able to produce calcium-dependent rings and clumps.

I sought to confirm Louise's preliminary results at 24°C, which promoted stronger shaking biofilm formation as explained above (Figure 13). My results phenocopied what Louise observed, where a *binK* mutant was able to produce both rings and clumps in the presence of calcium, but not in its absence (Figure 19A). Additionally, I investigated the biofilm competency of a *binK* mutant in pellicle and wrinkled colony assays, and confirmed the specificity of calcium-induced biofilm formation. Similar to the *rscS*$^{++}$ strain, the *binK* mutant strain formed robust pellicles in the presence of calcium (Figure 19B). Conversely, where the *rscS*$^{++}$ strain is sufficient to form wrinkled colonies in the absence of calcium, the *binK* mutant strain alone formed smooth, non-cohesive colonies (Figure 19C). However, on plates with calcium, the *binK* mutant formed canonical, cohesive wrinkled colonies (Figure 19C). Lastly, the biofilm formation we saw was specific to calcium, as no other seawater salts were able to induce biofilm formation by the *binK* mutant (Figure 19D). Together, these data identify a powerful new tool where a combination of a single gene deletion and salt supplementation was sufficient to induce biofilm formation, overcoming the need for genetic overexpression.

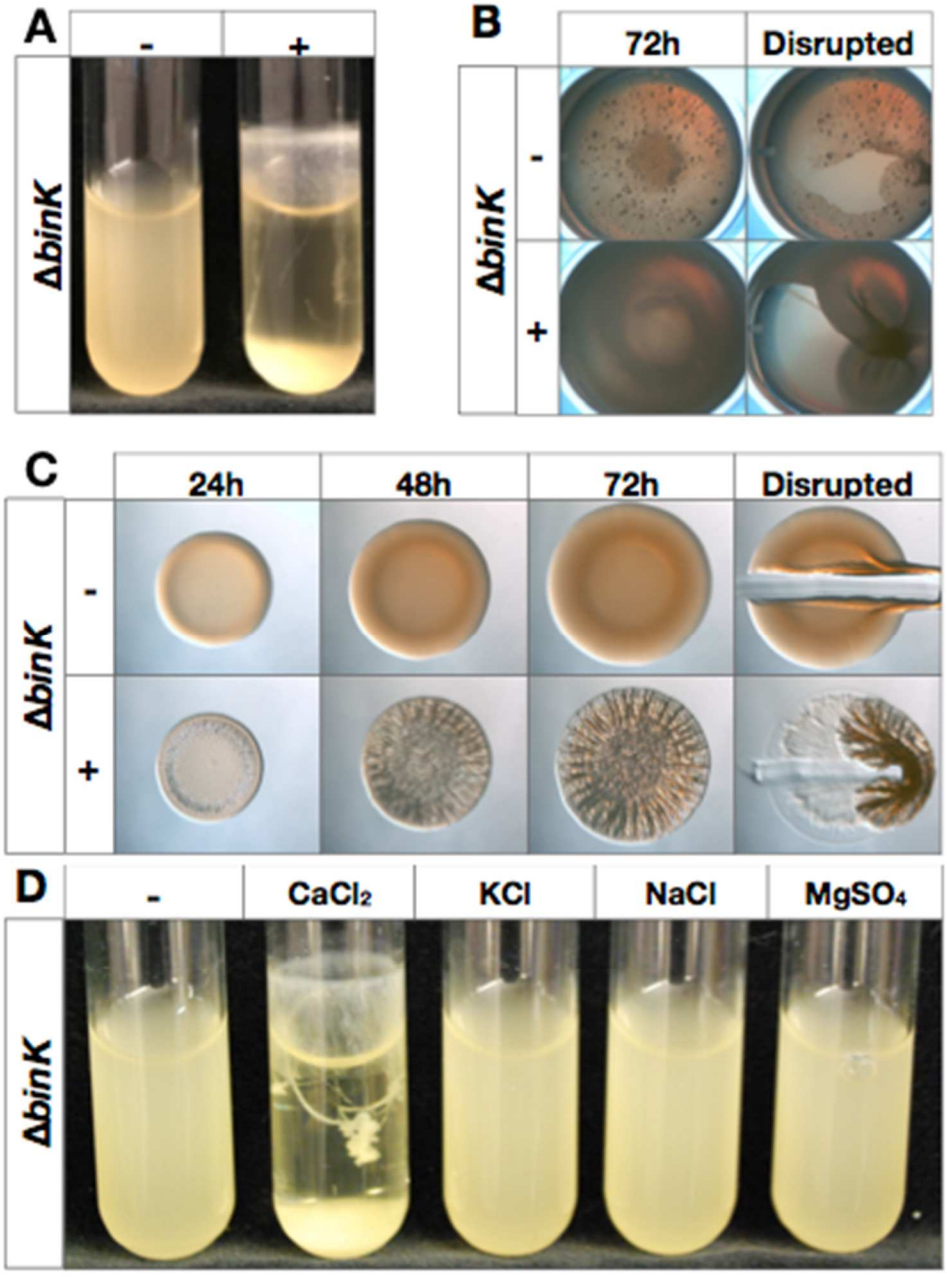

Figure 19. Calcium Induces Biofilm Formation by a *binK* Mutant. Biofilm formation was assessed for the V. fischeri Δ*binK* (KV7860) strain. (A) Δ*binK* strain was grown in LBS medium, with shaking, either lacking or containing 10 mM $CaCl_2$. (B) Pellicle formation was assessed at 72 h after static incubation in LBS either lacking or containing 10 mM $CaCl_2$ as indicated. Pellicles were disrupted to determine cohesiveness. (C) Wrinkled colony formation was assessed by a time course on LBS agar plates lacking or containing 10 mM $CaCl_2$, as indicated. Colonies were disrupted at the final time point to evaluate SYP production. (D) Δ*binK* strain was grown in LBS medium alone or medium supplemented with 10 mM $CaCl_2$, KCl, NaCl, or $MgSO_4$, as indicated.

Biofilm Rings and Clumps are Dependent on Cellulose and SYP, Respectively

We determined that calcium-dependent adherent ring formation in ES114 required cellulose polysaccharide, and therefore asked what polysaccharide(s) contributed to the ring and clump formation seen in the *rscS*$^{++}$ strain and *binK* mutant strains. RscS has historically been strongly linked to SYP as a positive regulator of *syp* transcription. To first test the role of SYP and cellulose due to RscS, Louise Lie assayed the biofilm phenotypes of *rscS*-overexpressing strains with mutations in *sypG, vpsR,* or *bcsA* grown with and without calcium at 28°C. Without calcium, all cultures were turbid, but with calcium, the strains with mutations in *bcsA* and *vpsR* formed no rings, but retained the cohesive cellular clump. Additionally, the *sypG* mutant had no clump, but retained ring formation. These results suggested that the cohesive cellular clump was dependent on SYP and the ring was dependent on cellulose.

As a calcium-induced biofilm formation in a *binK* mutant strain phenocopies *rscS*-overexpressing strains, we sought to confirm the type(s) of biofilm produced by a *binK* mutant strain under these conditions. Louise evaluated liquid shaking biofilms while I evaluated wrinkled colony formation. Deletion of *sypK* resulted in complete abrogation of wrinkled colony formation, but in liquid cultures, only the clump was lost; the adherent ring remained (Figure 20). This suggested that SYP was likely sufficient for solid plate biofilm phenotypes, and responsible for clump formation. Similar to ES114, deletion of the main cellulose synthase subunit, *bcsA,* resulted in loss of the adherent ring, but the cohesive clump remained, and disruption of both *sypK* and *bcsA* allowed for complete loss of calcium-dependent liquid biofilms (Figure 20). I quantified these biofilms via crystal violet staining, confirming that disruption of *sypK* resulted in a significant loss of biomass (Figure 20A). Disruption of *bcsA* alone resulted in a visual decrease in biomass, but this was not statistically significant, while a double *sypK bcsA*

mutant strain resulted in significantly decreased biomass (Figure 20A). Additionally, assessment of wrinkled colony formation in *bcsA* and *sypK bcsA* mutant backgrounds confirmed that SYP, but not cellulose contributes to wrinkled colony formation. Overall, these data corroborate that both SYP and cellulose as polysaccharides required for calcium-dependent liquid biofilm formation, while only SYP is required for solid agar wrinkled colony formation, and importantly confirm conditions for induction of SYP-dependent biofilms in the absence of positive regulator overexpression.

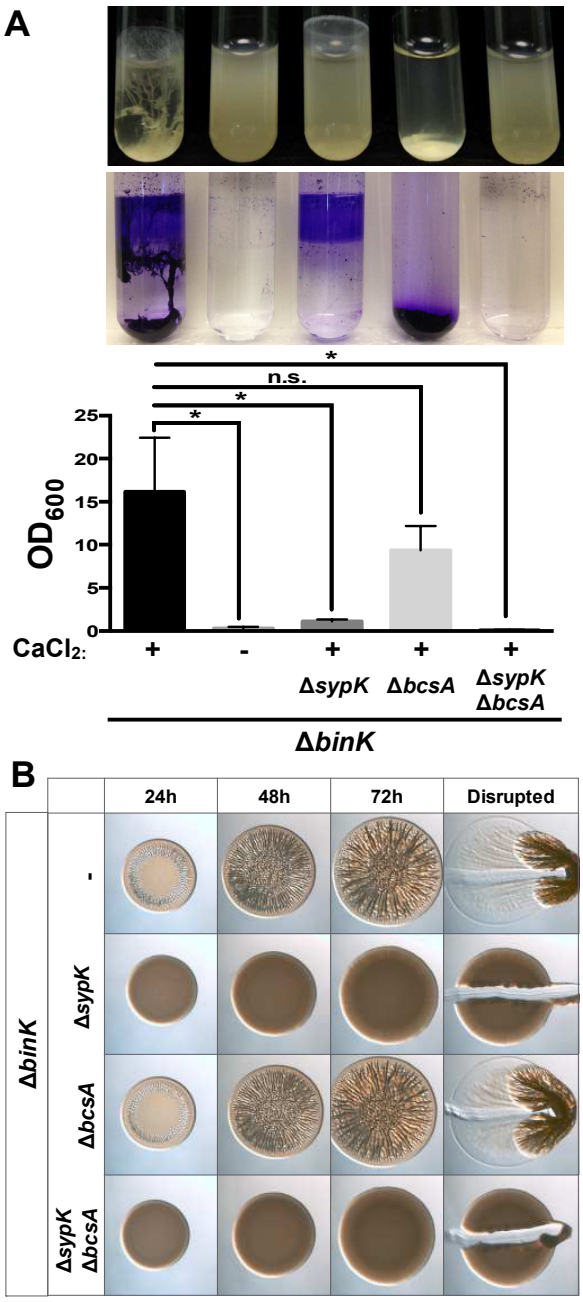

Figure 20. **Calcium-Induced Biofilms are *syp* and *bcs* Dependent.** The contribution of specific polysaccharides to calcium-induced *V. fischeri* biofilms was evaluated using Δ*binK* (KV7860), Δ*binK* Δ*sypK* (KV7906), ΔbinK ΔbcsA (KV7908), and Δ*binK* Δ*sypK* Δ*bcsA* (KV7914) strains. (A, top) Strains were grown shaking in LBS medium either lacking or containing 10 mM $CaCl_2$, as indicated, and imaged 16 h postinoculation. (Middle) Tubes were stained with crystal violet and imaged. (Bottom) Crystal violet was quantified, and a one-way ANOVA was performed (p values of 0.01, 0.01, 0.1 [not significant n.s.], and 0.01). (B) Wrinkled colony formation was assessed by a time course on LBS agar plates lacking or containing 10 mM $CaCl_2$, as indicated. Colonies were disrupted at the final time point to evaluate SYP production.

Calcium Induces Both *syp* and *bcs* at the Level of Transcription

Calcium was able to induce both SYP and cellulose polysaccharide-dependent biofilms by RscS-overproducing and Δ*binK* mutant strains in liquid culture, and while I determined that VpsR, BinA, and calcium all regulate *bcs* transcription in a WT background, neither the level where SYP regulation occurred or the impact of a *binK* deletion was known. I hypothesized that like *bcs*, calcium could modulate *syp* transcription. Previous data have shown that *syp* transcription is controlled by a network of regulators with inputs from the SKs RscS and SypF, leading to activation of RR and direct transcriptional activator SypG.

I assessed the impact of calcium and a *binK* mutation on transcription of the *syp* and *bcs* loci, using transcriptional reporter strains in the Visick lab collection. At first, the Miller units were quite variable, which I determined to be linked to optical density of the biofilm-forming cultures grown in the presence of calcium. Thus, I introduced a *sypQ::*FRT-Cm mutation into all reporter backgrounds to alleviate this issue. I saw a significant increase in Miller units for both ES114-based reporters when the strains grown with 10 mM calcium relative to no addition (Figure 21). The increase was quite small for *sypA*, but still statistically significant. These results correlate with the phenotypes observed in liquid culture, and what I had previously seen for the *bcs* locus (Figure 16). I also assessed transcription in a *binK* mutant background. When *binK* was deleted, *bcsQ* transcription increased significantly in response to calcium, similar to the WT strain (Figure 21A). *sypA* transcription was also significantly increased in response to calcium, and this response was much more robust in a *binK* mutant than in a WT strain. These results demonstrate that calcium is able to drive transcription of both *syp* and *bcs* loci.

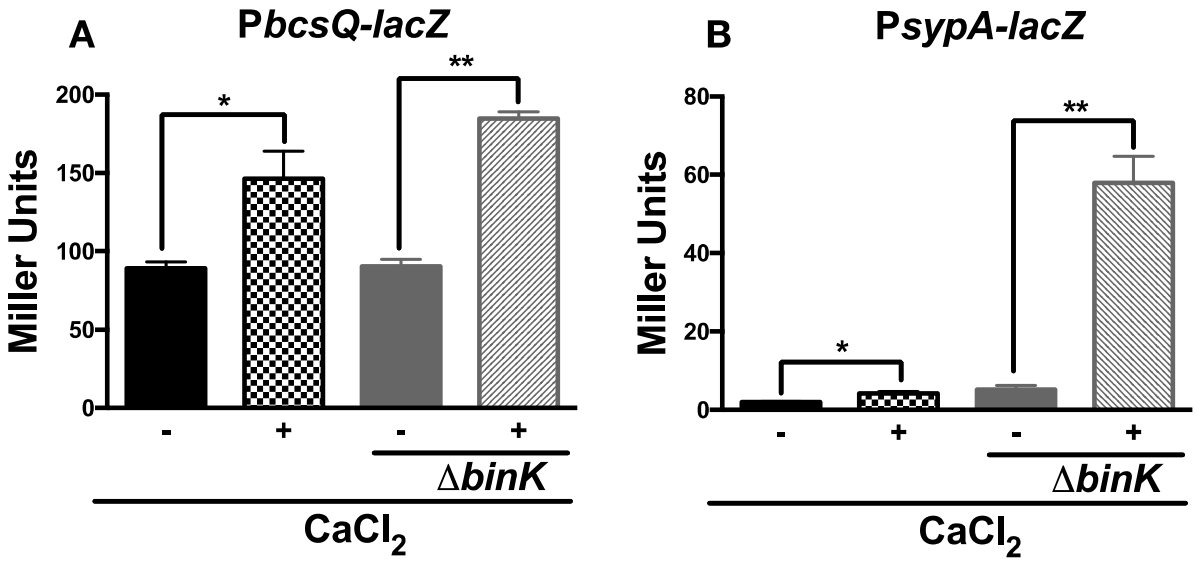

Figure 21. Calcium Induces *syp* and *bcs* Transcription. Transcription of the *bcs* and *syp* genes was assessed using a promoterless *lacZ* reporter gene fused to the promoter regions of *bcsQ* (A) and *sypA* (B). *V. fischeri* cells were grown at 24°C with shaking in 20 ml of LBS supplemented, as indicated, with 10 mM $CaCl_2$. (A) The effect of calcium on *bcsQ* transcription was monitored using P*bcsQ-lacZ* (KV8078) (p=0.02) and Δ*binK* P*bcsQ-lacZ* (KV8076) (p=0.0025) strains. (B) The effect of calcium on *sypA* transcription was monitored using P*sypA-lacZ* (KV8079) (p=0.03) and Δ*binK* P*sypA-lacZ* (KV8077) (p=0.004) strains.

Summary

In this study, I identified calcium as a major signal to induce biofilm formation by *V. fischeri*. Specifically, I showed that ES114 is competent to produce calcium-induced, cellulose-dependent biofilm rings adherent to the sides of test tubes in shaking liquid culture, and that these rings are impacted by BinA, VpsR, tetracycline, and temperature. Additionally, I along with my colleagues, determined that calcium is sufficient to induce shaking-liquid biofilms when RscS is overproduced, and shaking-liquid biofilms, wrinkled colonies, and pellicles when *binK* is deleted. Finally, I determined that calcium induces both *syp* and *bcs* through a significant increase in transcription, and that *bcs* transcription is also impacted by VpsR and BinA. The combination of a *binK* disruption plus calcium gives us a powerful new tool to probe SYP-dependent biofilms and *syp* transcriptional regulation since we no longer need to overexpress

positive regulators to induce biofilm formation. The application of these biofilm-competent conditions will be explored in a later section.

Exploring Regulatory Complexity of Calcium-Induced SYP-Dependent Biofilm Formation

Introduction

In the previous section, I introduced the discovery of calcium as a biofilm promoting factor, inducing cellulose-dependent adherent rings, and SYP-dependent cohesive cellular clumps. While previous reports had identified adherence to the side of test tubes (Geszvain & Visick, 2008, O'Shea *et al.*, 2006, Bassis & Visick, 2010, Darnell *et al.*, 2008), the strong cohesive clumps were a novel phenotype, as shaking-liquid culture is typically non-permissible to biofilm formation. Additionally, we found that loss of the recently identified negative regulator, BinK (Brooks & Mandel, 2016, Pankey *et al.*, 2017), in the presence of calcium was sufficient to induce biofilm formation in shaking-liquid culture, as well as wrinkled colony and pellicle formation.

syp transcription is induced by calcium is controlled by three known regulators SypG, SypF, and RscS. SypG is a RR and direct transcriptional activator of the *syp* locus (Norsworthy & Visick, 2015). SypF and RscS are both hybrid SKs, with similar domain architecture, and seem to work together to promote transcription (Norsworthy & Visick, 2015). They are both thought to autophosphorylate and engage in a phosphorelay that results in phosphorylation and subsequent activation of SypG (Norsworthy & Visick, 2015). While the C-terminal Hpt domain of RscS seems to be superfluous under these conditions, SypF's Hpt domain is required for biofilm formation (Norsworthy & Visick, 2015). We therefore used this opportunity to validate previous work studying *syp* regulators using both a new phenotype and a background free from overexpression of transcriptional regulators.

Calcium-Induced Cell Clumping Requires SypF and SypG

We first asked if SypF, SypG, and/or RscS were required for calcium- dependent biofilm formation. We generated double deletion mutants of each regulator in a *binK* mutant background, and former technician Louise Lie first assessed cell clumping in shaking cultures. She observed that all of the mutants retained the ability to form rings, but the *binK sypF* and *binK sypG* mutants produced turbid instead of clumped cultures, while the *binK rscS* double mutant looked like the *binK* parent strain. I confirmed her results and quantified the biomass produced by each strain using crystal violet staining. Visual observation of both cultures and quantification of crystal violet-stained tubes confirmed that the *sypF* and *sypG* double mutants formed substantially less biofilm than a single *binK* mutant (Figure 22). Additionally, Dr. Cecilia Thompson confirmed these phenotypes in wrinkled colony formation, indicating that the calcium-dependent cell clumping and wrinkled colony formation that occur under these conditions in the absence of *binK* require *sypF* and *sypG* but not *rscS*.

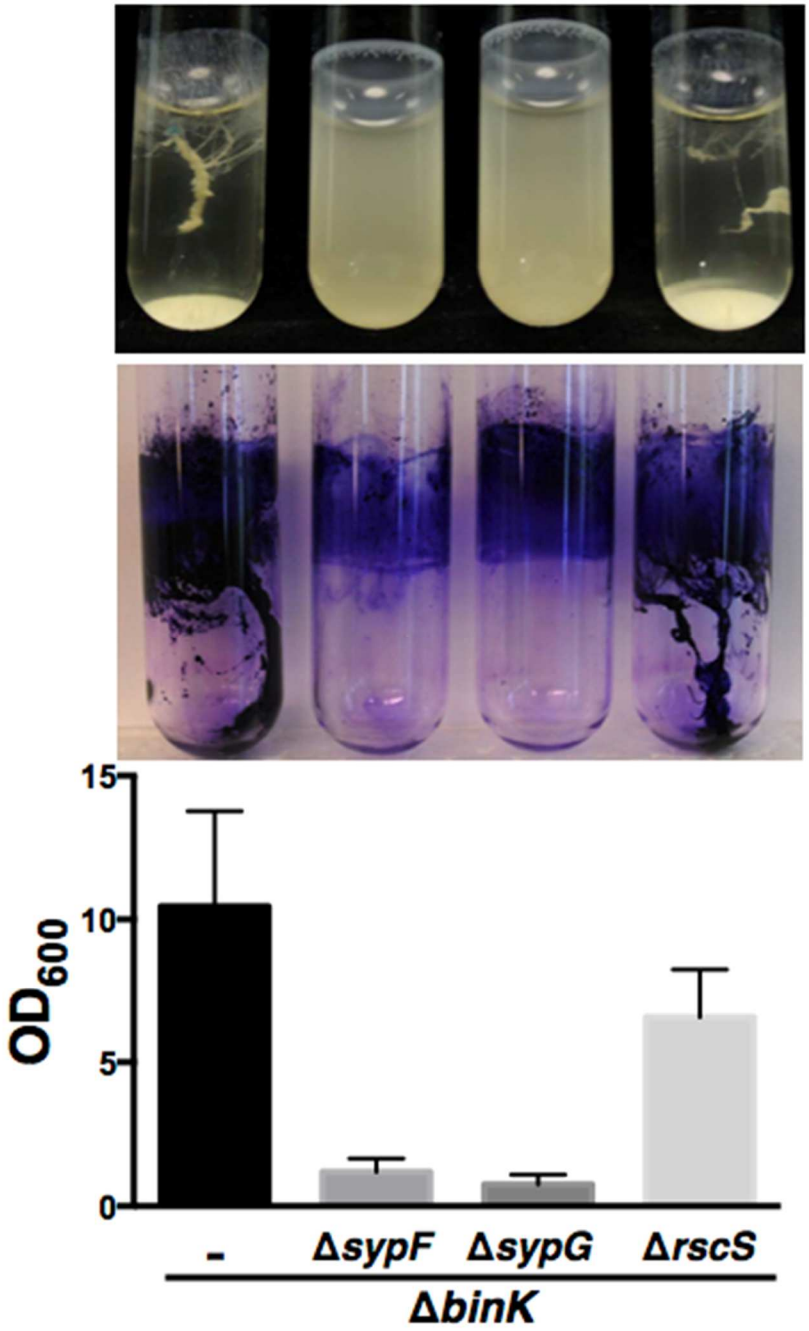

Figure 22. Calcium-Dependent Cell Clumping Requires SypF and SypG. The contribution of SypF, SypG, and RscS to calcium-induced *V. fischeri* biofilms was evaluated in Δ*binK* (KV7860), Δ*binK* Δ*sypF* (KV7862), Δ*binK* Δ*sypG* (KV7933), and Δ*binK* Δ*rscS* (KV7861) strains. (top) Strains were grown shaking in LBS medium supplemented with 10 mM $CaCl_2$ and imaged 16 h postinoculation. (Middle) Tubes were stained with crystal violet and imaged. (Bottom) Crystal violet was quantified, and a one-way ANOVA was performed (P values of 0.09, 0.07, and 0.5 compared to KV7860).

SypF-Hpt is Sufficient for Formation of Cohesive Cellular Clumps

Dr. Allison Norsworthy previously determined that only the Hpt domain of SypF was required for biofilm formation when RscS was overproduced (Norsworthy & Visick, 2015). Since SypF, but not RscS, is necessary for biofilms in a *binK* mutant, we asked if full-length SypF was required or if only a specific domain(s) would be sufficient for calcium-induced, SYP-dependent cell clumping. Using the double *binK sypF* mutant, we complemented *sypF* using alleles that encode variants with substitutions in residues predicted to be involved in the phosphorelay, H250Q, D549A, and H705Q, as well as expressing the Hpt domain alone. Louise first tested these phenotypes and found that, consistent with previous work, expression of the WT-Hpt domain alone, not the H705Q variant, was sufficient to restore clumping. I confirmed and quantified these data, determining that loss of a phosphorylatable SypF-Hpt variant resulted in significantly less biomass than complementation with full length SypF (Figure 23). These data indicate that a SypF-Hpt domain able to engage in phosphotransfer is required for BinK-inhibited, calcium-dependent cell clumping.

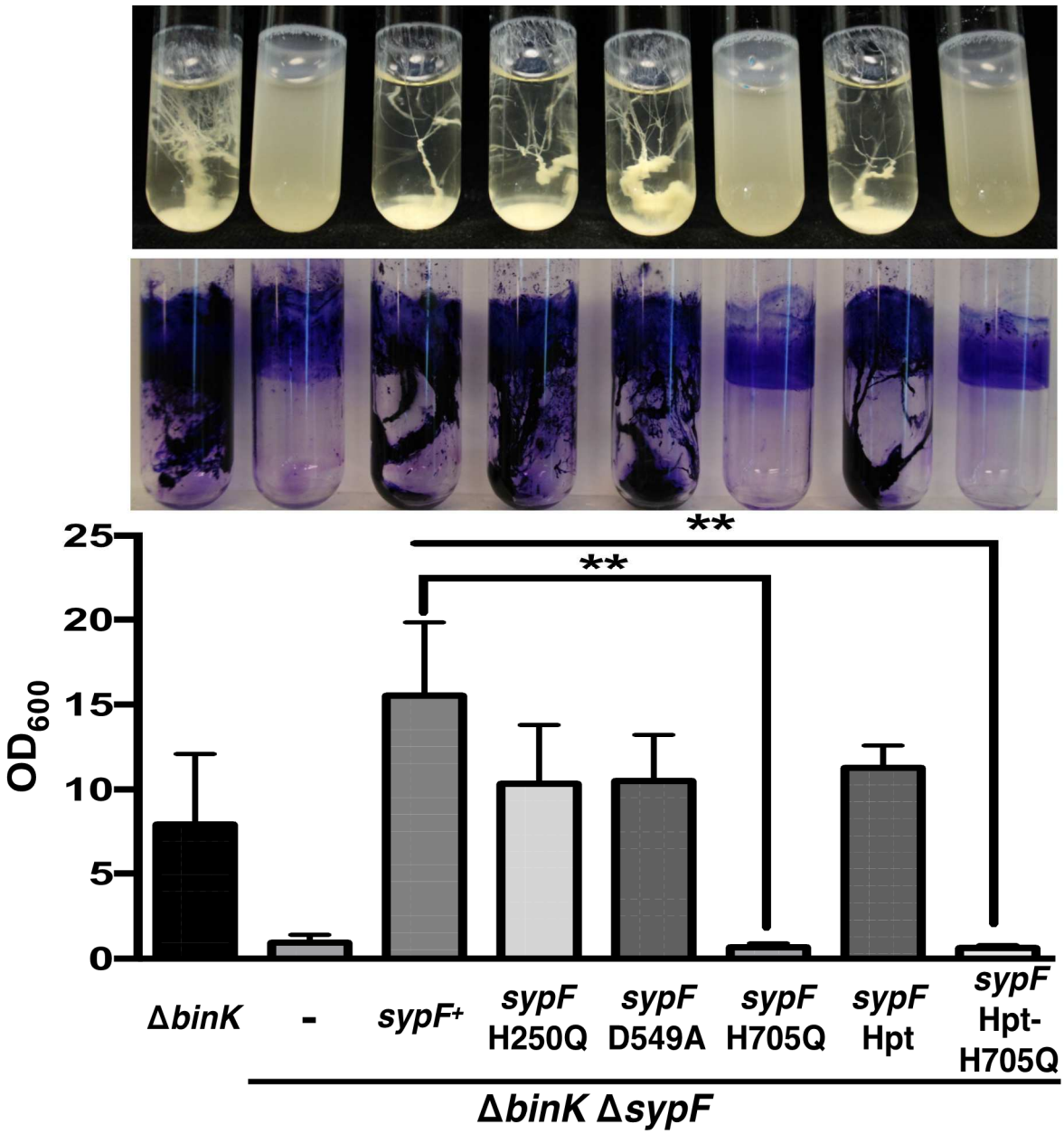

Figure 23. Hpt Domain of SypF is Required for Calcium-Induced Clumps. The requirement for specific SypF residues and domains in calcium-induced *V. fischeri* biofilm formation was evaluated. (Top) Strains were grown shaking in LBS medium containing 10 mM $CaCl_2$ and imaged 16 h postinoculation. (Middle) Tubes were stained with crystal violet and imaged. (Bottom) Crystal violet was quantified, and a one-way ANOVA was performed (*P* values were not significant [ns], 0.004, ns, and 0.004). Strains, from left to right, are the Δ*binK* (KV7860), Δ*binK* Δ*sypF* (KV7862), Δ*binK* Δ*sypF sypF*$^+$ (KV7878), Δ*binK* Δ*sypF sypF*-H250Q (KV7875), Δ*binK* Δ*sypF sypF*-D549A (KV7879), Δ*binK* Δ*sypF sypF*-H705Q (KV7873), Δ*binK* Δ*sypF sypF*-HPT (KV7877), and Δ*binK* Δ*sypF sypF*-HPT-H705Q (KV7871).

HahK Promotes SYP-Dependent Clump Formation

Since only the Hpt domain of SypF was required for clump formation, and not RscS or SypF autophosphorylation, we hypothesized that another SK must be responsible for phosphorylating the Hpt domain to drive *syp* transcription and polysaccharide production. Dr. Karen Visick performed a search through the ES114 genome looking for a SK that was not linked to a RR, with a REC domain that would allow for phosphotransfer to SypF's Hpt domain, with an emphasis on genes that appeared important for symbiosis (Ruby *et al.*, 2005, Mandel *et al.*, 2008, Brooks *et al.*, 2014). She identified and tested four candidate genes, and found only one, *VF_A0072,* which impacted clump formation. While *VF_A0072* was uncharacterized, it had previously been named *hahK* (*H*noX-*a*ssociated *h*istidine *k*inase) due to its location in an operon downstream of *hnoX* (*VF_A0071*) (Wang *et al.*, 2010, Nisbett & Boon, 2016).

We hypothesized that, when SypF is intact, it is capable of promoting calcium-induced biofilm formation independent of *hahK* and that the role of HahK, if any, would be more apparent when only the Hpt domain of SypF was present. To test this, we generated a triple *binK*, *sypF*, and *hahK* mutant strain, and then introduced either *sypF*-Hpt or full length *sypF* into the chromosome. Louise first assessed shaking-liquid biofilm formation by this strain and found that the Δ*binK sypF* +*sypF*-Hpt control strain was competent to produce cell clumps in response to calcium, and that the equivalent strain that lacking *hahK* formed very small clumps, while complementation with full length *sypF* mostly restored clumping. I confirmed and quantified these data, determining that significantly less biomass was present in a *hahK* mutant strain complemented with *sypF*-Hpt compared to the *binK sypF* mutant strain (Figure 24). Complementation with full length *sypF* also resulted in significantly less biomass than the Δ*binK sypF* mutant parent strain, but substantially more than when only the Hpt domain was present

(Figure 24). Additionally, Dr. Thompson performed wrinkled colony assays confirming this phenotype on plates, and together these data indicated that HahK has a role in SYP-dependent biofilm formation, likely through SypF-Hpt.

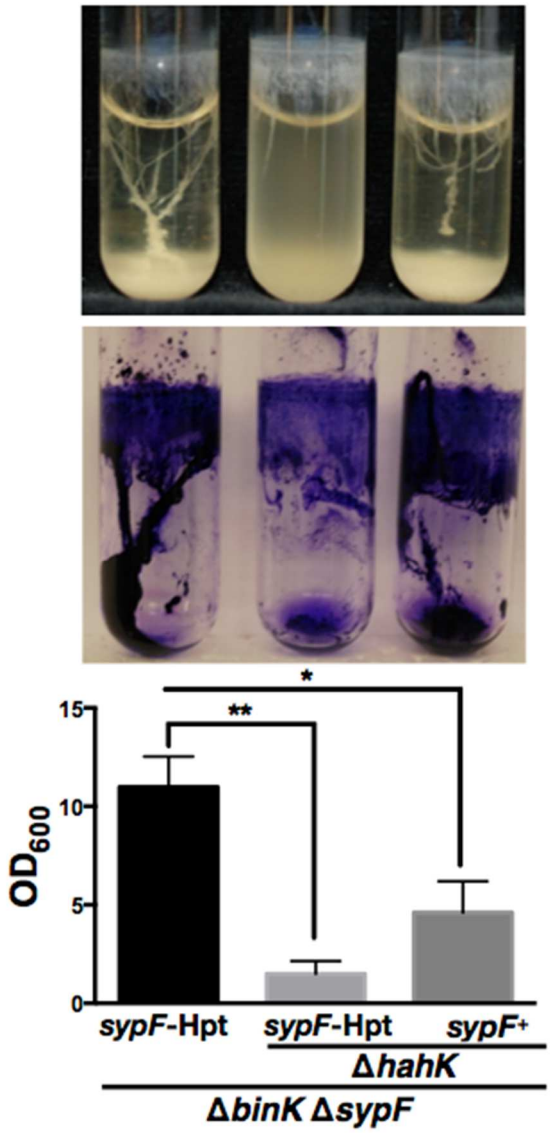

Figure 24. Sensor Kinase HahK Promotes Cell Clumping. The contribution of *hahK* to calcium-induced *V. fischeri* biofilms was evaluated in Δ*binK* Δ*sypF sypF-HPT* (KV7877), Δ*binK* Δ*sypF* Δ*hahK sypF-HPT* (KV8323), and Δ*binK* Δ*sypF* Δ*hahK sypF*$^{+}$ (KV8324) strains. (top) The strains were grown shaking in LBS medium containing 10 mM $CaCl_2$ and imaged 16 h postinoculation. (Middle) Tubes were stained with crystal violet and imaged. (Bottom) Crystal violet was quantified and a one-way ANOVA was performed (*P* values of 0.002 and 0.03).

HahK Promotes Wrinkled Colony Formation

To continue probing the function of HahK, I investigated overexpression of *hahK* in an ES114 background. Overexpression of *hahK* was sufficient to induce wrinkled colony formation in the absence of calcium (Figure 25). Similar to the above results, this wrinkling phenotype required the WT Hpt domain of SypF, able to engage in phosphotransfer, as a *sypF* deletion, either alone or with expression of the Hpt-H705Q variant, abrogated wrinkled colony formation, but wrinkling occurred with complementation of *sypF*-Hpt (Figure 25). This phenotype is similar to overexpression of *rscS* in an ES114 background, and supports a role for HahK as a positive SYP regulator, dependent on SypF-Hpt.

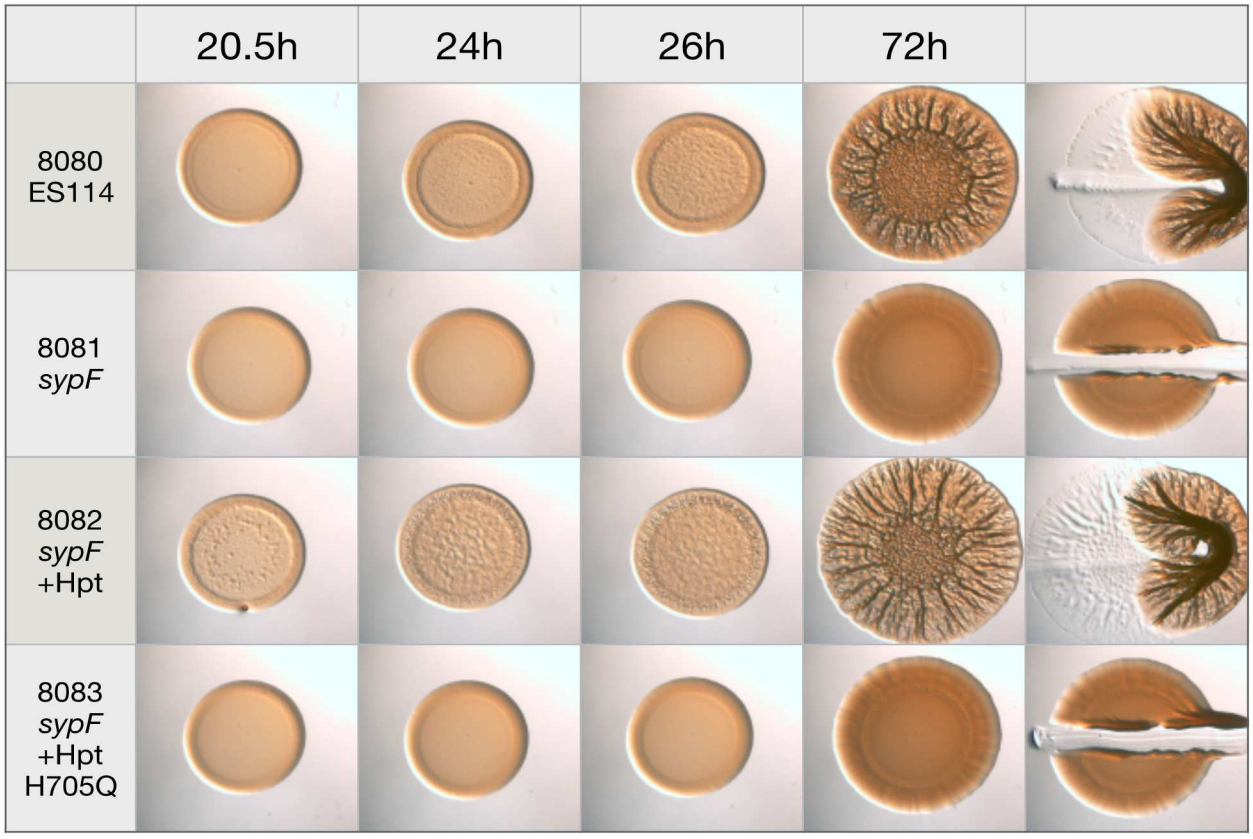

Figure 25. Overproduction of HahK Induces Wrinkled Colony Formation. Strains containing pKV498, which overexpresses *hahK*, were grown overnight, normalized to an OD_{600} of 0.2, and spotted onto LBS plates. Wrinkled colony formation was evaluated at the times indicated, and spots were disrupted at the final time point to evaluate cohesion.

HahK Regulates *syp* Transcription

Since the biofilm competency of a Δ*binK sypF* +*sypF*-Hpt strain required HahK, we hypothesized that HahK is likely acting at the level of *syp* transcription. To determine if HahK contributed to *syp* transcription, I utilized a P*sypA-lacZ* reporter strain in a Δ*binK* Δ*sypF* background, +/- Δ*hahK*, and complemented with an empty cassette (-), full length *sypF* (F), or *sypF*-Hpt (Hpt). In the strains with *hahK* present, *syp* transcription occurred when full length *sypF* was added back and was decreased but still occurred when only *sypF*-Hpt was present (Figure 26A). When *hahK* was deleted, *syp* transcription occurred only when full length *sypF* was present, and not when the Hpt domain alone was present (Figure 26A). To examine the impact of *hahK* on *sypA* transcription from an additional angle, I utilized an alternative strain background: Δ*binK* Δ*sypEF* with the *sypF*-Hpt domain expressed in the chromosome, with or without a Δ*hahK* mutation. *sypA* transcription occurred when *hahK* was present, but was significantly decreased when *hahK* was deleted (Figure 26B). Together, these data confirm that HahK impacts *syp* transcription.

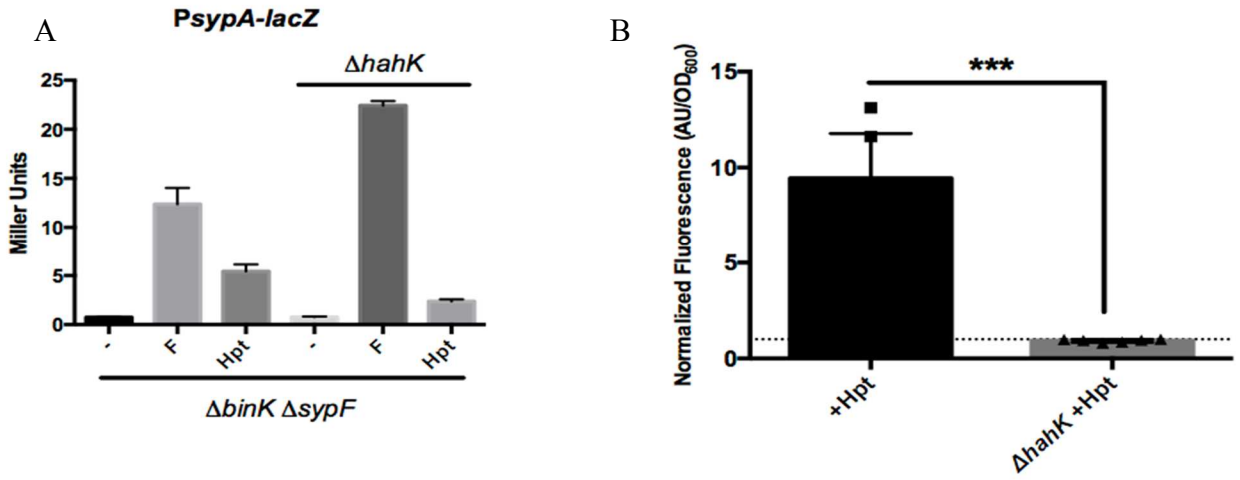

Figure 26. HahK Positively Regulates *syp* Transcription Dependent on SypF-Hpt. (A) Strains were grown overnight and subcultured 1:100 at 24°C for 22 h, and then samples were collected for a miller assay. From left to right, strains are: KV8091, KV8092, KV8093, KV8094, KV8095, and KV8112. (B) Strains expressing a P*sypA-GFP* reporter (pLL3) were grown overnight at 24°C. Strains were subcultured the next day at an OD_{600} = 0.05. The fluorescence and OD were measured at the indicated time points. The fluorescence/ OD_{600} for each strain was normalized to a biofilm (–) strain (indicated by the dotted line) to generate the normalized fluorescence. Strains are as follows: Δ*sypF* +Hpt (KV8086) and Δ*hahK* Δ*sypF* +Hpt (KV8107), normalized against KV6439. The data were analyzed by a one-way ANOVA (***$p \leq 0.001$).

A Role for RscS in Calcium-Dependent Biofilms

While a Δ*binK* Δ*sypF* Δ*hahK* +*sypF*-Hpt mutant strain was severely attenuated for biofilm formation, clump formation was not fully abolished (Figure 24). RscS has previously been shown to work through SypF-Hpt (Norsworthy & Visick, 2015); thus, we hypothesized that RscS may promote this residual biofilm formation. We first introduced an *rscS* mutation in the Δ*binK* Δ*sypF* +*sypF*-Hpt mutant background, and I assessed shaking-biofilm formation. I found that, in liquid culture, mutant strains with or without *rscS* were virtually indistinguishable from each other. However, since we had evidence that SypF, HahK, and RscS all work through the Hpt domain of SypF to promote *syp* transcription, we hypothesized that the presence of HahK in these strains may obscure the contribution of RscS. To test this hypothesis, I introduced both

rscS and *hahK* mutations into a Δ*binK* Δ*sypF* +*sypF*-Hpt strain background and assessed the ability of the resulting strain to form calcium-induced shaking biofilms. In this background, cell clumping was completely abrogated, ring formation substantially diminished, and there was a significant decrease in biomass via crystal violet staining (Figure 27). Dr. Thompson confirmed these phenotypes on solid agar in a wrinkled colony assay. These data support a role for RscS in calcium-dependent cell clumping that was previously concealed by multiple sensor kinase inputs. This marked the first phenotype in culture for an *rscS* deletion strain since its discovery (Visick & Skoufos, 2001) and highlighted the complexity and redundancy of regulators in the control of *V. fischeri* biofilm formation.

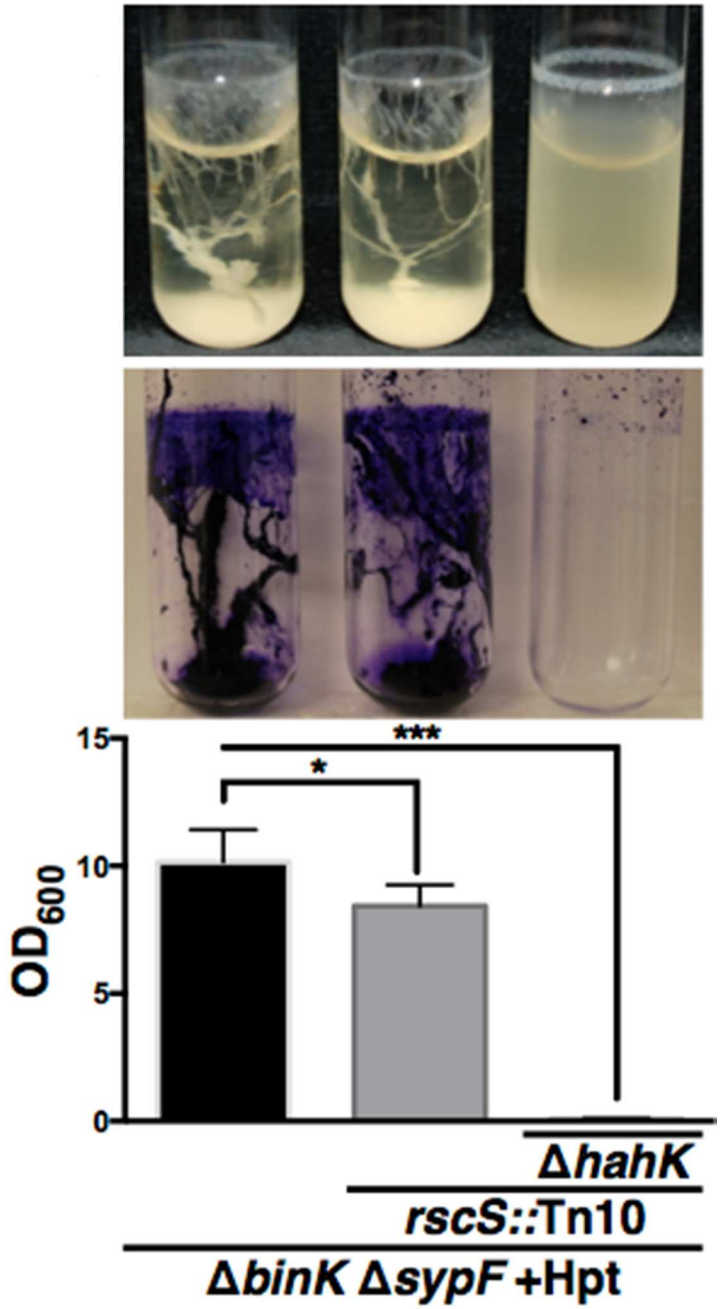

Figure 27. RscS Contributes to Calcium-Dependent Biofilms. The contributions of RscS and HahK to calcium-induced *V. fischeri* biofilms were evaluated using Δ*binK* Δ*sypF sypF*-Hpt (KV7877), Δ*binK* Δ*sypF rscS*::Tn*10 sypF*-Hpt (KV7949), and Δ*binK* Δ*sypF rscS*::Tn*10* Δ*hahK sypF*-HPT (KV8325) strains. (Top) Strains were grown shaking in LBS medium containing 10 mM $CaCl_2$ and imaged 16 h postinoculation. (Middle) Tubes were stained with crystal violet and imaged. (Bottom) Crystal violet was quantified, and a one-way ANOVA was performed (*p* values of 0.01 and 0.0009).

HahK Phosphotransfer Mutants are Stably Expressed

As we identified HahK as a SYP-dependent biofilm regulator, Dr. Thompson began to investigate the *h*eme *n*itric oxide/*ox*ygen binding protein, HnoX, which is in an operon immediately upstream of *hahK*. She identified that HnoX inhibited biofilm formation, dependent on HahK, and the ability of HahK to engage in phosphotransfer. I evaluated the expression and stability of WT-HahK, and the two phosphotransfer mutants, HahK-D506A, and HahK-H222Q (Figure 28), validating that her observed phenotypes were due to loss of phosphorelay, and not lack of protein production.

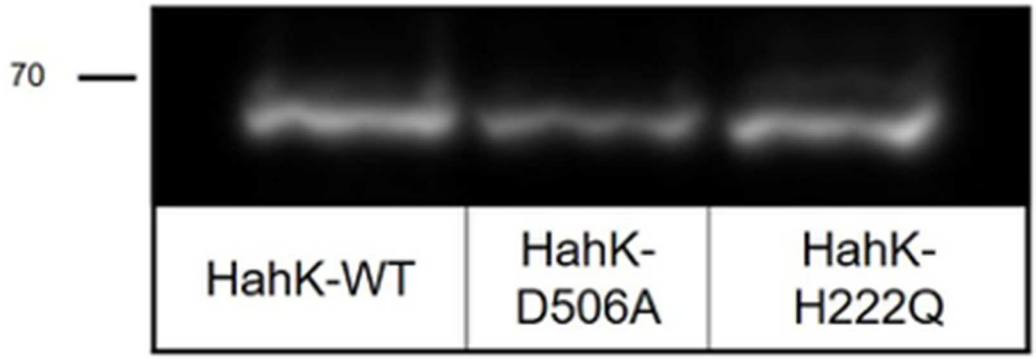

Figure 28. Protein Stability and Protein Production of HahK Phosphomutants. (A) Samples from overnight cultures of ES114 containing pKV522 (HahK-WT), pKV524 (HahK-D506A), and pKV523 (HahK-H222Q) respectively were collected to evaluate HA-tagged HahK protein production.

HnoX-Mediated Inhibiton of *syp* Transcription Depends on SypG

Dr. Thompson further investigated HnoX as an inhibitor of biofilm formation and determined that HnoX negatively regulates *syp* transcription. To confirm that the effect of HnoX on *syp* transcription was mediated by SypG, I performed a β-galactosidase assay to evaluate the epistatic relationship of SypG and HnoX. When either *sypG* or both *hnoX* and *sypG* were disrupted from the parent strain background, no *syp* transcription occurred (Figure 29), confirming that HnoX mediates *syp* transcription through SypG.

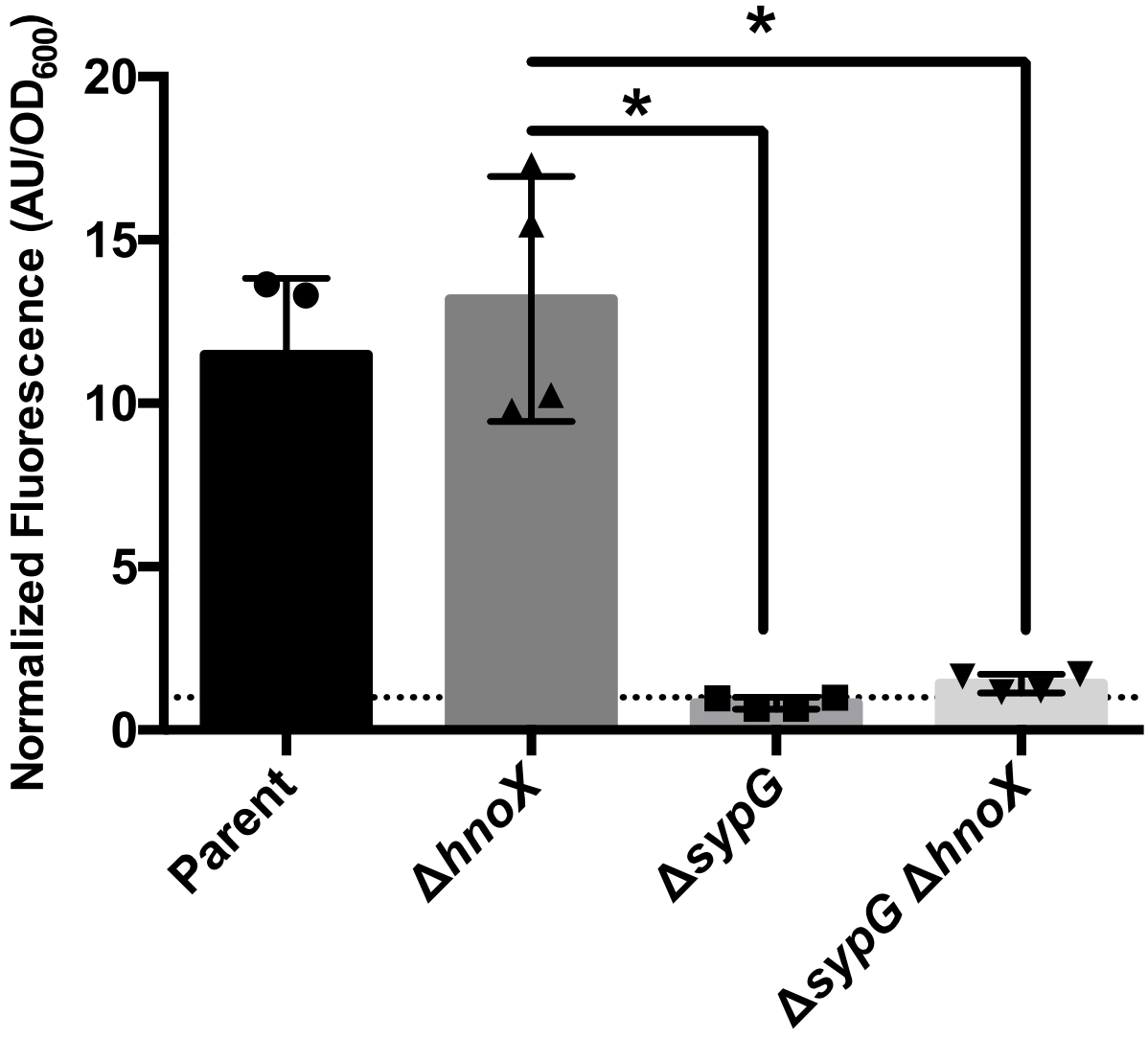

Figure 29. HnoX Mediates *syp* Transcription Through SypG. Strains expressing a P*sypA*-GFP reporter (pLL3) were grown overnight at 24°C. Strains were subcultured the next day at an OD_{600} = 0.05. The fluorescence and OD were measured at the indicated time points. The fluorescence/ OD_{600} for each strain was normalized to a biofilm (–) strain (indicated by the dotted line) to generate the normalized fluorescence. Strains are as follows: Parent (KV7856), Δ*hnoX* (KV8150), Δ*sypG* (KV8607) and Δ*hnoX* Δ*sypG* (KV8611), normalized against KV6567. The data were analyzed by a one-way ANOVA (*$p \leq 0.05$).

HnoX Inhibits Symbiotic Aggregation

Previous evidence demonstrated that an *hnoX* mutant outcompeted wild-type strains for colonization (Wang *et al.*, 2010), and Dr. Thompson identified HnoX as a negative regulator of biofilm formation. Therefore, we hypothesized that an *hnoX* mutant colonizes more efficiently because it forms a better biofilm. To test this possibility, in collaboration with Denise Tarnowski in Mark Mandel's lab at University of Wisconsin Madison, I exposed juvenile, aposymbiotic squid to approximately 3×10^6 of bacteria, of either a Δ*hnoX* mutant or parent strain. After a 3 h incubation, I then imaged and measured the symbiotic aggregates (biofilms). The *hnoX* mutant formed aggregates that consisted of a significantly larger surface area compared to the parent control strain, and the aposymbiotic control squid formed no aggregates (Figure 30). These results suggested that *hnoX* negatively regulates symbiotic biofilms, which may account, at least in part, for the colonization advantage previously seen by an *hnoX* mutant.

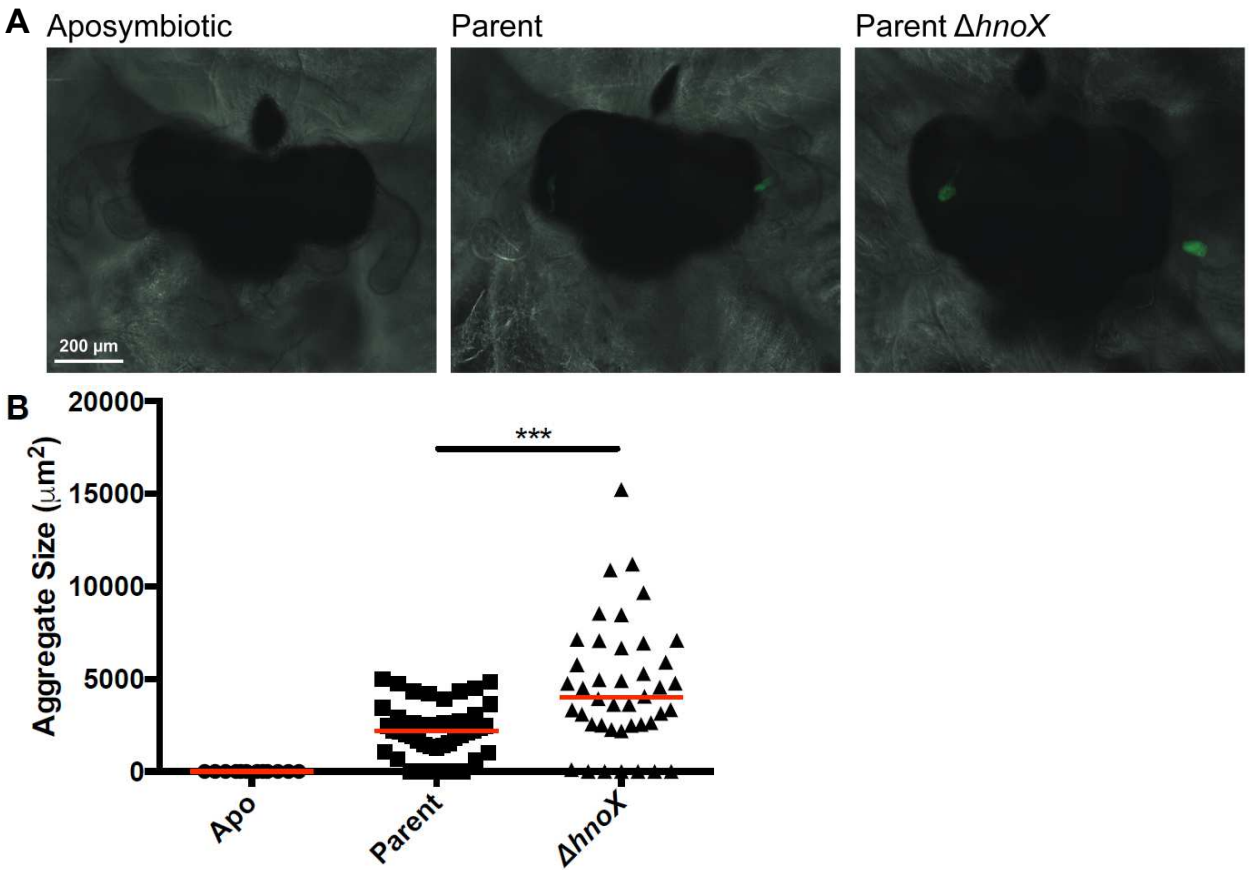

Figure 30. HnoX Inhibits Symbiotic Aggregation. (A) Aggregates at the entrance to the light organ were visualized at 3 h in either aposymbiotic juveniles or those inoculated with pVSV102-containing parent strain (KV3299) or the Δ*hnoX* derivative (KV8027). (B) Aggregate area was plotted for each inoculation condition as indicated above. Red lines indicate median. Samples were analyzed using a Mann-Whitney test ($p < 0.0001$, $p = 0.0002$); asterisks indicate significance between parent and Δ*hnoX* strains.

Summary

In this study, I helped to identify HahK as a positive regulator of SYP-dependent biofilm formation. We determined that HahK acts at the level of *syp* transcription and requires the Hpt domain of SypF to increase *syp* transcription, SYP-dependent shaking-liquid biofilms, and wrinkled colony formation. Utilizing a *hahK* mutant, I was able to identify the first *in vitro* phenotype for an *rscS* mutation, which highlights the complex redundancy of sensors modulating control of *syp* transcription. Additionally, the identification of HahK allowed us to identify and

characterize HnoX as an inhibitor of biofilm formation, epistatic to HahK, and dependent on the ability of HahK to engage in phosphotransfer. Finally, I found that HnoX is able to form larger symbiotic aggregates during symbiosis initiation, expanding on our understanding of HnoX as an inhibitor of biofilm formation and colonization.

Establishing a Direct Connection Between Calcium, C-di-GMP, and Biofilm Formation

Introduction

Bacteria adapt to their surroundings by recognizing environmental signals, resulting in changes in gene expression, protein production and/or activity, and other processes that permit them to survive and/or thrive accordingly. In many bacteria, internal signaling relies on cyclic dinucleotides, such as bis(3'-5')-cyclic dimeric guanosine monophosphate (c-di-GMP), a small ubiquitous second messenger that regulates numerous bacterial behaviors, including biofilm formation, motility, and virulence (Römling *et al.*, 2013, Valentini & Filloux, 2016). C-di-GMP is synthesized by diguanylate cyclases (DGC), which contain a GGDEF domain, and is degraded by phosphodiesterases (PDE), containing either EAL or HD-GYP domains (Hecht & Newton, 1995, Galperin *et al.*, 1999, Tal *et al.*, 1998). The number of DGCs and PDEs encoded within bacterial genomes can differ greatly between species with many organisms containing dozens of such genes, highlighting the importance of c-di-GMP as an intracellular signal (Römling *et al.*, 2013). *V. fischeri* contains 50 putative DGC/PDE genes: 28 with GGDEF domains, 9 with EAL domains, 11 containing both GGDEF and EAL domains, and 2 genes with HD-GYP domains (Figure 4) (Ruby *et al.*, 2005, Mandel *et al.*, 2008, Wolfe & Visick, 2010).

Calcium is one environmental signal linked to c-di-GMP and known to impact bacterial biofilm formation (King *et al.*, 2020). In addition to the strong positive regulation of *V. fischeri* biofilm formation detailed in the previous section, calcium affects biofilm formation in both *V.*

cholerae and *V. vulnificus* (Chodur *et al.*, 2018, Bilecen & Yildiz, 2009). In *V. cholerae,* the calcium-sensing two-component system CarRS decreases transcription of *vpsR*, resulting in decreased *vps* transcription and biofilm formation (Bilecen & Yildiz, 2009). While calcium and c-di-GMP have not been directly linked in *V. cholerae,* c-di-GMP has been shown to increase VpsR activity (Srivastava *et al.*, 2011). In *V. vulnificus,* calcium increases c-di-GMP, increasing transcription of the *b*iofilm and *r*ugose *p*olysaccharide (*brp*) locus, dependent on both the IamA pilin and VpsR homolog, BrpR (Chodur *et al.*, 2018, Pu *et al.*, 2020, Guo & Rowe-Magnus, 2010). The calcium-binding matrix protein, CabA, which is also induced by calcium, contributes to rugosity and matrix structure (Park *et al.*, 2015, Chodur & Rowe-Magnus, 2018). *V. fischeri* does not encode homologs of *V. cholerae*'s CarRS SK/RR system, or CabA in *V. vulnificus*. As described above, in *V. fischeri*, calcium coordinately induces transcription of genes for the synthesis of two polysaccharides known to contribute to biofilm formation, *bcs* (cellulose) and *syp* (*sy*mbiosis *p*olysaccharide (SYP)). The mechanism by which calcium increases transcription of polysaccharide loci and induces biofilm in *V. fischeri* is as yet unknown. Calcium also inhibits *V. fischeri* motility, a behavior considered to be the opposite of sessile biofilm formation, which modulated by changes in c-di-GMP levels; however, the mechanism by which calcium inhibits motility also is unknown (O'Shea *et al.*, 2005, O'Shea *et al.*, 2006). Understanding how *V. fischeri* biofilm formation and motility are controlled in response to environmental signals, specifically calcium, is important as both phenotypes represent key behaviors for symbiotic colonization (Yip *et al.*, 2005, Yip *et al.*, 2006, Millikan & Ruby, 2002).

Given the strong links between c-di-GMP and both biofilm formation and motility, my goal was to find a link between calcium and c-di-GMP. This initial search and subsequent work was aided by two sets of tools (1) a biosensor generously gifted to us by Dr. Fitnat Yildiz at

University of California Santa Cruz (Zamorano-Sánchez *et al.*, 2019), and (2) a set of strains containing single deletions of every putative DGC and PDE in the *V. fischeri* genome created by former technician, Ali Razvi. Access to these tools allowed me to introduce the c-di-GMP biosensor into each of the 50 single mutant strains created by Ali in order to screen for changes in c-di-GMP levels in response to calcium, as well as screen the mutant strains for calcium-dependent biofilm phenotypes. For concision and clarity, the results of these screens are only briefly touched on here, and are explored in greater detail in **Appendix A**. In this section, I focus on establishing a connection between calcium and c-di-GMP, and identifying, functionally characterizing, and uncovering a role in cellulose-dependent biofilm formation for a calcium-sensing DGC, CasA.

Calcium Increases Intracellular C-di-GMP

My previous results demonstrated that calcium induces biofilm formation through transcriptional activation of the genes for two distinct polysaccharides, SYP and cellulose. Calcium also impacts *V. fischeri* motility, where low levels of calcium (up to 20 mM) increase migration distance and high levels (40+ mM) inhibit migration (O'Shea *et al.*, 2005). Both biofilm formation and motility are classic behaviors regulated by c-di-GMP, and motility in *V. fischeri* has previously already been linked to c-di-GMP (O'Shea *et al.*, 2006). Therefore, we hypothesized calcium could alter c-di-GMP in *V. fischeri*, resulting in altered bacteria behaviors.

To ask if calcium altered intracellular c-di-GMP, we used a c-di-GMP biosensor plasmid pFY4535, from the Yildiz lab at University of California Santa Cruz (Zamorano-Sánchez *et al.*, 2019). Briefly, this plasmid works by expressing a constitutive AmCyan cassette, followed by a c-di-GMP binding riboswitch that controls expression of a Turbo-RFP cassette (Figure 31A) (Zamorano-Sánchez *et al.*, 2019). Therefore, the more RFP that is detected, the higher the

relative levels of c-di-GMP within the cell, with the AmCyan functioning as an internal control. Additionally, this plasmid contains both a Gent^r resistance cassette, and a *hok/sok* toxin/antitoxin system allowing for maintenance without antibiotic selection after the initial conjugation/selection event. I conjugated this plasmid first into ES114 and used flow cytometry as a method to assess and measure AmCyan and RFP. In previous experiments I had used 10 mM calcium to assess calcium-related phenotypes, because 10 mM is approximately the level found in seawater. However, I found that while addition of 10 mM calcium did result in a small increase in c-di-GMP, it was difficult to see meaningful differences via flow cytometry (Figure 31B). Therefore, I explored a range of calcium concentrations, up to 50 mM, and found that increasing amounts of calcium led to a fairly stepwise increase in relative c-di-GMP levels based on the mean fluorescence intensity (MFI) of RFP in live AmCyan$^+$ RFP$^+$ cells (Figure 31B). These data indicated that increasing calcium resulted in increased relative c-di-GMP. Current student, Michael Vanek performed a motility experiment showing that calcium impacted *V. fischeri* motility up to 100 mM, which led me to increase my calcium range to 100 mM and assess c-di-GMP. Consistent with my earlier results, the MFI of live AmCyan$^+$ RFP$^+$ cells increased in a linear fashion as calcium increased (Figure 31C). I performed a linear regression analysis to evaluate a best fit line for the data and determined that the line is significantly non-zero with a slope of 68.48 (Figure 31C). Additionally, I compared histograms from representative samples of live AmCyan$^+$ RFP$^+$ cells grown with 0, 20, and 60 mM calcium, which revealed a definite shift and increase in RFP as calcium increased (Figure 31D). These data indicate that calcium is able to increase relative levels of c-di-GMP in *V. fischeri* in a dose-dependent manner.

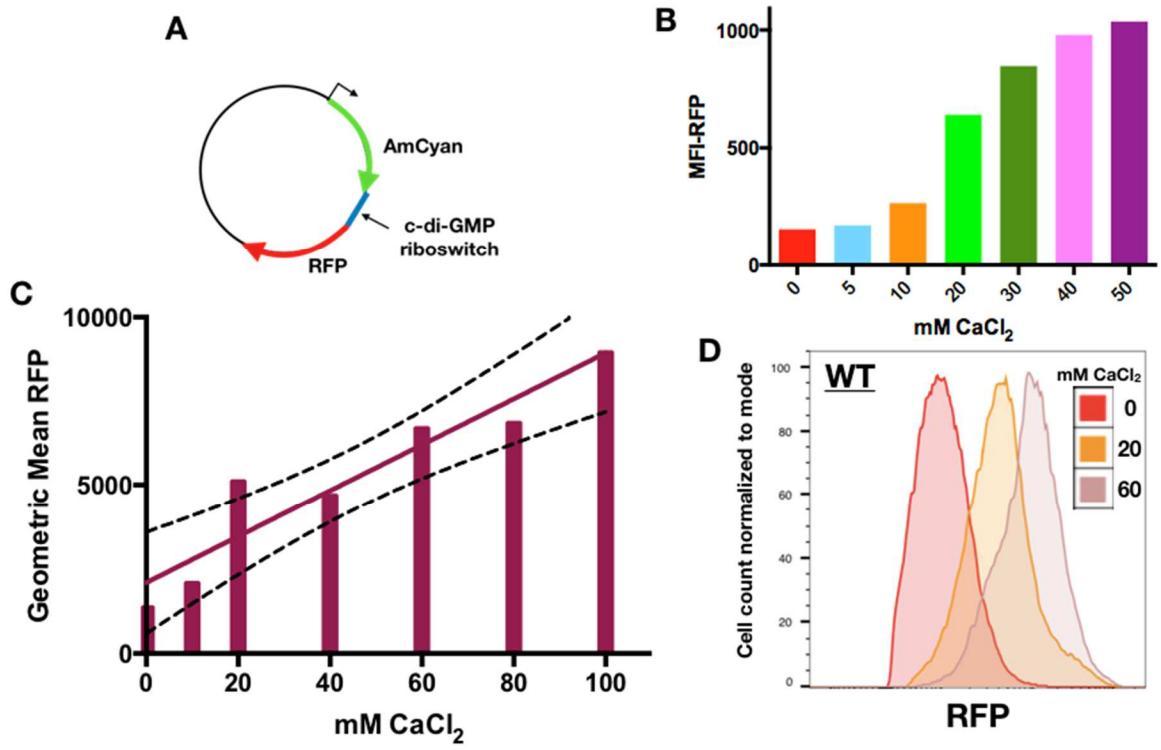

Figure 31. Calcium Increases Relative C-di-GMP. (A) Schematic of pFY4535 c-di-GMP biosensor plasmid, which contains a constitutive AmCyan cassette and a c-di-GMP binding riboswitch that controls Turbo-RFP expression. (B) Mean fluorescence intensity (MFI) of RFP from WT ES114 containing biosensor grown with increasing concentrations of calcium. (C) Geometric mean of RFP, the area under the curve as determined via flow cytometry for ES114 (WT) containing the pFY4535 biosensor plasmid. Data points represent three biological replicates at increasing concentrations of $CaCl_2$ as indicated. Solid lines indicate linear regression fitted slope lines, and dotted lines indicated the confidence interval. (D) Representative histogram showing $AmCyan^+$ RFP^+ live cells, with cell count normalized to mode. X-axis shows increasing RFP. Colors represent different amounts of calcium, 0, 20, 60 mM as indicated.

A *casA* Mutant Strain Displays Calcium-Dependent Phenotypes

I hypothesized that calcium could signal to activate a DGC(s) or deactivate a PDE(s) to result in a calcium-dependent increase in c-di-GMP levels. To assess this possibility, I took the 50 single DGC/PDE mutant strains constructed by Ali Razvi and screened them for changes in (1) wrinkled colony formation, (2) Congo red binding (indicative of cellulose production), and (3) c-di-GMP levels as determined by the biosensor. The majority of mutant strains either did not

display strong phenotypes under the conditions tested or responded to calcium similarly to ES114. One strain in particular that displayed strong calcium-dependent phenotypic changes had a deletion of the gene *VF_1639*. Based on experimental results, we named *VF_1639 ca*lcium *s*ensing protein A (CasA), and I will use CasA throughout for consistency and clarity.

I first evaluated wrinkled colony formation, which is a measure of SYP-dependent biofilms. To date, SYP is the only polysaccharide with an established role in symbiotic colonization and is known to be required for colonization (Yip *et al.*, 2005, Yip *et al.*, 2006). A *casA* mutant strain displayed very mild phenotypic differences compared to WT and Δ*binK* parent strains (Figure 32). No differences were seen compared to the parent strain in the absence of calcium. When 10 mM calcium was added, ES114 contained subtle architecture distinct from wrinkling, and a *casA* mutant strain was missing some, but not all of the architecture (Figure 32, left). In a *binK* mutant strain, a *casA* mutation resulted in a very slight increase in wrinkling at the center of the colony (Figure 32, right). Overall, the solid agar phenotypes dependent on CasA were extremely mild, which suggests that CasA likely does not impact SYP-dependent biofilm formation.

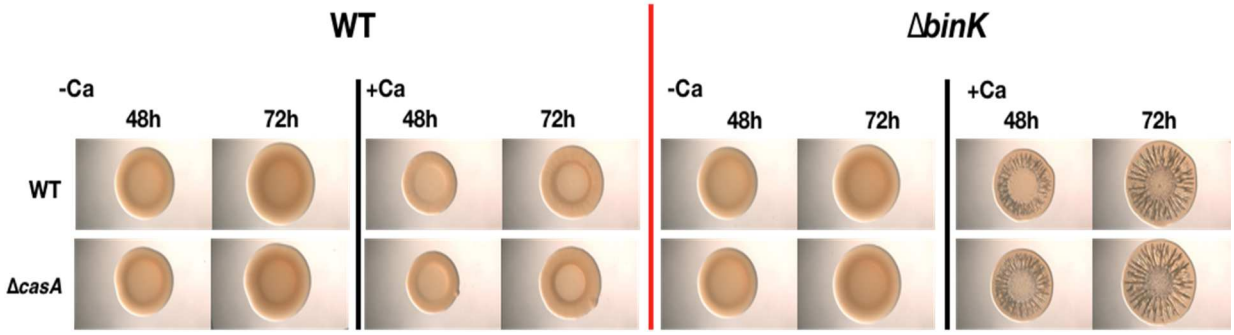

Figure 32. Wrinkled Colony Phenotypes of a Δ*casA* Mutant Strain. A *casA* mutant strain in either a WT or *binK* mutant background was assess for wrinkled colony formation at the indicated time points on one day old LBS plates. – or + Ca refers to 0 or 10 mM added calcium, respectively.

I next assessed binding to Congo red. Congo red is a dye that binds to a variety of polysaccharides and amyloid fibers, including cellulose. Visualizing color on Congo red is standard for evaluating cellulose and curli-dependent biofilms in *E. coli* and *Salmonella* spp., which are among the best studied cellulose-dependent biofilms (Römling *et al.*, 2000, Römling, 2005, Zogaj *et al.*, 2001). I saw no color differences between ES114 and a *casA* mutant strain on LBS Congo red agar without calcium (Figure 33, top). Dr. Karen Visick had previously assessed several DGC/PDE mutant strains on Congo red agar with added calcium, and found that a *casA* mutant strain bound less dye than WT. I repeated that assay, and confirmed that on plates with calcium a *casA* mutant strain did bind less dye than WT, resulting in a lighter color (Figure 33, bottom). This result was particularly intriguing as it suggests that CasA could affect cellulose polysaccharide production, but only in the presence of calcium.

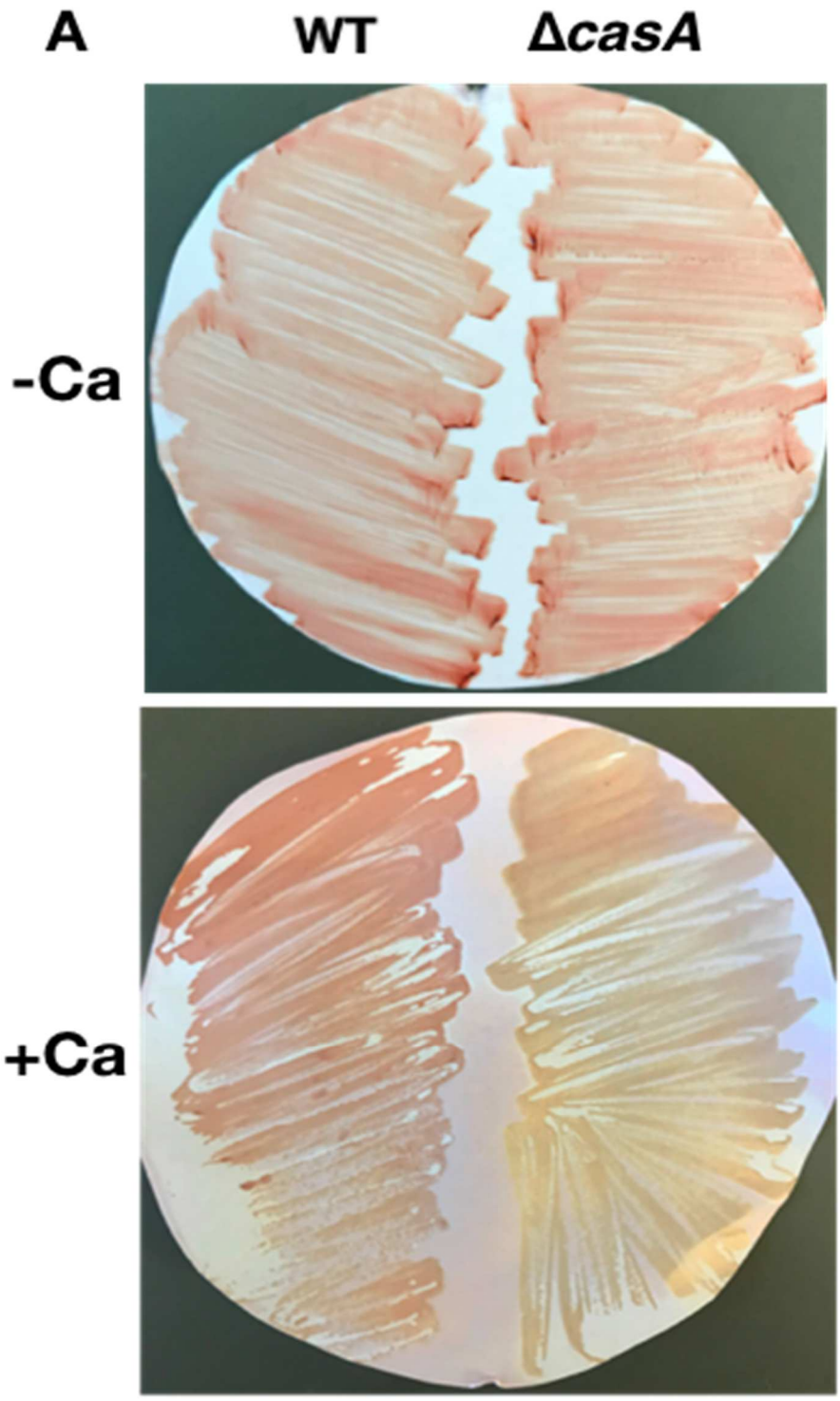

Figure 33. Congo Red Binding Phenotypes Dependent on CasA. WT or a *casA* mutant strain were grown on LBS Congo red plates at 24°C for 24 h, and then bacteria was collected using a piece of white paper to assess color. Plate on the top has no added calcium, plate on the bottom had 10 mM added calcium.

Finally, I evaluated relative c-di-GMP levels using the c-di-GMP biosensor. I first determined the fold change of RFP (c-di-GMP) in response to 40 mM calcium in a *casA* mutant. WT increased relative c-di-GMP approximately 3-fold in response to calcium. However, a *casA* mutant strain showed no change in relative c-di-GMP in response to calcium (Figure 34A). This result was a single snapshot of one calcium concentration, so I repeated this experiment at increasing calcium levels from 10-100 mM. Representative histograms and the geometric mean of RFP, from $AmCyan^+$ RFP^+ live cells, revealed that c-di-GMP levels in the Δ*casA* mutant continued to stay approximately the same, regardless of calcium concentration (Figure 34B & C). ES114's response to calcium is shown as a comparison (Figure 34C). Linear regression analysis of the best fit line of the values from the *casA* mutant revealed that this line is significantly greater than zero, with a slope of 10.27, indicating that between 0-100 mM calcium, a *casA* mutant strain did have a small increase in c-di-GMP in response to calcium (Figure 34C). However, visually and statistically, the best fit lines were significantly different between WT and a *casA* mutant, confirming statistically that CasA is responsible for a significant portion of the calcium-dependent increase in c-di-GMP.

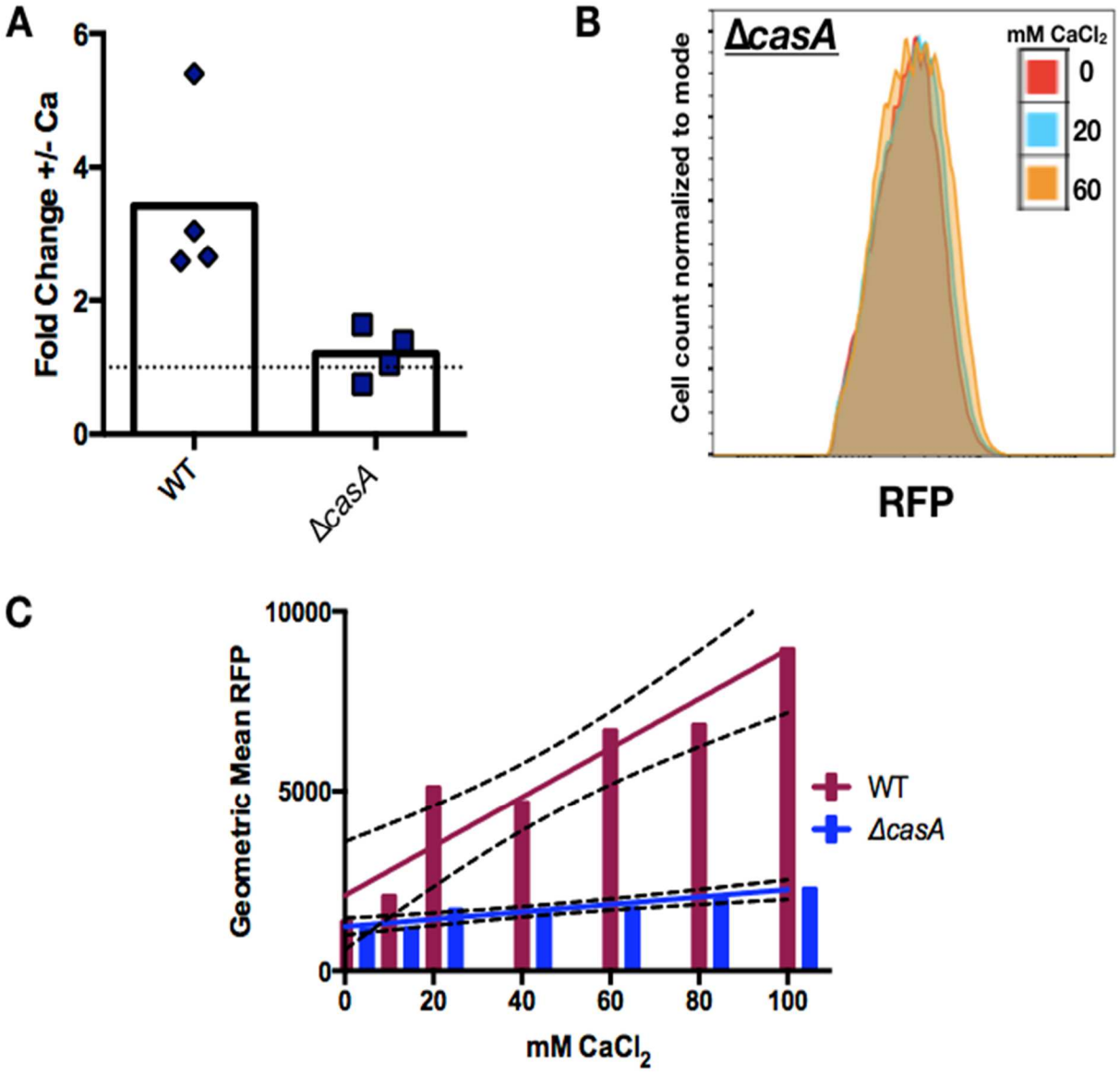

Figure 34. A *casA* Mutant Strain Does Not Increase C-di-GMP in Response to Calcium. (A) Fold change in the MFI-RFP levels of both WT and a *casA* mutant grown with and without 40 mM calcium. (D) Representative histogram showing AmCyan^{+} RFP^{+} live cells, with cell count normalized to mode. X-axis shows increasing RFP. Colors represent different amounts of calcium, 0, 20, 60 mM as indicated. (C) Geometric mean of RFP, the area under the curve as determined via flow cytometry comparing WT and Δ*casA* containing the pFY4535 biosensor plasmid. Data points represent three biological replicates at increasing concentrations of $CaCl_2$ as indicated. Solid lines indicate linear regression fitted slope lines, and dotted lines indicated the confidence interval. *Note, the values for WT here are the same as in Figure 31 C.

In addition to biofilm formation, c-di-GMP also impacts motility as they are directly opposite behaviors. Other lab members including Dr. Karen Visick and Steven Eichinger were screening c-di-GMP mutant strains for motility phenotypes, and noted increased motility in the Δ*casA* mutant strain in the presence of calcium. I repeated these experiments, comparing WT and a Δ*casA* mutant strain in soft-agar with either no supplementation (TBS-), 35 mM magnesium (TBS Mg^{2+}), and 10 mM calcium (TBS Ca^{2+}). Magnesium is added because it promotes bacterial flagellation and migration (O'Shea *et al.*, 2005); however, *V. fischeri* will migrate without magnesium. In media with either no supplementation or magnesium, WT and a Δ*casA* mutant migrated the same distance over time (Figure 35). However, when calcium was added, as others had previously observed, I also found that the Δ*casA* mutant strain was able to migrate farther than WT over time (Figure 35). Additionally, Michael Vanek explored motility at a higher range of calcium concentrations with and without magnesium. He found that on soft-agar with 35 mM magnesium, WT decreased migration when calcium is added in a dose dependent manner; however, a Δ*casA* mutant strain exhibited no change in migration up to 100 mM calcium. Together, these data demonstrate that, in addition to biofilm formation, CasA also has a role in calcium-inhibited motility.

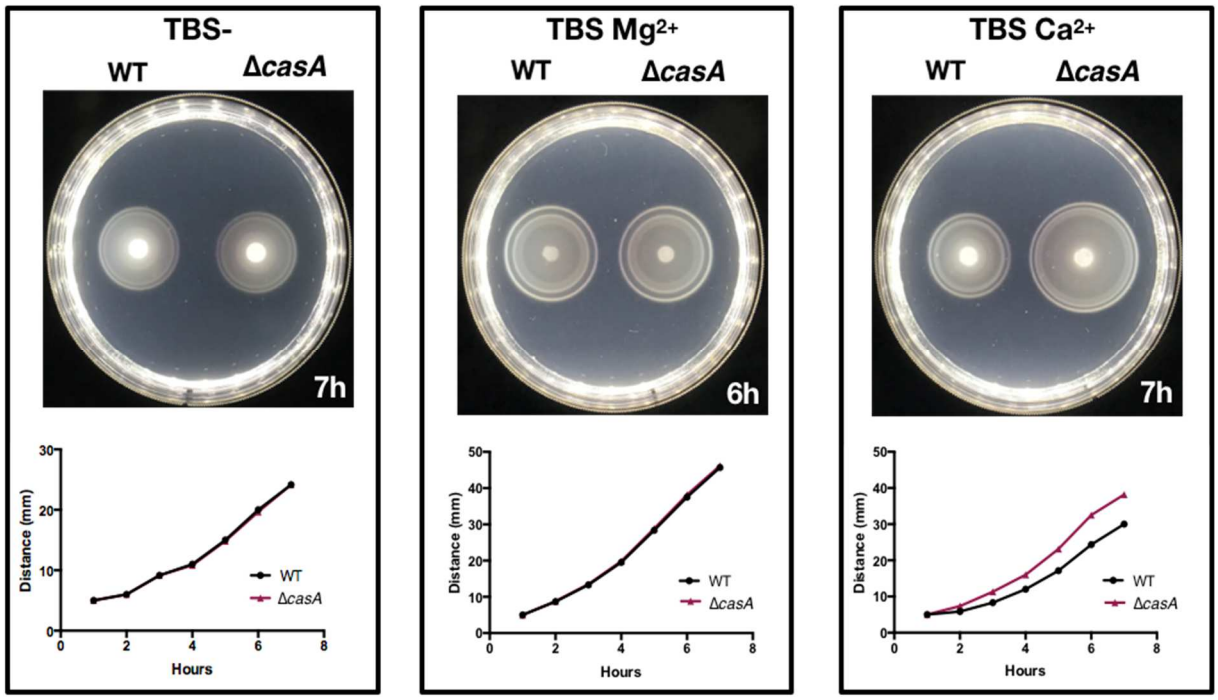

Figure 35. CasA Has a Role in Calcium-Inhibited Motility. WT and *casA* mutant strains were grown overnight and subbed in TBS media, before being normalized and spotted onto TBS soft agar plates with either no supplementation, 35 mM magnesium, or 10 mM calcium. Strains were incubated at 28°C, and diameters were measured every hour up to 8 h. Representative images were take at the times indicated.

Calcium-Induced Cellulose is Dependent on CasA

Based on the preliminary screens, I hypothesized that calcium increases cellulose polysaccharide dependent on CasA. Therefore, I performed a Congo red assay with WT, Δ*casA*, complemented Δ*casA* (Δ*casA*/*casA*$^+$), and Δ*bcsA* mutant strains to confirm that CasA impacts cellulose. On plates without calcium, I observed that WT, Δ*casA*, and Δ*casA/casA*$^+$ strains were all the same color, while a Δ*bcsA* mutant strain was less red, meaning that it bound less dye (Figure 36, top). In contrast, on plates containing calcium, WT and Δ*casA/casA*$^+$ remained the same color, while a Δ*casA* mutant strain bound less dye, appearing the same color as a Δ*bcsA* mutant strain (Figure 36, bottom). These data support a connection between calcium, CasA, and cellulose.

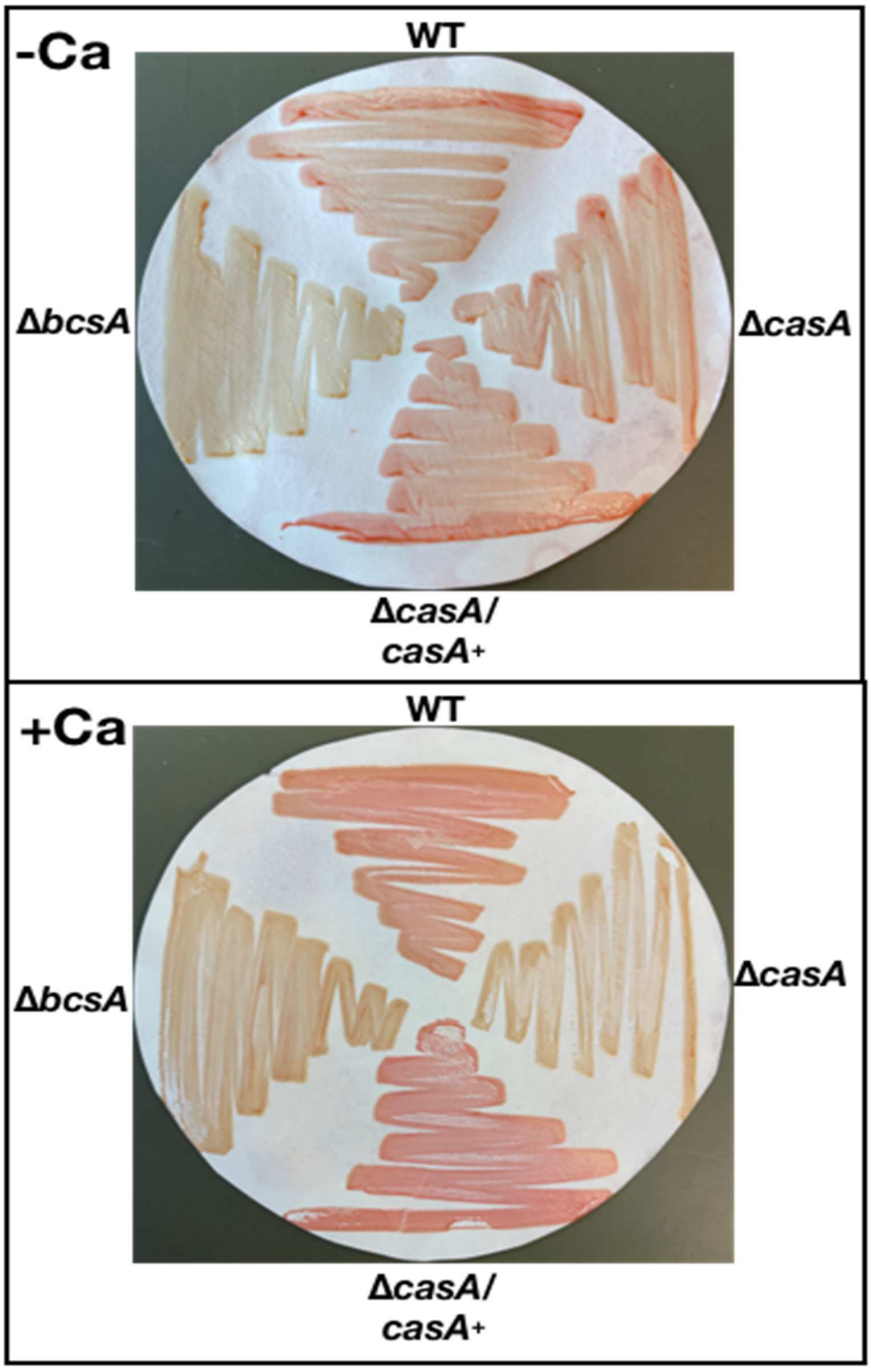

Figure 36. CasA Induces Congo Red Binding in Response to Calcium. Congo red dye bound to bacteria grown on LBS plates without (top) and with (bottom) added 40 mM calcium. Clockwise from the top, the strains are: WT (ES114) and Δ*casA* (KV9179), Δ*casA/casA*$^{+}$ (KV9821), and Δ*bcsA* (KV7894) mutants.

To further support this hypothesis, I examined shaking-liquid biofilm phenotypes with increasing amounts of calcium. I observed robust ring formation in WT increasing as calcium levels increased (Figure 37A). Conversely, a Δ*casA* mutant strain was defective for ring formation; however, Δ*casA/casA*$^{+}$ phenocopied WT, displaying strong surface attachment (Figure 37A). I stained tubes with crystal violet (Figure 37A, right, representative image), destained, and measured biomass via OD_{600} (Figure 37B). I analyzed the resulting graphs with linear regression analysis and determined that the best fit lines of WT and Δ*casA/casA*$^{+}$ were both significantly different from zero, but not significantly different from each other. Additionally, the best fit line from the Δ*casA* mutant strain was not significantly different from zero, indicating no increase in biomass in response to calcium. Overall, these data confirm that calcium-induced ring formation is dependent on CasA.

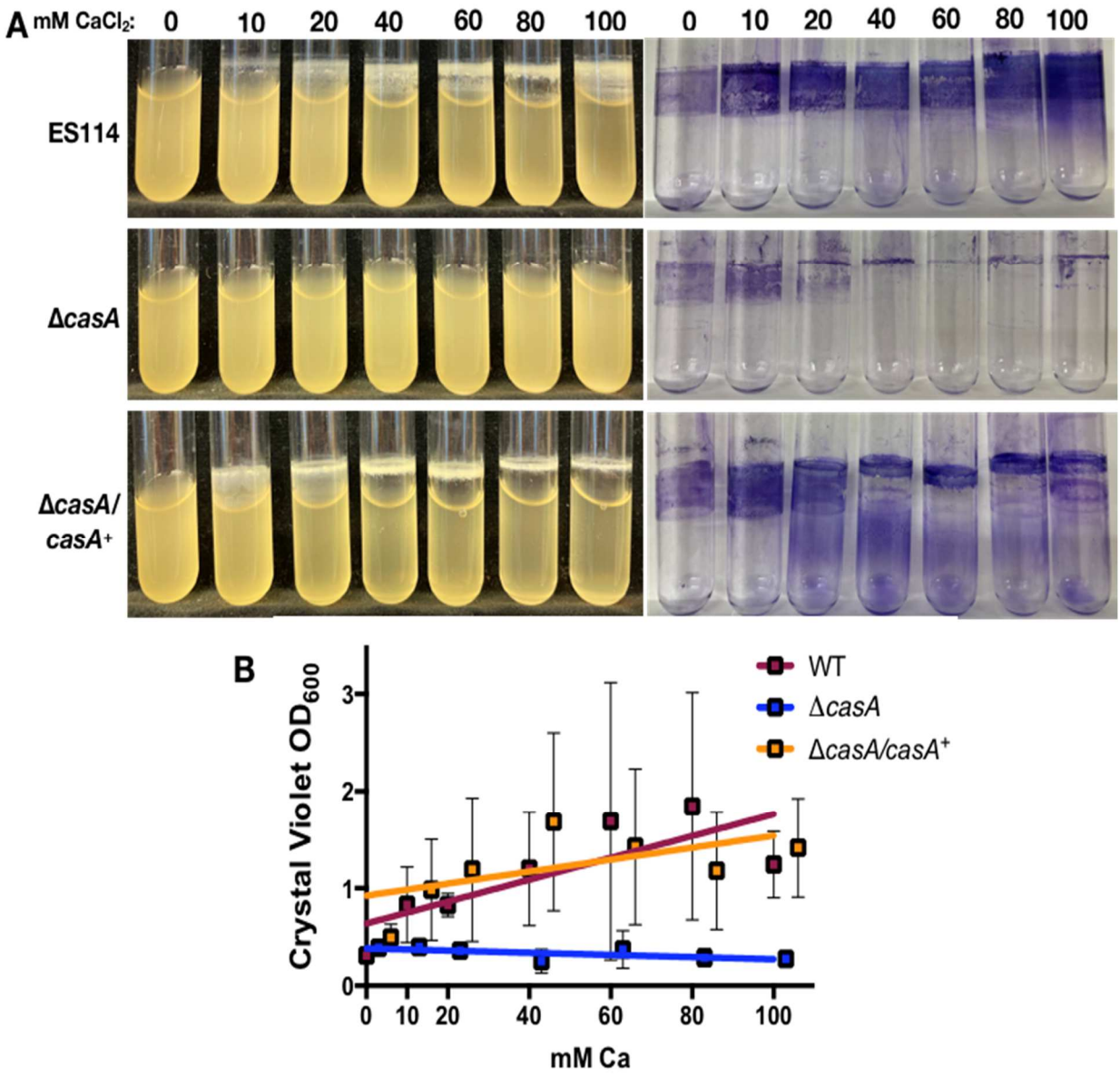

Figure 37. CasA Induces Cellulose-Dependent Biofilms in Response to Calcium. (A) Shaking biofilm assay with increasing amounts of exogenous calcium added to cultures. Strains are ES114 (WT), Δ*casA* (KV9179), and Δ*casA/casA*$^{+}$ (KV9821). Left- representative set of tubes stained with crystal violet before destaining (B) Quantification of crystal violet staining of biofilms like those show in panel A. Symbols represent the mean of each sample and error bars are the standard deviation. Solid lines indicate linear regression analysis, where the lines that represent WT (red) and the ΔcasA/casA+ strain (orange) are not significantly different from each other but are significantly different from the ΔcasA mutant (blue, p=0.02).

CasA is Responsible for Calcium-Dependent Increase in *bcs* Transcription.

Because I previously saw that calcium significantly increases transcription of the *bcs* locus, leading to an increase in cellulose polysaccharide, I hypothesized that CasA might control cellulose production at the level of transcription. To evaluate this possibility, I used a P*bcsQ-lacZ* transcriptional reporter. While *bcsQ* transcription in WT increased significantly after addition of calcium, transcription of *bcsQ* in the Δ*casA* mutant remained constant regardless of calcium (Figure 38A). These data suggested that CasA is necessary for the calcium-dependent increase in *bcs* transcription.

As I previously saw, VpsR is an activator of *bcs* transcription (Figure 16A). Since both VpsR and CasA impact *bcs* transcription, I asked if CasA were epistatic to VpsR. Previously, I saw that *vpsR* overexpression resulted in a calcium-dependent increase in *bcs* transcription (Figure 16B). I overexpressed *vpsR* in a Δ*casA* Δ*vpsR* double mutant strain background. *vpsR* overexpression increased *bcsQ* transcription but did not induce a response to calcium (Figure 38B). This indicated that CasA is needed for the calcium-dependent increase in *bcs* transcription.

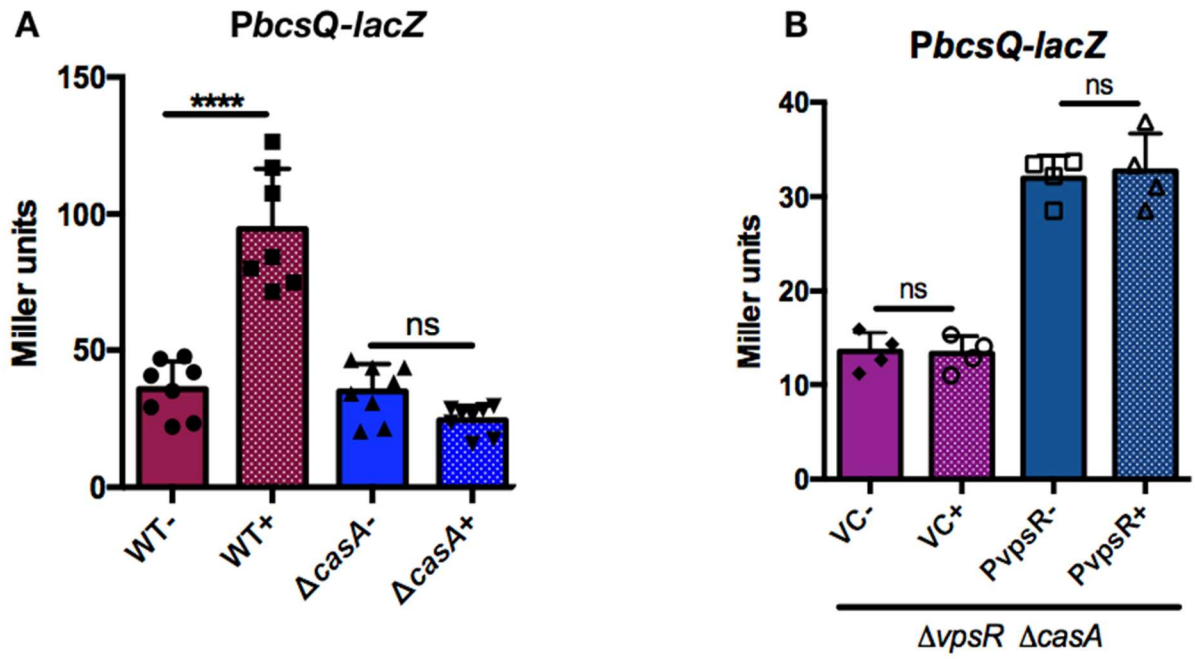

Figure 38. Impact of Calcium, CasA and VpsR on *bcs* Transcription. (A) PbcsQ-lacZ reporter strains WT (KV8078) and Δ*casA* (KV9864) grown with (+) or without (-) 40 mM added calcium as indicated. Only WT exhibited a significant increase in bcsQ transcription when calcium is added,(p=0.0001****). (B) Δ*vpsR* Δ*casA* double (KV9868) mutants containing either vector control (VC; pKV69) or *vpsR* over expression (PvpsR; pCLD42) grown with (+) or without (-) 40 mM added calcium as indicated.

vpsR Transcription is Independent of Calcium and Negatively Autoregulated

In *V. cholerae*, calcium decreases transcription of *vpsR* (Bilecen & Yildiz, 2009). While *V. fischeri* does not encode the CarRS SK/RR TCS responsible, it was still possible that calcium, through CasA could alter *vpsR* transcription. To test this, I designed a P*vpsR-lacZ* reporter construct, and measured β-galactosidase activity with and without calcium. I found that in a WT strain, calcium had no effect on *vpsR* transcription (Figure 39A), suggesting that *vpsR* is independent of calcium. Therefore, CasA and the calcium-dependent increase in *bcs* transcription likely occurs after *vpsR* transcription.

Additionally, VpsR in *V. cholerae* positively autoregulates, which has downstream impacts for *vps* transcription and subsequent *V. cholerae* biofilm formation (Casper-Lindley & Yildiz, 2004). Therefore, I asked if VpsR in *V. fischeri* also had autoregulatory activity by assessing *vpsR* transcription in WT and a Δ*vpsR* mutant strain. Surprisingly, I found that *vpsR* transcription was significantly increased in a Δ*vpsR* mutant compared to WT, suggesting negative autoregulation (Figure 39B). To confirm this, I measured *vpsR* transcription when *vpsR* was overexpressed in WT. Consistent with the Δ*vpsR* mutant strain results, overexpression resulted in decreased transcription (Figure 39C). Together, these data suggest that VpsR negatively autoregulates- opposite to VpsR in *V. cholerae*.

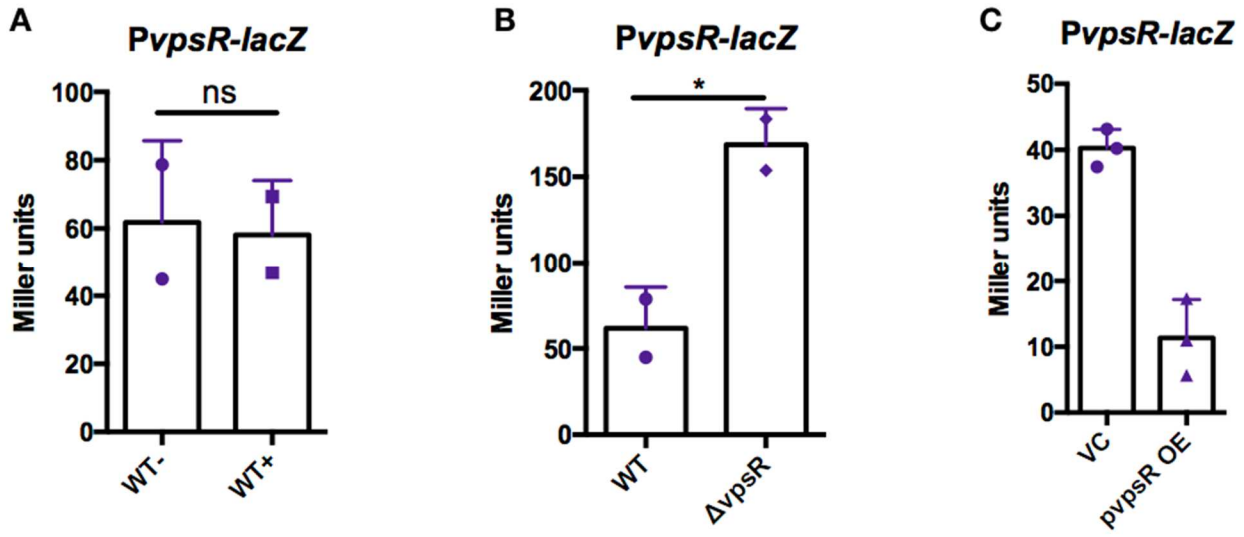

Figure 39. Expression of the *vpsR* Promoter. **(A)** P*vpsR-lacZ* (KV9573) reporter strain with and without addition of 10mM $CaCl_2$. **(B)** P*vpsR-lacZ* (KV9573) and Δ*vpsR* P*vpsR-lacZ* (KV9867) strains without any added calcium. Note, "WT" values are the same in panel A and panel B. **(C)** P*vpsR-lacZ* reporter strain (KV9573) containing either a vector control, pKV69, or over expression of *vpsR*, pCLD42.

CasA is a Functional DGC

I determined that CasA is responsible for calcium-dependent motility and cellulose biofilm phenotypes and is specifically required for a calcium-dependent increase in *bcs*

transcription. To begin to probe how CasA functions to cause these downstream phenotypes, I examined the structure of CasA (Figure 40). Domain prediction in BLAST (Altschul *et al.*, 1990, Altschul *et al.*, 1997, Boratyn *et al.*, 2012, Camacho *et al.*, 2009) identify a sensory domain and a GGDEF domain on the N and C-terminal ends, respectively. The enzymatic GGDEF domain has a RXXD motif for an inhibitory (I-site) and a GGEEF motif indicative of an active site. I-sites are found in many DGCs and allosterically bind c-di-GMP, inhibiting c-di-GMP production (Christen *et al.*, 2006), while active sites are responsible for signal synthesis (Tal *et al.*, 1998, Paul *et al.*, 2007). Function of these motifs is typically probed by mutating the R in the I-site and either the second G or the following E/D residue. I used site directed mutagenesis to make R400A and G410A substitutions (Figure 40, red letters). These alleles were expressed under the control of the constitutive *nrdR* promoter followed by an idealized RBS and were HA tagged on the C-terminal end. I inserted these constructs single copy into the chromosome of a *casA* mutant strain, at the intergenic region between *yeiR* and *glmS*, which is a site we commonly use for gene insertions (Visick *et al.*, 2018). All variants were stably expressed (Figure 41A).

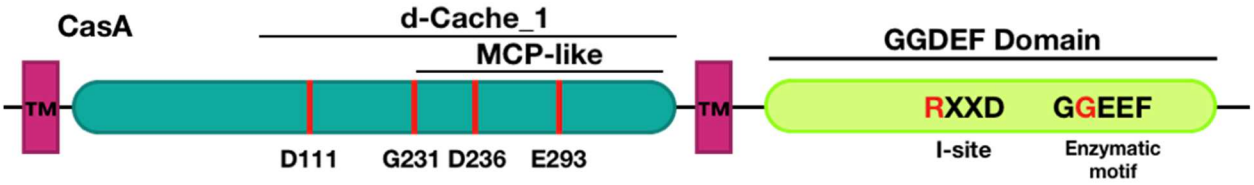

Figure 40. Schematic of General CasA Protein Structure. Two transmembrane regions flank a N-terminal sensory domain (teal) with predicted d-Cache-1 and MCP-like domains. The C-terminal domain consists of a GGDEF DGC domain containing an enzymatic GGEEF motif. Red lines and letters indicate substituted residues. All locations are approximate and not to scale.

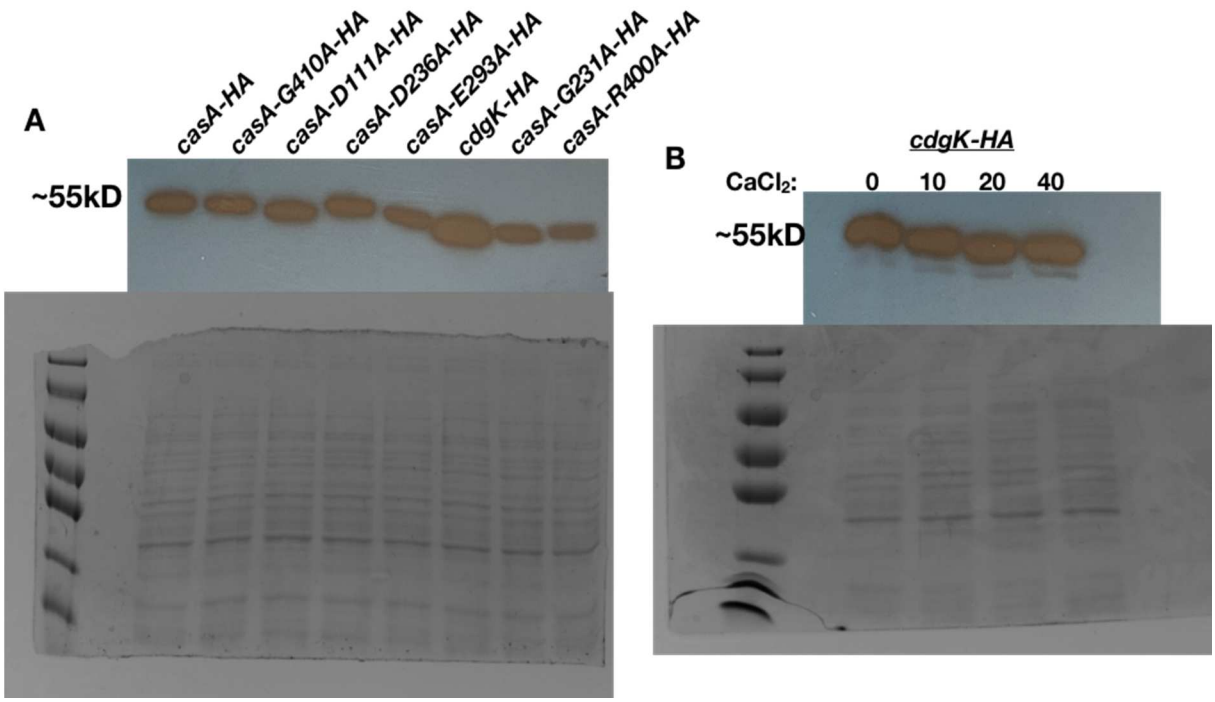

Figure 41. Western Blots Confirming Expression and Ctability of CasA and CdgK Variants. Bacterial strains containing the indicated alleles inserted in the intergenic region between *yieR-glmS* in a Δ*casA* mutant background (see methods). Cultures were normalized and run on two gels in tandem, one was stained with Coomassie blue as a loading control (bottom), and the other was transferred and probed with an α-HA antibody (Top). Blot is representative of over three replicates (A) Strains are: Δ*casA* IG::*casA*-HA (KV9821), Δ*casA* IG::*casA*-G410A-HA (KV9822), Δ*casA* IG::*casA*-D111A-HA (KV9825), Δ*casA* IG::*casA*-D236A-HA (KV9826), Δ*casA* IG::*casA*-E293A-HA (KV9827), Δ*casA* IG::*cdgK*-HA (KV9828), and Δ*casA* IG::*casA*-G231A-HA (KV9824). (B) Δ*casA* IG::*cdgK*-HA (KV9828) grown with the indicated amount of calcium.

Assessing relative c-di-GMP levels with the biosensor, I found that the CasA-G410A-expressing strain phenocopied its Δ*casA* parent, failing to increase c-di-GMP levels in response to calcium as seen by the Δ*casA/casA*$^{+}$ complement strain (Figure 42A). The CasA-G410A variant also failed to complement the Congo red phenotype, binding similar amounts of dye as the Δ*casA* parent strain (Figure 42B). Conversely, looking at both relative c-di-GMP levels and Congo red phenotypes, I found that the CasA-R400A variant phenocopied the Δ*casA/casA*$^{+}$

strain, demonstrating no phenotype specific to the I-site disruption (Figure 42A & B). Additionally, Michael Vanek performed motility experiments of these strains, and the results were consistent with the data presented here, where CasA-G410A phenocopied the Δ*casA* parent, and CasA-R400A phenocopied the WT CasA complement. Together, these data suggest that while the I-site has no phenotype under these conditions, c-di-GMP production is necessary for the calcium-dependent biofilm formation controlled by CasA.

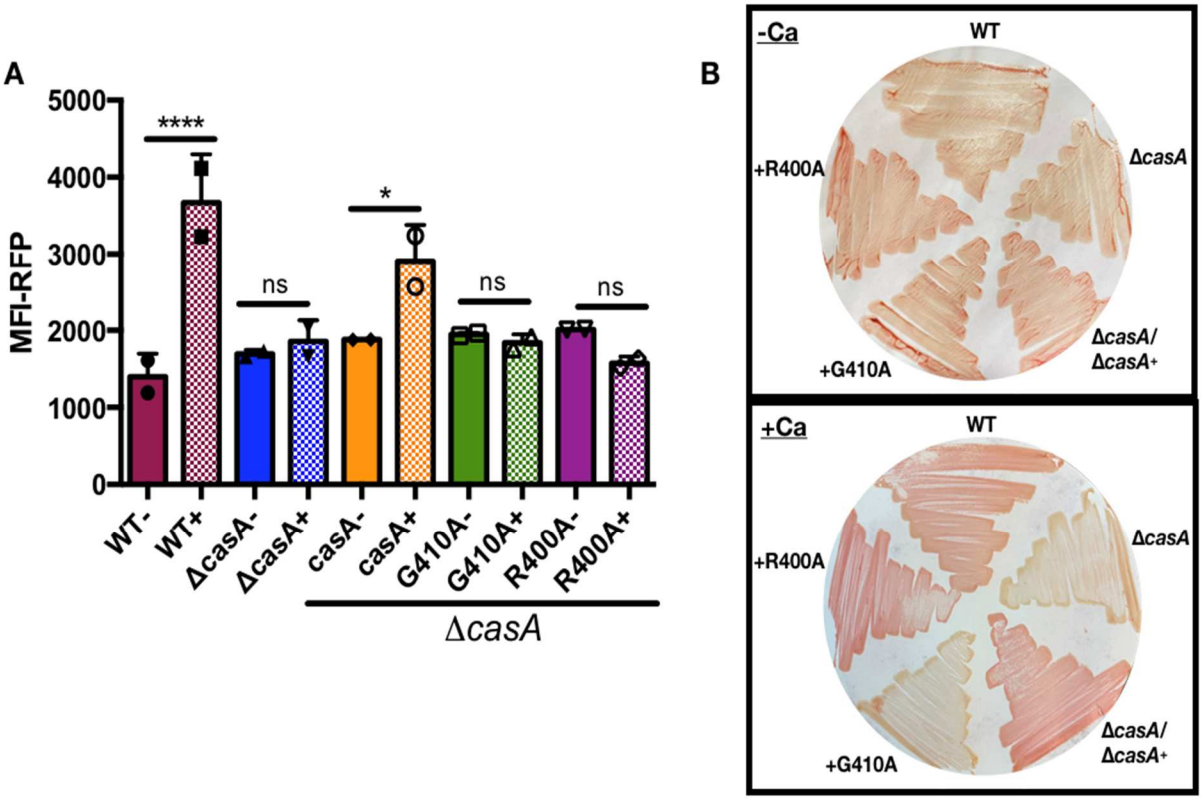

Figure 42. Calcium-Dependent Phenotypes Require CasA's Enzymatic GGEEF Motif. (A) MFI of RFP in AmCyan^{+} RFP^{+} live cells, with or without 40 mM added calcium. Only WT and Δ*casA/casA*$^{+}$ increase c-di-GMP in response to calcium (p=0.0001****, p= 0.01*) (B) Congo red dye bound to bacteria grown on LBS plates without (top) or with (bottom) 40 mM calcium.

N-Terminal Sensory Domain Controls CasA Function

The N-terminal sensory domain contains a predicted d-Cache_1 (*ca*lcium and *che*motaxis), and an MCP-like (*m*ethyl-accepting *c*hemotaxis *p*rotein) domain. However, CasA lacks conserved motifs typical of such sensory domains such as N, F, and G1-3 boxes (Dutta & Inouye, 2000, Parkinson & Kofoid, 1992). Thus, to identify residues potentially important for function, I aligned CasA with homologous proteins from closely related *Vibrio* spp. and chose several highly conserved residues to mutate, with a focus on aspartates and glutamates because calcium is known to bind such residues: D111, G231, D236, and E293 (Figure 43) (Pidcock & Moore, 2001, Madeira *et al.*, 2019). Complementation experiments revealed two classes of phenotypes:

```
V. fischeri          ---MPKFNLKHIFLIPTLFLVLIVGFILNNHMNSVQRQVNREYDRIINSLQRSIKVIISL     57
V. cholerae          --MNQRMSLTWIICAPLFIVFVLAASVFQQYLYDLNQEIDDAYADIQQQLERAEKVVTAL     58
V. sonorensis        MKTERHFSLAAVFFIPGVVTVILL GLIVKNYFDSVARDVSEEYQRIETSIERATKILTAL     60
V. crassostreae      MKVNRHFSLTFIFGFPAVIATMLLGLIGKNHFDSVKKDIDSEFHRIEEVFKRTTKVVTAL     60
V. coralliirubri     MKVNRHFSLTFVFGFPAVIAAMLLGLIGKNHFDLVKKDISSEFQRIEEVFKRTTKVVTAL     60
V. splendidus        MKVNRHFSLTFVFGFPAVIAAM LLGLIGKNHFDAVEKDISSEFHRIEDVFKRTTKVVTAL     60
                           ::.*  ::  * ..  :: . : ::::  : :::.  :  *   ::*: *:: :*

V. fischeri          DYNISQLYKQNQGSFYNHNFEIKKDSGLCVIRPSENLDAVMA -EQDISVAEGRLDYSIAG     116
V. cholerae          DYTFTHNQRPAENILFKHSARV --VANVCQIKPIDGLVLAQGLSSSFAVPKLDLSYMLIG     116
V. sonorensis        DYSFSNYYKSGTALLLEHNRTA --EDGLCRMWPIDALLLSEGKNQ--AIPAVDISYMLVG     116
V. crassostreae      DYSFSNYYKSGNPLFLDHNKQV --VDGLCQIWPIDVLLLADGKTS--DIPSVDIDYMLVG     116
V. coralliirubri     DYSFSNYYKSGNPLFLDHN KQV--VDGLCQIWPIDVLLLADGKTS--DIPSVDIDYMLVG     116
V. splendidus        DYSFSNYYKSGNPLFLDHNKHV --VDGLCQIWPIDVLLLADGKTS--DIPSVDIDYMLIG     116
                     **.:::  :     : .*.       .:* : * : *    .  .   :    :.* : *

V. fischeri          KKDLCDPSSEVYEIASKKVS LAPVISFIHDYESYLHGIYFISKYNYIISSPKEIAENLSQ     176
V. cholerae          DASLCDSKPSHDPSLQIKLSMAPILSFLHDMDEYIYGVHYVDSSGYIISSPDTISEKVTY     176
V. sonorensis        DKSLCDPNSPLYKRVSSKVSLAPILSFLHDLDDYVLGMHYIDKSGYVMSSPETLAKNINK     176
V. crassostreae      QESLCSETSDSYKSA SEKIALAPILSFLSQLDEYHDGVHFIDTSGYVISSPEDFAKGLSK     176
V. coralliirubri     EESLCSESSDSYKSASKKIALAPILSFLSQLDEFHSGVHFIDKRGYVISSPEGFAKKLSK     176
V. splendidus        QESLCSESSDSYKSASEKIALAPILSFLSQLDEYHAGVHFIDTSGYVISSPEGFAKGLSK     176
                     . .**. .       . *:::**::**: : :.:  *:::::.. .*::***. ::: :.

V. fischeri          K-TLDVIYSRPYWKNSMKNDSEKYITFTPPYTDAFFD -GLEVLTFSTPIYYKGIFKGVLV     234
V. cholerae          QQIKDFISESPLWSHAIAAPN --MIAVDGPYRSVIREQHEWLLTLILPVYRDADYQGLVA     234
V. sonorensis        S-LLETVKARPVWHITINNRE --TITIAGPANVY--SLSDRVVTMTVPIYFQDELQGIVS     231
V. crassostreae      E-LLSTIKSRPYWQKTANNPD --KLTLSGPGYRF--DSLDRMISMTIPVFHKGVHQGMLS     231
V. coralliirubri     E-LLSTIKSRPYWQKTANNPE --KLTLTGPAYRF--ESLDRMISMTIPVFHQGVHQGMLS     231
V. splendidus        E-LLSTIKSRPYWQKTANNPD --QLTLSGPGYRF--DSLDRIISMTIPVFHKGVHQGMLS     231
                     .   . :   * *  :    .   ::.  *      .    ::::  *:: .   :*: :

V. fischeri          IDLSVEKLLRSS-NEISQHIQLLNSDEYKRFEQYRFMQPVNLDFTDFTYFLYYKTSIKEE     293
V. cholerae          VDIGLRELLSRM-PHLASRFDMIDLNEMAIPTFAYRPHKLTSEYADYHQVVFYKLDIQSE     293
V. sonorensis        LDLDIDALLSTN-GKLASPIHFSSDEPQLTPATARWIYPLKMEGVKFHHHLYYQFE WQPQ     290
V. crassostreae      VDINAGRLLENSNEHLAGRIDIIDTTRSAPIDSAAFYHEINLEGVASHHAMYYELDIAKE     291
V. coralliirubri     VDIDADKLLANSNEHLAGRIDIIDTTLATPVDSAAFYHELKLDGVASHHAMYYELDIAKE     291
V. splendidus        VDINADKLLANSNEHLAGRIDIIDTTLATPVDSAAFYHEIKLDGVSSHHAM YYELDIAKE     291
                     :*:.   **     .::  :.: .                :. : .     ::*: .   :

V. fischeri          LKGFLVHDSNSLILTLVMYILSLLSMFYYQSRVSQKYYRDLAKQDPMTGLYNRRGFEMSL     353
V. cholerae          LSNFLTEKSGNLLVVALVYLFLTGVLIYLNTRWDRQHYAQLAARDPMTGLLN RRGMESFL     353
V. sonorensis        VQHFFALESDSLAVIASLYVMSVFVLFYINTHVEKSYFRELSAKDPMTGLLNRRGLEAFL     350
V. crassostreae      IEHFFVYEKDSLIVAIIVYLFSVTIFFYVNSTIERGYFKDLAAKDPMTGLLNRRGLEAFW     351
V. coralliirubri     VEHFFVYEKDSLIVAIIVYLFSVTIFFYVNSNIERGYFKDLAAKDPM TGLLNRRGLEAFW     351
V. splendidus        VEHFFVYEKDSLIVAIIVYLFSVTIFFYVNSNIERGYFKDLAAKDPMTGLLNRRGLEAFW     351
                     :. *:. ....* :   :*::    ::* ::  .: :: :*: :****** ****:*

V. fischeri          QDRVVKKYVGFAIYDIDDFKQINDVFGHDVGDEAIKYVARMLNKSVRD SDIVSRFGGEEF     413
V. cholerae          KGKRHSQYLAIAVLDIDDFKQINDAYGHDMGDRVICYIGEQIENHIRSSDAVARFGGEEF     413
V. sonorensis        GNAQHGNYLAIAIFDIDNFKSINDTWGHDVGDDVIRHIGKELEKNLRSNDSVARFGGEEF     410
V. crassostreae      RSVEHDQLFALTVFDIDDFKSINDTYGHDKGDDVIRYMSRQIG NSVRSSDVAARFGGEEF     411
V. coralliirubri     RSVEHDQLFALTVFDIDDFKSINDTYGHDKGDDVIRYMSRQINNSIRSSDVAARFGGEEF     411
V. splendidus        RSVEHDQLFALTVFDIDDFKSINDTYGHDKGDDVIRYMSRQISNSIRSSDVAARFGGEEF     411
                       .    : ..::: ***:**.***.:*** ** .* ::.. : : :*..* .:*******

V. fischeri          VICINAESRNSLESVCERVRKSIQDSSGKVVKGGFTVSGGVTVIDS -HQEFSFEHVIKKA     472
V. cholerae          VVYVTAKEKEQITRIMQRIFDAVCRESPLILEPGFTISGGIEVVES -TTDRSFEDLFKAA     472
V. sonorensis        VIYMTGDAKDGLVASMQRVRSAIGESSFKVLEKGFTLSGGIEVAKS -EAGWDFETMFKAA     469
V. crassostreae      VVYMRGEDRETLMRTLERVKNAICSTSADIIPNGFTVSGGVCIVETEQSKLNFDEIFKYA     471
V. coralliirubri     VVYMKGEDRETLMRTLERVKNAICSTSADIIPNGFTVSGGVCIVETEQSKLNFDEIFKYA     471
V. splendidus        VVYMKGEDRETLMRTLERVKNAICSTSADIIPNGFTVSGGICLVETEQSKLNFDEIFKYA     471
                     *: : .. :: :    :*: .::   *  ::  ***:***: : .:     .*: ::*  *

V. fischeri          DALLYKAKQDGKNRVYFS        490
V. cholerae          DEKLYVAKTSGKNQLVY -       489
V. sonorensis        DEKLYLAKNQGKDQLVS -       486
V. crassostreae      DEKLYVAKTTGKDRLEF -       488
V. coralliirubri     DEKLYVAKTTGKDRLEF -       488
V. splendidus        DEKLYV AKTTGKDRLEF-       488
                     *  ** **  **:::
```

Figure 43. Alignment of Homologous Proteins. A Blast search of *V. fischeri* CasA turned up several similar proteins found in a variety of *Vibrio* spp., and the 5 top hits are aligned here. The *V. fischeri* and *V. cholerae* proteins are CasA and CdgK, respectively. The enzymatic GGEEF motif is highlighted in blue, and residues that were mutated are highlighted in purple.

First, one variant, CasA-D111A, exhibited increased activity while maintaining a response to calcium. Specifically, in the absence of calcium, this strain produced substantially higher levels of c-di-GMP (Figure 44A, light blue bars) and increased red color on Congo Red (Figure 44B). However, c-di-GMP was still significantly increase in response to calcium, indicating an intact calcium-response mechanism.

Second, three of the substitutions (G231A; D236A; E293A) diminished the apparent calcium-responsiveness of CasA. All three variants lost the ability to increase c-di-GMP in response to calcium, and without calcium maintained similar (G231A, D236A) or slightly higher (E293A) c-di-GMP levels than Δ*casA/casA*$^{+}$ (Figure 44A). However, these variants phenocopied Δ*casA/casA*$^{+}$ on Congo red agar containing calcium (Figure 44B), indicating that they must retain some function. Michael Vanek also performed motility experiments evaluating the N-terminal variants and found the phenotypes to be consistent with these data. Overall, these experiments reveal four sensory domain residues that impact CasA function and calcium-dependent phenotypes, suggesting that this domain may be responsible for sensing calcium as a signal.

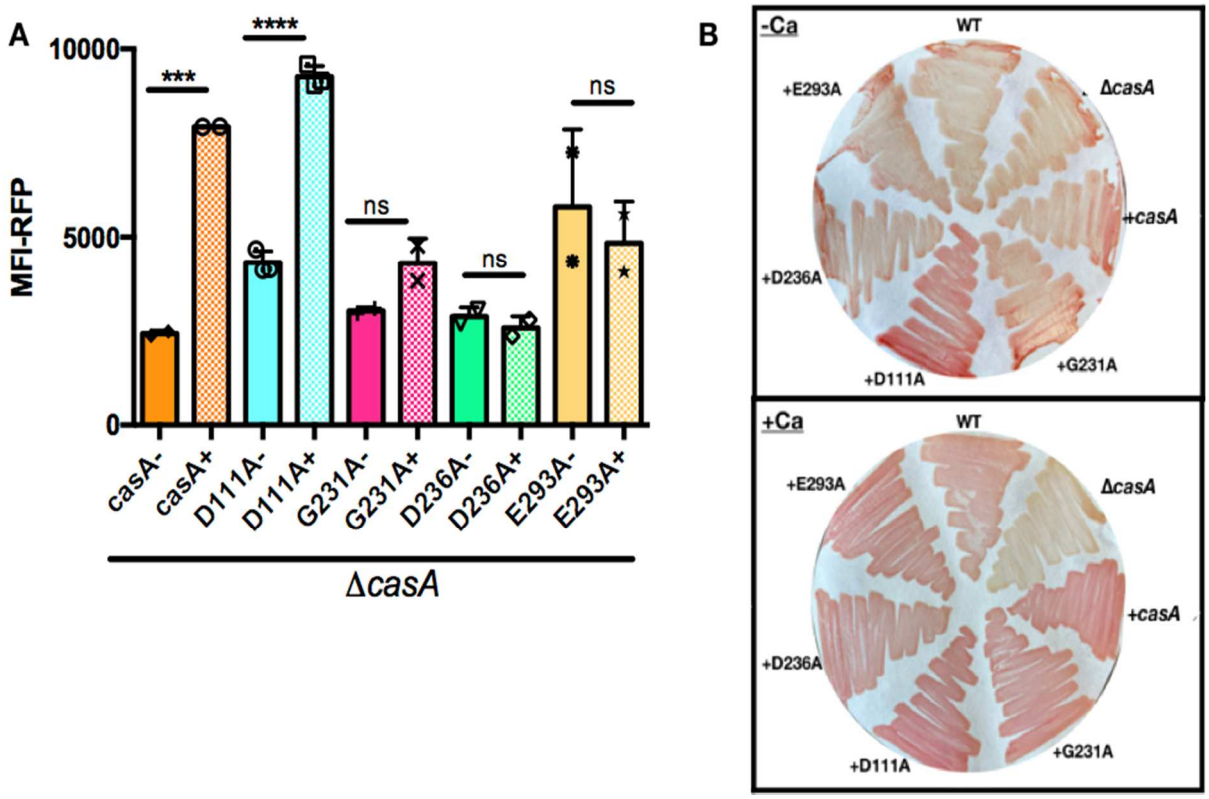

Figure 44. Calcium-Dependent Phenotypes Depend on CasA's N-Terminal Sensory Domain. (A) MFI of RFP in AmCyan^{+} RFP^{+} live cells, with or without 40 mM added calcium. Only the Δ*casA/casA*$^{+}$ and Δ*casA/casA*-D111A strains increased c-di-GMP in response to calcium (p=0.002***, p=0.0001****). (B) Congo red dye bound to bacteria grown on LBS plates without (top) or with (bottom) 40 mM calcium.

CasA is Sufficient for the Response to Calcium

While CasA is responsible for several calcium-dependent phenotypes, it was unclear whether CasA directly senses calcium as a signal, or if it requires a partner(s) to sense and respond to calcium. To explore the sufficiency of CasA in response to calcium, we used *E. coli* as a heterologous system with plasmid-borne *casA*. I cloned *casA* and transformed it into an *E. coli* strain containing the c-di-GMP biosensor. Under these conditions, I found that low calcium levels exerted minimal effects on c-di-GMP levels in *E. coli* (Figure 45). However, when *casA*

was overexpressed, addition of 10 mM calcium resulted in a significant increase in c-di-GMP (Figure 45). These data suggest that CasA alone is sufficient produce c-di-GMP in response to calcium.

I was not able to assess Congo red biofilm phenotypes, as *E. coli* makes cellulose and curli containing biofilms, which produce color on Congo red (Römling *et al.*, 2000, Zogaj *et al.*, 2001). Additionally, I transformed the *casA* overexpression plasmid into a motile *E. coli* strain, and Michael Vanek and Natasha Peterson performed motility assays to evaluate CasA. They found that *casA* overexpression had a very minimal impact on motility at 0 mM calcium, but 10 mM calcium addition resulted in significantly decreased motility. This calcium-dependent decrease in motility is likely due to increased c-di-GMP production.

To determine if this response was (1) dependent on the ability of CasA to make c-di-GMP and (2) required a functional sensory domain, I evaluated the G410A enzymatic domain and D236A sensory domain variants. I cloned these mutant alleles and transformed the plasmids into *E. coli* containing the c-di-GMP biosensor and a motile *E. coli* strain. I found that strains expressing either variant phenocopied the vector control strain, with no calcium-dependent change in c-di-GMP levels (Figure 45). Michael Vanek and Natasha Peterson also performed a motility assay using the motile *E. coli* strain, and also observed that both variants phenocopied the vector control strain. These data suggest that both the periplasmic sensory domain and DGC enzymatic domain are required for CasA to sense and respond to calcium. Thus, CasA appears to be a novel calcium sensor that controls cellulose-dependent biofilm formation via a calcium-mediated induction of c-di-GMP.

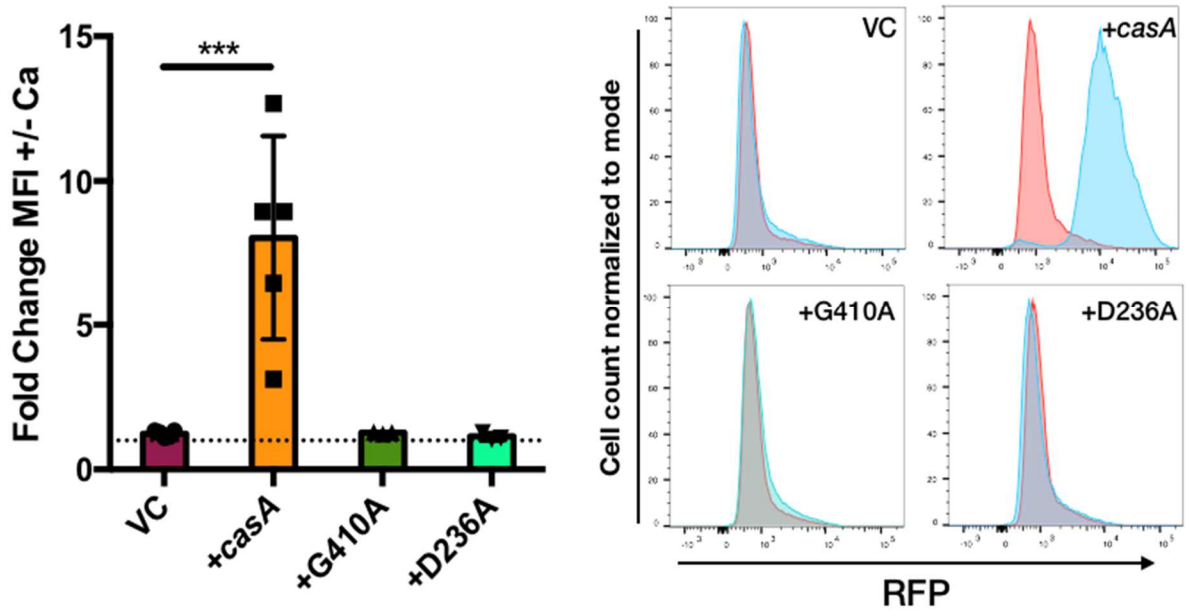

Figure 45. Calcium Activates *casA* in *E. coli.* Fold change of MFI-RFP in response to 10 mM calcium in AmCyan^{+} RFP^{+} live cells. Overexpression of *casA* alone resulted in a significant increase in RFP in response to calcium (p=0.0006 ***). Right- representative histograms.

CdgK Decreases C-di-GMP in the Presence of Calcium

V. fischeri CasA exhibits significant homology to *V. cholerae* CdgK, one of a set of DGCs that work upstream of VpsR to activate *vps* transcription (Townsley & Yildiz, 2015, Shikuma *et al.*, 2012). I hypothesized that *cdgK* could complement Δ*casA* and tested my hypothesis by expressing *cdgK* in the chromosome of a Δ*casA* mutant. The *cdgK* gene was synthesized by IDT as a gblock, and I used PCR SOE to fuse sequences that would drive *cdgK* transcription via the *nrdR* promoter, with an idealized RBS, and added an HA tag on the C-terminus, the same as the various *casA* alleles. This construct was then inserted into the intergenic region between *yeiR* and *glmS*. CdgK was stably produced both in the presence and absence of calcium (Figure 41). Experimentally, the Δ*casA*/*cdgK*$^{+}$ strain exhibited approximately a 5-fold decrease c-di-GMP levels in response to calcium (Figure 46). This suggested that CdgK

is an active DGC when expressed in *V. fischeri*, as it was still able to produce c-di-GMP, but that this activity may be negatively modulated by exogenous calcium. Consistent with these findings, I assessed Congo red binding in the Δ*casA*/*cdgK*$^{+}$ strain, and in the absence of calcium the *cdgK*-expressing strain was visually redder, compared to WT, Δ*casA*, and Δ*casA/casA*$^{+}$ strains, indicating increased Congo red binding (Figure 46). However, with calcium supplementation, it failed to bind Congo red, phenocopying the Δ*casA* parent (Figure 46). Michael Vanek performed motility assays to evaluate the *cdgK*-expressing strain, and found similar differences in motility, but only in the absence of magnesium. Together, these data suggest that CdgK is functional as a DGC in *V. fischeri*, but that this DGC activity only occurs in the absence of added calcium.

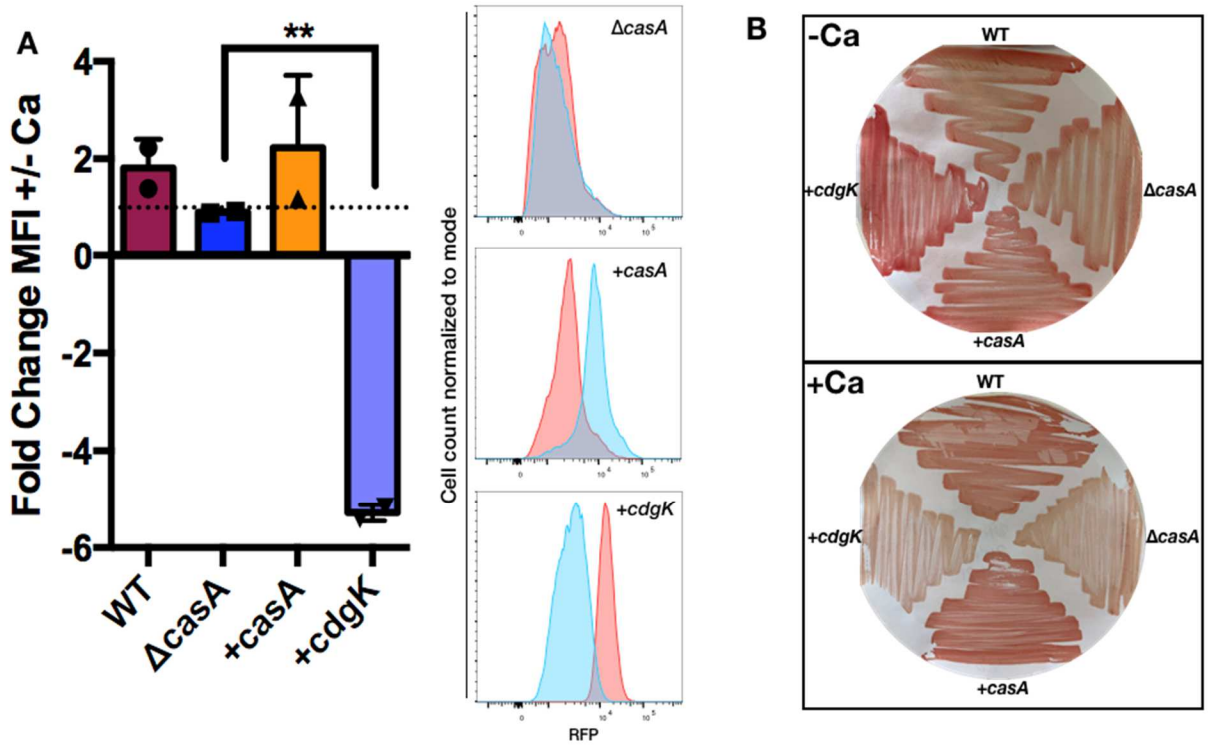

Figure 46. *V. cholerae* CdgK Displays Calcium-Dependent Phenotypes. (A) Fold change of RFP-MFI (left) in response to calcium and representative histograms (right) as determined by flow cytometric analysis of AmCyan^{+} RFP^{+} live cells containing pFY4535. Δ*casA/cdgK*$^{+}$ is significantly different from its parent Δ*casA* strain (p=0.0053**) (B) Congo red dye bound to bacteria grown on LBS plates without (top) or with (bottom) 40 mM calcium.

Summary

In this study, I determined one way in which calcium promotes biofilm formation and inhibits motility is through modulation of the second messenger, c-di-GMP. Specifically, I showed that calcium induces a dose-dependent increase in relative c-di-GMP levels, and this is dependent on the DGC CasA. CasA impacts biofilm formation at the level of *bcs* transcription, epistatic to VpsR. I also determined that CasA is a functional DGC, and that residues in the N-terminal sensory domain modulate how CasA responds to calcium, suggesting that these residues

may be involved in binding calcium. Additionally, I used *E. coli* as a heterologous system to determine that CasA alone is sufficient to sense and respond to calcium, without any binding partners specific to *V. fischeri*. Lastly, I investigated CasA's *V. cholerae* homolog, CdgK, and found that CdgK responds oppositely to CasA, seemingly turned off by calcium.

CHAPTER FOUR

DISCUSSION

Introduction

The overall goal of my dissertation was to advance our understanding of regulatory networks and signaling pathways that control biofilm formation by *V. fischeri*. Biofilm formation is a required step for initiation of the symbiosis between *V. fischeri*, and its host *E. scolopes*. The canonical WT strain ES114 is highly genetically tractable, and mutations can easily be made and moved, making *V. fischeri* an ideal bacterial species to study the questions of how environmental signals can be sensed and processed to promote behaviors such as biofilm formation. Symbiosis depends on production of SYP-dependent biofilms; their formation by *V. fischeri* is tightly controlled, and regulation of these biofilms is well-studied and understood. Yet, gaps remain in our understanding of how ES114 forms biofilms in the marine environment, during symbiosis, and in the laboratory. As ES114 was originally isolated from a squid host and remains proficient at colonizing juvenile squid, this strain must be biofilm competent; however, at the start of this dissertation, observing robust biofilm production by ES114 at the bench required overexpression of positive regulators. Such overexpression strains produce several easily assayed and distinct forms of biofilms including wrinkled colonies, pellicles, clumps and rings, and Congo red binding, while ES114 largely fails to do so under standard laboratory conditions.

Below, I will expand on my findings, framing them in the context of the literature, and discuss how this advances our knowledge of biofilm regulation in *V. fischeri*. Additionally, I put

forward hypotheses and my thoughts on future directions that could further our understanding of these regulatory mechanisms in the context of the laboratory and squid colonization.

Identification of Calcium as a Biofilm Promoting Signal

Overexpression of positive regulators, while necessary for induction of biofilm formation *in vitro,* unintentionally limited the scope of investigations by bypassing contributions of regulators including HahK and HnoX, and signals such as NO. Specifically, work performed by myself and others was able to identify calcium as a signal to induce biofilm formation by *V. fischeri*.

Previous work has explored calcium in the context of biofilm formation, but its importance was overlooked. This was likely due to robust biofilm formation when RscS is overproduced, regardless of calcium. Calcium has a minimal impact on phenotypes in RscS overproducing strains, and in ES114 seawater levels of calcium alone are insufficient to induce either the wrinkled colonies or pellicles indicative of SYP-dependent biofilm formation. Since RscS overproduction is so permissive to biofilm formation, it was surprising to see calcium have such a strong impact on shaking-liquid cultures, inducing SYP-dependent biofilm formation by *rscS*$^{++}$. This indicates the existence of a biofilm-inhibiting factor in shaking-liquid conditions that RscS overproduction is unable to overcome. However, calcium alone is also insufficient to induce SYP-dependent biofilms in liquid, requiring overexpression of *syp* through either overproduction of RscS or SypG (and lack of SypE), or lack of BinK. Additionally, while RscS overproduction is able to bypass calcium to produce wrinkled colonies and pellicles, lack of BinK still requires calcium under these conditions, suggesting that despite comparable liquid phenotypes, the functions of BinK and RscS cannot be equivalent or directly cancel each other

out. If that was the case, then loss of BinK alone would be permissive for wrinkled colony and pellicle production.

Even in the context of cellulose-dependent ring formation, calcium alone does not induce robust rings in shaking-liquid culture at 28°C, which is the field's standard for overnight growth. I was only able to see measurable and reproducible ring formation when bacteria were grown at 24°C or with the addition of antibiotics, supporting the hypothesis that calcium alone cannot overcome all barriers to biofilm formation. Both temperature and antibiotics have been identified as signals for that can impact biofilm formation in a variety of species. For example, aminoglycoside antibiotics and low temperature are both biofilm-promoting signals in *Pseudomonas aeruginosa*, dependent on c-di-GMP (Hoffman *et al.*, 2005, Kim *et al.*, 2020). Additionally, bacterial efflux pumps, including pumps that confer tetracycline resistance, can promote biofilm formation (Soto, 2013, Kvist *et al.*, 2008). However, the tetracycline resistance gene we use in the laboratory is *tetM*, which works to protect ribosomes from tetracycline and not as an efflux pump, meaning that antibiotics must be promoting calcium-dependent biofilm formation through a different mechanism (Roberts, 1996). As I demonstrated, calcium increases c-di-GMP levels in *V. fischeri*; however, we have not probed the impact of temperature or low levels of antibiotics on c-di-GMP. Overall, the phenotypes we observed in both liquid and solid media suggest that, despite calcium being a strong signal, it is not sufficient to induce biofilm formation (SYP or cellulose) under every condition. Identification of other inhibitory factor(s) could potentially allow for robust SYP-dependent biofilm formation by ES114 in laboratory conditions, significantly advancing our understanding of biofilm regulation.

The way that calcium acts as a signal in *V. fischeri* is likely multifaceted and goes beyond signaling through CasA, as explored later in this chapter. CasA has a prominent role in cellulose-

dependent biofilm formation (Figure 33 & 36 & 37), but not in SYP-dependent biofilm formation as seen by minimal impact on calcium-induced wrinkled colony formation (Figure 32), suggesting that calcium is affecting SYP and cellulose polysaccharide through different mechanisms. Additionally, calcium has been shown to induce the Lap system in *V. fischeri*, although the precise connection between calcium and Lap has yet to be explored (Christensen *et al.*, 2020a). Simply put, CasA alone is insufficient to account for all the ways calcium influences *V. fischeri* and calcium is likely being regulated on multiple levels. While calcium may have an extracellular role stabilizing the biofilm matrix (Kierek & Watnick, 2003), we have shown that calcium is also able to enter cells (Natasha Peterson, Tischler *et al*. 2021, submitted). The *V. fischeri* genome contains multiple putative calcium transporters that could regulate and/or facilitate calcium entry (Ruby *et al.*, 2005, Mandel *et al.*, 2008). Once calcium has entered the cell, calcium could be acting in any number of ways, including signaling through sensory proteins (explored in chapter one) or binding to riboswitches. Both calcium and c-di-GMP have been previously shown to bind to riboswitches and could using this mechanism to alter translation (Zamorano-Sánchez *et al.*, 2019, Zhou *et al.*, 2016, Breaker, 2018). Investigating how calcium is acting on and within *V. fischeri* cells could increase our understanding of the diversity of ways that a single cation can affect bacterial behavior.

Calcium as a Tool to Study SYP-Dependent Biofilm Formation

A *binK* mutant exposed to calcium is both biofilm-competent and able to significantly increase *syp* transcription. Thus, this combination of genetic alteration and nutrient supplementation can be used as a tool to probe biofilm formation. Indeed, using this tool, we were able to confirm previous work performed using *rscS* overexpression, which determined that RscS functioned upstream of SypF and required both the Hpt domain of SypF and SypG to

induce *syp* transcription. However, under our new conditions, SYP-dependent biofilm required only SypG and a SypF-Hpt domain that could be phosphorylated, meaning that SypF-Hpt could be phosphorylated in the absence of both RscS and SypF autophosphorylation. We hypothesized that another SK must be involved to phosphorylate SypF-Hpt, and identified HahK as another input into this pathway. HahK was able to impact wrinkled colony phenotypes and *syp* transcription, and loss of HahK severely diminished clumping phenotypes, cementing its role as a regulatory input. However, a *hahK* mutation did not completely abrogate biofilm formation, suggesting the involvement of yet another sensor kinase; indeed, the remaining biofilm phenotypes were lost when *rscS* was also disrupted (Figure 8). Thus, in addition to the opportunity to verify and validate the function and signaling pathway of known regulators, inducing SYP-dependent biofilms in a novel way resulted in (1) identification of HahK as a new biofilm regulator and (2) the first mutant phenotype in culture for *rscS* since it was identified in 2001 (Visick & Skoufos, 2001).

The discovery of HahK as regulatory input to biofilm formation pointed to the involvement of the linked regulator HnoX. Dr. Cecilia Thompson determined that HnoX senses NO, inhibiting HahK, and resulting in decreased biofilm formation. NO had been previously identified as a host-relevant signal on the surface of the light organ that is induced during symbiosis (Davidson *et al.*, 2004), suggesting that HnoX would sense NO, and decrease SYP, resulting in decreased symbiotic aggregation on the surface of the symbiotic organ. I found that indeed, this is the case, and strains lacking HnoX formed significantly larger aggregates than the parent strain (Figure 30). Many other studies have shown that aggregation is required for colonization initiation, and that hyper-biofilm forming strains with larger aggregates actually have a colonization advantage (Yip *et al.*, 2005, Yip *et al.*, 2006, Bongrand & Ruby, 2018,

Koehler *et al.*, 2018, Pankey *et al.*, 2017, Brooks & Mandel, 2016, Wang *et al.*, 2010). Correspondingly, strains lacking *hnoX* outcompete WT for colonization (Wang *et al.*, 2010). If aggregation is a colonization advantage, and presence of HnoX is a colonization disadvantage, then why does *V. fischeri* retain *hnoX* in the genome? I hypothesize that beyond other roles for HnoX during colonization and persistence, perhaps the presence of HnoX helps to prevent inefficient or ineffective aggregation. When imaging and measuring symbiotic aggregates, I noticed that strains lacking HnoX tended to form more oblong and disparate aggregates than the parent strain. Additionally, Davidson *et al.* report that the highest levels of NO on the juvenile squid light organ are present in newly hatched squid and these levels diminish over time, presenting images with distinct NO free areas surrounding the pores of symbiotic animals (Davidson *et al.*, 2004). While there are many other factors, both host and bacterial involved at this stage of initiation, and I am presenting a simplified view, it is possible that NO could be involved in positioning aggregates by preventing aggregation from occurring too far away from the pores or spread out, which could benefit bacterial dispersal and the continuation of colonization.

All together, these findings reveal an increased complexity of the regulatory pathway controlling *syp*-dependent biofilm formation and highlights the need for multiple tools to approach the complicated mechanism of biofilm induction/repression. Just as the contributions of HahK and HnoX were masked when RscS or SypG were overproduced, the loss of BinK and the presence of calcium may conceal other unknown regulatory inputs. Current work in the lab is expanding to look at other signals, and Courtney Dial has determined a combination of nutrients and supplements that allows for SYP and cellulose-dependent biofilm formation by ES114 (Dial 2021 in review). These conditions, and others, are almost certainly guaranteed to identify new

regulatory inputs, advancing our understanding of how, why, what, when and where *V. fischeri* forms biofilms.

Differences Between SYP and Cellulose-Dependent Biofilms

In liquid culture, calcium coordinately induces both cellulose and SYP-dependent biofilm formation in permissive strain backgrounds (i.e. Δ*binK*, *rscS*$^{++}$). Work by others in the lab have determined that these polysaccharides are temporally regulated with the cellulose-dependent ring occurring first, sometimes within the first hour of growth. SYP is induced later on, producing cohesive cellular clumps. Additionally, others have seen that the large adhesin protein LapV contributes to these biofilms, and seems to play a greater role in adhesive, cellulose-dependent biofilms, rather than the cohesive SYP-dependent biofilms (Christensen *et al.*, 2020a). Overall, calcium addition permits formation of two distinct biofilms, dependent on three known components, and defined by either adherence or coherence. This highlights both the diversity of factors calcium regulates and the distinct differences between cellulose and SYP-dependent biofilms.

Biofilm formation in the simplest form is often thought of as a community of bacteria that first attach to a surface before secreting the extracellular matrix to form a mature biofilm. Cellulose-dependent rings adherent to the sides of test tubes are an example of this type of biofilm; however, biofilm communities do not require surface attachment, as exemplified by SYP-dependent clumps (Flemming *et al.*, 2016, Flemming & Wuertz, 2019, Bossier & Verstraete). These non-surface attached aggregates are prevalent in environmental settings and can be major contributors to host-associated biofilms. For example, non-surface attached *P. aeruginosa* and *S. typhimurium* aggregates can be found embedded in host mucus in the lungs and intestines, respectively, similar to how *V. fischeri* aggregates within the mucus of the squid's

light organ (Nyholm *et al.*, 2000, Cai, 2020). These adherence and coherence properties suggest that cellulose and SYP-dependent biofilms could be important under different environmental conditions. Since SYP-dependent aggregation is required for colonization initiation, it is possible that cellulose-dependent biofilms are more environmentally relevant, supporting surface attachment in the marine environment, and/or required post-symbiosis initiation.

CasA as a Calcium Sensing DGC

C-di-GMP is a ubiquitous bacterial signal that permits many organisms to change their behavior in response to varied internal and external signals. Calcium was one of the first signals identified as an activator of c-di-GMP through inhibition of PDE activity in *G. xylinus*, even before the discovery of c-di-GMP in 1987 (Ross *et al.*, 1985, Ross *et al.*, 1987, Aloni *et al.*, 1983). This inhibition occurred through outcompeting magnesium, which activates the PDE, and was not due to direct calcium sensing (Ross *et al.*, 1985). In the intervening decades, the connection between calcium and c-di-GMP has been investigated in a variety of organisms and signaling pathways. For example, in *Mycobacterium tuberculosis*, calcium alters PDE activity, affecting growth and survival during macrophage infection (Advani *et al.*, 2014, Koul *et al.*, 2009, King *et al.*, 2020). In the c-di-GMP-activated Lap systems of *P. aeruginosa* and *Leigonella pneumophila*, calcium activates the protease LapG, which promotes biofilm dispersal (Boyd *et al.*, 2012, Chatterjee *et al.*, 2012). Additionally, similar to what we observed here, calcium increases intracellular c-di-GMP levels in *V. vulnificus* (Boyd *et al.*, 2012, Chatterjee *et al.*, 2012, Chodur *et al.*, 2018, King *et al.*, 2020, Advani *et al.*, 2014, Koul *et al.*, 2009). My work adds to this literature by identifying CasA as a DGC whose activity is induced in response to calcium. To the best of my knowledge, no other DGCs that respond to calcium have been

identified. Other DGCs and PDEs responsive to calcium in a variety of organisms are likely to be uncovered as the connection between calcium and c-di-GMP continues to be explored.

The architecture of CasA includes a putative N-terminal periplasmic sensory domain—putatively involved in binding calcium—and a well-conserved C-terminal cytoplasmic GGDEF enzymatic domain responsible for c-di-GMP production. I found that residues in both these domains are required for function. Protein prediction programs identify both dCache-1 (*ca*lcium and *che*motaxis) and MCP-like (*m*ethyl accepting *c*hemotaxis *p*rotein) domains in the N-terminus. Class I MCPs have a periplasmic ligand binding domain (LBD), with another, functional domain in the cytoplasm (Salah Ud-Din & Roujeinikova, 2017), matching the general structure of CasA. Identification of calcium binding pockets can be surprisingly tricky, considering that calcium-binding proteins (CBP) are ubiquitous and some of the most well studied proteins in eukaryotes. Certain calcium binding superfamilies, such as EF-hand motifs and the βγ-crystallin Greek key motif, are conserved across domains of life, and associated with protein structure; however, the study of bacterial CBPs is a relatively young field, and calcium binding sites for many bacterial CPBs that don't contain these known motifs are yet unknown (Domínguez *et al.*, 2015, Dominguez, 2018, King *et al.*, 2020, Aravind *et al.*, 2009). Additionally, structure is not necessarily correlated with the ability to bind ions, nor can structure predict affinity for ion binding, as in eukaryotes the affinity for EF-hand domains can vary ~100,000 fold (Pidcock & Moore, 2001, Clapham, 2007). This is not just a structural issue, but also a chemical issue, as the reduced/oxidized state of a protein impacts electrostatic interactions between Ca^{2+} and putative binding residues. Additionally, Ca^{2+} can induce conformational changes in protein structure, and even the number of molecules (water, carboxyl groups, amino acid side chains, etc.) bound to Ca^{2+} have no correlation with binding affinity (Pidcock & Moore,

2001). Despite this variability, some patterns have emerged, and aspartates and glutamates have proven to be common calcium-coordinating residues (Pidcock & Moore, 2001). Consistent with those known interactions, N-terminal CasA residues D236 and E293 likely contribute to sensing/binding calcium in some way, as mutating these residues resulted in partial loss of the calcium response. Conversely, mutation of D111 allowed for an increase in basal CasA function without disrupting the ability to sense/respond to calcium. Given the complexities of ion-protein interactions, one or even two single residue changes may not be sufficient to fully abrogate the calcium response by CasA. Potentially, identifying a calcium binding site in the N-terminal domain through X-ray structures and other analyses could provide insight into CasA function and biological conditions that best support activity (e.g.. redox state, multimer formation).

Coordination of CasA, Calcium, and Cellulose

I found that CasA responds to calcium by synthesizing c-di-GMP to control cellulose production through increasing *bcs* transcription. Cellulose is the most abundant polysaccharide in the world and is synthesized by a wide variety of bacterial species, leading to a diversity of *bcs* operon structures, genes, cellulose products, and regulatory mechanisms. But throughout this heterogeneity, bacterial cellulose remains inextricably linked to c-di-GMP, as all identified BCS complexes contain a BcsA subunit with a PilZ c-di-GMP binding domain (Römling & Galperin, 2015). *E. coli* and *Salmonella* spp. are the best studied organisms with type II *bcs* operons, the same kind found in *V. fischeri*. In *V. fischeri,* I have shown that regulation starts at the transcriptional level, where *bcs* transcription depends on VpsR, is decreased by the PDE BinA, and significantly increased by calcium dependent on the DGC CasA. Without CasA, calcium has a negligible impact on either the internal levels of c-di-GMP or *bcs* transcription. Conversely, in *E. coli* and *Salmonella* spp., *bcs* transcription is thought to be constitutively active, and therefore

unregulated (Zogaj *et al.*, 2001). However, post-transcription regulation of cellulose by c-di-GMP is well established in these organisms and can be split up into three distinct levels. On the first level, c-di-GMP activates expression of key transcription factor CsgD. CsgD activates many biofilm components, including DgcC (AdrA in *Salmonella*), which produces the pool of c-di-GMP for the second level of regulation- allosteric activation of the BcsA subunit, allowing for polysaccharide synthesis (Zogaj *et al.*, 2001, Brombacher *et al.*, 2006, Chan *et al.*, 2004, Römling *et al.*, 2000, Simm *et al.*, 2004). The third level of regulation involves c-di-GMP binding to BcsE, thought to control BcsG, which is responsible for post-synthetic modification of cellulose in the periplasm (Thongsomboon *et al.*, 2018, Chan *et al.*, 2004). While not yet investigated, c-di-GMP almost certainly regulates cellulose synthesis in *V. fischeri* by binding to and activating the predicted BcsA and BcsE proteins, perhaps due to CasA-relayed calcium and/or additional signals. BinA is also a likely candidate for regulation of cellulose synthesis, and/or post-synthesis modification. BinA is a major regulator of cellulose polysaccharide at least at one or more levels, as it impacts global c-di-GMP levels, and *bcs* transcription, and lack of BinA allows for robust binding to Congo red dye, and adherent ring formation (Figures 10-14) (Bassis & Visick, 2010). It is possible that CasA and BinA work together as a pair to modulate the pool of c-di-GMP that contributes to cellulose production (Figure 47), and investigation of if and how these two proteins interact could increase our understanding of cellulose regulation in *V. fischeri*.

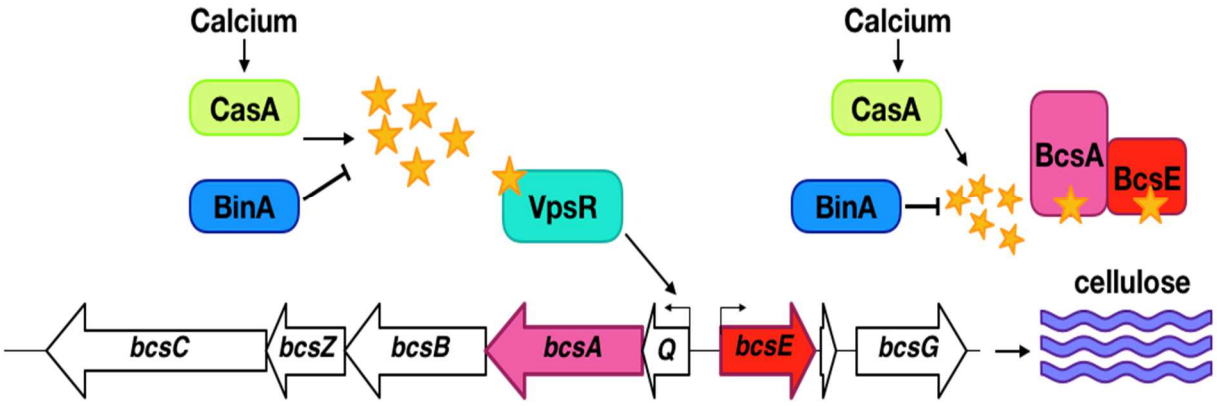

Figure 47. Updated Model for Regulation of Cellulose-Dependent Biofilm Formation. Calcium induces an increase in *bcs* transcription dependent on the DGC, CasA. CasA directly senses calcium, and produces c-di-GMP, which is hypothesized to activate VpsR. VpsR is required for bcs transcription. BinA is a PDE which negatively regulates cellulose, and this could occur transcriptionally or post-transcriptionally.

The Role of CasA in Motility

Opposite to its impact on biofilm formation, c-di-GMP inhibits bacterial motility, and this can occur through a variety of mechanisms. C-di-GMP can interact directly with flagellar proteins, including the flagellar motor to slow rotation, or to switch direction of flagellar rotation, acting as a "backstop break" (Römling *et al.*, 2013). Alternatively, c-di-GMP can have transcriptional affects, binding to master transcriptional regulators FlrA in *V. cholerae*, and FleQ in *Pseudomonas aeruginosa* (Römling *et al.*, 2013). Beyond direct interaction with flagellar regulation and machinery, c-di-GMP can also inhibit motility through production of polysaccharide. In *Salmonella*, cellulose polysaccharide directly interferes with motility through steric hindrance of flagellar rotation (Zorraquino *et al.*, 2013), and c-di-GMP activation of *vps* inhibits motility in *V. cholerae* (Srivastava *et al.*, 2013). These mechanisms offer a variety of ways that CasA could be inhibiting motility. I confirmed initial screens that identified CasA as a

calcium-dependent inhibitor of motility. While an excellent hypothesis would be that CasA inhibits motility the same way it induces biofilm formation- through cellulose polysaccharide, this was not the case. I identified and confirmed that both *bcsA* and *vpsR* mutant strains phenocopy ES114 migration, regardless of calcium. If cellulose was an inhibition factor, both mutations should have phenocopied migration of a *casA* mutant strain. Additionally, if VpsR, activated by CasA in the presence of calcium, promoted transcription of a motility factor/component, then a *vspR* mutant strain would have migrated farther in the presence of calcium. However, since this was not the case, we are left with several possibilities. CasA could be making c-di-GMP that impacts another transcription factor/regulator that controls motility. Both calcium and high c-di-GMP have previously been shown to decrease *V. fischeri* motility, with high c-di-GMP leading to a substantial post-transcriptional decrease in flagellin (O'Shea *et al.*, 2005, O'Shea *et al.*, 2006). This mechanism was previously identified through overexpression of the DGCs *mifA* and *mifCB* to simulate high c-di-GMP conditions, as the *mif* genes are named for and specifically related to *m*agnesium-dependent *i*nduction of *f*lagellation (O'Shea *et al.*, 2006). Surprisingly, this study also uncovered a specific connection between MifA and cellulose induction but showed no corresponding impact on cellulose by MifB or MifC, providing another intriguing, yet elusive connection between cellulose, c-di-GMP, and motility (O'Shea *et al.*, 2006). The role of calcium in motility was not probed in relation to the Mif proteins, but it is unlikely that this phenotype is solely dependent on high c-di-GMP, as not every DGC and PDE mutant has a specific calcium-dependent migration phenotype. However, both a role for CasA in flagellin stability and potential interactions between MifA and CasA should be probed to better understand how these regulators impact motility.

Parallels Between Calcium and Polysaccharide Regulation in *Vibrio* spp.

Regulation of the *bcs* locus in *V. fischeri* shows parallels to regulation of other *Vibrio* polysaccharide loci and is often directly inverse to regulation in *V. cholerae*. First, calcium affects transcription of a major polysaccharide locus in at least three different *Vibrio* spp., activating *bcs* and *brp* transcription in *V. fischeri* and *V. vulnificus,* respectively, and downregulating *vps* transcription in *V. cholerae* (Chodur *et al.*, 2018, Tischler *et al.*, 2018, Bilecen & Yildiz, 2009). Calcium acts to increase c-di-GMP in both *V. fischeri* and *V. vulnificus,* activating CasA in *V. fischeri* to increase *bcs* transcription (Chodur *et al.*, 2018). The specific calcium-dependent mechanism activating *brp* transcription is yet unknown but also dependent on c-di-GMP (Chodur *et al.*, 2018). Conversely, *vps* transcription is decreased by calcium, through downregulation of *vpsR* transcription by the calcium-sensing two component system CarRS (Bilecen & Yildiz, 2009). Second, the homologous transcriptional regulators VpsR in both *V. fischeri* and *V. cholerae* autoregulate their own transcription, albeit in opposite directions, with *V. fischeri* VpsR negatively autoregulating and *V. cholerae* VpsR engaging in positive autoregulation (Casper-Lindley & Yildiz, 2004). Third, the homologous DGCs CasA and CdgK respond oppositely to calcium, with CasA increasing and CdgK decreasing c-di-GMP levels in the presence of calcium, paralleling the effects on *bcs* and *vps* transcription. In *V. cholerae*, VpsR activity is increased by c-di-GMP (Hsieh *et al.*, 2018, Krasteva *et al.*, 2010). This is likely to be the case for the *V. fischeri* protein as well; if so, this could account for CasA-mediated induction of *bcs* transcription in response to calcium. Overall, these differences in regulation speak to the evolutionary divergence between species, with the same signal allowing each organism to adapt to its environmental niches without major functional changes.

V. cholerae CdgK was originally identified as one of a cohort of regulators that respond to temperature to create a pool of c-di-GMP that alters VpsR activity, and subsequent VPS-dependent biofilm formation (Townsley & Yildiz, 2015). Therefore, a CdgK-dependent change in c-di-GMP levels in response to calcium was an unexpected result. However, two other DGCs in *V. cholerae,* CdgH and CdgM, were identified as sensing and responding to bile acids and to temperature (Townsley & Yildiz, 2015, Koestler & Waters, 2014). These three cases suggest that either many more DGCs/PDEs may be responsive to multiple sensory inputs, or that temperature could be a proxy condition impacting other signals. For example, temperature can alter bacterial membrane fluidity (Cronan, 1975, Aguilar *et al.*, 2001). Membrane fluidity itself may be a signal, and could potentially impact other signals, including calcium. For example, chloroplasts are able to respond to temperature by altering concentrations of free calcium in the stroma, although the specific mechanism how this happens is yet unknown (Lenzoni & Knight, 2019, Navazio *et al.*, 2020). Calcium flux in bacteria is not well understood, but it has been shown to concentrate in the periplasm*,* which is likely to be impacted by membrane fluidity (Jones *et al.*, 2002, King *et al.*, 2020). The periplasm is also where the sensory domains of both CasA and CdgK are predicted to be located (Townsley & Yildiz, 2015). If CdgK is calcium responsive in *V. cholerae*, it may present an answer to a lingering question about calcium inhibition of VPS-dependent biofilm formation. The CarRS TCS is able to sense calcium, and downregulate *vspR* transcription, resulting in a decrease in *vps* transcription (Bilecen & Yildiz, 2009). However, even when *carS* or *carR* are deleted, transcription of *vpsA* and *vpsL* have a calcium-dependent decrease in transcription, meaning that in addition to CarRS, there must be another calcium-sensing mechanism that decreases *vps* transcription (Bilecen & Yildiz, 2009). In this hypothetical scenario, instead of and/or in addition to responding to temperature, CdgK could decrease c-di-

GMP in response to calcium, resulting in decreased VpsR activation and subsequent transcription of the *vps* locus. To be clear, the evidence supporting this hypothesis is all correlative and coincidental, but assessing calcium-inhibition of biofilm formation in a *cdgK* mutant is an intriguing experiment.

As a caveat to my conjecture above, nothing in the work presented here accounts for conditions permissive to expression of CdgK or CasA. All gene expression constructs were engineered using the non-native (native to *V. fischeri*, but not *casA*), constitutive *nrdR* promoter and contained an idealized RBS. I utilized these expression conditions because I had great difficulty creating a construct that resulted in detectible CasA protein. I worked through several iterations of promoters, sequences, and tags that could have impacted gene expression, protein production, and/or protein stability. It was not until adding the idealized RBS that I saw CasA complementation phenotypes and was able to detect protein by immunoblotting. Therefore, I used this construct as a template to express all other alleles, so that I would be able to compare the different variants without worrying about differences in expression.

While I made numerous attempts to express *casA* under its native promoter, other troubleshooting options remain that can be explored in further work. One possibility is simply that the promoter region I tested was not long enough. *casA* is independently transcribed, and there are 124 bp in the intergenic region between *VF_1640* and *casA*. I utilized only a marginally longer sequence for my initial promoter construct, which included putative -35 and -10 regions, but could easily lack enhancers that promote transcription. Due to DNA supercoiling, enhancers can be located as far as 2.5 kb up or downstream of a promoter start site (Liu 2001). Thus, assessing longer putative promoter regions could allow for *casA* transcription under the control of its native promoter.

Relevance of Cellulose During Colonization

Bacterial aggregation, or biofilm formation, on the surface of the symbiotic light organ is directly related to successful *V. fischeri* colonization of the Hawaiian bobtail squid. Strains defective in aggregation are unable to initiate colonization, while hyper-aggregating strains have dominant colonization behaviors (Yip *et al.*, 2005, Yip *et al.*, 2006, Bongrand & Ruby, 2018). However, the necessity of biofilm-competence at this early stage has made it challenging to evaluate or define any role for biofilm formation post-initiation. Recently, however, biofilm-competence dependent on RscS has been linked to successful maintenance of the *Vibrio*-squid symbiosis, beyond just the initial colonization stage (Ludvik *et al.*, 2021). These aggregation phenotypes have been almost exclusively tied to SYP, and to date there is only strong correlative, but not fully conclusive, evidence of a role for cellulose polysaccharide in colonization. On the symbiont side, a *vspR* mutant is defective for colonization and outcompeted by WT in a direct competition assay (Hussa *et al.*, 2007). Also, deletion of the gene for the negative cellulose regulator, BinA, results in increased colonization (Pankey *et al.*, 2017). While neither of these studies are fully conclusive, as a *bcs* mutant is not directly tested, the combination of two known cellulose regulators both presenting colonization phenotypes provides strong hypothesis for a role for cellulose in squid colonization. On the squid side, CasA and BinA are both differentially regulated during the daily cycle, upregulated in the hours before dawn and expulsion. CasA is downregulated immediately after dawn, while BinA is downregulated later on, during the day (Wier *et al.*, 2010). This regulation, and the strong cellulose phenotypes due to both CasA and BinA suggest that cellulose could be involved in symbiont maintenance following the dawn expulsion event. As our understanding of non-SYP dependent biofilm formation grows (e.g. cellulose, LapV, VPS-like polysaccharide), it is

important to understand the physiological relevance of each biofilm factor and where they fit into the life cycle of *V. fischeri* in the context of the host or the marine environment.

Environmental Relevance of Calcium Concentrations

I found that a range of calcium concentrations is sufficient to induce biofilm formation by *V. fischeri*, along what seems to be an almost linear trajectory. These findings beg the question, what calcium concentrations are environmentally relevant? The approximate calcium concentration of seawater is 10 mM (PubChem, 2021), which is the calcium concentration used for much of the work reported here. However, while 10 mM calcium promotes biofilm formation, environmental *V. fischeri* will not always reside in sessile biofilm communities in nature. For example, one of the first steps in colonization is recruitment of small particles to a sheltered zone by the squid's light organ appendages and cilia (Nawroth *et al.*, 2017). This recruitment is size specific, and only particles approximately 1-2 microns in length make it to the sheltered zone. Larger particles get swept back into the flow of water exiting the mantle cavity (Nawroth *et al.*, 2017). These data suggest that at least some *V. fischeri* must be planktonic in seawater, in order to start the colonization process. However, regions within the squid such as the mucus on the surface of the light organ and inside the symbiotic organ itself may represent microenvironments where increased calcium concentrations exist to promote symbiotic aggregation or other symbiont phenotypes. While I have been unable to investigate calcium staining on the surface of the light organ, several pieces of evidence support this hypothesis.

(1) A previous study investigated the role of NO in *E. scolopes* during colonization initiation (Davidson *et al.*, 2004). To accomplish this, they probed the surface of the juvenile light organ with both a NO-specific stain, and a calcium-sensitive fluorochrome as an internal control. While the specific data were not shown, Davidson reported altered calcium staining

patterns in apo vs symbiotic squid, indicating that calcium levels in the light organ may be associated with symbiosis. Additionally, the authors noted that calcium staining of the ducts and the crypts was “barely detectable”. Motility is required to swim through the ducts and crypts in order to access the deep crypts where bacteria settle and grow to complete colonization of the organ (Reviewed in: (Visick *et al.*, 2021)), and therefore promoting sessile behaviors would be counterproductive in the ducts and crypts.

(2) Similar to *V. fischeri*, *V. vulnificus* also has colonization and biofilm phenotypes that are induced by calcium. Calcium induces production of several adherence factors in *V. vulnificus* that promote colonization of their host organism, oysters. These colonization events typically happen in oysters found in estuaries, which have lower calcium concentrations than marine environments, typically ranging between 1.5-10 mM calcium; however, oysters are able to enrich calcium from the environment for growth and shell repair (Sillanpää *et al.*, 2016). This means that local calcium levels within oyster tissue and haemolymph can be quite high, having been reported up to six-fold higher than the surrounding water (Pu *et al.*, 2020). This particular increase in host calcium levels was reported three days after oysters were subjected to shell injury (Pu *et al.*, 2020). Unlike mollusks, cephalopods do not have shells, and while many squid do maintain an internal vestigial version called a gladius, or pen, bobtail squids do not (Sanchez *et al.*, 2019). Therefore, while *E. scolopes* likely does not sequester calcium for shell, or gladius, repair specifically, there might be other tools or mechanisms allowing for retention of calcium from the environment, and/or producing microenvironments with high calcium levels.

Conclusion

This dissertation has identified calcium as a major biofilm regulator and elucidated a mechanism by which *V. fischeri* is able to sense and respond to calcium. Calcium as a biofilm

signal permits formation of a novel biofilm phenotype in liquid culture, coordinately inducing both SYP and cellulose polysaccharide at the level of transcription. In first identifying calcium as a signal, we were able to develop a new method of biofilm induction, which allowed us to probe and validate the signaling network controlling *syp* transcription in the absence of genetic overexpression. In turn, this revealed the contributions of the regulators HahK and HnoX, which were previously masked. This dissertation also established a link between calcium and c-di-GMP, identifying the calcium-sensing DGC, CasA, as a regulator of cellulose-dependent biofilm formation and motility. Knowledge gained from the work presented here has already begun to benefit and inform biofilm studies to date, contributing to identification of two additional biofilm signals, and the characterization of the large adhesin protein, LapV. Future studies will continue to use calcium as a signal and a tool to further our understanding of biofilm formation and host-symbiont dynamics.

APPENDIX A

ADDITIONAL STUDIES

Screen for Calcium-Dependent Phenotypes in DGC and PDE Mutants

Biofilm formation and motility are two phenotypes that are required for symbiotic colonization by *V. fischeri* (Yip *et al.*, 2005, Yip *et al.*, 2006, Brennan *et al.*, 2013), and both of these behaviors are governed by the small signaling molecule, c-di-GMP (Römling *et al.*, 2013). C-di-GMP has been studied to some extent in *V. fischeri* with several studies establishing connections between this small molecule and either cellulose-dependent biofilm formation or motility (Bassis & Visick, 2010, O'Shea *et al.*, 2006). However, the *V. fischeri* genome contains 50 putative DGC and/or PDEs, making in depth characterization of these genes and the subsequent phenotypes extremely difficult until recently (Wolfe & Visick, 2010, Ruby *et al.*, 2005, Mandel *et al.*, 2008). In the fall of 2016, Dr. Karen Visick began developing a new set of tools that allow for rapid genetic manipulation of *V. fischeri* using antibiotic cassettes for allelic replacement of genes of interest. These new methods allowed us to quickly and easily delete genes in a matter of days, whereas using older techniques can take a month or more from start to finish (Visick *et al.*, 2018). Using this technique, former technician Ali Razvi was able to delete all 50 putative DGC/PDEs in approximately 5 months, and many lab members set out to screen these mutants for various phenotypes of interest.

As calcium induces both SYP and cellulose polysaccharide-dependent biofilms, I decided to screen these mutant strains for wrinkled colony formation (+/- calcium) and Congo red binding (only – calcium), which are indicative of SYP and cellulose production, respectively. I also screened for changes in levels of c-di-GMP using the c-di-GMP biosensor plasmid,

pFY4535, generous gifted by the Yildiz Lab (Zamorano-Sánchez *et al.*, 2019). Additionally, certain calcium-induced phenotypes are only visible in biofilm-competent conditions, one of which is deletion of the negative regulator *binK.* Since individual mutations have selectable antibiotic markers, I along with others in the lab moved each of these mutations into a *binK* mutant background, and ultimately performed phenotypic screens of both ES114 and *binK* mutant versions of many DGC/PDE mutants. Of note, of these mutants were only assessed one time, and all phenotypes should be considered preliminary. Phenotypes are summarized by gene in Table 4.

Wrinkled Colony Formation

While several mutations resulted in altered colony biofilm phenotypes, these phenotypes were overall very mild, and none altered SYP-dependent cohesive phenotypes- either increasing cohesion in a WT background, or disrupting wrinkling/cohesion in a *binK* mutant background. Several ES114-based mutations in a WT background did increase architecture typically associated with cellulose; disruption of either *VF_0494* or *binA* (*VF_A1038*) caused altered architecture regardless of calcium. Mutations in *VF_1350, VF_A0976, VF_0087, VF_1014, VF_1603,* and *VF_2480* caused a slight increase in architecture only in response to calcium (Figure 48). All differences are marked by a star on the appropriate colony image. The phenotype of a *binK* mutant is so strong that subtle differences in architecture were difficult to ascertain; however, several strains did display slightly increased or decreased wrinkling at the center of spots (Figure 48). In a *binK* mutant background, *VF_0494* and *VF_1603* mutations resulted in slightly increased wrinkling regardless of calcium, while *casA* (*VF_1639*) and *VF_A0216* both caused a slight increase in wrinkling only on plates with calcium. Additionally, a *binK* mutation paired with both *binA* (*VF_A1038*) and *VF_A0056* mutations resulted in a slight

increase in architecture on plates without calcium. It is possible that these mutations also impact phenotypes on plates with calcium and that I did not capture the moment where differences were visible. Overall, the subtle phenotypes observed suggest that either c-di-GMP does not impact SYP-dependent biofilm formation, or more likely, that multiple c-di-GMP regulators modulate SYP-dependent biofilm formation and are therefore redundant. If the second scenario is true, then multiple mutant strains would be required to see changes in SYP-dependent wrinkled colony phenotypes.

Congo Red Binding

On plates with no added calcium, most c-di-GMP mutants, generated in either a WT or *binK* mutant background, had minimal color changes, or exhibited just a slight increase in color on Congo red. Two notable exceptions were mutations in *VF_0494* and *VF_A1038* (*binA*), which are extremely red, indicating a high level of cellulose binding (Figure 49). Both genes contain dual GGDEF and EAL domains, although for BinA, only the EAL domain is thought to be functional (Bassis & Visick, 2010). BinA in particular has been shown to be a strong and specific regulator of cellulose, first by Christine Bassis and colleagues (Bassis & Visick, 2010), and later on in work detailed here in chapter 3.

C-di-GMP Levels

Overall, I found that screening for c-di-GMP levels using the biosensor was quite variable. However, despite this variation, repeated samples with a smaller number of strains allowed for a few patterns to emerge. The most reliable patterns came from mutants that had a decreased response to calcium, which included those with mutations in *casA* (*VF_1639*)*, pdeV* (*VF_A1014*), *binA* (*VF_A1038*), and *VF_0494.* Of these four genes, only *VF_1639* is a DGC, while the rest contain both putative GGDEF and EAL domains (Figure 50).

Summary

These screens provided us with a starting point to evaluate calcium-dependent c-di-GMP phenotypes and allowed for identification of *VF_1639* as a DGC with calcium-specific phenotypes. These results can also be very useful in evaluating differences between WT and c-di-GMP mutant strains of interest in the future. Additionally, mutants may behave differently under different conditions. It is important to note that all assays were performed in LBS media, wrinkled colony assays contained 10 mM calcium, Congo red plates were incubated at 24°C for 48 h before visualization, and the c-di-GMP screens with pFY4535 were performed with 40 mM calcium.

Table 4. Overview of C-di-GMP Mutant Phenotype Screen

C-di-GMP mutant phenotype screen overview

Gene	Wrinkled colony- WT	Wrinkled colony- Δ*binK*	Congo red-WT	Congo red- Δ*binK*	Avg. fold change + Ca (WT)
VF0596	X	X	+	X	12.01
VF0989 (mifA)	n/n	n/n	n	n	7.92
VF1200	n/n	n/n	(-)	n	6.47
VF1245	n/n	X	n	n	2.60
VF1350	n/+	n/n	+	+	5.08
VF1515	X	X	n	X	1.99
VF1561	n/n	n/n	n	n	X
VF1639 (casA)	n/n	n/+	n	n	1.01
VF2261	n/n	n/n	n	n	2.44
VF2362	n/n	n/n	n	n	2.74
VFA0056	n/n	+/n	n	n	4.33
VFA0057	n/n	n/n	n	n	2.49
VFA0152	n/n	n/n	n	n	2.27
VFA0155	n/n	n/n	n	n	X
VFA0276	n/n	n/n	n	n	X
VFA0323	n/n	n/n	n	n	2.05
VFA0342	n/n	n/n	n	n	3.08
VFA0343	n/n	n/n	n	n	3.76
VFA0368	X	X	n	X	X
VFA0381	n/n	n/n	n	n	X
VFA0398	n/n	n/n	n	n	X
VFA0476	n/n	n/n	n	n	9.17
VFA0567	n/n	n/n	n	n	X
VFA0692	n/n	n/n	n	n	X
VFA0796	n/n	n/n	n	++	X
VFA0959 (mifB)	n/n	n/n	n	n	3.10
VFA0976	n/+	n/n	n	n	2.14
VFA1012	n/n	n/n	n	+	X
VF0087 (mifD)	n/+	n/-	+	+	8.23
VF0091	n/n	n/n	n	poor growth	2.23
VF0094	n/n	n/n	n	+	7.37
VF0355	n/n	n/n	n	+	2.81
VF0494	+/+	+/+	++	++	1.44
VF0985	n/n	n/n	n	n	3.45
VFA0244	n/n	n/n	n	n	X
VFA0475	n/n	n/n	n	n	3.00
VFA1014 (pdeV)	n/+	n/n	+	n	1.28
VFA1038 (binA)	+/+	+/n	+++	+++	1.32
VFA1166 (lapD)	X	X	n	X	4.73
VF1603	n/+	+/+	+	+	1.82
VF2480	n/+	n/n	n	n	X
VFA0216	n/n	n/+	+	no growth	6.94
VFA0344	n/n	n/n	n	+	4.35
VFA0526	-/-	n/n	-	n	2.38
VFA0551	n/n	n/n	n	n	X
VFA0706	n/n	n/n	n	n	2.24
VFA0879	n/n	n/n	n	n	X
VFA1076	n/n	n/n	n	n	3.82
VF1367	n/n	n/n	n	n	2.07
VFA0506	n/n	n/n	+	n	1.93
Wrinkled colony formation was assessed -/+ calcium (- results on the left, + 10 mM calcium results bolded on the right)					
Congo red was only assessed on LBS with no calcium					
Fold change indicates average median of live AmCyan+ RFP+ cells in response to 40 mM calcium					
n= no change compared to parent strain (WT or *binK* mutant)					
- and += decreased and increased, respectively					
X= no results					
Teal= DGCs Yellow= DGC/PDEs Purple= PDEs (EAL) Green= PDEs (HD-GYP)					

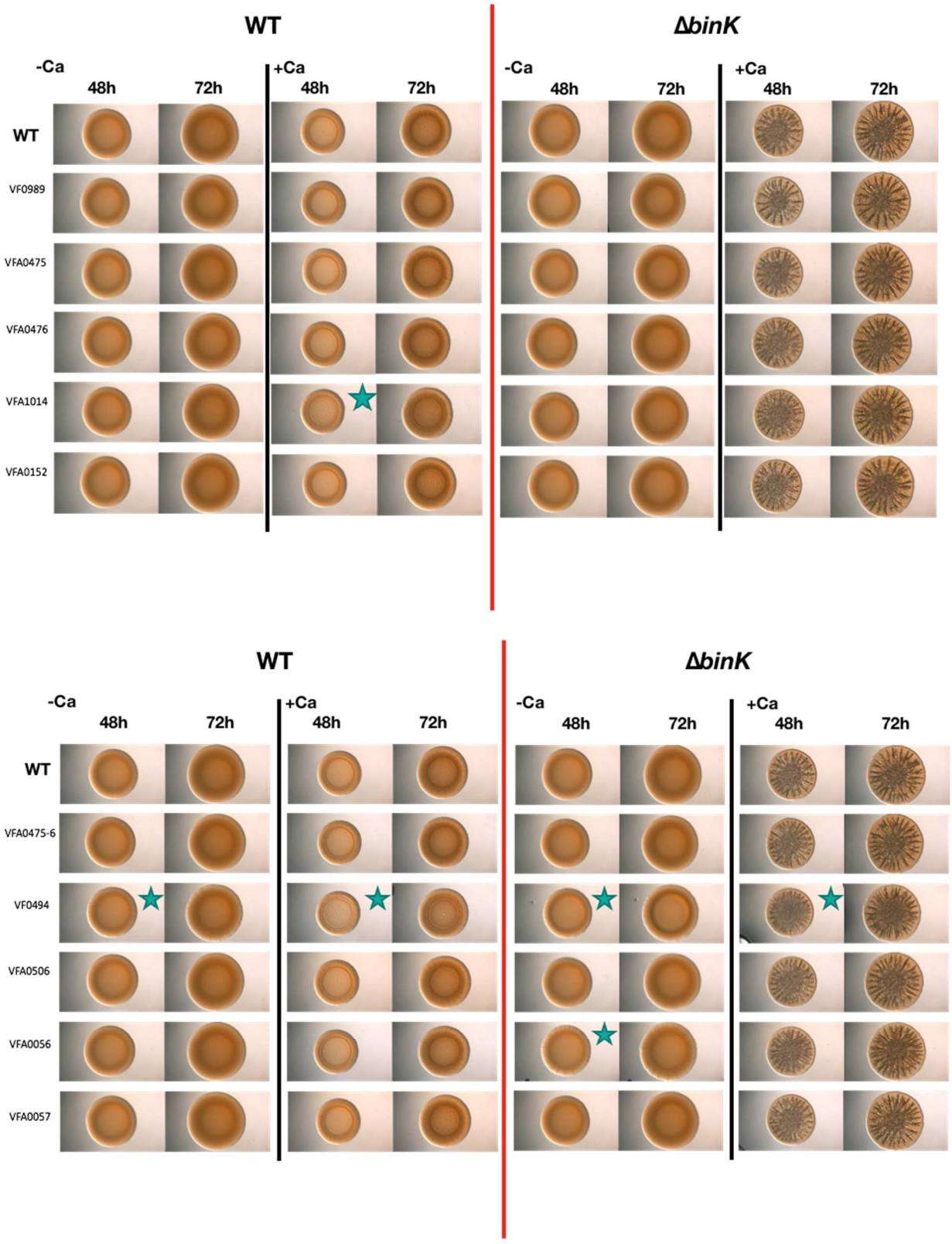
WT
ΔbinK
-Ca
+Ca
48h
72h
WT
VF0989
VFA0475
VFA0476
VFA1014
VFA0152
WT
ΔbinK
-Ca
+Ca
48h
72h
WT
VFA0475-6
VF0494
VFA0506
VFA0056
VFA0057

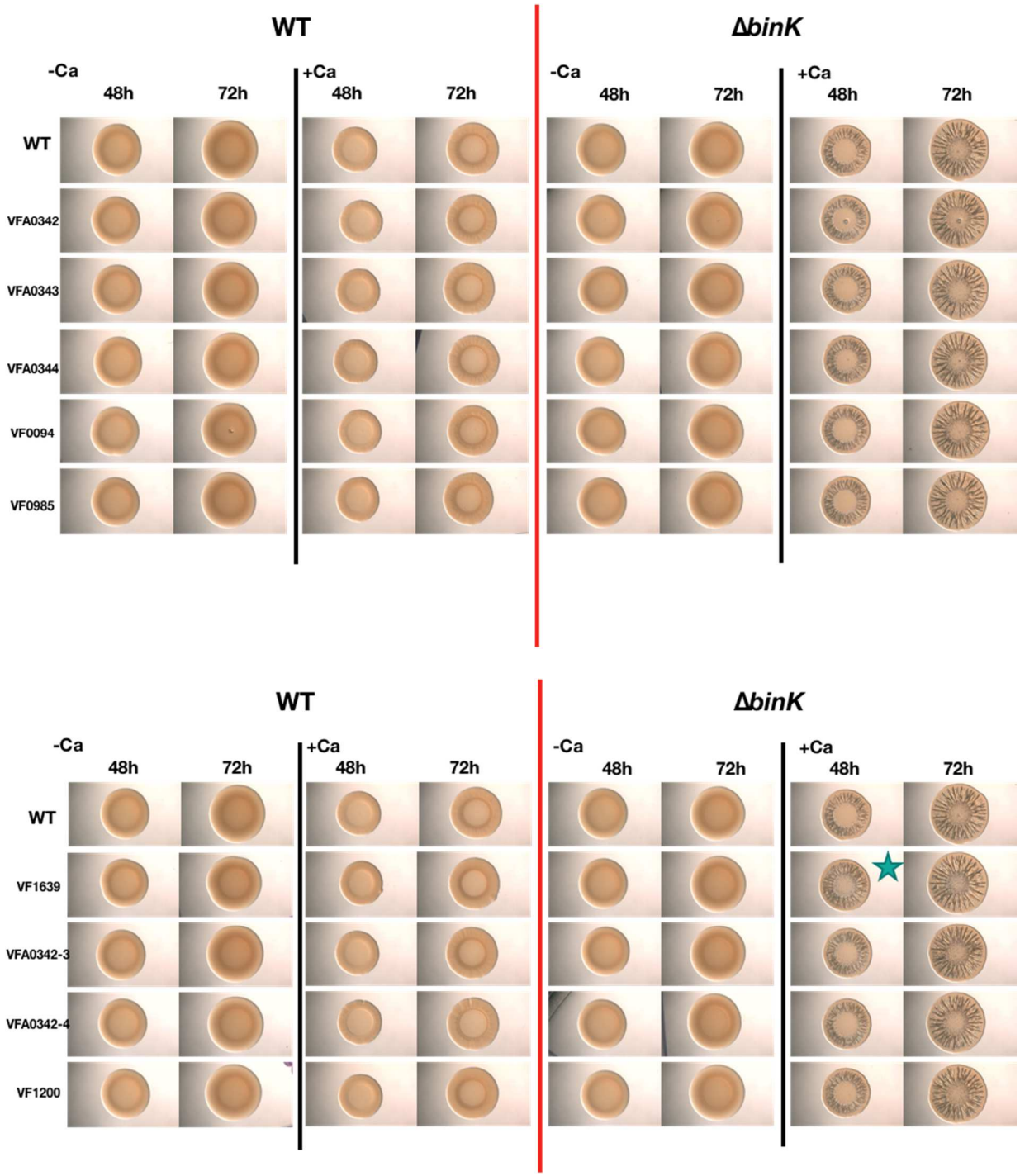
WT
ΔbinK
-Ca
+Ca
48h
72h
WT
VFA0342
VFA0343
VFA0344
VF0094
VF0985
WT
ΔbinK
-Ca
+Ca
48h
72h
WT
VF1639
VFA0342-3
VFA0342-4
VF1200

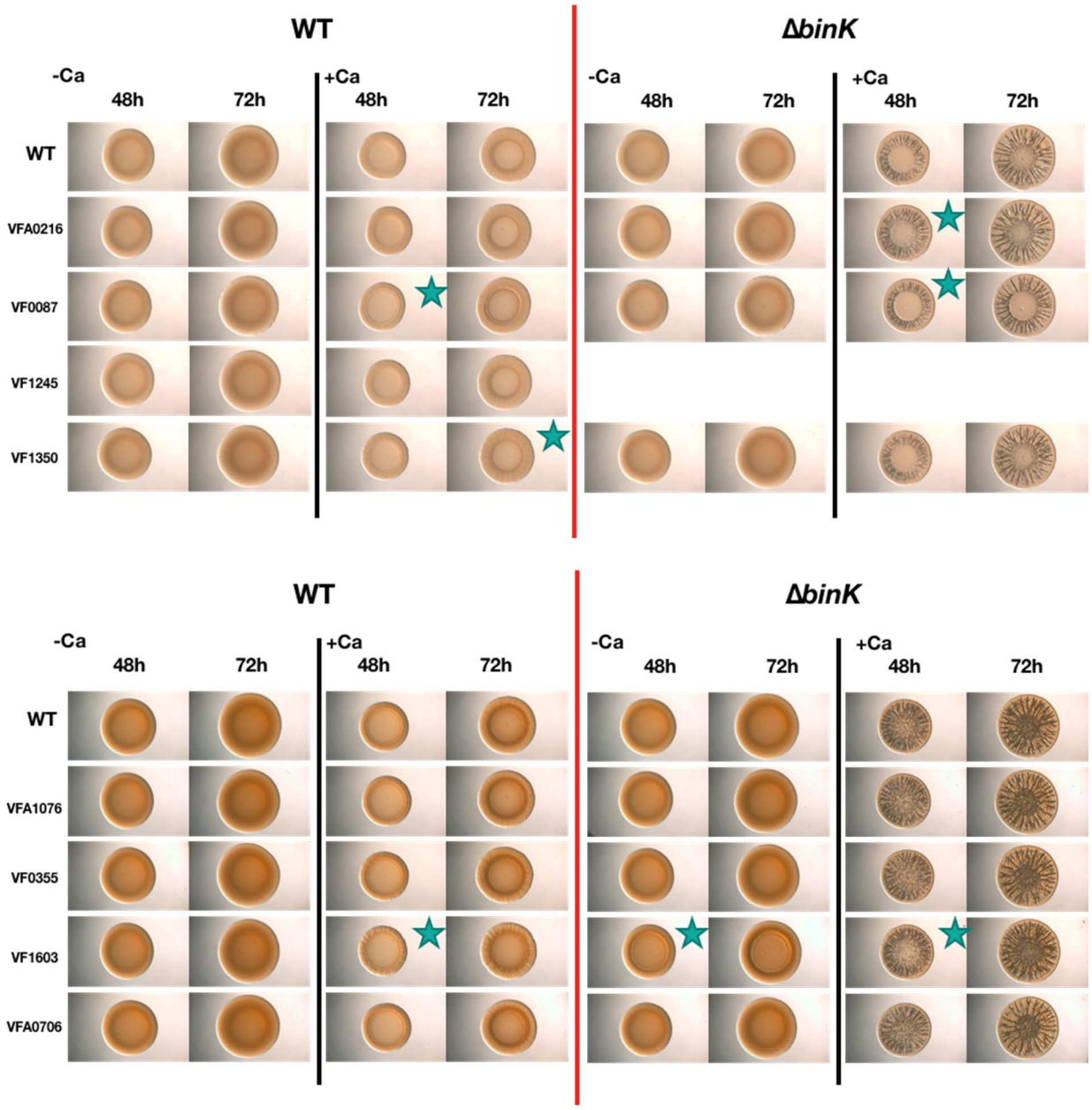
WT
ΔbinK
-Ca
+Ca
48h
72h
WT
VFA0216
VF0087
VF1245
VF1350
WT
ΔbinK
-Ca
+Ca
48h
72h
WT
VFA1076
VF0355
VF1603
VFA0706

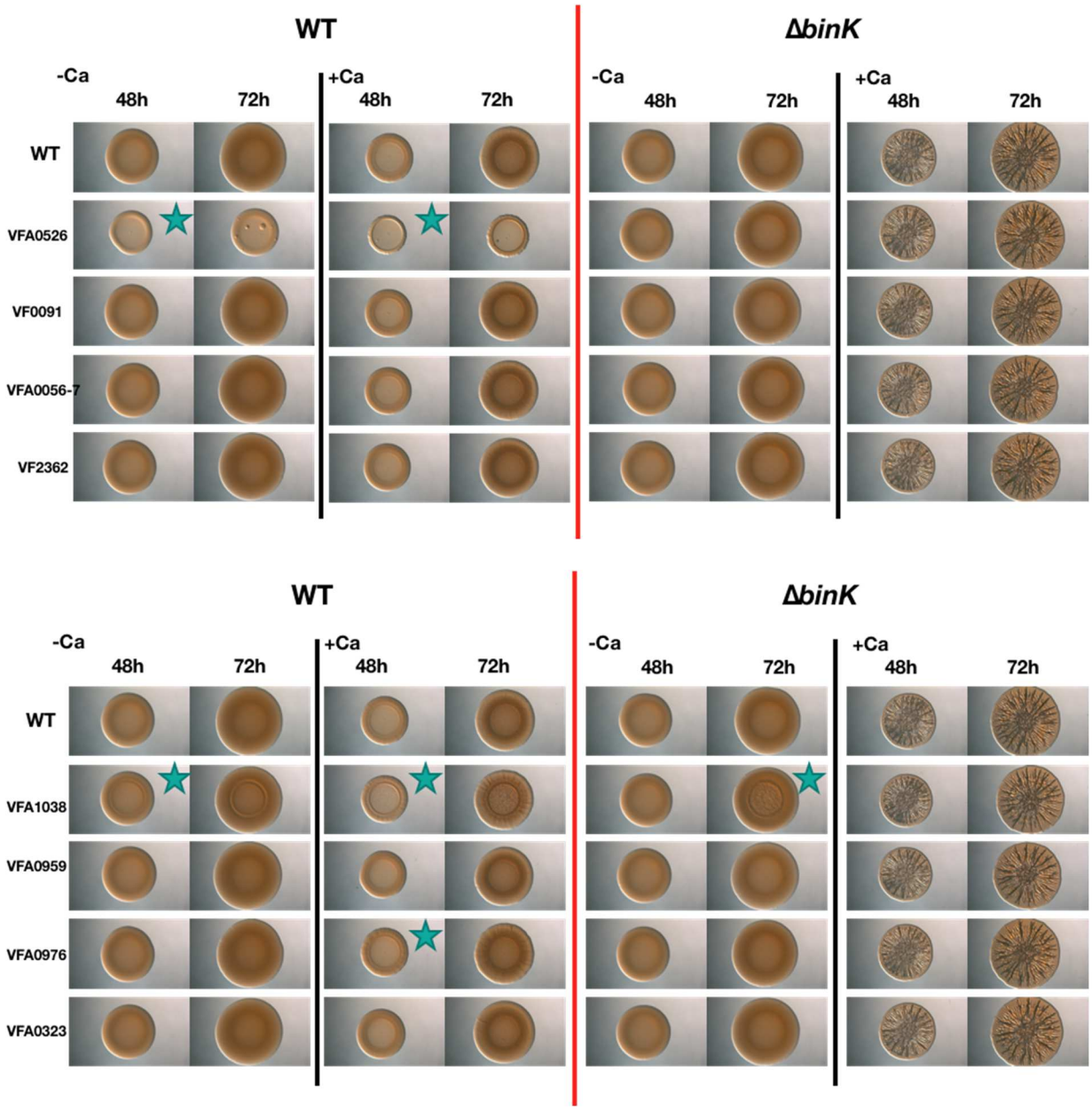
WT
ΔbinK
-Ca
+Ca
48h
72h
WT
VFA0526
VF0091
VFA0056-7
VF2362
WT
ΔbinK
-Ca
+Ca
48h
72h
WT
VFA1038
VFA0959
VFA0976
VFA0323

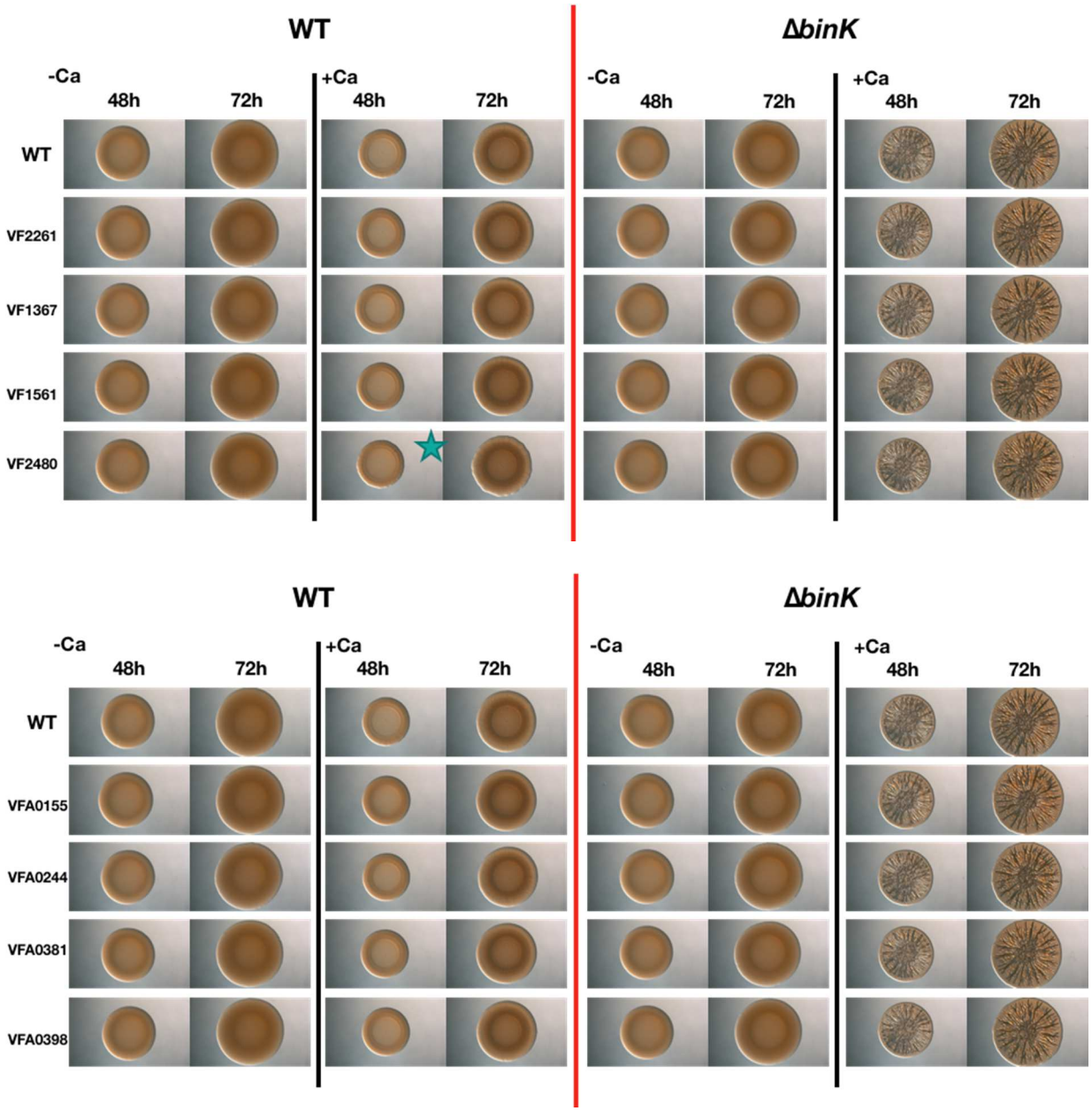
WT
ΔbinK
-Ca
+Ca
48h
72h
WT
VF2261
VF1367
VF1561
VF2480
WT
ΔbinK
-Ca
+Ca
48h
72h
WT
VFA0155
VFA0244
VFA0381
VFA0398

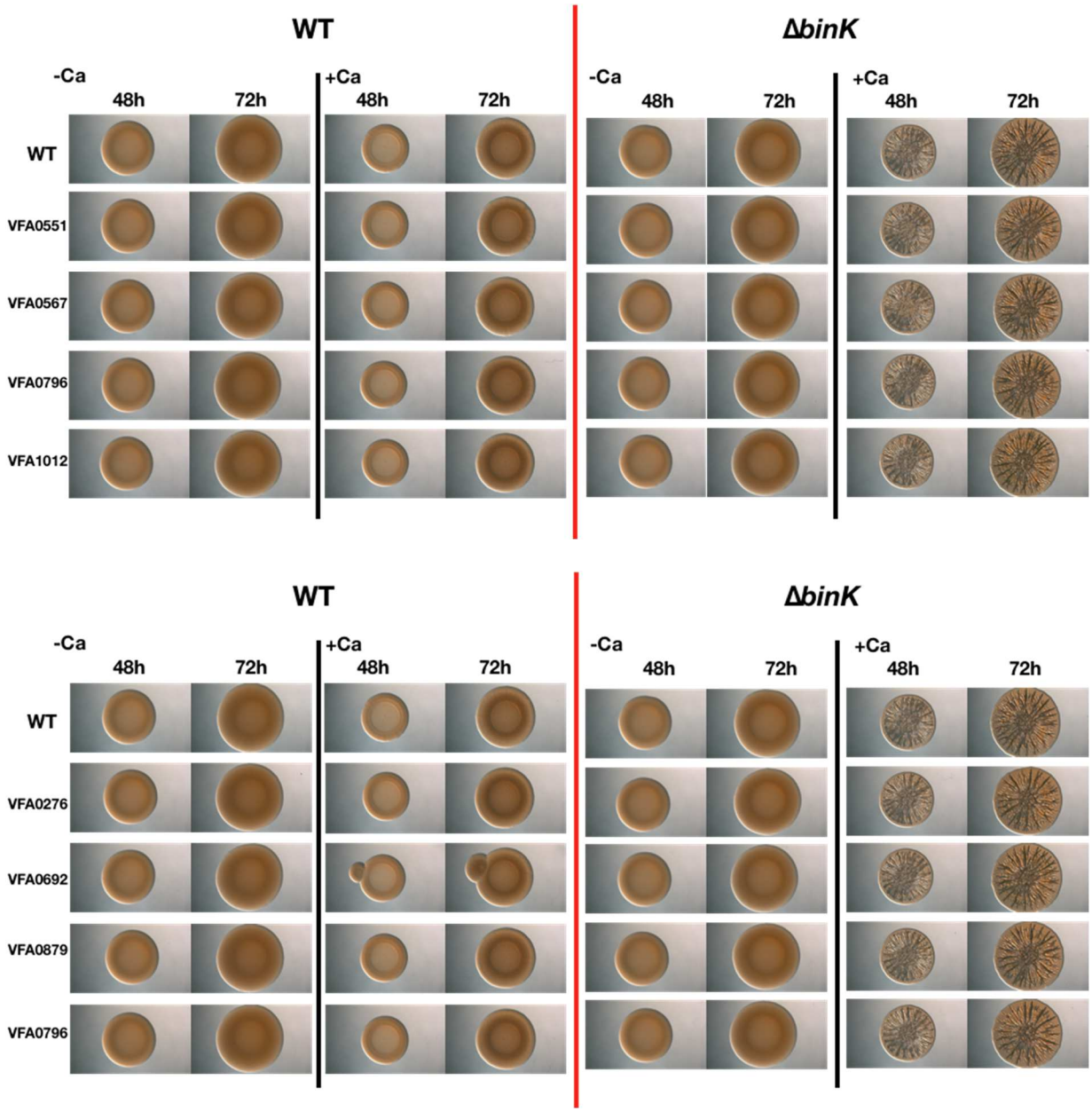

Figure 48. Screen of Wrinkled Colony Formation by C-di-GMP Mutant Strains. Each single (WT) or double (*binK*) mutant strain was evaluated on one day old LBS plates either without added calcium, or with 10 mM added calcium. Spots were all disrupted; however, no mutants generated in a WT background showed cohesion, and no mutants generated in the *binK* mutant background lost cohesion. Name of gene on the righthand side refers to which gene was deleted in that row.

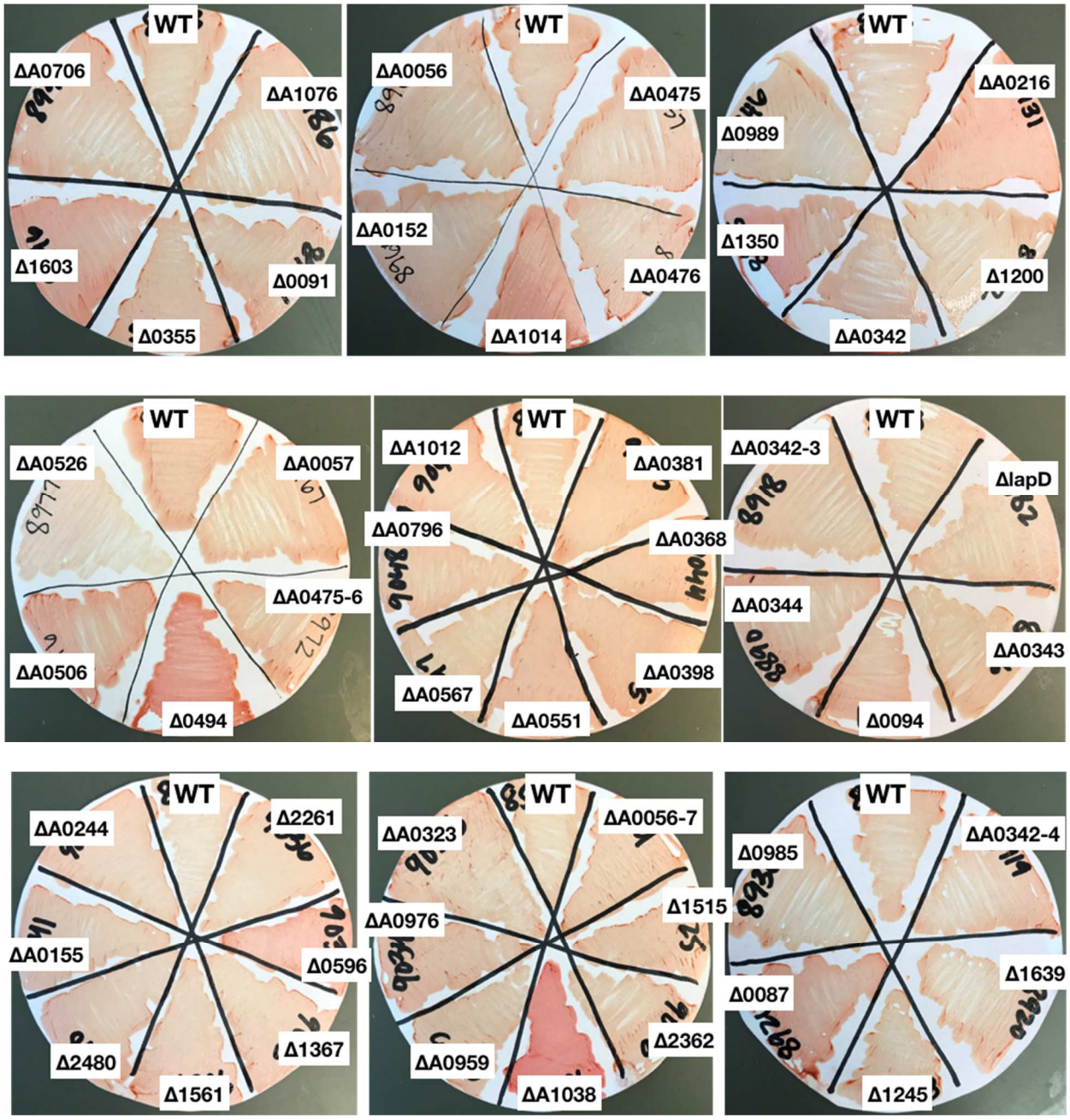
WT
ΔA0706
ΔA1076
Δ1603
Δ0091
Δ0355
WT
ΔA0056
ΔA0475
ΔA0152
ΔA0476
ΔA1014
WT
ΔA0216
Δ0989
Δ1350
Δ1200
ΔA0342
WT
ΔA0526
ΔA0057
ΔA0475-6
ΔA0506
Δ0494
WT
ΔA1012
ΔA0381
ΔA0796
ΔA0368
ΔA0567
ΔA0398
ΔA0551
WT
ΔA0342-3
ΔlapD
ΔA0344
ΔA0343
Δ0094
WT
ΔA0244
Δ2261
ΔA0155
Δ0596
Δ2480
Δ1367
Δ1561
WT
ΔA0323
ΔA0056-7
ΔA0976
Δ1515
ΔA0959
Δ2362
ΔA1038
WT
Δ0985
ΔA0342-4
Δ0087
Δ1639
Δ1245

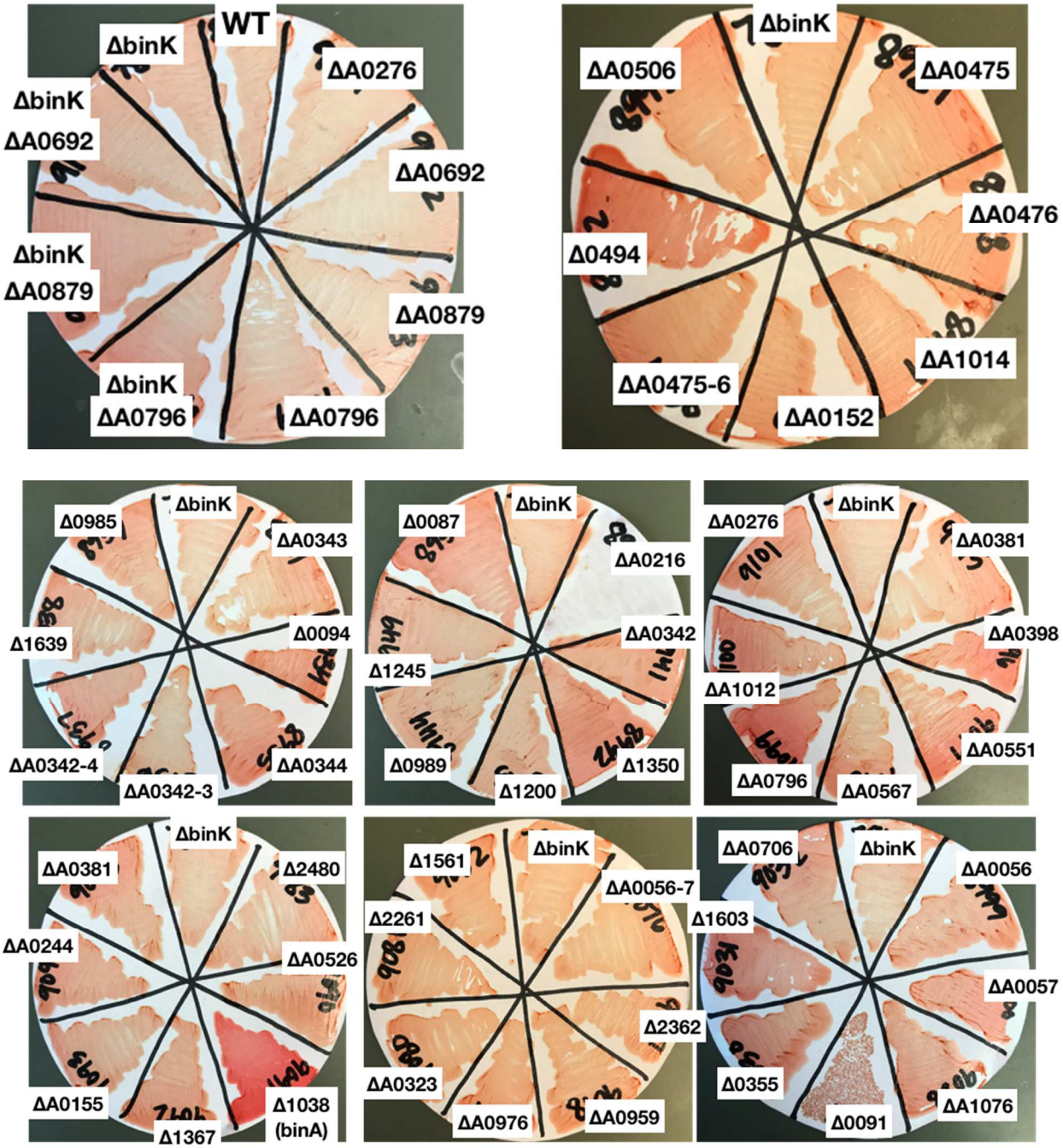

Figure 49. Screen of Congo Red Binding in c-di-GMP Mutant Strains. Mutations were present in either a WT or *binK* mutant background as indicated by control at the top of each individual piece of paper. Strains were streaked onto LBS Congo red agar without added calcium, and incubated at 24°C for 48 h before being removed with paper and imaged.

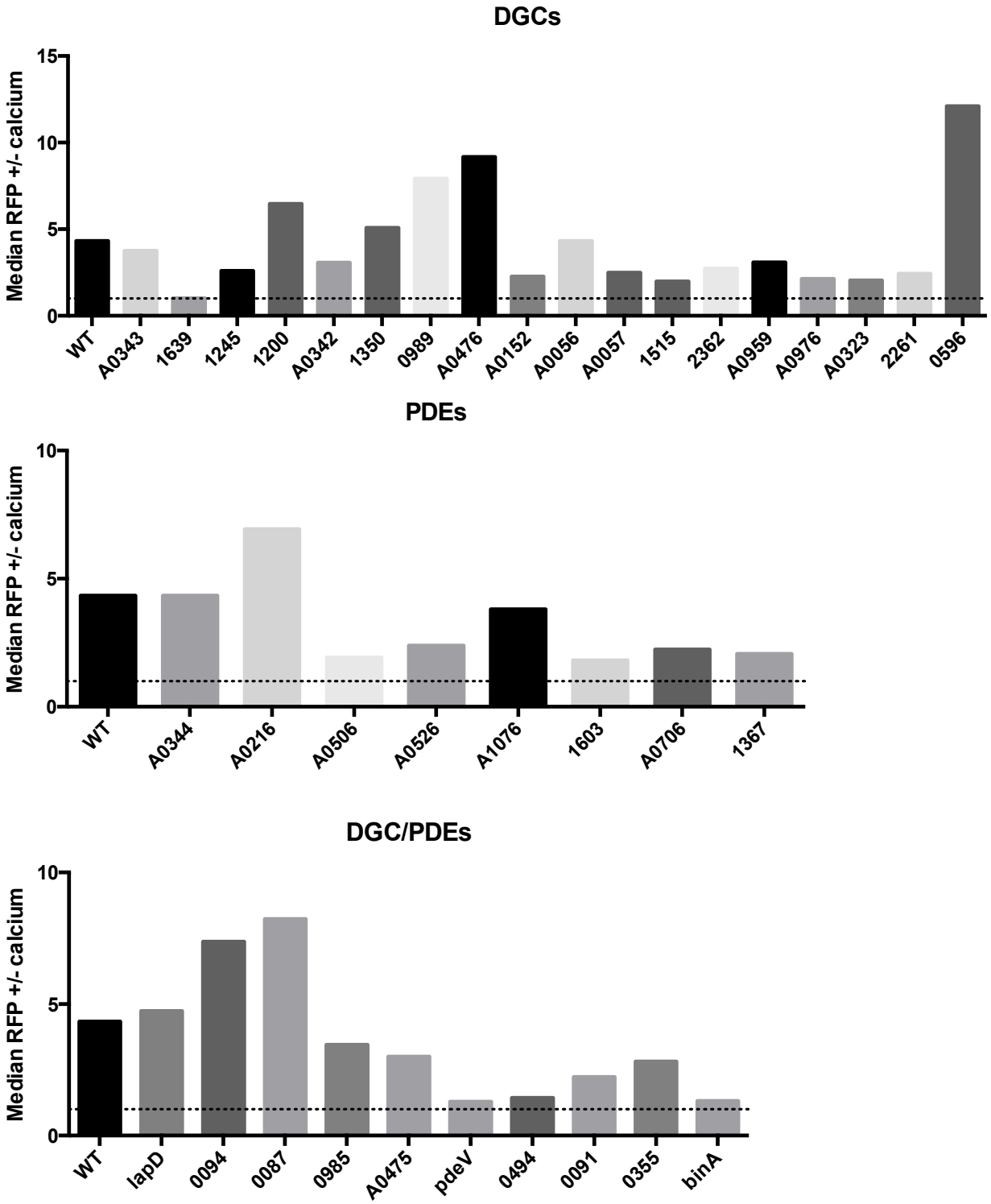

Figure 50. Screen of Relative C-di-GMP Levels in C-di-GMP Mutant Strains. Single mutants generated in a WT background were assessed for changes in c-di-GMP in response to 40 mM calcium. All strains are compared against the same WT values, but binned by putative domain function as indicated. Gene number following "VF" are indicated on the x-axis.

REFERENCE LIST

Advani, M.J., Rajagopalan, M., and Reddy, P.H. (2014) Calmodulin-like protein from M. tuberculosis H37Rv is required during infection. *Sci Rep* **4**: 6861.

Aguilar, P.S., Hernandez-Arriaga, A.M., Cybulski, L.E., Erazo, A.C., and de Mendoza, D. (2001) Molecular basis of thermosensing: a two-component signal transduction thermometer in Bacillus subtilis. *Embo j* **20**: 1681-1691.

Aloni, Y., Cohen, R., Benziman, M., and Delmer, D. (1983) Solubilization of the UDP-glucose:1,4-beta-D-glucan 4-beta-D-glucosyltransferase (cellulose synthase) from Acetobacter xylinum. A comparison of regulatory properties with those of the membrane-bound form of the enzyme. *J Biol Chem* **258**: 4419-4423.

Altschul, S.F., Gish, W., Miller, W., Myers, E.W., and Lipman, D.J. (1990) Basic local alignment search tool. *J Mol Biol* **215**: 403-410.

Altschul, S.F., Madden, T.L., Schäffer, A.A., Zhang, J., Zhang, Z., Miller, W., and Lipman, D.J. (1997) Gapped BLAST and PSI-BLAST: a new generation of protein database search programs. *Nucleic Acids Res* **25**: 3389-3402.

Altura, M.A., Heath-Heckman, E.A., Gillette, A., Kremer, N., Krachler, A.M., Brennan, C., Ruby, E.G., Orth, K., and McFall-Ngai, M.J. (2013) The first engagement of partners in the *Euprymna scolopes*-*Vibrio fischeri* symbiosis is a two-step process initiated by a few environmental symbiont cells. *Environ Microbiol* **15**: 2937-2950.

Altura, M.A., Stabb, E., Goldman, W., Apicella, M., and McFall-Ngai, M.J. (2011) Attenuation of host NO production by MAMPs potentiates development of the host in the squid-*Vibrio* symbiosis. *Cell Microbiol* **13**: 527-537.

Andree, M., Seeger, J.M., Schüll, S., Coutelle, O., Wagner-Stippich, D., Wiegmann, K., Wunderlich, C.M., Brinkmann, K., Broxtermann, P., Witt, A., Fritsch, M., Martinelli, P., Bielig, H., Lamkemeyer, T., Rugarli, E.I., Kaufmann, T., Sterner-Kock, A., Wunderlich, F.T., Villunger, A., Martins, L.M., Krönke, M., Kufer, T.A., Utermöhlen, O., and Kashkar, H. (2014) BID-dependent release of mitochondrial SMAC dampens XIAP-mediated immunity against Shigella. *Embo j* **33**: 2171-2187.

Aravind, P., Mishra, A., Suman, S.K., Jobby, M.K., Sankaranarayanan, R., and Sharma, Y. (2009) The betagamma-crystallin superfamily contains a universal motif for binding calcium. *Biochemistry* **48**: 12180-12190.

Aschtgen, M.S., Wetzel, K., Goldman, W., McFall-Ngai, M., and Ruby, E. (2016) *Vibrio fischeri*-derived outer membrane vesicles trigger host development. *Cell Microbiol* **18**: 488-499.

Asmat, T.M., Tenenbaum, T., Jonsson, A.B., Schwerk, C., and Schroten, H. (2014) Impact of calcium signaling during infection of Neisseria meningitidis to human brain microvascular endothelial cells. *PLoS One* **9**: e114474.

Augimeri, R.V., Varley, A.J., and Strap, J.L. (2015) Establishing a Role for Bacterial Cellulose in Environmental Interactions: Lessons Learned from Diverse Biofilm-Producing Proteobacteria. *Front Microbiol* **6**: 1282.

Bao, Y., Lies, D.P., Fu, H., and Roberts, G.P. (1991) An improved Tn7-based system for the single-copy insertion of cloned genes into chromosomes of gram-negative bacteria. *Gene* **109**: 167-168.

Barraud, N., Schleheck, D., Klebensberger, J., Webb, J.S., Hassett, D.J., Rice, S.A., and Kjelleberg, S. (2009) Nitric oxide signaling in Pseudomonas aeruginosa biofilms mediates phosphodiesterase activity, decreased cyclic di-GMP levels, and enhanced dispersal. *J Bacteriol* **191**: 7333-7342.

Bassis, C.M., and Visick, K.L. (2010) The cyclic-di-GMP phosphodiesterase BinA negatively regulates cellulose-containing biofilms in Vibrio fischeri. *J Bacteriol* **192**: 1269-1278.

Bergounioux, J., Elisee, R., Prunier, A.L., Donnadieu, F., Sperandio, B., Sansonetti, P., and Arbibe, L. (2012) Calpain activation by the Shigella flexneri effector VirA regulates key steps in the formation and life of the bacterium's epithelial niche. *Cell Host Microbe* **11**: 240-252.

Bilecen, K., and Yildiz, F.H. (2009) Identification of a calcium-controlled negative regulatory system affecting Vibrio cholerae biofilm formation. *Environ Microbiol* **11**: 2015-2029.

Boettcher, K.J., and Ruby, E.G. (1990) Depressed light emission by symbiotic Vibrio fischeri of the sepiolid squid Euprymna scolopes. *J Bacteriol* **172**: 3701-3706.

Boettcher, K.J., Ruby, E.G., and McFall-Ngai, M.J. (1996) Bioluminescence in the symbiotic squid *Euprymna scolopes* is controlled by a daily biological rhythm. *Journal of Comparative Physiology A* **179**.

Bongrand, C., Koch, E.J., Moriano-Gutierrez, S., Cordero, O.X., McFall-Ngai, M., Polz, M.F., and Ruby, E.G. (2016) A genomic comparison of 13 symbiotic *Vibrio fischeri* isolates from the perspective of their host source and colonization behavior. *ISME J* **10**: 2907-2917.

Bongrand, C., and Ruby, E.G. (2018) Achieving a multi-strain symbiosis: strain behavior and infection dynamics. *ISME J*.

Bonnet, M., and Tran Van Nhieu, G. (2016) How Shigella Utilizes Ca(2+) Jagged Edge Signals during Invasion of Epithelial Cells. *Front Cell Infect Microbiol* **6**: 16.

Boratyn, G.M., Schäffer, A.A., Agarwala, R., Altschul, S.F., Lipman, D.J., and Madden, T.L. (2012) Domain enhanced lookup time accelerated BLAST. *Biol Direct* **7**: 12.

Bossier, P., and Verstraete, W. Triggers for microbial aggregation in activated sludge?

Boyd, C.D., Chatterjee, D., Sondermann, H., and O'Toole, G.A. (2012) LapG, required for modulating biofilm formation by *Pseudomonas fluorescens* Pf0-1, is a calcium-dependent protease. *J Bacteriol* **194**: 4406-4414.

Breaker, R.R. (2018) Riboswitches and Translation Control. *Cold Spring Harb Perspect Biol* **10**.

Brennan, C.A., Mandel, M.J., Gyllborg, M.C., Thomasgard, K.A., and Ruby, E.G. (2013) Genetic determinants of swimming motility in the squid light-organ symbiont Vibrio fischeri. *Microbiologyopen* **2**: 576-594.

Brombacher, E., Baratto, A., Dorel, C., and Landini, P. (2006) Gene expression regulation by the Curli activator CsgD protein: modulation of cellulose biosynthesis and control of negative determinants for microbial adhesion. *J Bacteriol* **188**: 2027-2037.

Brooks, J.F., Gyllborg, M.C., Cronin, D.C., Quillin, S.J., Mallama, C.A., Foxall, R., Whistler, C., Goodman, A.L., and Mandel, M.J. (2014) Global discovery of colonization determinants in the squid symbiont Vibrio fischeri. *Proc Natl Acad Sci U S A* **111**: 17284-17289.

Brooks, J.F., and Mandel, M.J. (2016) The histidine kinase BinK is a negative regulator of biofilm formation and squid colonization. *J Bacteriol* **198**: 2596-2607.

Cai, Y.M. (2020) Non-surface Attached Bacterial Aggregates: A Ubiquitous Third Lifestyle. *Front Microbiol* **11**: 557035.

Camacho, C., Coulouris, G., Avagyan, V., Ma, N., Papadopoulos, J., Bealer, K., and Madden, T.L. (2009) BLAST+: architecture and applications. *BMC Bioinformatics* **10**: 421.

Carneiro, L.A., Travassos, L.H., Soares, F., Tattoli, I., Magalhaes, J.G., Bozza, M.T., Plotkowski, M.C., Sansonetti, P.J., Molkentin, J.D., Philpott, D.J., and Girardin, S.E. (2009) Shigella induces mitochondrial dysfunction and cell death in nonmyleoid cells. *Cell Host Microbe* **5**: 123-136.

Casper-Lindley, C., and Yildiz, F.H. (2004) VpsT is a transcriptional regulator required for expression of vps biosynthesis genes and the development of rugose colonial morphology in Vibrio cholerae O1 El Tor. *J Bacteriol* **186**: 1574-1578.

Castillo, M.G., Goodson, M.S., and McFall-Ngai, M. (2009) Identification and molecular characterization of a complement C3 molecule in a lophotrochozoan, the Hawaiian bobtail squid Euprymna scolopes. *Dev Comp Immunol* **33**: 69-76.

Chamnongpol, S., Cromie, M., and Groisman, E.A. (2003) Mg2+ sensing by the Mg2+ sensor PhoQ of Salmonella enterica. *J Mol Biol* **325**: 795-807.

Chan, C., Paul, R., Samoray, D., Amiot, N.C., Giese, B., Jenal, U., and Schirmer, T. (2004) Structural basis of activity and allosteric control of diguanylate cyclase. *Proc Natl Acad Sci U S A* **101**: 17084-17089.

Chang, W.S., van de Mortel, M., Nielsen, L., Nino de Guzman, G., Li, X., and Halverson, L.J. (2007) Alginate production by Pseudomonas putida creates a hydrated microenvironment and contributes to biofilm architecture and stress tolerance under water-limiting conditions. *J Bacteriol* **189**: 8290-8299.

Chatterjee, D., Boyd, C.D., O'Toole, G.A., and Sondermann, H. (2012) Structural characterization of a conserved, calcium-dependent periplasmic protease from Legionella pneumophila. *J Bacteriol* **194**: 4415-4425.

Cherepanov, P.P., and Wackernagel, W. (1995) Gene disruption in Escherichia coli: TcR and KmR cassettes with the option of Flp-catalyzed excision of the antibiotic-resistance determinant. *Gene* **158**: 9-14.

Chodur, D.M., Coulter, P., Isaacs, J., Pu, M., Fernandez, N., Waters, C.M., and Rowe-Magnus, D.A. (2018) Environmental Calcium Initiates a Feed-Forward Signaling Circuit That Regulates Biofilm Formation and Rugosity in Vibrio vulnificus. *mBio* **9**.

Chodur, D.M., and Rowe-Magnus, D.A. (2018) Complex Control of a Genomic Island Governing Biofilm and Rugose Colony Development in Vibrio vulnificus. *J Bacteriol* **200**.

Christen, B., Christen, M., Paul, R., Schmid, F., Folcher, M., Jenoe, P., Meuwly, M., and Jenal, U. (2006) Allosteric control of cyclic di-GMP signaling. *J Biol Chem* **281**: 32015-32024.

Christensen, D.G., Marsden, A.E., Hodge-Hanson, K., Essock-Burns, T., and Visick, K.L. (2020a) LapG mediates biofilm dispersal in Vibrio fischeri by controlling maintenance of the VCBS-containing adhesin LapV. *Mol Microbiol* **114**: 742-761.

Christensen, D.G., Tepavčević, J., and Visick, K.L. (2020b) Genetic Manipulation of Vibrio fischeri. *Curr Protoc Microbiol* **59**: e115.

Chun, C.K., Troll, J.V., Koroleva, I., Brown, B., Manzella, L., Snir, E., Almabrazi, H., Scheetz, T.E., Bonaldo, M.e.F., Casavant, T.L., Soares, M.B., Ruby, E.G., and McFall-Ngai, M.J. (2008) Effects of colonization, luminescence, and autoinducer on host transcription during development of the squid-*Vibrio* association. *Proc Natl Acad Sci U S A* **105**: 11323-11328.

Claes, M.F., and Dunlap, P.V. (2000) Aposymbiotic culture of the sepiolid squid *Euprymna scolopes*: role of the symbiotic bacterium *Vibrio fischeri* in host animal growth, development, and light organ morphogenesis. *J Exp Zool* **286**: 280-296.

Clapham, D.E. (2007) Calcium signaling. *Cell* **131**: 1047-1058.

Cohen, J.J., Eichinger, S.J., Witte, D.A., Cook, C.J., Fidopiastis, P.M., Tepavčević, J., and Visick, K.L. (2021) Control of Competence in Vibrio fischeri. *Appl Environ Microbiol* **87**.

Collins, A.J., Schleicher, T.R., Rader, B.A., and Nyholm, S.V. (2012) Understanding the role of host hemocytes in a squid/*Vibrio* symbiosis using transcriptomics and proteomics. *Front Immunol* **3**: 91.

Conner, J.G., Zamorano-Sánchez, D., Park, J.H., Sondermann, H., and Yildiz, F.H. (2017) The ins and outs of cyclic di-GMP signaling in Vibrio cholerae. *Curr Opin Microbiol* **36**: 20-29.

Costerton, J.W., Cheng, K.J., Geesey, G.G., Ladd, T.I., Nickel, J.C., Dasgupta, M., and Marrie, T.J. (1987) Bacterial biofilms in nature and disease. *Annu Rev Microbiol* **41**: 435-464.

Cronan, J.E. (1975) Thermal regulation of the membrane lipid composition of Escherichia coli. Evidence for the direct control of fatty acid synthesis. *J Biol Chem* **250**: 7074-7077.

Cui, Y., Zhao, D., Barrow, P.A., and Zhou, X. (2016) The endoplasmic reticulum stress response: A link with tuberculosis? *Tuberculosis (Edinb)* **97**: 52-56.

Darnell, C.L., Hussa, E.A., and Visick, K.L. (2008) The putative hybrid sensor kinase SypF coordinates biofilm formation in Vibrio fischeri by acting upstream of two response regulators, SypG and VpsR. *J Bacteriol* **190**: 4941-4950.

Davidson, S.K., Koropatnick, T.A., Kossmehl, R., Sycuro, L., and McFall-Ngai, M.J. (2004) NO means 'yes' in the squid-vibrio symbiosis: nitric oxide (NO) during the initial stages of a beneficial association. *Cell Microbiol* **6**: 1139-1151.

Davis, R.W., Botstein, D., and Roth, J.R., (1980) A Manual for Genetic Engineering, Advanced Bacterial Genetics. In.: Cold Spring Harbor press, pp.

Dominguez, D.C. (2004) Calcium signalling in bacteria. *Mol Microbiol* **54**: 291-297.

Dominguez, D.C., (2018) Calcium Signaling in Prokaryotes. In: Calcium and Signal Transduction. J.N. Buchholz & E.J. Behringer (eds). IntechOpen, pp.

Domínguez, D.C., Guragain, M., and Patrauchan, M. (2015) Calcium binding proteins and calcium signaling in prokaryotes. *Cell Calcium* **57**: 151-165.

Donlan, R.M. (2002) Biofilms: microbial life on surfaces. *Emerg Infect Dis* **8**: 881-890.

Dunn, A.K., Millikan, D.S., Adin, D.M., Bose, J.L., and Stabb, E.V. (2006) New rfp- and pES213-derived tools for analyzing symbiotic Vibrio fischeri reveal patterns of infection and lux expression in situ. *Appl Environ Microbiol* **72**: 802-810.

Dupont, N., Lacas-Gervais, S., Bertout, J., Paz, I., Freche, B., Van Nhieu, G.T., van der Goot, F.G., Sansonetti, P.J., and Lafont, F. (2009) Shigella phagocytic vacuolar membrane remnants participate in the cellular response to pathogen invasion and are regulated by autophagy. *Cell Host Microbe* **6**: 137-149.

Dutta, R., and Inouye, M. (2000) GHKL, an emergent ATPase/kinase superfamily. *Trends Biochem Sci* **25**: 24-28.

Elíes, J., Yáñez, M., Pereira, T.M.C., Gil-Longo, J., MacDougall, D.A., and Campos-Toimil, M. (2020) An Update to Calcium Binding Proteins. *Adv Exp Med Biol* **1131**: 183-213.

Fang, X., Ahmad, I., Blanka, A., Schottkowski, M., Cimdins, A., Galperin, M.Y., Römling, U., and Gomelsky, M. (2014) GIL, a new c-di-GMP-binding protein domain involved in regulation of cellulose synthesis in enterobacteria. *Mol Microbiol* **93**: 439-452.

Fishman, M.R., Giglio, K., Fay, D., and Filiatrault, M.J. (2018) Physiological and genetic characterization of calcium phosphate precipitation by Pseudomonas species. *Sci Rep* **8**: 10156.

Flemming, H.C., and Wingender, J. (2010) The biofilm matrix. *Nat Rev Microbiol* **8**: 623-633.

Flemming, H.C., Wingender, J., Szewzyk, U., Steinberg, P., Rice, S.A., and Kjelleberg, S. (2016) Biofilms: an emergent form of bacterial life. *Nat Rev Microbiol* **14**: 563-575.

Flemming, H.C., and Wuertz, S. (2019) Bacteria and archaea on Earth and their abundance in biofilms. *Nat Rev Microbiol* **17**: 247-260.

Galperin, M.Y., Natale, D.A., Aravind, L., and Koonin, E.V. (1999) A specialized version of the HD hydrolase domain implicated in signal transduction. *J Mol Microbiol Biotechnol* **1**: 303-305.

García Véscovi, E., Soncini, F.C., and Groisman, E.A. (1996) Mg2+ as an extracellular signal: environmental regulation of Salmonella virulence. *Cell* **84**: 165-174.

Geszvain, K., and Visick, K.L. (2008) The hybrid sensor kinase RscS integrates positive and negative signals to modulate biofilm formation in Vibrio fischeri. *J Bacteriol* **190**: 4437-4446.

Grab, D.J., Nyarko, E., Nikolskaia, O.V., Kim, Y.V., and Dumler, J.S. (2009) Human brain microvascular endothelial cell traversal by Borrelia burgdorferi requires calcium signaling. *Clin Microbiol Infect* **15**: 422-426.

Graf, J., Dunlap, P.V., and Ruby, E.G. (1994) Effect of transposon-induced motility mutations on colonization of the host light organ by Vibrio fischeri. *J Bacteriol* **176**: 6986-6991.

Graf, J., and Ruby, E.G. (1998) Host-derived amino acids support the proliferation of symbiotic bacteria. *Proc Natl Acad Sci U S A* **95**: 1818-1822.

Graw, J. (1997) The crystallins: genes, proteins and diseases. *Biol Chem* **378**: 1331-1348.

Guo, Y., and Rowe-Magnus, D.A. (2010) Identification of a c-di-GMP-regulated polysaccharide locus governing stress resistance and biofilm and rugose colony formation in Vibrio vulnificus. *Infect Immun* **78**: 1390-1402.

Guragain, M., King, M.M., Williamson, K.S., Pérez-Osorio, A.C., Akiyama, T., Khanam, S., Patrauchan, M.A., and Franklin, M.J. (2016) The Pseudomonas aeruginosa PAO1 Two-Component Regulator CarSR Regulates Calcium Homeostasis and Calcium-Induced Virulence Factor Production through Its Regulatory Targets CarO and CarP. *J Bacteriol* **198**: 951-963.

Ha, D.G., and O'Toole, G.A. (2015) c-di-GMP and its Effects on Biofilm Formation and Dispersion: a Pseudomonas Aeruginosa Review. *Microbiol Spectr* **3**: Mb-0003-2014.

Hay, I.D., Remminghorst, U., and Rehm, B.H. (2009) MucR, a novel membrane-associated regulator of alginate biosynthesis in Pseudomonas aeruginosa. *Appl Environ Microbiol* **75**: 1110-1120.

Hecht, G.B., and Newton, A. (1995) Identification of a novel response regulator required for the swarmer-to-stalked-cell transition in Caulobacter crescentus. *J Bacteriol* **177**: 6223-6229.

Hickman, J.W., Tifrea, D.F., and Harwood, C.S. (2005) A chemosensory system that regulates biofilm formation through modulation of cyclic diguanylate levels. *Proc Natl Acad Sci U S A* **102**: 14422-14427.

Hoffman, L.R., D'Argenio, D.A., MacCoss, M.J., Zhang, Z., Jones, R.A., and Miller, S.I. (2005) Aminoglycoside antibiotics induce bacterial biofilm formation. *Nature* **436**: 1171-1175.

Horton, R.M., Hunt, H.D., Ho, S.N., Pullen, J.K., and Pease, L.R. (1989) Engineering hybrid genes without the use of restriction enzymes: gene splicing by overlap extension. *Gene* **77**: 61-68.

Hsieh, M.L., Hinton, D.M., and Waters, C.M. (2018) VpsR and cyclic di-GMP together drive transcription initiation to activate biofilm formation in Vibrio cholerae. *Nucleic Acids Res* **46**: 8876-8887.

Hu, L., Raybourne, R.B., and Kopecko, D.J. (2005) Ca2+ release from host intracellular stores and related signal transduction during Campylobacter jejuni 81-176 internalization into human intestinal cells. *Microbiology (Reading)* **151**: 3097-3105.

Hussa, E.A., Darnell, C.L., and Visick, K.L. (2008) RscS functions upstream of SypG to control the syp locus and biofilm formation in Vibrio fischeri. *J Bacteriol* **190**: 4576-4583.

Hussa, E.A., O'Shea, T.M., Darnell, C.L., Ruby, E.G., and Visick, K.L. (2007) Two-component response regulators of Vibrio fischeri: identification, mutagenesis, and characterization. *J Bacteriol* **189**: 5825-5838.

Johnson, M.D., Garrett, C.K., Bond, J.E., Coggan, K.A., Wolfgang, M.C., and Redinbo, M.R. (2011) Pseudomonas aeruginosa PilY1 binds integrin in an RGD- and calcium-dependent manner. *PLoS One* **6**: e29629.

Jones, B.W., and Nishiguchi, M.K. (2004) Counterillumination in the Hawaiian bobtail squid, *Euprymna scolopes* Berry (Mollusca: Cephalopoda). *Marine Biology* **144**: 1151-1155.

Jones, H.E., Holland, I.B., and Campbell, A.K. (2002) Direct measurement of free Ca(2+) shows different regulation of Ca(2+) between the periplasm and the cytosol of Escherichia coli. *Cell Calcium* **32**: 183-192.

Karatan, E., Duncan, T.R., and Watnick, P.I. (2005) NspS, a Predicted Polyamine Sensor, Mediates Activation of Vibrio cholerae Biofilm Formation by Norspermidine. *Journal of Bacteriology* **187**: 7434-7443.

Kierek, K., and Watnick, P.I. (2003) The Vibrio cholerae O139 O-antigen polysaccharide is essential for Ca2+-dependent biofilm development in sea water. *Proc Natl Acad Sci U S A* **100**: 14357-14362.

Kim, S., Li, X.H., Hwang, H.J., and Lee, J.H. (2020) Thermoregulation of Pseudomonas aeruginosa Biofilm Formation. *Appl Environ Microbiol* **86**.

King, M.M., Kayastha, B.B., Franklin, M.J., and Patrauchan, M.A. (2020) Calcium Regulation of Bacterial Virulence. *Adv Exp Med Biol* **1131**: 827-855.

Koch, E.J., Miyashiro, T., McFall-Ngai, M.J., and Ruby, E.G. (2014) Features governing symbiont persistence in the squid-*Vibrio* association. *Mol Ecol* **23**: 1624-1634.

Koehler, S., Gaedeke, R., Thompson, C., Bongrand, C., Visick, K.L., Ruby, E., and McFall-Ngai, M. (2018) The model squid-*Vibrio* symbiosis provides a window into the impact of strain- and species-level differences during the initial stages of symbiont engagement. *Environ Microbiol*.

Koestler, B.J., and Waters, C.M. (2014) Bile acids and bicarbonate inversely regulate intracellular cyclic di-GMP in Vibrio cholerae. *Infect Immun* **82**: 3002-3014.

Koropatnick, T.A., Engle, J.T., Apicella, M.A., Stabb, E.V., Goldman, W.E., and McFall-Ngai, M.J. (2004) Microbial factor-mediated development in a host-bacterial mutualism. *Science* **306**: 1186-1188.

Koropatnick, T.A., Kimbell, J.R., and McFall-Ngai, M.J. (2007) Responses of host hemocytes during the initiation of the squid-*Vibrio* symbiosis. *Biol Bull* **212**: 29-39.

Kostakioti, M., Hadjifrangiskou, M., and Hultgren, S.J. (2013) Bacterial biofilms: development, dispersal, and therapeutic strategies in the dawn of the postantibiotic era. *Cold Spring Harb Perspect Med* **3**: a010306.

Koul, S., Somayajulu, A., Advani, M.J., and Reddy, H. (2009) A novel calcium binding protein in Mycobacterium tuberculosis--potential target for trifluoperazine. *Indian J Exp Biol* **47**: 480-488.

Krasteva, P.V., Fong, J.C., Shikuma, N.J., Beyhan, S., Navarro, M.V., Yildiz, F.H., and Sondermann, H. (2010) Vibrio cholerae VpsT regulates matrix production and motility by directly sensing cyclic di-GMP. *Science* **327**: 866-868.

Kremer, N., Philipp, E.E., Carpentier, M.C., Brennan, C.A., Kraemer, L., Altura, M.A., Augustin, R., Häsler, R., Heath-Heckman, E.A., Peyer, S.M., Schwartzman, J., Rader, B.A., Ruby, E.G., Rosenstiel, P., and McFall-Ngai, M.J. (2013) Initial symbiont contact orchestrates host-organ-wide transcriptional changes that prime tissue colonization. *Cell Host Microbe* **14**: 183-194.

Kretsinger, R.H., Ison, R.E., and Hovmöller, S. (2004) Prediction of protein structure. *Methods Enzymol* **383**: 1-27.

Kuchma, S.L., Brothers, K.M., Merritt, J.H., Liberati, N.T., Ausubel, F.M., and O'Toole, G.A. (2007) BifA, a cyclic-Di-GMP phosphodiesterase, inversely regulates biofilm formation and swarming motility by Pseudomonas aeruginosa PA14. *J Bacteriol* **189**: 8165-8178.

Kvist, M., Hancock, V., and Klemm, P. (2008) Inactivation of efflux pumps abolishes bacterial biofilm formation. *Appl Environ Microbiol* **74**: 7376-7382.

Le Roux, F., Binesse, J., Saulnier, D., and Mazel, D. (2007) Construction of a Vibrio splendidus mutant lacking the metalloprotease gene vsm by use of a novel counterselectable suicide vector. *Appl Environ Microbiol* **73**: 777-784.

Lenzoni, G., and Knight, M.R. (2019) Increases in Absolute Temperature Stimulate Free Calcium Concentration Elevations in the Chloroplast. *Plant Cell Physiol* **60**: 538-548.

Lesley, J.A., and Waldburger, C.D. (2001) Comparison of the Pseudomonas aeruginosa and Escherichia coli PhoQ sensor domains: evidence for distinct mechanisms of signal detection. *J Biol Chem* **276**: 30827-30833.

Lewit-Bentley, A., and Réty, S. (2000) EF-hand calcium-binding proteins. *Curr Opin Struct Biol* **10**: 637-643.

Ludvik, D.A., Bultman, K.M., and Mandel, M.J. (2021) Hybrid histidine kinase BinK represses. *J Bacteriol*.

Lyell, N.L., Dunn, A.K., Bose, J.L., and Stabb, E.V. (2010) Bright mutants of Vibrio fischeri ES114 reveal conditions and regulators that control bioluminescence and expression of the lux operon. *J Bacteriol* **192**: 5103-5114.

López, D., Vlamakis, H., and Kolter, R. (2010) Biofilms. *Cold Spring Harb Perspect Biol* **2**: a000398.

Madeira, F., Park, Y.M., Lee, J., Buso, N., Gur, T., Madhusoodanan, N., Basutkar, P., Tivey, A.R.N., Potter, S.C., Finn, R.D., and Lopez, R. (2019) The EMBL-EBI search and sequence analysis tools APIs in 2019. *Nucleic Acids Res* **47**: W636-w641.

Mandel, M.J., and Dunn, A.K. (2016) Impact and influence of the natural *Vibrio*-squid symbiosis in understanding bacterial-animal interactions. *Front Microbiol* **7**: 1982.

Mandel, M.J., Schaefer, A.L., Brennan, C.A., Heath-Heckman, E.A., Deloney-Marino, C.R., McFall-Ngai, M.J., and Ruby, E.G. (2012) Squid-derived chitin oligosaccharides are a chemotactic signal during colonization by *Vibrio fischeri*. *Appl Environ Microbiol* **78**: 4620-4626.

Mandel, M.J., Stabb, E.V., and Ruby, E.G. (2008) Comparative genomics-based investigation of resequencing targets in Vibrio fischeri: focus on point miscalls and artefactual expansions. *BMC Genomics* **9**: 138.

Mandel, M.J., Wollenberg, M.S., Stabb, E.V., Visick, K.L., and Ruby, E.G. (2009) A single regulatory gene is sufficient to alter bacterial host range. *Nature* **458**: 215-218.

Marsden, A.E., Grudzinski, K., Ondrey, J.M., DeLoney-Marino, C.R., and Visick, K.L. (2017) Impact of Salt and Nutrient Content on Biofilm Formation by Vibrio fischeri. *PLoS One* **12**: e0169521.

Matz, C., McDougald, D., Moreno, A.M., Yung, P.Y., Yildiz, F.H., and Kjelleberg, S. (2005) Biofilm formation and phenotypic variation enhance predation-driven persistence of Vibrio cholerae. *Proc Natl Acad Sci U S A* **102**: 16819-16824.

McCann, J., Stabb, E.V., Millikan, D.S., and Ruby, E.G. (2003) Population dynamics of Vibrio fischeri during infection of Euprymna scolopes. *Appl Environ Microbiol* **69**: 5928-5934.

McFall-Ngai, M., and Bosch, T.C.G. (2021) Animal development in the microbial world: The power of experimental model systems. *Curr Top Dev Biol* **141**: 371-397.

McFall-Ngai, M., and Montgomery, M.K. (1990) The anatomy and morphology of the adult bacterial light organ of *Euprymna scolopes* Berry (Cephalopoda:Sepiolidae). *Biol Bull* **179**: 332-339.

McFall-Ngai, M.J. (2014) The importance of microbes in animal development: lessons from the squid-vibrio symbiosis. *Annu Rev Microbiol* **68**: 177-194.

Merritt, J.H., Brothers, K.M., Kuchma, S.L., and O'Toole, G.A. (2007) SadC reciprocally influences biofilm formation and swarming motility via modulation of exopolysaccharide production and flagellar function. *J Bacteriol* **189**: 8154-8164.

Merritt, J.H., Ha, D.G., Cowles, K.N., Lu, W., Morales, D.K., Rabinowitz, J., Gitai, Z., and O'Toole, G.A. (2010) Specific control of Pseudomonas aeruginosa surface-associated behaviors by two c-di-GMP diguanylate cyclases. *mBio* **1**.

Miller, J.H., (1972) Experiments in molecular genetics. In. Cold Spring Harbor Laboratory, New York, NY, pp.

Millikan, D.S., and Ruby, E.G. (2002) Alterations in *Vibrio fischeri* motility correlate with a delay in symbiosis initiation and are associated with additional symbiotic colonization defects. *Appl Environ Microbiol* **68**: 2519-2528.

Miyashiro, T., and Ruby, E.G. (2012) Shedding light on bioluminescence regulation in *Vibrio fischeri*. *Mol Microbiol* **84**: 795-806.

Montgomery, M.K., and McFall-Ngai, M.J. (1992) The muscle-derived lens of a squid bioluminescent organ is biochemically convergent with the ocular lens. Evidence for recruitment of aldehyde dehydrogenase as a predominant structural protein. *J Biol Chem* **267**: 20999-21003.

Montgomery, M.K., and McFall-Ngai, M.J. (1998) Late postembryonic development of the symbiotic light organ of *Euprymna scolopes* (Cephalopoda: Sepiolidae). *Biol Bull* **195**: 326-336.

Morris, A.R., Darnell, C.L., and Visick, K.L. (2011) Inactivation of a novel response regulator is necessary for biofilm formation and host colonization by Vibrio fischeri. *Mol Microbiol* **82**: 114-130.

Morris, A.R., and Visick, K.L. (2013) Inhibition of SypG-induced biofilms and host colonization by the negative regulator SypE in Vibrio fischeri. *PLoS One* **8**: e60076.

Navazio, L., Formentin, E., Cendron, L., and Szabò, I. (2020) Chloroplast Calcium Signaling in the Spotlight. *Front Plant Sci* **11**: 186.

Nawroth, J.C., Guo, H., Koch, E., Heath-Heckman, E.A.C., Hermanson, J.C., Ruby, E.G., Dabiri, J.O., Kanso, E., and McFall-Ngai, M. (2017) Motile cilia create fluid-mechanical microhabitats for the active recruitment of the host microbiome. *Proc Natl Acad Sci U S A* **114**: 9510-9516.

Nisbett, L.M., and Boon, E.M. (2016) Nitric Oxide Regulation of H-NOX Signaling Pathways in Bacteria. *Biochemistry* **55**: 4873-4884.

Norsworthy, A.N., and Visick, K.L. (2015) Signaling between two interacting sensor kinases promotes biofilms and colonization by a bacterial symbiont. *Mol Microbiol* **96**: 233-248.

Nyholm, S.V., and McFall-Ngai, M. (2004) The winnowing: establishing the squid–*Vibrio* symbiosis. *Nature Reviews Microbiology* **2**: 632.

Nyholm, S.V., and McFall-Ngai, M.J. (1998) Sampling the light-organ microenvironment of *Euprymna scolopes*: description of a population of host cells in association with the bacterial symbiont *Vibrio fischeri*. *Biol Bull* **195**: 89-97.

Nyholm, S.V., and McFall-Ngai, M.J. (2021) A lasting symbiosis: how the Hawaiian bobtail squid finds and keeps its bioluminescent bacterial partner. *Nat Rev Microbiol*.

Nyholm, S.V., Stabb, E.V., Ruby, E.G., and McFall-Ngai, M.J. (2000) Establishment of an animal-bacterial association: recruiting symbiotic *Vibrios* from the environment. *Proc Natl Acad Sci U S A* **97**: 10231-10235.

Nyholm, S.V., Stewart, J.J., Ruby, E.G., and McFall-Ngai, M.J. (2009) Recognition between symbiotic *Vibrio fischeri* and the haemocytes of *Euprymna scolopes*. *Environ Microbiol* **11**: 483-493.

O'Shea, T.M., Deloney-Marino, C.R., Shibata, S., Aizawa, S., Wolfe, A.J., and Visick, K.L. (2005) Magnesium promotes flagellation of Vibrio fischeri. *J Bacteriol* **187**: 2058-2065.

O'Shea, T.M., Klein, A.H., Geszvain, K., Wolfe, A.J., and Visick, K.L. (2006) Diguanylate cyclases control magnesium-dependent motility of Vibrio fischeri. *J Bacteriol* **188**: 8196-8205.

O'Toole, G., Kaplan, H.B., and Kolter, R. (2000) Biofilm formation as microbial development. *Annu Rev Microbiol* **54**: 49-79.

Ondrey, J.M., and Visick, K.L. (2014) Engineering Vibrio fischeri for Inducible Gene Expression. *Open Microbiol J* **8**: 122-129.

Pankey, S.M., Foxall, R.L., Ster, I.M., Perry, L.A., Schuster, B.M., Donner, R.A., Coyle, M., Cooper, V.S., and Whistler, C.A. (2017) Host-selected mutations converging on a global regulator drive an adaptive leap towards symbiosis in bacteria. *Elife* **6**: e24414.

Park, J.H., Jo, Y., Jang, S.Y., Kwon, H., Irie, Y., Parsek, M.R., Kim, M.H., and Choi, S.H. (2015) The cabABC Operon Essential for Biofilm and Rugose Colony Development in Vibrio vulnificus. *PLoS Pathog* **11**: e1005192.

Parkinson, J.S., and Kofoid, E.C. (1992) Communication modules in bacterial signaling proteins. *Annu Rev Genet* **26**: 71-112.

Paul, R., Abel, S., Wassmann, P., Beck, A., Heerklotz, H., and Jenal, U. (2007) Activation of the diguanylate cyclase PleD by phosphorylation-mediated dimerization. *J Biol Chem* **282**: 29170-29177.

Paul, R., Weiser, S., Amiot, N.C., Chan, C., Schirmer, T., Giese, B., and Jenal, U. (2004) Cell cycle-dependent dynamic localization of a bacterial response regulator with a novel di-guanylate cyclase output domain. *Genes Dev* **18**: 715-727.

Persat, A., Nadell, C.D., Kim, M.K., Ingremeau, F., Siryaporn, A., Drescher, K., Wingreen, N.S., Bassler, B.L., Gitai, Z., and Stone, H.A. (2015) The mechanical world of bacteria. *Cell* **161**: 988-997.

Peyer, S.M., Kremer, N., and McFall-Ngai, M.J. (2018) Involvement of a host Cathepsin L in symbiont-induced cell death. *Microbiologyopen* **7**: e00632.

Pidcock, E., and Moore, G.R. (2001) Structural characteristics of protein binding sites for calcium and lanthanide ions. *J Biol Inorg Chem* **6**: 479-489.

Pollack-Berti, A., Wollenberg, M.S., and Ruby, E.G. (2010) Natural transformation of Vibrio fischeri requires tfoX and tfoY. *Environ Microbiol* **12**: 2302-2311.

Pu, M., Storms, E., Chodur, D.M., and Rowe-Magnus, D.A. (2020) Calcium-dependent site-switching regulates expression of the atypical iam pilus locus in Vibrio vulnificus. *Environ Microbiol* **22**: 4167-4182.

PubChem, (2021) Element Summary for Atomic Number 20, Calcium. In.: National Center for Biotechnology Information, pp.

Ray, V.A., Driks, A., and Visick, K.L. (2015) Identification of a novel matrix protein that promotes biofilm maturation in Vibrio fischeri. *J Bacteriol* **197**: 518-528.

Ray, V.A., Eddy, J.L., Hussa, E.A., Misale, M., and Visick, K.L. (2013) The syp enhancer sequence plays a key role in transcriptional activation by the σ54-dependent response regulator SypG and in biofilm formation and host colonization by Vibrio fischeri. *J Bacteriol* **195**: 5402-5412.

Regelmann, A.G., Lesley, J.A., Mott, C., Stokes, L., and Waldburger, C.D. (2002) Mutational analysis of the Escherichia coli PhoQ sensor kinase: differences with the Salmonella enterica serovar Typhimurium PhoQ protein and in the mechanism of Mg2+ and Ca2+ sensing. *J Bacteriol* **184**: 5468-5478.

Richter, A.M., Possling, A., Malysheva, N., Yousef, K.P., Herbst, S., von Kleist, M., and Hengge, R. (2020) Local c-di-GMP Signaling in the Control of Synthesis of the E. coli Biofilm Exopolysaccharide pEtN-Cellulose. *J Mol Biol* **432**: 4576-4595.

Roberts, M.C. (1996) Tetracycline resistance determinants: mechanisms of action, regulation of expression, genetic mobility, and distribution. *FEMS Microbiol Rev* **19**: 1-24.

Ross, P., Aloni, Y., Weinhouse, C., Michaeli, D., Weinberger-Ohana, P., Meyer, R., and Benziman, M. (1985) An unusual guanyl oligonucleotide regulates cellulose synthesis in Acetobacter xylinum. *FEBS Lett* **186**: 191-196.

Ross, P., Weinhouse, H., Aloni, Y., Michaeli, D., Weinberger-Ohana, P., Mayer, R., Braun, S., de Vroom, E., van der Marel, G.A., van Boom, J.H., and Benziman, M. (1987) Regulation of cellulose synthesis in Acetobacter xylinum by cyclic diguanylic acid. *Nature* **325**: 279-281.

Ruby, E.G., and Asato, L.M. (1993) Growth and flagellation of *Vibrio fischeri* during initiation of the sepiolid squid light organ symbiosis. *Arch Microbiol* **159**: 160-167.

Ruby, E.G., Urbanowski, M., Campbell, J., Dunn, A., Faini, M., Gunsalus, R., Lostroh, P., Lupp, C., McCann, J., Millikan, D., Schaefer, A., Stabb, E., Stevens, A., Visick, K., Whistler, C., and Greenberg, E.P. (2005) Complete genome sequence of Vibrio fischeri: a symbiotic bacterium with pathogenic congeners. *Proc Natl Acad Sci U S A* **102**: 3004-3009.

Rumbaugh, K.P., and Sauer, K. (2020) Biofilm dispersion. *Nat Rev Microbiol* **18**: 571-586.

Römling, U. (2005) Characterization of the rdar morphotype, a multicellular behaviour in Enterobacteriaceae. *Cell Mol Life Sci* **62**: 1234-1246.

Römling, U., and Galperin, M.Y. (2015) Bacterial cellulose biosynthesis: diversity of operons, subunits, products, and functions. *Trends Microbiol* **23**: 545-557.

Römling, U., Galperin, M.Y., and Gomelsky, M. (2013) Cyclic di-GMP: the first 25 years of a universal bacterial second messenger. *Microbiol Mol Biol Rev* **77**: 1-52.

Römling, U., Rohde, M., Olsén, A., Normark, S., and Reinköster, J. (2000) AgfD, the checkpoint of multicellular and aggregative behaviour in Salmonella typhimurium regulates at least two independent pathways. *Mol Microbiol* **36**: 10-23.

Salah Ud-Din, A.I.M., and Roujeinikova, A. (2017) Methyl-accepting chemotaxis proteins: a core sensing element in prokaryotes and archaea. *Cell Mol Life Sci* **74**: 3293-3303.

Sanchez, G., Jolly, J., Reid, A., Sugimoto, C., Azama, C., Marlétaz, F., Simakov, O., and Rokhsar, D.S. (2019) New bobtail squid (Sepiolidae: Sepiolinae) from the Ryukyu islands revealed by molecular and morphological analysis. *Commun Biol* **2**: 465.

Sano, R., and Reed, J.C. (2013) ER stress-induced cell death mechanisms. *Biochim Biophys Acta* **1833**: 3460-3470.

Saquib, N.M., Jamwal, S., Midha, M.K., Verma, H.N., and Manivel, V. (2015) Quantitative Proteomics and Lipidomics Analysis of Endoplasmic Reticulum of Macrophage Infected with Mycobacterium tuberculosis. *Int J Proteomics* **2015**: 270438.

Schaller, R.A., Ali, S.K., Klose, K.E., and Kurtz, D.M. (2012) A bacterial hemerythrin domain regulates the activity of a Vibrio cholerae diguanylate cyclase. *Biochemistry* **51**: 8563-8570.

Schleicher, T.R., VerBerkmoes, N.C., Shah, M., and Nyholm, S.V. (2014) Colonization state influences the hemocyte proteome in a beneficial squid-*Vibrio* symbiosis. *Mol Cell Proteomics* **13**: 2673-2686.

Schwartzman, J.A., Koch, E., Heath-Heckman, E.A., Zhou, L., Kremer, N., McFall-Ngai, M.J., and Ruby, E.G. (2015) The chemistry of negotiation: rhythmic, glycan-driven acidification in a symbiotic conversation. *Proc Natl Acad Sci U S A* **112**: 566-571.

Sender, R., Fuchs, S., and Milo, R. (2016) Revised Estimates for the Number of Human and Bacteria Cells in the Body. *PLoS Biol* **14**: e1002533.

Serra, D.O., and Hengge, R., (2019) Cellulose in Bacterial Biofilms. In: Extracellular Sugar-Based Biopolymers Matrices. E. Cohen & H. Merzendorfer (eds). Springer, Cham, pp.

Serra, D.O., Richter, A.M., and Hengge, R. (2013) Cellulose as an architectural element in spatially structured Escherichia coli biofilms. *J Bacteriol* **195**: 5540-5554.

Shibata, S., Yip, E.S., Quirke, K.P., Ondrey, J.M., and Visick, K.L. (2012) Roles of the structural symbiosis polysaccharide (syp) genes in host colonization, biofilm formation, and polysaccharide biosynthesis in Vibrio fischeri. *J Bacteriol* **194**: 6736-6747.

Shikuma, N.J., Fong, J.C., and Yildiz, F.H. (2012) Cellular levels and binding of c-di-GMP control subcellular localization and activity of the Vibrio cholerae transcriptional regulator VpsT. *PLoS Pathog* **8**: e1002719.

Sillanpää, J.K., Ramesh, K., Melzner, F., Sundh, H., and Sundell, K. (2016) Calcium mobilisation following shell damage in the Pacific oyster, Crassostrea gigas. *Mar Genomics* **27**: 75-83.

Simm, R., Morr, M., Kader, A., Nimtz, M., and Römling, U. (2004) GGDEF and EAL domains inversely regulate cyclic di-GMP levels and transition from sessility to motility. *Mol Microbiol* **53**: 1123-1134.

Soto, S.M. (2013) Role of efflux pumps in the antibiotic resistance of bacteria embedded in a biofilm. *Virulence* **4**: 223-229.

Speare, L., Cecere, A.G., Guckes, K.R., Smith, S., Wollenberg, M.S., Mandel, M.J., Miyashiro, T., and Septer, A.N. (2018) Bacterial symbionts use a type VI secretion system to eliminate competitors in their natural host. *Proc Natl Acad Sci U S A* **115**: E8528-E8537.

Spormann, A.M. (2008) Physiology of microbes in biofilms. *Curr Top Microbiol Immunol* **322**: 17-36.

Srivastava, D., Harris, R.C., and Waters, C.M. (2011) Integration of cyclic di-GMP and quorum sensing in the control of vpsT and aphA in Vibrio cholerae. *J Bacteriol* **193**: 6331-6341.

Srivastava, D., Hsieh, M.L., Khataokar, A., Neiditch, M.B., and Waters, C.M. (2013) Cyclic di-GMP inhibits Vibrio cholerae motility by repressing induction of transcription and inducing extracellular polysaccharide production. *Mol Microbiol* **90**: 1262-1276.

Stabb, E.V., and Millikan, D.S., (2009) Is the *Vibrio fischeri-Euprymna scolopes* symbiosis a defensive mutualism? In: Defensive Mutualism in Microbial Symbiosis. J.F. White Jr. & M.S. Torres (eds). CRC Press, pp. 85-96.

Stabb, E.V., Reich, K.A., and Ruby, E.G. (2001) Vibrio fischeri genes hvnA and hvnB encode secreted NAD(+)-glycohydrolases. *J Bacteriol* **183**: 309-317.

Stabb, E.V., and Ruby, E.G. (2002) RP4-based plasmids for conjugation between Escherichia coli and members of the Vibrionaceae. *Methods Enzymol* **358**: 413-426.

Stabb, E.V., Schaefer, A., Bose, J.L., and Ruby, E.G., (2008) Quorum signaling and symbiosis in the marine luminous bacterium *Vibrio fischeri*. In: Chemical Communication among Bacteria. S.C. Winans & B.L. Bassler (eds). Washington, DC: ASM Press, pp. 233-250.

Stabb, E.V., and Visick, K.L., (2013) *Vibrio fischeri*: A bioluminescent light-organ symbiont of the bobtail squid *Euprymna scolopes* In: The Prokaryotes- Prokaryotic Biology and Symbiotic Associations. E. Rosenberg, E.F. DeLong, E. Stackebrandt, S. Lory & F. Thompson (eds). Springer-Verlag Berlin Heidelberg, pp. 497-525.

Stock, A.M., Robinson, V.L., and Goudreau, P.N. (2000) Two-component signal transduction. *Annu Rev Biochem* **69**: 183-215.

Tal, R., Wong, H.C., Calhoon, R., Gelfand, D., Fear, A.L., Volman, G., Mayer, R., Ross, P., Amikam, D., Weinhouse, H., Cohen, A., Sapir, S., Ohana, P., and Benziman, M. (1998) Three cdg operons control cellular turnover of cyclic di-GMP in Acetobacter xylinum: genetic organization and occurrence of conserved domains in isoenzymes. *J Bacteriol* **180**: 4416-4425.

Thompson, C.M., Marsden, A.E., Tischler, A.H., Koo, J., and Visick, K.L. (2018) Vibrio fischeri Biofilm Formation Prevented by a Trio of Regulators. *Appl Environ Microbiol* **84**.

Thompson, C.M., Tischler, A.H., Tarnowski, D.A., Mandel, M.J., and Visick, K.L. (2019) Nitric oxide inhibits biofilm formation by *Vibrio fischeri* via the nitric oxide sensor HnoX. *Mol Microbiol*.

Thompson, C.M., and Visick, K.L. (2015) Assessing the function of STAS domain protein SypA in Vibrio fischeri using a comparative analysis. *Front Microbiol* **6**: 760.

Thongsomboon, W., Serra, D.O., Possling, A., Hadjineophytou, C., Hengge, R., and Cegelski, L. (2018) Phosphoethanolamine cellulose: A naturally produced chemically modified cellulose. *Science* **359**: 334-338.

Tischler, A.D., and Camilli, A. (2004) Cyclic diguanylate (c-di-GMP) regulates Vibrio cholerae biofilm formation. *Mol Microbiol* **53**: 857-869.

Tischler, A.H., Lie, L., Thompson, C.M., and Visick, K.L. (2018) Discovery of calcium as a biofilm-promoting signal for *Vibrio fischeri* reveals new phenotypes and underlying regulatory complexity. *J Bacteriol* **200**.

Townsley, L., and Yildiz, F.H. (2015) Temperature affects c-di-GMP signalling and biofilm formation in Vibrio cholerae. *Environ Microbiol* **17**: 4290-4305.

Tran Van Nhieu, G., Dupont, G., and Combettes, L. (2018) Ca(2+) signals triggered by bacterial pathogens and microdomains. *Biochim Biophys Acta Mol Cell Res* **1865**: 1838-1845.

Valentini, M., and Filloux, A. (2016) Biofilms and Cyclic di-GMP (c-di-GMP) Signaling: Lessons from Pseudomonas aeruginosa and Other Bacteria. *J Biol Chem* **291**: 12547-12555.

Visick, K.L., Foster, J., Doino, J., McFall-Ngai, M., and Ruby, E.G. (2000) *Vibrio fischeri lux* genes play an important role in colonization and development of the host light organ. *J Bacteriol* **182**: 4578-4586.

Visick, K.L., Hodge-Hanson, K.M., Tischler, A.H., Bennett, A.K., and Mastrodomenico, V. (2018) Tools for Rapid Genetic Engineering of Vibrio fischeri. *Appl Environ Microbiol* **84**.

Visick, K.L., Quirke, K.P., and McEwen, S.M. (2013) Arabinose induces pellicle formation by Vibrio fischeri. *Appl Environ Microbiol* **79**: 2069-2080.

Visick, K.L., and Ruby, E.G. (2006) Vibrio fischeri and its host: it takes two to tango. *Curr Opin Microbiol* **9**: 632-638.

Visick, K.L., and Skoufos, L.M. (2001) Two-component sensor required for normal symbiotic colonization of *Euprymna scolopes* by *Vibrio fischeri*. *J Bacteriol* **183**: 835-842.

Visick, K.L., Stabb, E.V., and Ruby, E.G. (2021) A lasting symbiosis: how Vibrio fischeri finds a squid partner and persists within its natural host. *Nat Rev Microbiol*.

Véscovi, E.G., Ayala, Y.M., Di Cera, E., and Groisman, E.A. (1997) Characterization of the bacterial sensor protein PhoQ. Evidence for distinct binding sites for Mg2+ and Ca2+. *J Biol Chem* **272**: 1440-1443.

Wang, Y., Dufour, Y.S., Carlson, H.K., Donohue, T.J., Marletta, M.A., and Ruby, E.G. (2010) H-NOX-mediated nitric oxide sensing modulates symbiotic colonization by Vibrio fischeri. *Proc Natl Acad Sci U S A* **107**: 8375-8380.

Wang, Y., and Ruby, E.G. (2011) The roles of NO in microbial symbioses. *Cell Microbiol* **13**: 518-526.

Watson, R.O., Bell, S.L., MacDuff, D.A., Kimmey, J.M., Diner, E.J., Olivas, J., Vance, R.E., Stallings, C.L., Virgin, H.W., and Cox, J.S. (2015) The Cytosolic Sensor cGAS Detects Mycobacterium tuberculosis DNA to Induce Type I Interferons and Activate Autophagy. *Cell Host Microbe* **17**: 811-819.

Wei, S., and Young, R. (1998) Development of symbiotic bioluminescence in a nearshore cephalopod, *Euprymna scolopes*. *Marine Biology* **103**: 541–546.

West, A.H., and Stock, A.M. (2001) Histidine kinases and response regulator proteins in two-component signaling systems. *Trends Biochem Sci* **26**: 369-376.

Whitman, W.B., Coleman, D.C., and Wiebe, W.J. (1998) Prokaryotes: the unseen majority. *Proc Natl Acad Sci U S A* **95**: 6578-6583.

Wier, A.M., Nyholm, S.V., Mandel, M.J., Massengo-Tiassé, R.P., Schaefer, A.L., Koroleva, I., Splinter-Bondurant, S., Brown, B., Manzella, L., Snir, E., Almabrazi, H., Scheetz, T.E., Bonaldo, M.e.F., Casavant, T.L., Soares, M.B., Cronan, J.E., Reed, J.L., Ruby, E.G., and McFall-Ngai, M.J. (2010) Transcriptional patterns in both host and bacterium underlie a daily rhythm of anatomical and metabolic change in a beneficial symbiosis. *Proc Natl Acad Sci U S A* **107**: 2259-2264.

Wingender, J., and Flemming, H.C. (2011) Biofilms in drinking water and their role as reservoir for pathogens. *Int J Hyg Environ Health* **214**: 417-423.

Wolfe, A., and Visick, K., (2010) Roles of Diguanylate Cyclases and Phosphodiesterases in Motility and Biofilm Formation in *Vibrio fischeri*. In: The Second Messenger Cyclic-Di-GMP. A. Wolfe & K. Visick (eds). Washington, DC: ASM Press, pp. 186-200.

Yip, E.S., Geszvain, K., DeLoney-Marino, C.R., and Visick, K.L. (2006) The symbiosis regulator *rscS* controls the syp gene locus, biofilm formation and symbiotic aggregation by *Vibrio fischeri*. *Mol Microbiol* **62**: 1586-1600.

Yip, E.S., Grublesky, B.T., Hussa, E.A., and Visick, K.L. (2005) A novel, conserved cluster of genes promotes symbiotic colonization and sigma-dependent biofilm formation by Vibrio fischeri. *Mol Microbiol* **57**: 1485-1498.

Zamorano-Sánchez, D., Xian, W., Lee, C.K., Salinas, M., Thongsomboon, W., Cegelski, L., Wong, G.C.L., and Yildiz, F.H. (2019) Functional Specialization in *Vibrio cholerae* Diguanylate Cyclases: Distinct Modes of Motility Suppression and c-di-GMP Production. *mBio* **10**.

Zhang, M., Tanaka, T., and Ikura, M. (1995) Calcium-induced conformational transition revealed by the solution structure of apo calmodulin. *Nat Struct Biol* **2**: 758-767.

Zhou, H., Zheng, C., Su, J., Chen, B., Fu, Y., Xie, Y., Tang, Q., Chou, S.H., and He, J. (2016) Characterization of a natural triple-tandem c-di-GMP riboswitch and application of the riboswitch-based dual-fluorescence reporter. *Sci Rep* **6**: 20871.

Zogaj, X., Nimtz, M., Rohde, M., Bokranz, W., and Römling, U. (2001) The multicellular morphotypes of Salmonella typhimurium and Escherichia coli produce cellulose as the second component of the extracellular matrix. *Mol Microbiol* **39**: 1452-1463.

Zorraquino, V., García, B., Latasa, C., Echeverz, M., Toledo-Arana, A., Valle, J., Lasa, I., and Solano, C. (2013) Coordinated cyclic-di-GMP repression of Salmonella motility through YcgR and cellulose. *J Bacteriol* **195**: 417-428.

VITA

The author, Alice Hannah Tischler was born in Knoxville, Tennessee on September 10, 1992 to Monica and Jonathan Tischler. She received a Bachelor of Science degree from Allegheny College (Meadville, PA) in May 2015.

In August 2015, Alice matriculated into the Integrated Program in Biomedical Sciences at Loyola University Chicago and joined the Department of Microbiology and Immunology shortly thereafter. Alice completed her doctoral work in the laboratory of Dr. Karen L. Visick, where she focused on identification and characterization of calcium as a signal to promote biofilm formation by the marine bacterium, *Vibrio fischeri*. While at Loyola, her work was partially funded by the Arthur J. Schmitt Foundation.

After receiving her Ph.D., Alice will begin a post-doctoral position with Dr. Shumin Tan at Tufts University School of Medicine in Boston, MA, studying *Mycobacterium tuberculosis*.